University of Strathclyde

Department of Chemical & Process Engineering

Investigation of Premixed Sooting Flames by Combined Laser Induced Incandescence and Laser Induced Fluorescence

Jaclyn Dunn

A thesis submitted to the Department of Chemical and Process Engineering, University of Strathclyde in fulfilment of the requirements for the degree of Doctor of Philosophy

2014

This thesis is the result of the author's original research. It has been composed by the author and has not been previously submitted for examination which has led to the award of a degree.

Signed: Date:

f.e.a.r.

ACKNOWLEDGEMENTS

Firstly, I would like to thank my supervisor, Dr Iain Burns, for the help and support through these last four years. I would like to offer thanks to the technical staff in the department – without their help much of the initial work and "problem solving" would have been much more difficult. My thanks also to the EPSRC for the funding of this work.

I would like to extend my gratitude to Dr Alison Nordon and Dr Ashleigh Fletcher for many encouraging discussions and support through this time. Also Yuxuan Hu for all the useful conversations, especially around laboratory matters. I should also, at this point, thank everyone in the department of Pure and Applied Chemistry analytical group for welcoming me to their office (Melissa Black, Laura Palmer and David Wilsdon – you all deserve special mentions) and offering much needed laughter after I was displaced. To all my fellow chemical engineering PhD students – our lunchtime chatter will always be unrivalled and the special and sincere friendship we have will, I'm sure, last many years. Lynsey Anderson, we've had the best and worst times over the last ten years, I couldn't have got through some of it without you! Colin Jones, you've probably suffered more than anyone when things were going wrong but your calm head and reassurance have got me to this point: thank you for being there through all the tough times, as well as the great times. A special thanks to all of my friends - both fellow students (who know the highs and lows), and "civilians" (who hear all about the highs and lows) without you I could not have come this far.

Last, but not least, I would like to thank my family – Dad, Joyce, Colin, Stephanie and Gran – it's been a hard time for us but your support in my continuing study has been invaluable. Sadly, Mum, you won't get to read this but your and Dads encouragement - initially of me to be an inquisitive child and latterly to pursue this path - won't, like you, be forgotten.

ABSTRACT

This study applies the techniques of laser induced incandescence (LII) and laser induced fluorescence (LIF) to investigate laminar sooting flames of premixed ethylene air. The approach involves using three different excitation wavelengths, together with temporally and spectrally resolved detection, generating a rich dataset concerning the formation of soot and polycyclic aromatic hydrocarbons (PAHs).

Both prompt and delayed detection are used to perform LII when exciting with short wavelengths, both with issues involved. Delayed detection gives an underestimation of soot volume fraction at low heights in the flame, as a result of particle size effects. Prompt detection gives overestimation of soot volume fraction due to fluorescence in the measurement volume. It is shown that care must be taken with either method and through evaluation of the associated errors this study shows delayed detection provides a more accurate measure of soot volume fraction.

The ability to obtain the fluorescence signals over a range of heights above burner and stoichiometries is demonstrated. The approach relies on heating the soot particles equivalently with three excitation wavelengths so the LII contribution to the signals can be subtracted, leaving only fluorescence. Fluorescence profiles obtained show similar features to those seen in the literature for invasive measurements, including a reduction in the fluorescence signal generated by 283 nm excitation at intermediate heights above the burner surface followed by a re-increase. Although the data do not allow species-selective measurements of PAHs, these *in-situ* measurements allow inferences to be drawn about changing concentration of different size classes of these precursors to soot formation.

Finally the method of obtaining subtracting the LII contribution to signals was used to obtain fluorescence spectra both for 283 nm and 532 nm excitation. This showed the possibility that fluorescence can yield useful information that it is otherwise impossible to obtain *in-situ* under sooting conditions.

TABLE OF CONTENTS

TABLE OF FIGURES

1 INTRODUCTION

1.1 COMBUSTION IN SOCIETY

Since the early days of civilisation combustion has played a key role in society – from the use of fire for heat, light, and cooking, to the relatively modern invention and progression of jet engines. Taking into consideration the role which combustion processes have in our everyday life it is widely agreed that society as it is today could not continue in its current state without them. Although there has been a recent drive towards, and consequently much work focusing on, renewable energies there is still a gap which must be filled by either hydrocarbon combustion or nuclear energy. There are commonly discussed pros and cons for each – but there is an acceptance that at present a combination of all three sources are required[1]. It is also widely recognised though that the current levels of combustion cannot be maintained without there being greater consideration of the impact which it is having on the environment and consequently human health.

With this in mind it becomes apparent that there is still much need to better understand the fundamentals of the combustion process in order it be better understood. This would allow not only the ability to better design combustors, which are more efficient, but which are also kinder to the environment. However, due to the complex nature of the mechanism of formation of soot, and the number of intermediaries, the greater understanding of combustion processes is not a straightforward goal and as such much of the work focuses on the fundamentals of flames in order a better understanding be developed. This is a shift from the previous "end goal" where much of combustion research was more focused on improving the efficiency[2].

As well as the importance of the study of soot itself, it has become apparent that there is a need to study the intermediaries and precursors to soot, namely polycyclic aromatic hydrocarbons (PAHs). Since the 1960s it has been known that these molecules are not only pollutants in their own right but are also highly carcinogenic and mutagenic[3], thus presenting the release of these is of optimum importance, especially as they are harder to detect than soot.

An initial response to the problem of incomplete combustion reactions would be to suggest that all combustion reactions could be driven to completion, and hence no soot released into the environment. However, in reality this is overly simplistic. Even if it were possible from a design point of view to have complete combustion there are many processes which require the production of soot in order to be effective (due to the heat transfer properties of soot) or to produce carbon (for example for use as a filler in rubber or as a component of ink)[4, 5]. There are also issues surrounding the adequate control of processes where there is a need for soot formation and the negative impact soot can have on the process if it sticks to the combustor. This highlights that the necessity to understand soot formation is not one purely driven from an environmental point of view[6-10] but one which is motivated by industry.

It could be argued that necessity to understand combustion will decline along with the use of fossil fuels, however, this may not be the case. Even if all energy could be obtained via renewable means there will remain processes reliant on combustion, for example aviation and obtaining carbon black. Furthermore, there is a potential that the measurements techniques which are developed for the study of combustion, some of which will be further discussed here, are equally applicable to other areas of research with minimal modification, and can find use in fields such as research of nanoparticulate materials.

1.2 HISTORY OF THE STUDY OF SOOT AND POLLUTION

In 1860 Michael Faraday gave his famous six lecture series on the "Chemical History of a Candle"[11]. Many regard this as being around the infancy of the study of combustion, however, this is not the case. For many centuries previously fire had been looked upon with some curiosity and various theories around how fire propagates had been suggested over many years.

Due to the complex nature of the impact which soot has on the body, historically there was not the physiological knowledge to understand the mechanisms of action. There was, however, the realisation that the inhalation of smoke filled air could have a large negative impact on health as early as the 13th century when King Edward 1st of England issued an order that sea coal should not be burned in the vicinity of London, in order to minimise the thick smog this created[12]. It was the 18th century before the health concerns shown were directly related to soot, with medical observers noting that there was a high proportion of chimney sweeps who were being diagnosed with scrotal cancer[13]. The link between the soot and the observance of cancer led to soot being identified as a carcinogen was a major step forward, though it would be another two centuries before it was recognised that it was the component molecules of soot, the PAHs, which were causing the carcinogenic effect.

Real scientific study of the impact of soot as we now it began in the 1920s, with the work of Kuroda and Kawahata, showing the link between lung cancer and soot inhalation[13]. At this point the study of carcinogens was in its infancy and as a known carcinogen soot was one of the initial substances to be tested. By the 1960s that there began a growing realisation within the wider community that the PAHs can be highly carcinogenic and mutagenic[6, 14, 15] and the real study of them began in earnest. With this there became an importance of not only understanding and reducing the amount of soot produced but also the precursors of soot.

As much as there has been progress over the last few decades this has been slow, especially in the early days where the wide range of techniques available today were not available. Pace is being gathered in the study of soot formation, however, with the number of published papers growing massively in the last 20 years. This can be illustrated by examining how the number of papers including the keyword soot formation has grown over the last 45 year, as shown in Figure 1-1[16].

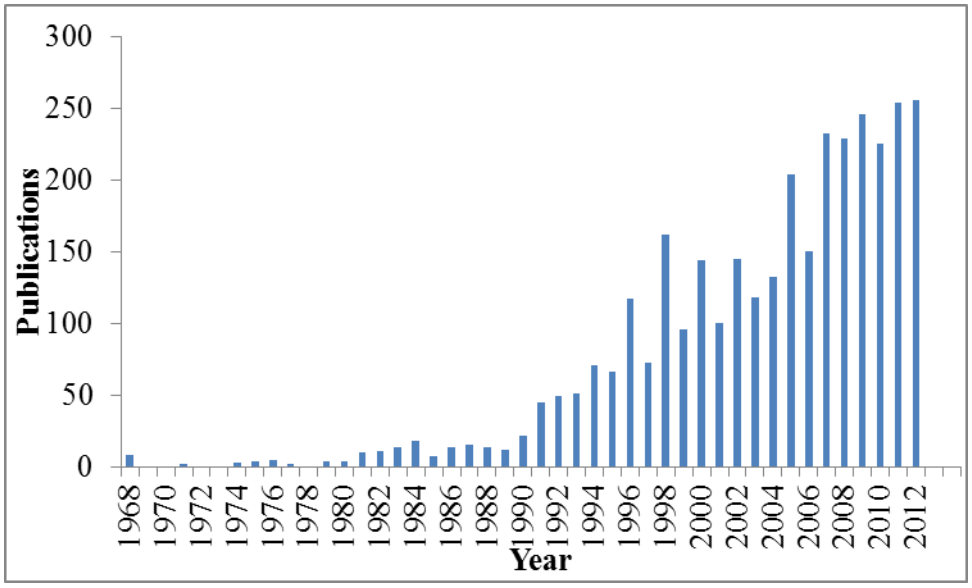

Figure 1-1 : Papers published over last 45 years on the study of soot formation

Much work is still required, however, as to understand the most simple of flames fully there is a great deal of data which must be gathered. This was noted by Bladh[17] in his thesis where he discusses the impossibility to predict particulate formation within a flame from a single parameter, such as particle size or temperature, and as such to understand the mechanisms through which combustion progresses there must be a wide range of information obtained from several different experiments.

1.3 AIMS AND OUTLINE OF THESIS

This work aimed firstly to investigate the impact which obtaining laser induced incandescence measurements with short wavelengths of excitation has on the soot volume fraction. In the literature, although it is well established that fluorescence can have an impact on the signal which is acquired at the peak and particle size effects will have an impact on the signal obtained after a delay, both of these methods are reported as being used. This work aims to highlight the errors associated with these methods through thorough investigation of the signals gathered over a wide range of flame conditions and heights above burner.

It has been established in the literature that through recording the emitted signal with a short wavelength of excitation (532 m) and subtracting the signal obtained with a long wavelength of excitation (1064 nm) that the remaining signal will be attributable to fluorescence. This is as a result of the signal obtained with short excitation wavelengths being a combination of fluorescence and incandescence and the signal obtained with a long excitation wavelength. This was investigated in order to ascertain how the fluorescence signal would change over the wide range of stoichiometries and heights above burner employed in this study, and also how this compares to measurements which are seen in the literature which have been made through invasive processes.

The challenge of being able to obtain fluorescence information non-invasively in sooting flames is outlined in the literature[18]. If this were possible it would open the door to many interesting studies and potentially an easier and more accurate way of obtaining fluorescence profiles without having to sample from the flame. Building on the ability to separate fluorescence and incandescence contributions at one wavelength, the ability to obtain fluorescence using the method outlined in the previous paragraph over a range of detection wavelengths to yield a fluorescence spectrum is investigated.

In the work presented here there will firstly be consideration given to the large body of work presented in the literature, where the current developments are and where work is

still needed. This is discussed in chapter 2 with an emphasis on what methods are currently used and the benefits and shortcomings of these techniques. The rationale behind the development of laser based techniques are outlined along with the implications of the successful developments and implementation of these techniques.

In chapter 3 there is detailed discussion of how the optimum set up and flame conditions to be used in this work were identified. Careful consideration had to be given to how the burner and flame conditions which were being employed in this work could be considered adequate and how the results which were obtained throughout the work could be considered reliable.

The results which are presented here are split into three chapters, each of which covers a different aspect of the work. In the first chapter there is consideration made of the methods by which the incandescence signal, from which we can obtain information on the soot which is present in the flame is recorded and used. The first of these techniques involves examining the peak signal, which can be influenced by fluorescence interference, and the other involves examining the signal after a delay, to avoid the fluorescence, though this can cause issues associated with changes in particle size. Each of these methods will have associated errors and, as such, a comprehensive comparison of these methods is made through assessment of the signal obtained.

If a long wavelength of excitation is used then the emitted signal will be attributable only to incandescence, where if a shorter wavelength of excitation is used the emitted signal will be attributable to both incandescence and fluorescence. In the second of the results chapters it is shown that if all conditions – including the degree to which the particles are being heated – are kept constant then it is possible to subtract the signal obtained with a long wavelength of excitation from the signal obtained with a short wavelength of excitation, leaving the fluorescence signal. This is examined to show the capability of utilising this fluorescence signal to obtain valuable information about the flame.

The third chapter progresses this idea and proposes recording the emitted signal over a range of detection wavelengths. This ensures that not only can information be obtained about the relative signals resulting from fluorescence but that it is possible to obtain a spectra which is attributable to fluorescence. This is a significant step forward to be being able to obtain information on PAHs without having to withdraw samples from the flame.

As is the case with all work of this type there are many questions which remain upon the completion of the work. For this reason there is a dedicated section, after the conclusions, about further work which could be undertaken. This section not only suggests further conditions which should be used and experiments which would expand upon the work shown, but also reflects upon the work suggesting ways which the work could be improved upon – both in terms of technique and range of measurement. There are also comments upon further work which could be undertaken if wholesale changes were made to the setup and how this would help to move the technique forward.

1.4 REFERENCES

1. C. W. Forsberg, *Progress in Nuclear Energy*, 2009, **51**, 192-200.
2. M. D. Smooke, C. S. McEnally, L. D. Pfefferle, R. J. Hall and M. B. Colket, *Combustion and Flame*, 1999, **117**, 117-139.
3. V. V. Kislov, N. I. Islamova, A. M. Kolker, S. H. Lin and A. M. Mebel, *Journal of Chemical Theory and Computation*, 2005, **1**, 908-924.
4. R. Viskanta and M. P. Mengüç, *Progress in Energy and Combustion Science*, 1987, **13**, 97-160.
5. Z. A. Mansurov, *Combustion Explosion and Shock Waves*, 2005, **41**, 727-744.
6. J. A. Miller, M. J. Pilling and E. Troe, *Proceedings of the Combustion Institute*, 2005, **30**, 43-88.

7. Q. N. Chan, P. R. Medwell, P. A. M. Kalt, Z. T. Alwahabi, B. B. Dally and G. J. Nathan, *Proceedings of the Combustion Institute*, 2011, **33**, 791-798.
8. F. Cignoli, S. Benecchi and G. Zizak, *Applied Optics*, 1994, **33**, 5778-5782.
9. K. Siegmann, K. Sattler and H. C. Siegmann, *Journal of Electron Spectroscopy and Related Phenomena*, 2002, **126**, 191-202.
10. R. Hadef, K. P. Geigle, W. Meier and M. Aigner, *International Journal of Thermal Sciences*, 2010, **49**, 1457-1467.
11. http://www.fordham.edu/halsall/mod/1860Faraday-candle.asp, Accessed 20 September, 2013.
12. http://www.fordham.edu/halsall/mod/1860Faraday-candle.asp, Accessed 25/08/13.
13. T. R. Barfknecht, *Progress in Energy and Combustion Science*, 1983, **9**, 199-237.
14. S. Senkan and M. Castaldi, *Combustion and Flame*, 1996, **107**, 141-150.
15. B. S. Haynes and H. G. Wagner, *Progress in Energy and Combustion Science*, 1981, **7**, 229-273.
16. http://apps.webofknowledge.com/, accessed 1/11/13 (keywords "soot formation").
17. H. Bladh, Lund University Sweden, 2007.
18. P. Desgroux, X. Mercier and K. A. Thomson, *Proceedings of the Combustion Institute*, 2013, **34**, 1713-1738.

2 SOOT FORMATION AND DIAGNOSTICS

Over the last 60 years although there has been much work done in the study of soot formation crucial questions remain unanswered. Even though there is a well-established general pathway of soot formation there is still much work which needs to be done to understand key steps. The problem is a complex one with many different fuels, burner configurations, and vast array of applications; there is no one size fits all approach to the study of combustion mechanisms. As such consideration must be given to what information needs to be obtained before deciding upon which method can be successfully employed.

With such a wide variety information required for complete understanding there have been several experimental techniques developed to investigate flames and the species within them. All diagnostic techniques have advantages and disadvantages, and as such different systems to which they are most applicable. Some techniques are useful for species specific information, while others give broader but more general information. Through the development and application of various techniques a more complete picture can be obtained: it is not possible to validate model predictions using information obtained from only one measurement technique.

This chapter firstly details what is currently accepted to be the route of soot formation highlighting the major gaps in our current understanding and the difficulties with recent models. The relevant experimental methods employed in previous studies are then discussed and their advantages and disadvantages outlined. Finally the methods used in this work are introduced along with discussion of how these will be of benefit.

2.1 SOOT FORMATION

Due to the complex nature of soot formation, and the simultaneous breakdown and growth mechanisms, there are many paths through which a molecule can progress when growing[1-4]. Therefore, although combustion has been studied for many years there is still a great deal information which still has to be obtained[5, 6].

During hydrocarbon combustion the fuel initially breaks down into small molecules and radicals, which under some conditions may react to form sequentially larger molecules. These molecules, which can be collectively classified as polycyclic aromatic hydrocarbons (PAHs) – react to form progressively larger PAH molecules which will eventually join together to form soot[7]. As the name suggests, PAHs are planar aromatic molecules, the smallest of which is naphthalene ($C_{10}H_8$) and the largest of which can be several hundred amu.

Though widely studied in order to obtain information on soot formation it is also important to study PAHs in their own right as they are well known pollutants which can be highly carcinogenic. The detrimental effect of PAHs on both health and the environment has been discussed since the 1960s but progress on the mechanism of formation is slow and although the general mechanism of the formation of PAHs has been widely investigated there remains significant gaps in the understanding of their formation and growth[8, 9]. Since the toxicity of PAHs is not dependent on the size of the molecule but on the structure of the molecule, it is important to investigate how these molecules grow[9].

2.1.1 Growth of PAHs

The gap in knowledge of what mechanisms are responsible for the evolution of small nanoparticles (that is those with diameters of a few nanometers) from large PAH molecules is an issue of central importance[10, 11]. One of the main issues is that there is a

need for computational tools that can predict PAH concentration and soot formation and a better understanding of the nature and origin of the incipient particles is crucial to achieving that.[12]

It is largely agreed upon that the main building block in the growth of PAHs is acetylene, and the hydrogen abstraction/acetylene addition (HACA) mechanism has been widely used[13, 14]. Although this is recognised as being an imperfect mechanism[15] it was the first mechanism, presented by Frenklach and co-workers[14] in 1985, that tackled the initial stages of soot formation and thus many subsequent models have their basis here.

The initial breakdown of the hydrocarbon fuel via pyrolysis results in small molecules and radicals. This is followed by their recombination to give acetylene molecules (C_2H_2), which are consumed in the growth of larger molecules. Through a simple ring closure, outlined in the HACA mechanism, the initial aromatic ring is formed.

An example of a route by which this can occur is shown in Figure 2-1, as described by Frenklach *et al.*[14].

Frenklach[14] continues by describing how upon ring closures phenylacetylene radical is initially formed. It is possible for the phenylacetylene radical to undergo further reaction with a molecule of acetylene, resulting in the formation of a naphthalene radical. There follows further acetylene addition and hydrogen loss resulting in the formation of acenaphthalene. This process continues with sequentially larger, yet still planar, PAH molecules forming.

After the PAHs reach a significant size (and hence mass) it is also possible for the molecules to grow through either reaction with other PAHs or through the addition of other small radicals present from the initial pyrolysation. It was hypothesised that due to the atoms and bonds lying in the one plane within the molecules it is only possible to achieve planar growth in this way[16]. This meant that in order for the molecules to become three dimensional there must be nucleation of some type – where one molecule acts as a surface for other molecules to join, Figure 2-2. However, more recently it has

been suggested that aliphatic chains attached to the molecules could have a large effect in allowing the molecules to grow via coalescence[17].

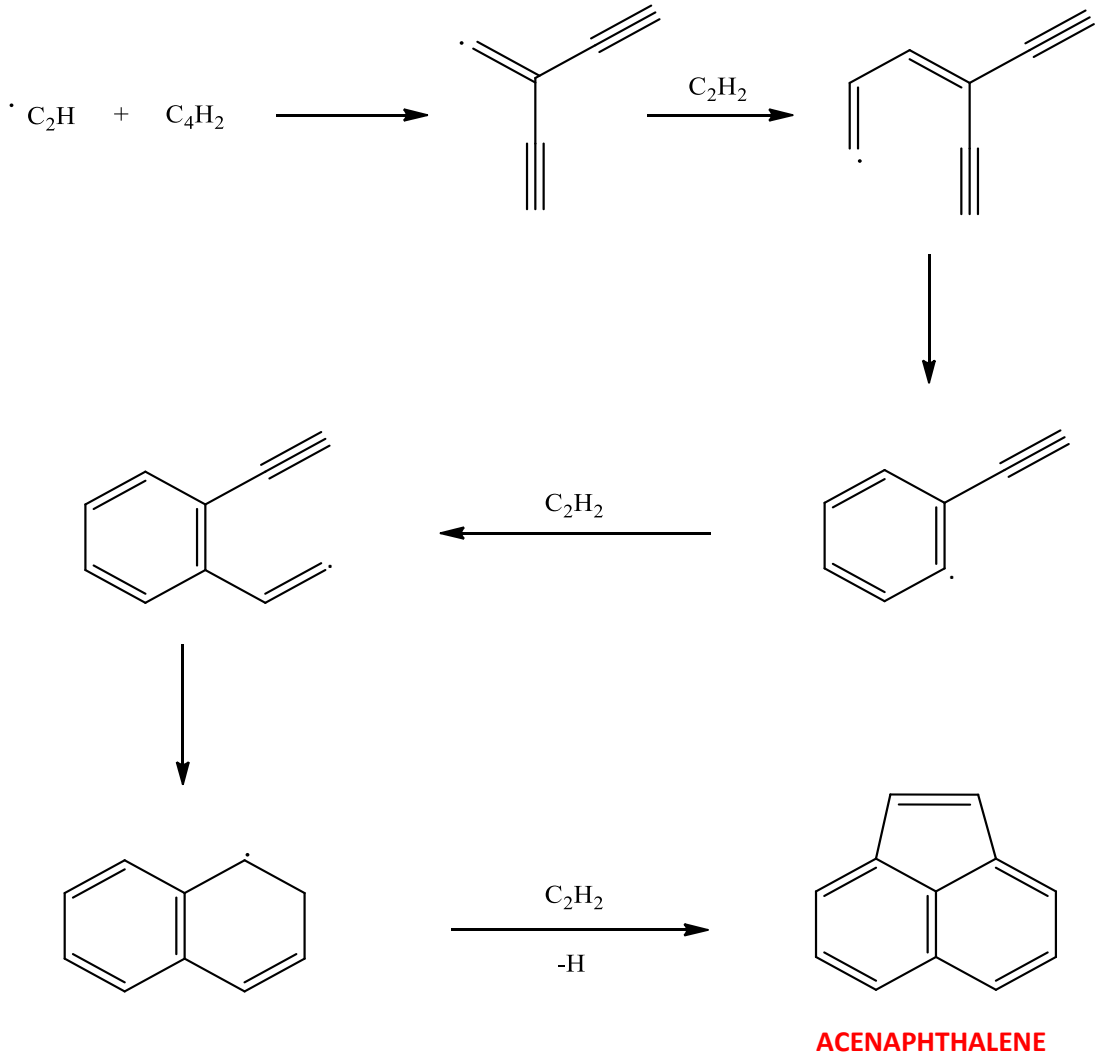

Figure 2-1 : HACA mechanism

This nucleation step can be highlighted as an excellent example of the difficulty involved in suggesting a plausible mechanism. It has been suggested, that this occurs through dimerization of large PAHs to form the so called “PAH-dimer” and that the

initial attraction which holds the two planar PAHs together in "sandwich like" formation are van der Waals forces[9].

However, it is discussed by Siegmann *et al.* in 2002[7] that, as van der Waals forces are inherently weak, that this mechanism can be thought of as highly unlikely for small molecules, such as pyrene at this temperature. More recently though it has been suggested that large molecules could be of great enough mass that van der Waals forces will be viable and hence molecules be able to condense in this way with the growth will be facilitated by aliphatic chains which are attached to PAHs[18, 19]. Due to the conflicting views, and the lack of a way of directly monitoring this step, even this, one of the earliest suggested mechanisms, requires greater understanding.

2.1.2 Soot Growth

Soot particles, it is widely accepted, grow via either surface growth (that is addition of PAHs or other gas phase molecules) or coagulation (of small particles colliding and joining)[20-22], although it has been shown that surface growth becomes less likely as the soot matures[23]. It was put forward by Frenklach *et al.*[16] that this is due to the falling concentration of hydrogen as the temperature of the flame decreases. The coagulation of the particles decreases the particle number concentration but while increasing in the particle mass[7].

Most of the initial work in the study of soot formation was collated in Frenklach's[14] 1985 paper. This paper presented the reaction model between gaseous molecules and soot particles being as a result of chemical growth mechanisms. In his 2001 paper Frenklach[24] describes how soot formation can be split into four parts – homogeneous nucleation of soot particles, particle coagulation, particle surface growth reactions, and particle agglomeration. He also describes how through work presented by himself and co-workers in 1991[16] and 1994[25] reaction models had been evolved such that when PAH molecules reach a certain size they will stick together to form dimers, and subsequently

trimmers and tetramers, which will continue to grow in this way until solid particles are formed.

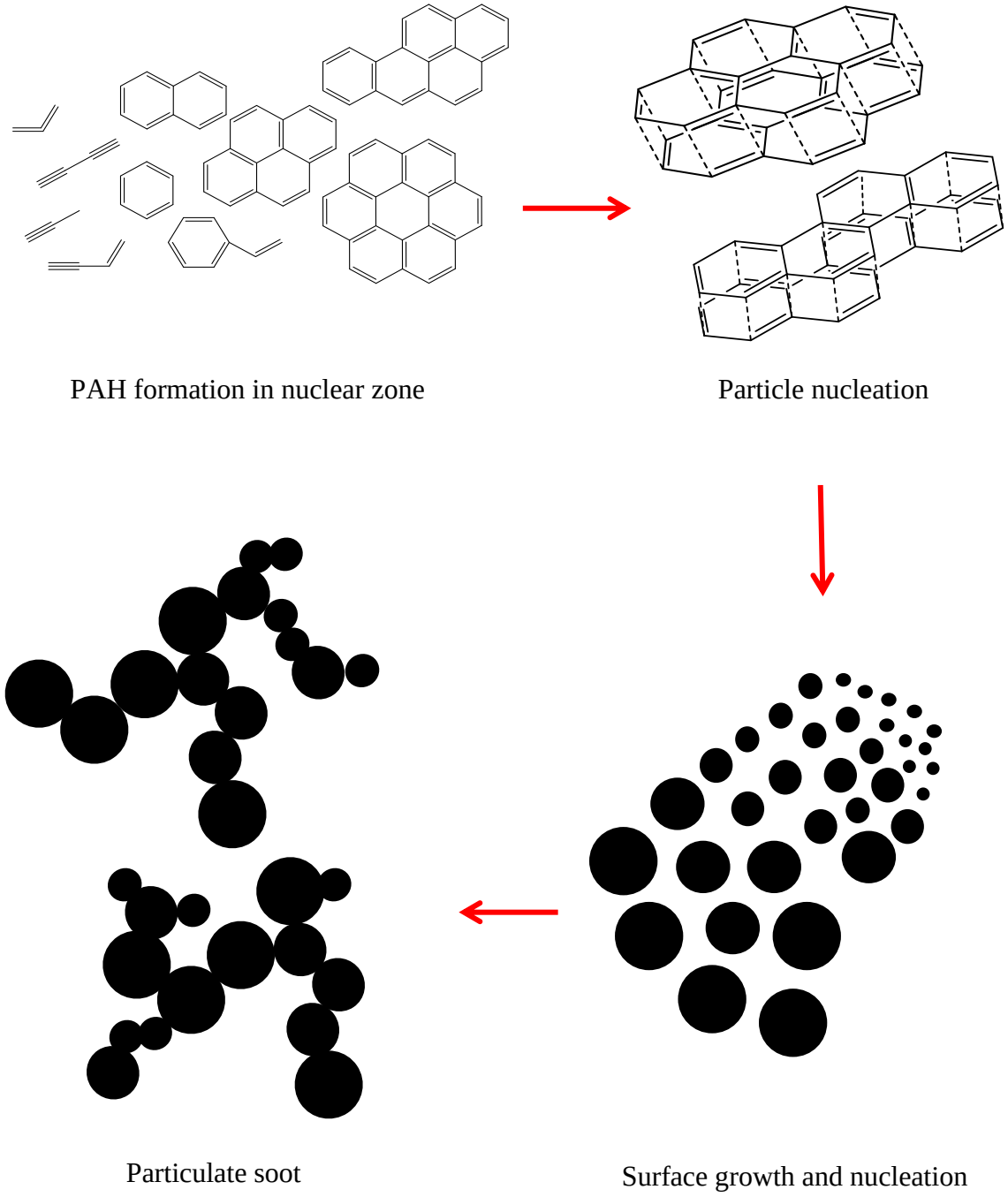

Figure 2-2 : General mechanism of soot formation

Once the particles reach a mass where the surface growth ceases particles will join to each other through aggregation, which leads to the clusters of smaller soot particles which have joined to form particles which are several hundred nanometers in size. When the particles are large enough, and as a result of the heat produced, the polyaromatic molecules can undergo graphitisation[7] - where the soot becomes a more thermodynamically stable graphite-like material. This causes the particle to increase in density, and with it brings new challenges when studying the mechanisms of growth. Simultaneously, to this there is also the competing process of oxidation which causes the loss of particle mass[9]. It is via this oxidation that some flames which appear sooting (that is they show an orange glow) never release soot particles, for example a candle flame.

The idea of there being a stepwise progression towards the formation of soot is an important consideration when designing experiments to study the formation. For example, one goal of this work is to differentiate between regions in the flame where there are small molecules (in this study this will only be identifiable through a lack of signal) then sequentially small PAHs, larger PAHs and finally soot. It was therefore important to allow the necessary reactions to take place in a controlled environment. This was achieved through use of a flat flame burner, which gives a pseudo one dimensional flame, allowing for it to be seen as different layers, with the concentration and temperature invariant with radial position. This is a standard type of flame where studies of particulate materials in flames are made and as such there are many studies in such flames[26, 27]. Turbulent flames are characterised by much more complex time variant structures[28] thus highlighting the need for fundamental studies to be made in the simplest flames possible[29]. This is in order that the simple mechanisms by which flames progress can be identified and understood, with new information on more complex flames and set ups added stepwise over time in order a full understanding is maintained.

2.1.3 Importance of nascent soot

As has been discussed, one of the most important, yet least understood, steps in the

process is the formation of nascent soot[2, 24] (that is what happens in the growth phase between gas molecules and particulate material). As highlighted by Sirignano *et al.*[3] in their 2013 paper, much of the work on kinetic models for soot formation in recent years has focussed on the stage from gas phase to particulate phase molecules[2, 30-32].

Experimentally, upon the change from small gaseous PAHs to larger particulate PAHs it was noted by Vander Wal and co-workers[33], using a diffusion flame as described by Santoro *et al.*[34], that there is a so called "dark zone" in incandescence or fluorescence measurements. This is where neither method shows a good signal, suggesting that the particles are not in a state where it is likely they will fluoresce and are not of a significant mass that they will incandescence. It is though, as discussed by Dobbins *et al.*[20], the case that the particles take on an almost liquid like state. This means that the particles cannot be detected in the same way as either smaller or larger particles which may be present elsewhere in the flame.

This was first discussed by D'Alessio *et al.* in 1992[35] when the presence of so called "*transparent particles*" were identified in premixed ethylene flames. These were noted as having an average size of 2 nm, not absorbing in the visible, and fluorescing in the ultraviolet range. It was noted that the concentration profile of these particles decreases through soot inception, leading to their identification as being soot precursors. This is further discussed by Köylü *et al.* in 1997[36] where "*translucent particles*" are observed. These particles were found to not absorb light in the same way as larger particles but were still large enough to be quantifiable when captured and examined by electron microscope. This suggests that although particulate material is present it is behaving in a very different way to the larger particles. It was presented that the optimum way to evaluate these particles was through use of thermophoretic sampling particle diagnostics[36].

Since it has been highlighted as an important step in the reaction and many modelling studies are focused on this region, there is an obvious need to carry out experimental measurements in this region. It may not always be possible due to the nature of combustion to use a thermophoretic sampling technique or examining through electron

microscopy, and these methods may not yield information which is useful when developing mechanisms of soot formation. An ideal way of carrying out such measurements would be through use of in-situ techniques, allowing the molecules to be examined in place and without the risk of further reaction upon removal from the flame.

2.2 EXPERIMENTAL STUDY OF SOOT FORMATION

Many papers have been published on technique development and the emerging picture of the pathway from small molecules to soot, including several reviews[10, 11, 24, 37, 38]. These highlight the large body of work from which new work can be derived and also highlights the difficulties which exist in studying soot formation.

As has been discussed the formation of soot is a complex problem and must be broken down into smaller more directed studies[29]. For example it is not possible to identify all of the species present and how these change with the flame propagation using one technique or even several techniques in the one experiment. For this reason many different techniques have been developed.

These techniques can be separated into two categories:

Invasive techniques

These involve extracting a sample from the flame and analysing it outwith the flame. This is generally achieved through probing the flame and transporting the sample to where it is to be analysed.

Non-invasive techniques

Non-invasive techniques involve exciting molecules within the flame so that they emit or scatter light.

Each technique has distinct advantages and disadvantages, leading to a variation in what information will be obtained. Beyond the techniques themselves there can also be a bottleneck with the available knowledge, such as necessary spectroscopic data, rendering some measurements either impossible or requiring that more assumptions be made than would be ideal.

2.2.1 Invasive techniques

There is a long history of and a wide range of extractive sampling techniques being used to study flames. Many of these techniques are well established in other fields and as such there is not a great deal of modifications which need to be made to make them suitable for use with gaseous samples which have been extracted from flames. The use of such techniques allows for simple particle sizing, soot volume fraction and the ability to identify several species in the same sample. There are, however, as with *in-situ* measurements, some disadvantages.

McEnally's review paper[10] puts forward that the main advantage of probe sampling over optical diagnostics is the ability to "selectively and sensitively" make measurements where the hydrocarbons present are unsuitable for spectroscopic methods. The argument is also made that in fuel rich flames it can be impossible to make non-invasive measurements, so although there are significant drawbacks to having to withdraw samples from the flame to make measurements it is better to have some sort of information from the flame rather than no information at all.

One commonly employed techniques is gravimetric sampling, which involves taking a sample from the flame, achieved by forcing gases through a porous disk in a chimney[39], and allowing any particulate material attaches itself to the disk. The disk can them be removed for weighing. The flow rate of the gas passing through the disk is a known quantity and thus by weighing the mass of particulates on the disc the mass fraction can be calculated. This is a common method to use for the calibration of laser induced incandescence[40] as it has many advantages as outlined by Zhou *at al*[39, 41]. It is insensitive

to the soot refractive index and does not require assumptions with respect to any light scattering which will occur and interfere with the measurement, as can be the case with extinction measurements. However, this technique is inherently ex-situ and as such it can be time consuming, involving the need for a sampling atmosphere which is both thermally stable, free from interferences and with a stable humidity. This, of course, is not always easy to achieve.

A second method which is often seen in the literature is transmission electron microscopy (TEM)[21, 42-45]. The method of sampling which must be employed for this type of analysis involves placing a fine mesh in the flame for a short period of time, allowing soot to move towards it by thermophoresis and become attached to it. The mesh may then be removed and the soot analysed via TEM. This is a highly useful diagnostic technique as it is able to yield morphological information as well as information about the particle sizes[46] which are present.

There are also several examples in the literature of examining soot from flames is scanning mobility particle sizing (SMPS)[47-50]. SMPS was first described by Wang and Flagan in 1990[51] and is a variation of differential mobility analysis. Zhou *et al*.[47] state that SMPS has benefits over TEM as it is avoids the potential of physisorbtion of organics from the soot surface in the vacuum chamber. However, due to particle coagulation and potential losses in the sampling line there can be significant issues with implementing this technique.

It is possible to effectively investigate PAHs which are present in a sample through use of photoionisation[11]. This involves the extraction of a sample to an ionisation chamber where the PAHs are photoionised (that is hitting the sample with photons so that electrons are ejected) before being analysed by time of flight mass spectrometry. Different methods of photoionisation are used, each with different advantages. Desgroux[11] puts forward that the most commonly used method for quantitative measurements of PAHs is to combine resonance enhanced multiphoton ionisation with molecular beam mass spectrometry, though to date this has been primarily used in non-

sooting flames. An important development by Siegmann and co-workers[7] was the use of photoionisation for the examination of nascent particles.

A further method of studying PAHs recently presented by the Lille group[52, 53] involves carrying out laser induced fluorescence (LIF) in an expanded low temperature jet of gas sampled from the flame. In this technique the sampled gas is transported to a low pressure chamber where it is cooled along the free jet expansion. A laser is then passed though the jet allowing LIF (which will be fully discussed in section 1.5) to be carried out. This technique was developed in order that measurements could be carried out where the temperature is limited to a "few dozen" Kelvin, meaning that only the first energy level will be significantly populated. This results in simplifying the spectra and thus allowing for much simpler interpretation of the obtained data, leading to species specific PAH concentration measurements for a few of the smaller species including naphthalene[52].

Techniques which involve extractively sampling from the flame, have many difficulties associated with them. It is obvious initially that this is not the most ideal method of making measurements in the flame as the sample may not be representative of the desired region in the flame. This is due to the lag between removing the sample and analysing it via, for example, gas chromatography or mass spectroscopy. Therefore there has to be careful consideration made about how the sample should be transported as if the sample is not treated correctly it will continue reacting, leaving the sample unrepresentative of the flame. This is commonly achieved using the same principle as for many other examples of extractive sampling – that is by using a low pressure heated line to minimise condensation and minimise further reaction[53].

In the same vein it must be ensured that there is no reactive gas or reactive species within the sample line or sampling chamber, though this can be easily achieved by flushing with and using an unreactive gas as the transport medium. Furthermore the probe will perturb the flame introducing the risk of the sample being unrepresentative of the undisturbed flame[11, 37]. This is because by inserting what is essentially a foreign body in the flame there will be a new surface in the flame which can promote or inhibit

soot formation and other reactions in a way that is difficult to interpret; it also changes the flame temperature[54]. Measurements which involve inserting a probe in the flame including the use of thermocouples for temperature measurements[55] are also characterised by poor spatial and temporal resolution.

More recently there have been developments on sampling systems[56] with the introduction of dilute sampling probes, allowing for better spatial resolution and faster particle size measurements. This, along with other newer techniques are briefly discussed by Echavarria *et al.*[57] in their paper on the evolution of soot size distribution in premixed flames.

The effect which the probe itself can have on the flame structure is thoroughly examined in the 2000 paper by Hartlieb *et al.*[58] and it can be assumed that the shortcomings discussed are common to all hydrocarbon flames. These findings suggest that great care must be taken when interpreting studies which have been carried out extractively. There are relatively few papers devoted to the study of the impact which the probe can have on flames compared to the number of papers which utilise extractive sampling.

Therefore, although there is a clear advantage to the use of extractive sampling in some situations due to its species selectivity, it is advantageous where possible to make other measurements in situ. Thus since the late 1970s there has been a progression towards using optical techniques, which are capable of making highly accurate *non-invasive* measurements.

2.2.2 Non-invasive techniques

Non-invasive techniques are employed in many fields and have developed since the advent of the laser in 1960 and the subsequent studies of various spectroscopic methods and light scattering techniques. In 1984 Dasch[59] stated that "*advances in soot formation and destruction kinetics have been hindered by a lack of in-situ techniques*" and it is fair to say that since the early 1990s there have been great strides in the application of non-invasive techniques.

One of the most commonly employed methods which has been used extensively since the 1970s to study particulate material during combustion is light scattering measurements[34, 60-62]. Having first been published by Senftleben and Benedict in 1919[63], in an experiment where a collimated beam of light heating soot particles was able to give particle size information, it is one of the earliest described methods of monitoring soot. These are fully discussed in Charalampopoulos's 1992 paper[64] where both the advantages and disadvantages are noted. It is highlighted that although using classical light scattering techniques it is possible to obtain the particle size of the soot particles it is important that the correct refractive index is accurately known as even small discrepancies can cause large errors in the particle size measurements. This can be aided through use of a continuous wave laser where the particle size can be predicted with a greater degree of accuracy. The main issue with all light scattering techniques is that it must be assumed that the particles are spherical, which is not the reality of the situation. Often though, the trade-off which needs to be made, with respect to the necessary assumptions, is worth it in order to obtain in situ real time analysis. A second benefit of light scattering measurements is that they may be made simultaneously with other laser diagnostic techniques[65].

It is also possible to make extinction measurements of light passing through a flame in order to obtain information on the soot volume present[66-69]. This is often used as a method of calibrating LII signals. Although, if used to calculate soot volume fraction caution must be taken if light lower than 700 nm is to be uses as large PAHs and nanoparticles can cause attenuation of the light, which will lead to an overestimation of the volume of soot present in the measurement volume[62, 70].

There are though, as with any techniques, drawbacks associated with the use of optical techniques. A major issue, as highlighted by Bladh[71], is the need to have optical access to the combustor which can lead to the need for reconstruction in order to achieve any measurements. He also highlights that there can be the requirement for complex set-ups if many species are to be studied simultaneously.

The two most widely used laser diagnostic techniques are laser induced incandescence and laser induced fluorescence, and these are discussed extensively in review papers by Daily[72] and Kohse-Hoinghaus *et al.*[29, 73], and also by Leipertz *et al.* in their chapter in Applied Combustion Diagnostics[74]. These techniques were utilised in this work and as such are discussed fully in sections 2.4 and 2.5. These techniques offer the potential of good temporal and spatial resolution while maintaining selectivity and sensitivity and offer the ability of obtaining information on many different parameters within the flame[73].

2.3 COMPUTATIONAL MODELLING

The role of computational work in kinetic studies to develop potential mechanisms has been highlighted above and such is its importance it has been discussed extensively in the community. Through using computational methods it is possible to investigate well defined systems[9], which can be difficult to achieve experimentally. While it remains impossible, for a variety of reasons such as lack of supporting spectroscopic data or sampling technique, to obtain information about the molecules which are present in the flame it is important to have good robust models, not only for flame chemistry but for heat and mass transfer for example, which match flame conditions as closely as possible.

Through use of computational modelling it is possible to test detailed reaction mechanisms and with increasing computing power this is becoming easier and faster[9]. This is an extremely important development, as in combustion mechanisms can contain around a hundred species and several hundred reaction pathways[75].

It is therefore widely agreed that the best way to move forward is to ensure that the experimental work which is carried out is amenable to modelling and can be used to both develop and corroborate suggested mechanisms[9, 76]. Models must consider many

things simultaneously and while there have been many studies on the routes to PAH molecule formation, PAH growth to soot particle inception remains poorly understood it is important to focus work and develop better methods of experimentally investigating what is occurring in these regions in order to support current kinetic modeling[3, 12, 23, 77].

2.4 LASER INDUCED INCANDESCENCE

Over the last 30 years there have been many reported uses of laser induced incandescence (LII) as a diagnostic technique to study the formation of soot *in-situ*. It is a technique well suited to the calculation of soot volume fraction, especially in non-steady flames, as well as offering the possibility for time resolved and two dimensional measurements[11]. It can also be used to characterise particle size of material in the flame[78]. The possibility of using laser diagnostics to examine particulate material was first discussed by Weeks and Duley in 1974[79]. They had noted that when laser light was passed through a dust filled environment there was an emission of visible light from the particles which had been heated by the incident beam. It was found that this emitted light could contain information on both the size and also the composition of the particles, and as such if harnessed could be of great importance. They presented an experiment in which they excite particles of well-defined sizes in a chamber and monitor the emitted light intensity differs. This illustrated that smaller particles had a shorter signal decay time than that of larger particles.

This was continued in the 1977 paper by Eckbreth when incandescence was recognised as an important source of interference when carrying out Raman diagnostics[80]. This paper built on the fact that the particle size could be identified by monitoring the incandescent decay and discussed how the particle temperature could be calculated from the incandescence. This was tied together, along with work by Greenhalgh[81] and

Dasch[59], in 1984, by Melton[82] who presented a method for utilising LII in examining soot formation.

The 1984 Melton paper[82] presented equations showing that, due to the cooling mechanisms of laser heated soot, the LII signal would be proportional to the soot volume fraction in the measurement volume. The importance of this correlation cannot be underestimated and this was the beginning of a new non-intrusive way of examining soot particles *in-situ* and throughout the last 30 years this original principle has been built on and many different techniques developed around it[38, 65, 83-96].

Throughout the time since the realisation of LII as a potential technique for monitoring particulate material in flames there have been many developments in the way of new methodologies and computational models[87]. Though much work has been done many questions still remain unanswered along with many opportunities for improved signal collection[78].

There is also a great deal of energy being put into the development of modelling the LII decay of the LII signal. The importance of effective modelling to predict signals which will be obtained from LII is highlighted in the 2006 paper by Schulz *et al.*[78] which resulted from the 2005 LII workshop in Duisburg. This states "*the evaluation of measured LII signals strongly depends on the underlying models*" which highlights that the argument for the development of new, and more effective, models is circular – with the need for good data to effectively test models to ensure models which are used for data analysis are as accurate as possible. As a result of this meeting target flames and conditions were identified as "target flames" to allow comparison of signals obtained between groups and add to the body of work which can be drawn upon when developing models. There is thus an importance to have a well defined set of conditions under which experimental work is being carried out, ensuring that the work can be compared to and used in parallel with the work of other groups.

As is highlighted the 2007 review paper by Michelsen et al.[97] the choice of seemingly unimportant parameters, such as the refractive index function or the thermal

accomodation coefficient can have a great effect on the predictions which models give. By better standardisation of models more useful data would be able to be obtained. There is also a summary of the parameters which would aid better experimental understanding, which again highlights the need for better understanding of what is needed for modelling when carrying out experimental work in order maximum benefit can be achieved.

2.4.1 Theory of Laser Induced Incandescence

LII relies on the general principle that particulate material within a flame can be heated using a laser to such a temperature that there is significant emission in the visible spectral range[98]. When a particle is heated in this way it cools via three key mechanisms: radiation, sublimation and conduction, Figure 2-3[99].

The information obtained by monitoring the emitted radiation can be used to calculate the particle size and soot volume fraction. It is important to note that this is due to not all of the energy being lost as the particle cools. Steps must therefore be taken to ensure that as much energy as possible is being lost via this route. It is important to ensure that the particle reaches the sublimation temperature in order that the soot volume fraction can be linearly related to the signal level[78, 100, 101]. The energy loss via sublimation can be minimised by adjusting the laser fluence. Furthermore, at temperatures of greater than about 3000 K the cooling process is dominated by radiative cooling, conversely at lower temperatures collisional cooling will dominate[102].

The emitted incandescence follows Plancks law, as shown in Equation 2-1 which relates the temperature of the particle to the emitted light intensity.

$$B_\lambda(T) = \frac{2hv^2}{\lambda^5} \frac{1}{\frac{hc}{e^{\lambda k_B T}} - 1}$$

Equation 2-1

Where: B = spectral radiance

h = Planck constant

c = speed of light in a vacuum

λ = wavelength

k_B = Boltzmann constant

T = temperature

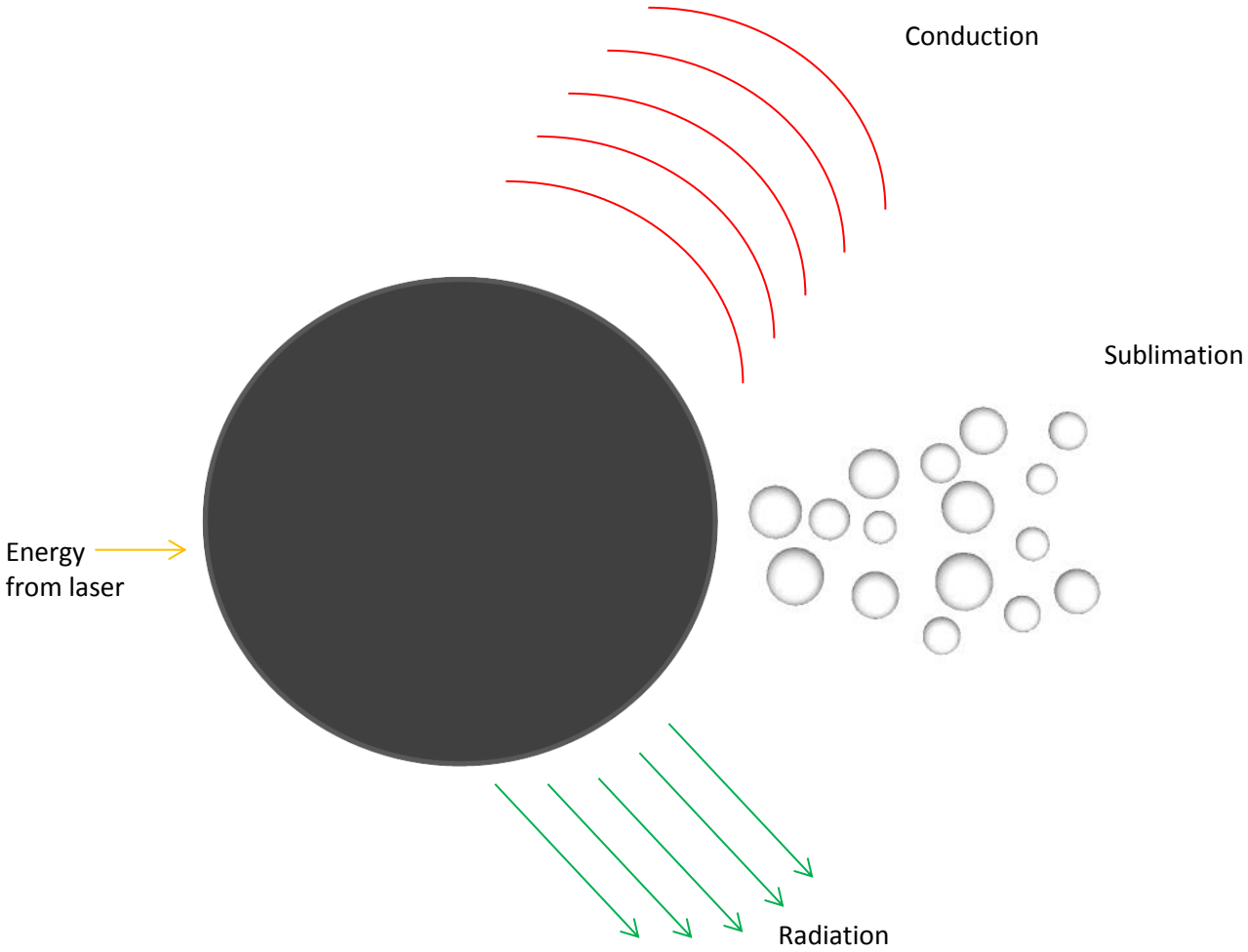

Figure 2-3 : Processes which occur upon laser heating particle

Hence if the spectral radiance is plotted against a spectra which is characteristic of the temperature of the blackbody will be obtained. Incandescence which occurs as a result of heating the particles in a flame will follow this blackbody decay and as such for a given particle incandescence the particle temperature can be inferred.

There are three different ways in which the light is emitted during incandescence can be recorded – each with its own advantages – temporally, spatially and spectrally. By monitoring the temporal decay of the emitted radiation it is possible to obtain information about the particle size, soot volume fraction and the temperature of the particles[44, 98, 103]. This is achieved through treating the data in a variety of ways outlined below.

SOOT VOLUME FRACTION CALCULATION

The soot volume fraction is a measure of the amount of soot is found in a specific measurement volume. The soot volume fraction is calculated through use of the peak LII signal. Although the peak LII signal is proportional to the soot volume fraction it is dependent on the soot temperature[11]. To address this, the particles are heated to near the temperature of sublimation, where, although there will be subsequent loss of mass due to sublimation, the peak LII signal will be quasi-linear to the soot volume fraction[78]. The measurement can then be calibrated through use of light extinction measurements (which will be used in this work) or cavity ring down spectroscopy. Alternatively colour pyrometry can be used to resolve the heated particle temperature by recording the LII emission at two (or more) wavelengths and using absolute intensity calibrated detectors.

Mewes *et al.* discussed how soot volume fraction can be described by their diameter, d_p, the average number of particles per aggregate, n_p and the number density of the aggregates which are in the measurement volume, N[86]. These combine to give an equation, Equation 2-2, which gives the soot volume fraction, *fv*, in the measurement volume.

$$fv = \frac{\pi}{6} N n_p d_p^3$$

Equation 2-2

Due to the near linear relationship which exists between the peak LII signal and the soot volume fraction, LII is useful for making such measurements, Equation 2-2

$$S_{LII} \propto N d^{3+0.154/\lambda_{det}}$$

Equation 2-2

Where: S_{LII} = LII signal

d = particle diameter

λ_{det} = detection wavelength

This relationship only holds true if the laser fluence is high enough[82], that is above the point of particle sublimation.

An extensive theoretical investigation of the dependence of soot volume fraction on the signal is presented by Bladh *et al.*[99], and more information can be found there.

In order for this information to be quantitative there must be calibration, generally via light extinction measurements, Equation 2-3

$$f_v \approx \frac{\lambda}{6\pi E(m)} K_{ext} = \frac{\lambda}{6\pi L E(m)} ln\left(\frac{I_0}{I_T}\right)$$

Equation 2-3

Where : λ = wavelength

$E(m)$ = absorption function

L = absorption path length

I_0 = incident intensity

K_{ext} = extinction coefficient

I_T = transmitted intensity

In situations where the extinction coefficient is low it is advantageous to use cavity ring down in order to carry out the extinction measurements[101, 104, 105]. However, there has been major strides more recently to different calibration methods, so all the work is carried out simultaneously within the flame in question, rather than having a separate calibration method[105-108].

In order to employ the above, it must be assumed that the particles are both monodisperse and non-aggregated[109], which of course will not be the case with large soot particles.

PARTICLE SIZE CALCULATION

In order to obtain particle size information, the cooling of the particle must be modelled and there are reviews of this produced by Michelsen *et al.*[97, 98, 110]. This is achieved through use of mass and energy balance equations. Due to uncertainties about the conduction heat transfer and particle aggregation there remains much work to be done, as discussed by Liu *et al.*[111]. When obtaining the primary particle size it must also be remembered that LII is inherently biased to larger particles as smaller particles will cool faster[92, 112]. The study of time resolved signals in order to obtain particle size measurements is often referred to as time-resolved laser induced incandescence (TIRE-LII) and there are several papers published on the subject[92, 96, 113-117].

PARTICLE TEMPERATURE CALCULATION

More recently the benefits of measuring LII signals at two different wavelengths of light has been demonstrated[90, 104, 118-121]. This two-colour LII (2C-LII) improves the accuracy of measurements as the maximum particle temperature can be estimated, allowing soot volume fraction to be calculated without having to rely on the accuracy of the ratio of the soot refractive index function - E(m)[122]. This is achieved by recording the emitted

signal simultaneously at two different wavelengths. It has also been shown by Maffi *et al.*[123] that it is possible to obtain information about the thermal accommodation coefficient and the soot absorption function through utilising the results in a numerical simulation.

LII has also been used in work to obtain more accurate E(m) measurements, which in turn increases the success of soot volume measurements. This can be achieved through use of 2C-LII if there is an accurate model for the absorption of the laser (as the soot particle temperature at the end of the laser pulse, that is the peak temperature, is almost independent of primary soot particle size), by obtaining the difference in temperature between heated and unheated particles[124]. Therssen *et al.*[119] achieve this through use of two excitation wavelengths, giving the opportunity to obtain a ratio, giving E(m), through observation of the respective fluence curves.

One important area of study is devoted to how the incandescence signal can be effected in highly sooting flames as a result of "signal trapping", that is the signal being reabsorbed by particles between the measurement volume and the edge of the flame[88, 108, 113, 125, 126]. This is an important consideration, especially if the results are going to be used comparatively or for models and thus the data must be well understood. This effect was considered not to have a large impact in this work.

It is key to remember when making incandescent measurements, that there are opportunities for interferences to arise[127]. The main source of interference occurs due to the presence of PAHs which exist within the flame. These can be excited by the laser, especially when shorter wavelengths of excitation light are employed, which can lead to laser induced fluorescence (LIF). Fluorescence of PAHs can result in the signal being red shifted with respect to the excitation wavelength[74]. Incident light may be scattered by soot or by the burner surface and there could be interference from other light sources within the lab. Steps must be taken to minimise any stray light, but this is not possible if the interference is coming from the measurement volume. Therefore, there must be a

detection technique employed which ensures that the region where the incandescence is being detected is either free from any interferences or that there is a method in place to eliminate the contribution to the signal by the interferences. The current methods for this are discussed in section 1.5.

It is also important to take into account that LII is an intrusive process and as such the physical properties may be affected in ways which cannot be accounted for[128].

2.5 LASER INDUCED FLUORESCENCE

Laser induced fluorescence has been cited by Cignoli *et al.*[129] as being one of the most useful techniques which can be applied to combustion diagnostics as an imaging technique. Unlike LII, which as discussed above is concerned with solid particles, the main strength of the LIF are its ability to identify small molecules[130-133], especially radical species[73, 134], within the flame and to determine the temperature of flames[135] without the necessity of inserting a probe into the flame[136, 137].

Fluorescence measurements are useful for monitoring the growth and development from small molecules to larger PAHs. This is as a result of the high absorption coefficient and quantum yield which are attributes of PAHs[138]. As the size of the aromatic structure increases the wavelength of the emitted light also increases[104]. This is as a result of the spectra being as a result of $\pi - \pi^*$ transitions. As the PAHs increase in size the energy gap which exist within the molecule decrease resulting in broadening of the absorption bands and a red shift of the emitted light[139]. Therefore, this may be used to identify regions in the flame where PAH formation is at a more advanced stage than others – it may be expected that larger PAHs will be found higher in the flame and smaller PAHs will be found lower in the flame.

When making incandescence measurements fluorescence is often described as being an interferent in the region of the flame where soot growth is at an early stage. In order to avoid this an excitation wavelength which does not give any fluorescence (at typical detection wavelengths), such as 1064 nm, is employed or the LII signal is recorded long enough after onset of signal that it can be assumed that the fluorescence, which has a much shorter lifetime than incandescence, has decayed.

2.5.1 Theory of Laser Induced Fluorescence

Fluorescence is, in this type of experiment, concurrent to LII and occurs due to the absorption and subsequent release of energy Figure 2-4

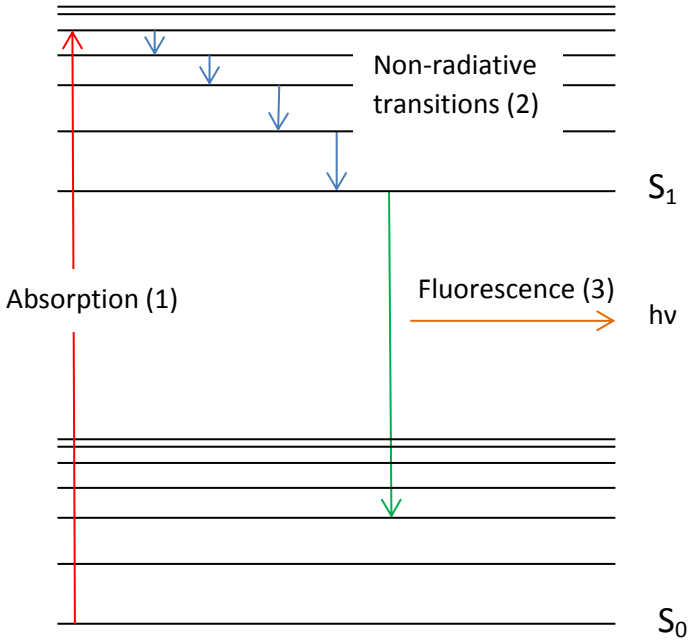

Figure 2-4 : Energy level diagram showing fluorescence emission : (1) excitation, (2) internal relaxation, (3) fluorescent emission, where h = Planck's constant ν = frequency and S_X = electronic energy level

When a molecule absorbs energy, in this case from the laser pulse it is excited to a higher energy level (see [1]). The molecule will then normally undergo internal relaxation, via vibrational and rotational energy transfer, which results in the relaxation to a lower energy band, through still within the upper energy electronic level (see [2]). This means that when the molecule relaxes back to the ground state (see [3]), with the energy loss via fluorescence emission, due to the energy being released being less than the energy being absorbed then the wavelength of the emitted light is longer than the wavelength of the excitation.

There are complications which are also evident when making fluorescent measurements. There can be other contributions to the relaxation of the molecule via processes such as quenching and this must be taken into account. This makes LIF more suited to the identification of small molecules such as OH, NO and CH, as they are well known and as such data concerning their spectroscopy, quenching and transfer rates already exist. It is for this reason that studying species for which the data is unknown can raise many problems[11, 140].

As the particles which are being examined increase in size incandescence will be by far the dominant process over fluorescence[102]. This is because as the molecular size increases the number of electronic states will also evidently increase. This causes the gap between the HOMO and LUMO levels of the molecule to decrease which will encourage non-radiative relaxation processes and hence incandescence will become the dominant cooling mechanism. As molecules grow during soot formation there is a boundary, at which particles obtain bulk properties causing a net shift from fluorescent processes to incandescence[102]. As a result of this, and taking into account the shape of the flame and the growth of soot within the flame, there should be more fluorescence in the flame at low heights.

Fluorescence occurs predominantly at wavelengths longer than the wavelength of excitation, with the very little fluorescence below this due to anti-Stokes fluorescence. Anti-Stokes fluorescence occurs when some of the thermal energy which is present is converted into light and will occur at high temperatures. Therefore there can be a

strategised approach with what wavelength of excitation light should be used in order to excite the PAHs which are looked to be identified as different excitation wavelengths can be chosen to target certain PAHs[33, 141]. Furthermore when exciting with low wavelengths in the UV range it is possible to carry out simultaneous measurements to observe both PAHs, OH and other small molecules[142-144].

It is highlighted in Desgroux 2013 review paper[11] that PAH concentration is not proportional to the LIF signal. This is because fluorescence relies on the structure of the PAHs and on the environment in which the measurements were being made due to the effects of collisional quenching[144]. The LIF signal is also the sum of contributions of a number of different PAH molecules so it cannot be used to quantify concentrations of individual species. This is one of the main limitations of LIF measurements, however, since it offers the ability to obtain information in-situ which is spatially and temporally resolved it still offers a huge advantage over other techniques[11]. In theory if it were possible to keep these constant it would be possible to relate the intensity of the signal to the concentration of the PAH.

2.6 Current Separation of Contributions from Laser Induced Incandescence and Laser Induced Fluorescence

Since, ordinarily, fluorescence is viewed as an interference in incandescence measurements then steps have been taken when developing the techniques to avoid fluorescence. The most obvious way which this is achieved is to use an excitation wavelength which will not lead to the occurrence of any fluorescence. Therefore the fundamental Nd:YAG wavelength, 1064 nm, is often employed as this ensures any emitted signal will be solely due to incandescence. However, it is not always

advantageous to use this wavelength as it removes the possibility to make simultaneous light scattering measurements – which can be achieved if a visible light is used. Furthermore the use of visible light also makes it easier to align the system – which can be highly advantageous when dealing with complex or difficult environments where alignment can be tricky. Finally sources for 532 nm of light easily available and since there have been methods developed to get around the fluorescent interference it is often employed even though it is not optimum.

There are two well developed methods of performing LII measurements; each has its benefits with one of the methods addressing the issues which can be seen when measuring with a shorter wavelength of excitation.

The first method – prompt LII - involves taking the signal at the peak of the LII signal or at the peak of the laser pulse[145, 146]. This method gives the best correlation between the signal and soot volume fraction and also for any effects due to particle size to be ignored[11, 146, 147]. Long wavelengths of light, such as 1064 nm, are preferred when using this method as shorter excitation wavelengths will result in a signal which has a fluorescence contribution. This would mean that the signal intensity would not be directly proportional to the soot concentration. Care must also be taken that there is no contribution to the signal from stray light, for example from the excitation laser beam.

To enable measurements with shorter wavelengths of light a method which will eliminate the fluorescent contribution without having an effect on the incandescent signal delayed detection is employed. In this method, as the name suggests, there is a delay from the laser pulse to the point where the measurement is taken. This allows the fluorescence to have decayed before the measurement is taken, so it can be assumed that the signal is due solely to incandescence. Although this method is successful the length of time which is left before recording the LII signal is seen largely as being arbitrary. It can lead to the loss of information on the peak incandescence and can also mean that the decay which is being fitted can be from a point a relatively long time after the LIF has fully decayed and the signal is due solely to LII. In order to accurately determine the length of time which should be left can be difficult and as the fluorescent lifetime is

different for each flame condition the norm is to slightly over estimate the decay time of LIF.

There are several examples in the literature where 532 nm light is used to heat the particles in the flame[84, 85, 117, 119, 124, 146, 148-151]. There are many reasons why someone may choose to do this but primarily it is because this excitation wavelength is readily available or because there is the possibility of making simultaneous scattering measurements using the same wavelength. In spite of this there has been no study published where the differences which could result in the obtained information depending on the detection technique, that is prompt or delayed, is examined. This work aims to investigate if there is a difference seen in the shape of the height above burner profiles when using prompt and delayed LII and how the excitation wavelength impacts upon this. It is the case that although many groups take account that they should not measure at the peak, a less methodical approach is taken when deciding how long after the peak to make the measurement or what impact this will have upon the signal.

2.7 WORK PRESENTED

As has been highlighted in the previous section much of the work which is described in the literature aims to eliminate any fluorescence which interferes with the incandescence signal. Since the valuable information which can be obtained from fluorescence has been highlighted it would be advantageous if, instead of eliminating this information that it could be utilised. A method of achieving this this was initially suggested by Vander Wal in 1997[74], expanded on by Schoemaeker Moreau *et al.*[105] in 2004 and further progressed in diesel flames by Lemaire *et al.* in 2009[106]. It has been shown here that since when exciting with 1064 nm light there will only be incandescence it is possible to subtract any light emitted with this excitation from a signal where a lower wavelength of

excitation has been used, in order that the remaining signal can be solely attributed to fluorescence. Schoemaeker Moreau and Lemaires work uses images which are obtained via an ICCD camera and the subtraction shows images of the regions in the flame where the PAHs could be expected. Although this yields valuable information on the region in the flame where the PAHs are and where the main region of soot growth is there is much more information which can be obtained through gathering data in a slightly different way. This is also important as there are great difficulties with examining PAHs in flames which are sooting[11] and the ability to achieve this *in-situ* would be a great development.

The work presented here differs in that instead of imaging the entire flame a specific point in the flame is used. Due to the flame being laminar, of a reasonable diameter and stable, the flame can be considered to be pseudo one dimensional. Therefore, the measurement can be repeated at a range of heights above burner in a number of flame conditions in order that a fuller picture of the burner can be gathered in a stepwise way. The signal was recorded both over time and over a range of wavelengths in order that for each point, at each detection wavelength, with each excitation wavelength there is the possibility to obtain information on the soot volume and particle size. As the emitted signal is being recorded over a range of wavelengths by subtracting the incandescence from this signal a spectra consisting purely of fluorescent light will be obtained.

It is known that PAHs are sensitive to the excitation wavelength which is being used. Without being species selective it is accepted that shorter wavelengths will excite smaller PAHs than longer wavelengths. Since the LII would show the soot particles and the fluorescence the PAHs it would be advantageous if this could be further refined. The incandescence measurements can differentiate between the size of soot particles as the decay time will change as the particles increase. The fluorescence however will not show this. In order, therefore, to illustrate that larger and smaller PAHs can be identified (in a qualitative way) two different excitation wavelengths were used – 283 nm and 532 nm. It was hypothesised that upon excitation with 283 nm PAHs which were smaller, and hence lower in the flame, would be excited and that when exciting with 532 nm larger PAHs, hence those higher in the flame, will be excited.

In order to observe if this is happening measurements were taken over a range of heights in the burner. When it was shown that this was indeed the case with one detection wavelength then the emitted light was observed over a range of detection wavelengths. This idea can be further developed in order that not only can PAH spectra be obtained that classes of spectra can be identified from them. This will be discussed further in the further work section.

2.8 EQUIPMENT EMPLOYED

2.8.1 Burner Employed

In this work a water cooled McKenna type burner was used. This is considered to be standard for this type of work as it allows for a stable laminar flame to be produced over a range of stoichiometies. The flame is also stabilised by the addition of a stainless steel metal plate 21 mm above the burner surface to further aid stabilisation of the flame. Due to the stability of the flame which is produced on such a burner the flame is highly repeatable which makes it suitable obtaining large data sets which can be used for developing or verifying models. Also due to the stability across the burner the flame which is produced can be considered to be one dimensional, which again makes it amenable for modelling.

A premixture of air and ethylene is used for the production of the flame, with a range of stoichiometries between 1.7 and 2.1 used. In all cases these are sooting flames, giving the opportunity to obtain both incandescence and fluorescence from the flame.

2.8.2 Lasers

In order that is be possible to make measurements using three different excitation wavelengths both and Nd:YAG (neodymium-doped yttrium aluminium garnet) (Surelite

Continuum, SLII-10) and dye laser (Cobra, Sirah Lasertechnik) were employed. This was achieved by using both the fundamental and frequency doubled wavelengths emitted from the Nd:YAG, 1064 nm and 532 nm respectively, and using the 532 nm light to excite rhodamine 590 dye in methanol in the dye laser (giving rise to 566 nm light), which was subsequently doubled to give 283 nm light.

There are several classes of laser which have been developed, each with their own advantages and disadvantages. In the work which will be presented here an Nd:YAG laser, which is an example of a solid state laser, is employed. Solid state lasers all rely upon a crystal, which can be doped with an ion that can be excited when pumped with energy from an external source, as shown in Figure 2-5.

The wavelength of the laser light which will be emitted is determined by the difference in energy between the higher energy level and the level to which the electrons relax. This means that although Nd:YAG lasers typically emit at 1064 nm there are also transitions around 1440, 1320, 1120 and 940 nm which can be used.

Many pulsed solid state lasers work in a Q-switching mode. This maximises the power which will be emitted through use of an optical switch blocking the excited electrons to relax until the maximum population inversion in a given time frame has been achieved. At this point the optical switch opens, allowing a light wave to depopulate the higher energy states, allowing all the light to escape the cavity as coherent light. In the case of the laser employed here the electons which are excited come from the neodymium ions which are hosted in the yttrium aluminium garnet crystal.

Since the light which is emitted through Q-switching has a high intensity it is suitable to being frequency doubled in order that 532 nm light can be obtained, and this is taken advantage of in this work. There is also the opportunity to obtain higher harmonics of the 1064 nm signal, allowing for the use of 266 and 355 nm light.

The Nd:YAG laser which was used has a pulse duration of 5 – 7 ns (FWHM) in the fundamental and 4 – 6 ns (FWHM) when frequency doubled, with maximum energies of 560 mJ and 280 mJ respectively.

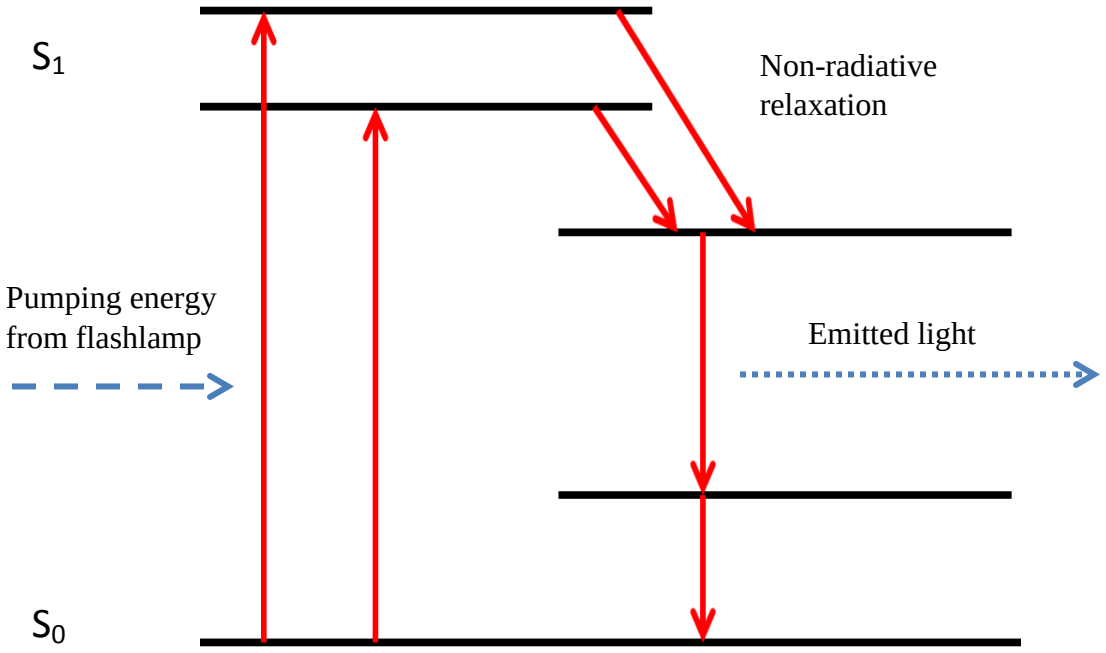

Figure 2-5 : Excitation of neodymium ions

The other laser which was employed in this work, in order that UV wavelengths could be utilised, was a Sirah pulsed dye laser. Dye lasers work through the excitation of an organic dye housed within the laser, hence giving light of this wavelength. In this case a solution of Rhodamine 590 in methanol was used, which giving a small region of wavelengths centred around 566 nm. This light passes through a grating to eliminate surrounding wavelengths leaving 566 nm light, which is then frequency doubled - resulting in light of centring around 283 nm. Through use of a carefully positioned slit the desired wavelength, in this case 283 nm, may be selected.

Inside the dye laser the dye solution is circulated through a loop of plastic tubing, in order that it can flow through the dye cell which is held within the laser casing. In order to excite the dye within the cell 532 nm light is pumped into the dye laser. The light passes through the dye solution causing the organic molecules electrons to be excite to a

higher energy level. When the molecules decay the excess energy is emitted as fluorescence, which will be at a higher wavelength than that of the exciting light. This is as a result of the electrons relaxing to the ground state, with the loss of the excess energy, energy will have been lost by the electrons relaxing to a lower vibrational energy band. This means the energy emitted will be less than that which it took to excite the electrons, resulting in a longer wavelength of light.

The specific wavelength of light which is required is obtained through moving the instrument grating. In the case here this resulted in light of 566 nm, however, for this work a wavelength in the ultraviolet spectrum was needed. This was achieved through frequency doubling, via a doubling crystal, to obtain a laser wavelength of 283 nm.

2.8.3 Monochromator

In order that spectrally resolved data could be obtained a monochromator (Oriel Cornerstone, 130) was employed so that the detection wavelength could be scanned. There are two ways in which a monochromator can work. The first employs a prism to separate the wavelengths contributing to the signal; the second, which will be used here, uses a diffraction grating.

As the name suggests the different wavelengths of light from a broadband source are separated via a diffraction grating. The diffraction grating consists of a sheet with an optically flat surface which has a series of gratings through which it can separate the wavelengths of light. As the grating moves to different angles the diffraction pattern of the light is different, allowing for the separation of the light. This light is refocused by the second mirror and passes through the exit slit, Figure 2-6.

As can be seen from the diagram the movement of the diffraction grating has to be extremely sensitive in order that the wavelengths of light can be separated. Following from this it can also be seen that both the inlet and outlet slits must be of a size which is amenable to the measurements which have to be made. By increasing the slit width the

resolution of the wavelength which will pass through the monochromator will increase also.

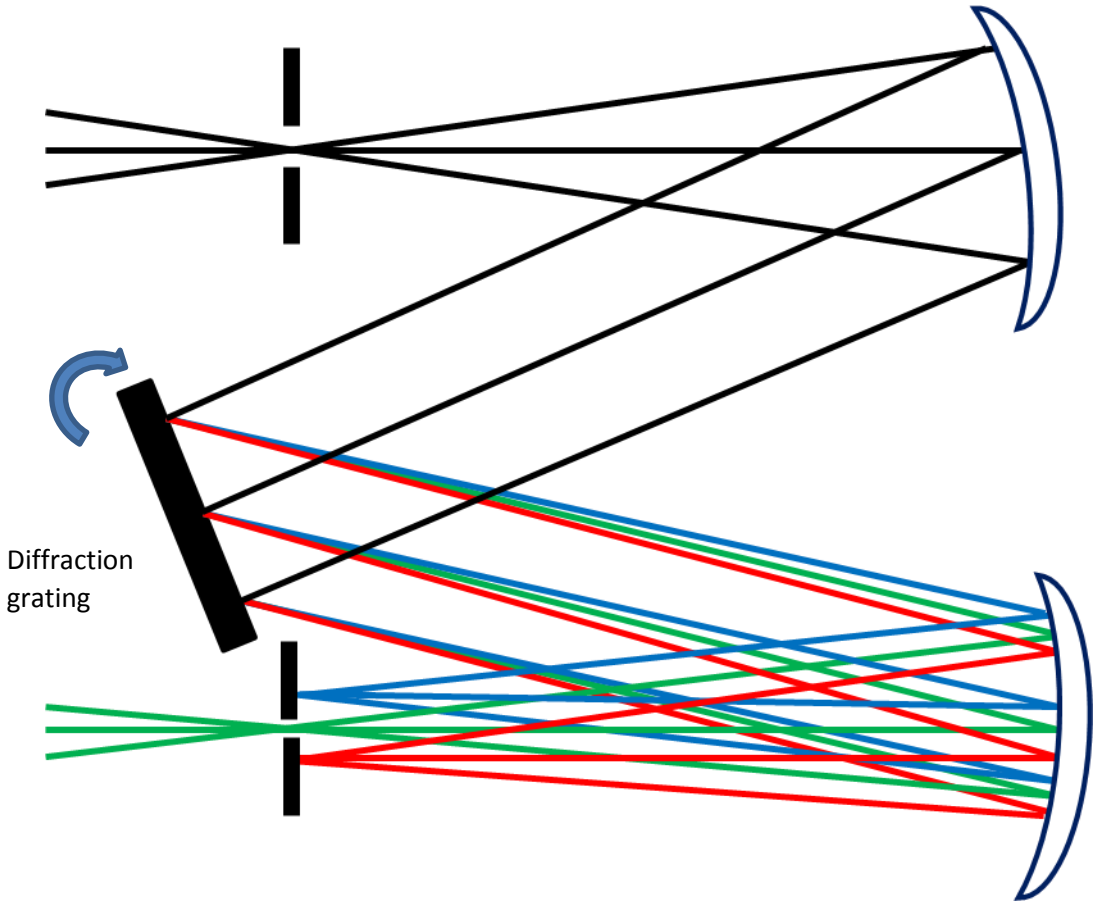

Figure 2-6 : Monochromator operation

2.8.4 Photomultiplier tube

Throughout all of this work a photomultiplier tube (PMT) (Hammamatsu R636-10) was employed as the detector, either behind a bandpass filter or a monochromator. A photomultiplier works by generating and amplifying electric current which is proportional to the intensity of the incident light upon it.

Initially the photons which enter the PMT will strike a negatively charged electrode, known as a photocathode, which is coated with a photosensitive material. When a photon hits the photocathode the energy which is absorbed cause the emission of electrons as a result of the photoelectric effect.

Within the PMT there is a series of dynodes (electrodes), Figure 2-7, and it is these which amplify the electric current. This is achieved by having the dynodes positioned in the sequential manner shown and having each one at a higher positive voltage than the previous one. When the photons enter the PMT they first encounter a negatively charged electrode – known as a photocathode. This absorbs the photons and due to the photoelectric effect will emit electrons. As the electrons move towards the positively charged dynode they are accelerated in the electric field and so reach the dynode with a higher energy than they left the photocathode with. When they hit the dynode this causes further low energy electrons to be released and accelerated towards the next dynode. Due to the precise geometry of the dynodes within the PMT there are always an increasing number of electrons produced after each dynode, Figure 2-7.

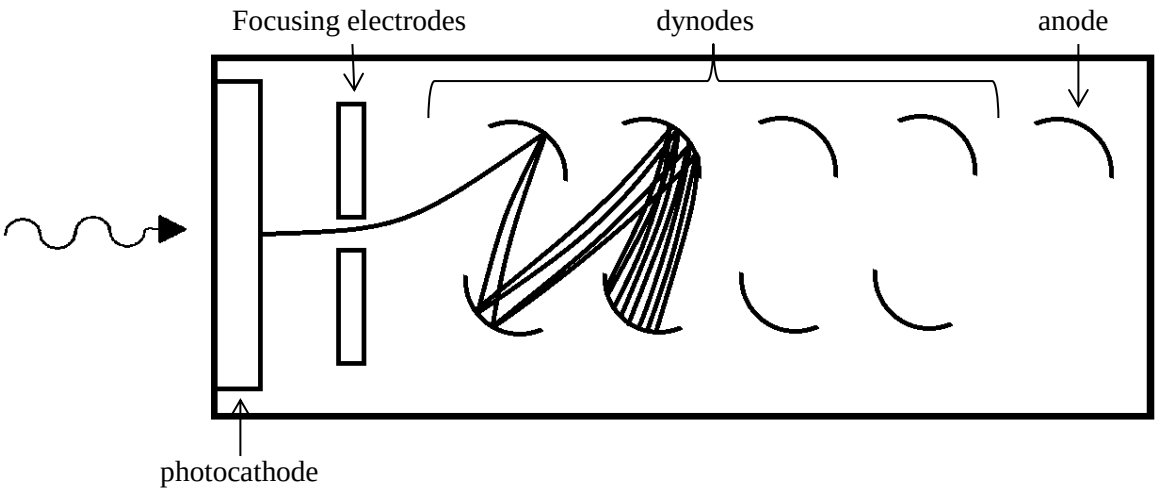

Figure 2-7 : Photomultiplier tube

Once the electrons have completed the amplification process by travelling the length of the dynode chain they are incident upon an anode, giving rise to an electric current which can be measured. In order that ever smaller numbers of incident photons be measured it is possible to change the gain which occurs by altering the input voltage

Photomultipliers are appropriate to use as a detector in this type of work because even for relatively high gain settings the noise level is low. This is advantageous since the aim is to perform sensitive measurements involving low signal levels.

2.9 REFERENCES

1. J. F. Roesler, S. Martinot, C. S. McEnally, L. D. Pfefferle, J. L. Delfau and C. Vovelle, *Combustion and Flame*, 2003, **134**, 249-260.
2. A. Raj, M. Celnik, R. Shirley, M. Sander, R. Patterson, R. West and M. Kraft, *Combustion and Flame*, 2009, **156**, 896-913.
3. M. Sirignano, J. Kent and A. D'Anna, *Energy & Fuels*, 2013, **27**, 2303-2315.
4. K. H. Homann, *Angewandte Chemie-International Edition*, 1998, **37**, 2435-2451.
5. A. Bruno, C. de Lisio and P. Minutolo, *Optics Express*, 2005, **13**, 5393-5408.
6. H. Wang, *Proceedings of the Combustion Institute*, 2011, **33**, 41-67.
7. K. Siegmann, K. Sattler and H. C. Siegmann, *Journal of Electron Spectroscopy and Related Phenomena*, 2002, **126**, 191-202.
8. J. P. Longwell, *Symposium (International) on Combustion*, 1982, **19**, 1339-1350.
9. H. Richter and J. B. Howard, *Progress in Energy and Combustion Science*, 2000, **26**, 565-608.
10. C. S. McEnally, L. D. Pfefferle, B. Atakan and K. Kohse-Hoinghaus, *Progress in Energy and Combustion Science*, 2006, **32**, 247-294.
11. P. Desgroux, X. Mercier and K. A. Thomson, *Proceedings of the Combustion Institute*, 2013, **34**, 1713-1738.
12. N. A. Slavinskaya and P. Frank, *Combustion and Flame*, 2009, **156**, 1705-1722.

13. O. I. Smith, *Progress in Energy and Combustion Science*, 1981, **7**, 275-291.
14. M. Frenklach, D. W. Clary, W. C. Gardiner Jr and S. E. Stein, *Symposium (International) on Combustion*, 1985, **20**, 887-901.
15. F. Xu, P. B. Sunderland and G. M. Faeth, *Combustion and Flame*, 1997, **108**, 471-493.
16. M. Frenklach and H. Wang, *Symposium (International) on Combustion*, 1991, **23**, 1559-1566.
17. J. P. Cain, J. Camacho, D. J. Phares, H. Wang and A. Laskin, *Proceedings of the Combustion Institute*, 2011, **33**, 533-540.
18. S. H. Chung and A. Violi, *Proceedings of the Combustion Institute*, 2011, **33**, 693-700.
19. J. D. Herdman and J. H. Miller, *Journal of Physical Chemistry A*, 2008, **112**, 6249-6256.
20. R. A. Dobbins, R. A. Fletcher and H. C. Chang, *Combustion and Flame*, 1998, **115**, 285-298.
21. W. Merchan-Merchan, S. G. Sanmiguel and S. McCollam, *Fuel*, 2012, **102**, 525-535.
22. M. Frenklach, *Twenty-Sixth Symposium (International) on Combustion*, 1996, 2285-2293.
23. F. Xu, K. C. Lin and G. M. Faeth, *Combustion and Flame*, 1998, **115**, 195-209.
24. M. Frenklach, *Physical Chemistry Chemical Physics*, 2002, **4**, 2028-2037.
25. M. Frenklach and H. Wang, *Soot Formation in Combustion: Mechanisms and Models*, Springer-Verlag, Heidleberg, 1994.
26. A. D'Anna, *Proceedings of the Combustion Institute*, 2009, **32**, 593-613.
27. F. Migliorini, S. de Iuliis, F. Cignoli and G. Zizak, *Combustion and Flame*, 2008, **153**, 384-393.
28. V. Sankaran and S. Menon, *Proceedings of the Combustion Institute*, 2000, **28**, 203-209.
29. K. Kohse-Hoinghaus, R. S. Barlow, M. Alden and E. Wolfrum, *Proceedings of the Combustion Institute*, 2005, **30**, 89-123.

30. A. D'Anna, *Energy & Fuels*, 2008, **22**, 1610-1619.
31. G. Blanquart and H. Pitsch, *Combustion and Flame*, 2009, **156**, 1614-1626.
32. A. D'Anna and J. H. Kent, *Combustion and Flame*, 2008, **152**, 573-587.
33. R. L. Vander Wal, K. A. Jensen and M. Y. Choi, *Combustion and Flame*, 1997, **109**, 399-414.
34. R. J. Santoro, H. G. Semerjian and R. A. Dobbins, *Combustion and Flame*, 1983, **51**, 203-218.
35. A. D'Alessio, A. D'Anna, A. D'Orsi, P. Minutolo, R. Barbella and A. Ciajolo, *Symposium (International) on Combustion*, 1992, **24**, 973-980.
36. Ü. Ö. Köylü, C. S. McEnally, D. E. Rosner and L. D. Pfefferle, *Combustion and Flame*, 1997, **110**, 494-507.
37. C. Lou, C. Chen, Y. P. Sun and H. C. Zhou, *Science China-Technological Sciences*, 2010, **53**, 2129-2141.
38. Z. A. Mansurov, *Combustion Explosion and Shock Waves*, 2005, **41**, 727-744.
39. R. L. Vander Wal, Z. Zhou and M. Y. Choi, *Combustion and Flame*, 1996, **105**, 462-470.
40. M. Y. Choi, G. W. Mulholland, A. Hamins and T. Kashiwagi, *Combustion and Flame*, 1995, **102**, 161-169.
41. Z. Q. Zhou, T. U. Ahmed and M. Y. Choi, *Experimental Thermal and Fluid Science*, 1998, **18**, 27-32.
42. R. L. Vander Wal, T. M. Ticich and A. B. Stephens, *Applied Physics B*, 1998, **67**, 115-123.
43. R. L. Vander Wal and K. A. Jensen, *Appl. Opt.*, 1998, **37**, 1607-1616.
44. B. Axelsson, R. Collin and P. E. Bengtsson, *Applied Optics*, 2000, **39**, 3683-3690.
45. F. Migliorini, K. A. Thomson and G. J. Smallwood, *Applied Physics B-Lasers and Optics*, 2011, **104**, 273-283.
46. J. Appel, H. Bockhorn and M. Wulkow, *Chemosphere*, 2001, **42**, 635-645.
47. B. Zhao, Z. W. Yang, M. V. Johnston, H. Wang, A. S. Wexler, M. Balthasar and M. Kraft, *Combustion and Flame*, 2003, **133**, 173-188.

48. M. Kasper, K. Siegmann and K. Sattler, *Journal of Aerosol Science*, 1997, **28**, 1569-1578.
49. W. S. Kim, S. H. Kim, D. W. Lee, S. Lee, C. S. Lim and J. H. Ryu, *Environmental Science & Technology*, 2001, **35**, 1005-1012.
50. G. Skillas, H. Burtscher, K. Siegmann and U. Baltensperger, *Journal of Colloid and Interface Science*, 1999, **217**, 269-274.
51. S. C. Wang and R. C. Flagan, *Aerosol Science and Technology*, 1990, **13**, 230-240.
52. M. Wartel, J. F. Pauwels, P. Desgroux and X. Mercier, *Applied Physics B*, 2010, **100**, 933-943.
53. X. Mercier, M. Wartel, J. F. Pauwels and P. Desgroux, *Applied Physics B-Lasers and Optics*, 2008, **91**, 387-395.
54. K. Kohse-Höinghaus and A. Brockhinke, *Combustion Explosion and Shock Waves*, 2009, **45**, 349-364.
55. A. C. Eckbreth, *Laser diagnostics for combustion temperature and species*, Gordon & Breach, Amsterdam, 1996.
56. B. Zhao, K. Uchikawa and H. Wang, *Proceedings of the Combustion Institute*, 2007, **31**, 851-860.
57. C. A. Echavarria, A. F. Sarofim, J. S. Lighty and A. D'Anna, *Combustion and Flame*, 2011, **158**, 98-104.
58. A. T. Hartlieb, B. Atakan and K. Kohse-Höinghaus, *Combustion and Flame*, 2000, **121**, 610-624.
59. C. J. Dasch, *Symposium (international) on Combustion*, 1984, **20**, 1231 - 1237.
60. A. Lamprecht, W. Eimer and K. Kohse-Hoinghaus, *Combustion and Flame*, 1999, **118**, 140-150.
61. W. H. Dalzell, G. C. Williams and H. C. Hottel, *Combustion and Flame*, 1970, **14**, 161-&.
62. T. C. Bond and R. W. Bergstrom, *Aerosol Science and Technology*, 2006, **40**, 27-67.
63. H. Senftleben and E. Benedict, *Annals of Physics*, 1919, **60**, 297.

64. T. T. Charalampopoulos, *Progress in Energy and Combustion Science*, 1992, **18**, 13-45.
65. B. Quay, T. W. Lee, T. Ni and R. J. Santoro, *Combustion and Flame*, 1994, **97**, 384-392.
66. J. Appel, B. Jungfleisch, M. Marquardt, R. Suntz and H. Bockhorn, *Twenty-Sixth Symposium (International) on Combustion, Vols 1 and 2*, 1996, 2387-2395.
67. R. Di Sante, *Optics and Lasers in Engineering*, 2013, **51**, 783-789.
68. K. A. Thomson, K. P. Geigle, M. Kohler, G. J. Smallwood and D. R. Snelling, *Applied Physics B-Lasers and Optics*, 2011, **104**, 307-319.
69. R. J. Santoro, H. G. Semerjian and R. A. Dobbins, *Combustion and Flame*, 1983, **51**, 203-218.
70. J. Zerbs, K. P. Geigle, O. Lammel, J. Hader, R. Stirn, R. Hadef and W. Meier, *Applied Physics B-Lasers and Optics*, 2009, **96**, 683-694.
71. H. Bladh, Doctoral Dissertation, Lund University, 2007.
72. J. W. Daily, *Progress in Energy and Combustion Science*, 1997, **23**, 133-199.
73. K. Kohse-höinghaus, *Progress in Energy and Combustion Science*, 1994, **20**, 203-279.
74. A. Leipertz, F. Ossler and M. Alder. in *Applied Combustion Diagnostics*, eds. K.-H. K and J. B. Jeffries, Taylor & Francis, New York, ch. 13, p. 359.
75. L. Cai and H. Pitsch, *Combustion and Flame*, 2014, **161**, 405-415.
76. S. Cheskis and A. Goldman, *Progress in Energy and Combustion Science*, 2009, **35**, 365-382.
77. S. B. Dworkin, Q. A. Zhang, M. J. Thomson, N. A. Slavinskaya and U. Riedel, *Combustion and Flame*, 2011, **158**, 1682-1695.
78. C. Schulz, B. F. Kock, M. Hofmann, H. Michelsen, S. Will, B. Bougie, R. Suntz and G. Smallwood, *Applied Physics B-Lasers and Optics*, 2006, **83**, 333-354.
79. R. W. Weeks and W. W. Duley, *Journal of Applied Physics*, 1974, **45**, 4661-4662.
80. A. C. Eckbreth, *Journal of Applied Physics*, 1977, **48**, 4473-4479.
81. D. A. Greenhalgh, *Applied Optics*, 1983, **22**, 1128-1130.

82. L. A. Melton, *Applied Optics*, 1984, **23**, 2201-2208.
83. R. L. Vanderwal and K. J. Weiland, *Applied Physics B-Lasers and Optics*, 1994, **59**, 445-452.
84. D. J. Bryce, N. Ladommatos and H. Zhao, *Applied Optics*, 2000, **39**, 5012-5022.
85. S. Will, S. Schraml and A. Leipertz, *Optics Letters*, 1995, **20**, 2342-2344.
86. B. Mewes and J. M. Seitzman, *Applied Optics*, 1997, **36**, 709-717.
87. R. Hadef, K. P. Geigle, W. Meier and M. Aigner, *International Journal of Thermal Sciences*, 2010, **49**, 1457-1467.
88. F. Migliorini, S. De Iuliis, F. Cignoli and G. Zizak, *Applied Optics*, 2006, **45**, 7706-7711.
89. B. Bougie, L. C. Ganippa, A. P. van Vliet, W. L. Meerts, N. J. Dam and J. J. ter Meulen, *Proceedings of the Combustion Institute*, 2007, **31**, 685-691.
90. S. De Iuliis, F. Migliorini, F. Cignoli and G. Zizak, *Proceedings of the Combustion Institute*, 2007, **31**, 869-876.
91. P. E. Bengtsson and M. Alden, *Applied Physics B-Lasers and Optics*, 1995, **60**, 51-59.
92. H. Bladh and P. E. Bengtsson, *Applied Physics B-Lasers and Optics*, 2004, **78**, 241-248.
93. H. Bladh, P. E. Bengtsson, J. Delhay, Y. Bouvier, E. Therssen and P. Desgroux, *Applied Physics B-Lasers and Optics*, 2006, **83**, 423-433.
94. H. Bladh, J. Johnsson, J. Rissler, H. Abdulhamid, N. E. Olofsson, M. Sanati, J. Pagels and P. E. Bengtsson, *Applied Physics B-Lasers and Optics*, 2011, **104**, 331-341.
95. Q. N. Chan, P. R. Medwell, P. A. M. Kalt, Z. T. Alwahabi, B. B. Dally and G. J. Nathan, *Proceedings of the Combustion Institute*, 2011, **33**, 791-798.
96. M. Charwath, R. Suntz and H. Bockhorn, *Applied Physics B-Lasers and Optics*, 2006, **83**, 435-442.
97. H. A. Michelsen, F. Liu, B. F. Kock, H. Bladh, A. Boiarciuc, M. Charwath, T. Dreier, R. Hadef, M. Hofmann, J. Reimann, S. Will, P. E. Bengtsson, H. Bockhorn, F. Foucher, K. P. Geigle, C. Mounaim-Rousselle, C. Schulz, R. Stirn,

B. Tribalet and R. Suntz, *Applied Physics B-Lasers and Optics*, 2007, **87**, 503-521.

98. H. A. Michelsen, *Journal of Chemical Physics*, 2003, **118**, 7012-7045.
99. H. Bladh, J. Johnsson and P. E. Bengtsson, *Applied Physics B-Lasers and Optics*, 2008, **90**, 109-125.
100. C. J. Dasch, *Applied Optics*, 1984, **23**, 2209-2215.
101. R. L. Vander Wal and K. J. Weiland, *Applied Physics B*, 1994, **59**, 445-452.
102. R. L. Vander Wal, *Applied Physics B-Lasers and Optics*, 2009, **96**, 601-611.
103. R. L. Vander Wal, T. M. Ticich and A. B. Stephens, *Combustion and Flame*, 1999, **116**, 291-296.
104. C. S. Moreau, E. Therssen, X. Mercier, J. F. Pauwels and P. Desgroux, *Applied Physics B-Lasers and Optics*, 2004, **78**, 485-492.
105. J. V. Pastor, J. M. Garcia, J. M. Pastor and J. E. Buitrago, *Measurement Science & Technology*, 2006, **17**, 3279-3288.
106. D. R. Snelling, G. J. Smallwood, F. Liu, O. L. Gulder and W. D. Bachalo, *Applied Optics*, 2005, **44**, 6773-6785.
107. P. Desgroux, X. Mercier, B. Lefort, R. Lemaire, E. Therssen and J. F. Pauwels, *Combustion and Flame*, 2008, **155**, 289-301.
108. M. Y. Choi and K. A. Jensen, *Combustion and Flame*, 1998, **112**, 485-491.
109. S. Dankers and A. Leipertz, *Applied Optics*, 2004, **43**, 3726-3731.
110. H. A. Michelsen, M. A. Linne, B. F. Kock, M. Hofmann, B. Tribalet and C. Schulz, *Applied Physics B-Lasers and Optics*, 2008, **93**, 645-656.
111. F. Liu, M. Yang, F. A. Hill, D. R. Snelling and G. J. Smallwood, *Applied Physics B-Lasers and Optics*, 2006, **83**, 383-395.
112. F. Liu, B. J. Stagg, D. R. Snelling and G. J. Smallwood, *International Journal of Heat and Mass Transfer*, 2006, **49**, 777-788.
113. K. J. Daun, *Journal of Heat Transfer-Transactions of the Asme*, 2010, **132**.
114. J. Hayashi, H. Watanabe, R. Kurose and F. Akamatsu, *Combustion and Flame*, 2011, **158**, 2559-2568.

115. M. Charwath, R. Suntz and H. Bockhorn, *Applied Physics B-Lasers and Optics*, 2011, **104**, 427-438.
116. S. Will, S. Schraml and A. Leipertz, *Twenty-Sixth Symposium (International) on Combustion*, 1996, 2277-2284.
117. S. Schraml, S. Dankers, K. Bader, S. Will and A. Leipertz, *Combustion and Flame*, 2000, **120**, 439-450.
118. A. Boiarciuc, F. Foucher and C. Mounaim-Rousselle, *Applied Physics B-Lasers and Optics*, 2006, **83**, 413-421.
119. E. Therssen, Y. Bouvier, C. Schoemaecker-Moreau, X. Mercier, P. Desgroux, M. Ziskind and C. Focsa, *Applied Physics B-Lasers and Optics*, 2007, **89**, 417-427.
120. S. De Iuliis, F. Cignoli and G. Zizak, *Appl. Opt.*, 2005, **44**, 7414-7423.
121. F. Liu, D. R. Snelling, K. A. Thomson and G. J. Smallwood, *Applied Physics B-Lasers and Optics*, 2009, **96**, 623-636.
122. H. Bladh, J. Johnsson, N. E. Olofsson, A. Bohlin and P. E. Bengtsson, *Proceedings of the Combustion Institute*, 2011, **33**, 641-648.
123. S. Maffi, S. De Iuliis, F. Cignoli and G. Zizak, *Applied Physics B-Lasers and Optics*, 2011, **104**, 357-366.
124. D. R. Snelling, F. S. Liu, G. J. Smallwood and O. L. Gulder, *Combustion and Flame*, 2004, **136**, 180-190.
125. C. R. Shaddix and K. C. Smyth, *Combustion and Flame*, 1996, **107**, 418-452.
126. F. Liu, K. A. Thomson and G. J. Smallwood, *Journal of Quantitative Spectroscopy & Radiative Transfer*, 2008, **109**, 337-348.
127. F. Goulay, P. E. Schrader, L. Nemes, M. A. Dansson and H. A. Michelsen, *Proceedings of the Combustion Institute*, 2009, **32**, 963-970.
128. R. J. Santoro and C. R. Shaddix, in *Applied Combustion Diagnostics*, eds. K.-H. K and J. B. Jeffries, Taylor & Francis, New York, ch. 9, p. 252.
129. F. Cignoli, S. Benecchi and G. Zizak, *Optics Letters*, 1992, **17**, 229-231.
130. J. B. Jeffries, R. A. Copeland, G. P. Smith and D. R. Crosley, *Symposium (International) on Combustion*, 1988, **21**, 1709-1718.
131. U. Westblom and M. Alden, *Applied Optics*, 1990, **29**, 4844-4851.

132. D. R. Crosley, *Combustion and Flame*, 1989, **78**, 153-167.
133. D. E. Heard, J. B. Jeffries, G. P. Smith and D. R. Crosley, *Combustion and Flame*, 1992, **88**, 137-148.
134. M. J. Dyer and D. R. Crosley, *Optics Letters*, 1982, **7**, 382-384.
135. K. J. Rensberger, J. B. Jeffries, R. A. Copeland, K. Kohsehöinghaus, M. L. Wise and D. R. Crosley, *Applied Optics*, 1989, **28**, 3556-3566.
136. M. Tamura, J. Luque, J. E. Harrington, P. A. Berg, G. P. Smith, J. B. Jeffries and D. R. Crosley, *Applied Physics B-Lasers and Optics*, 1998, **66**, 503-510.
137. K. McManus, B. Yip and S. Candel, *Experimental Thermal and Fluid Science*, 1995, **10**, 486-502.
138. I. D. Berlman, *Handbook of Fluorescence Spectra of Aromatic Molecules*, Academic Press, New York, 1971.
139. J. B. Birks, *Photophysics of Aromatic Molecules,* Wiley-Interscience, London, 1970.
140. K. C. Smyth and D. R. Crosley, *Applied Combustion Diagnostics*, Taylor & Francis, New York.
141. J. T. Wu, K. H. Song, T. Litzinger, S. Y. Lee, R. Santoro, M. Linevsky, M. Colket and D. Liscinsky, *Combustion and Flame*, 2006, **144**, 675-687.
142. S. Y. Lee, S. R. Turns and R. J. Santoro, *Combustion and Flame*, 2009, **156**, 2264-2275.
143. H. Böhm, K. Kohse-Höinghaus, F. Lacas, C. Rolon, N. Darabiha and S. Candel, *Combustion and Flame*, 2001, **124**, 127-136.
144. K. C. Smyth, C. R. Shaddix and D. A. Everest, *Combustion and Flame*, 1997, **111**, 185-207.
145. F. Migliorini, S. De Iuliis, S. Maffi, F. Cignoli and G. Zizak, *Applied Physics B-Lasers and Optics*, 2009, **96**, 637-643.
146. P. Witze, S. Shimpi, R. Durrett and L. Farrell, *JSME International Journal Series B-Fluids and Thermal Engineering*, 2005, **48**, 632-638.
147. P. R. Medwell, G. J. Nathan, Q. N. Chan, Z. T. Alwahabi and B. B. Dally, *Combustion and Flame*, 2011, **158**, 1814-1821.

148. G. Cleon, T. Amodeo, A. Faccinetto and P. Desgroux, *Applied Physics B-Lasers and Optics*, 2011, **104**, 297-305.
149. M. D. Smooke, C. S. McEnally, L. D. Pfefferle, R. J. Hall and M. B. Colket, *Combustion and Flame*, 1999, **117**, 117-139.
150. P. O. Witze, S. Hochgreb, D. Kayes, H. A. Michelsen and C. R. Shaddix, *Applied Optics*, 2001, **40**, 2443-2452.
151. P. E. Bengtsson and M. Alden, *Applied Physics B-Photophysics and Laser Chemistry*, 1989, **48**, 155-164.

3 EXPERIMENTAL AND METHOD DEVELOPMENT

This chapter describes the approach to make reliable and repeatable LII and LIF measurements. Two different experimental set-ups were employed, the first initial measurements recorded at one detection wavelength using a band pass filter. The second involved measurements made in the same flame but with the spectrum of light emitted recorded over a range of wavelengths through use of a monochromator.

The burner employed was of the same type but not exactly that which has been identified as standard for this type of measurement. In order for this to be possible the flame must be stable and reproducible. Also the conditions for use in these experiments were chosen in order that they were comparable with conditions which are often used and are considered suitable for this work – that is those which will give a stable sooting flame.

Finally, there had to be consideration given to the conditions which should be used with respect to the laser. It had been decided that three wavelengths of excitation should be used and as such conditions had to be chosen which would ensure that when using the different wavelengths the soot particles were being heated to the same extent in each in order that the incandescence would be equal.

3.1 OPTICAL SETUP

In order that is be possible to make measurements using three different excitation wavelengths both and Nd:YAG and dye laser were employed, Figure 3-1. This was achieved by using both the fundamental and frequency doubled wavelengths emitted from the Nd:YAG, 1064 nm and 532 nm respectively, and using the 532 nm light to

excite rhodamine 590 dye in the dye laser (giving rise to 566 nm light), which was subsequently doubled to give 283 nm light.

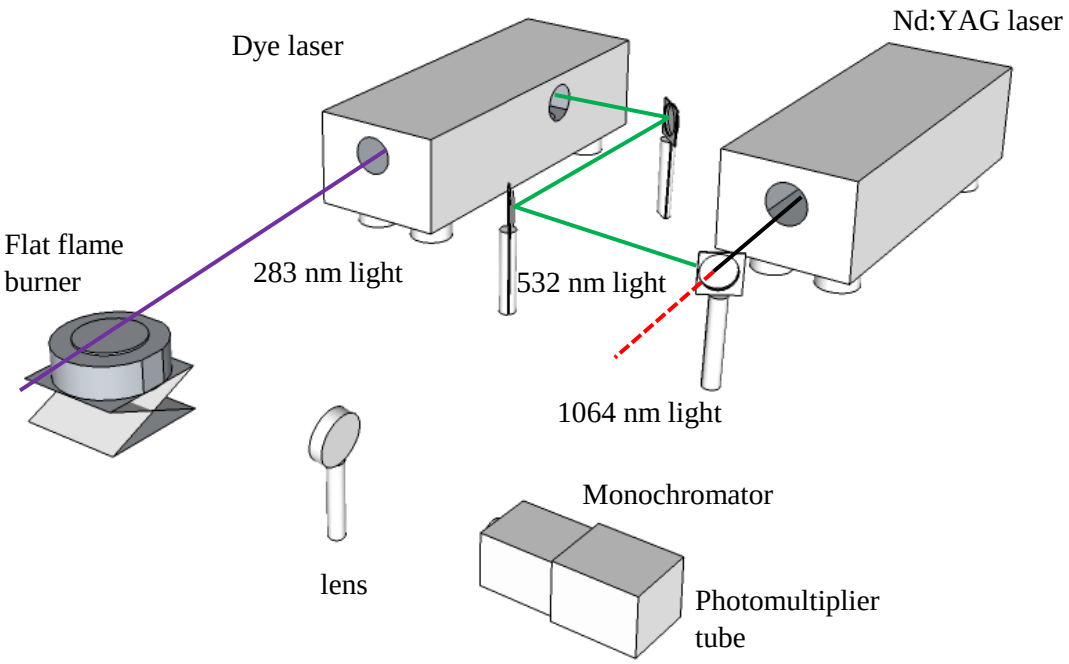

Figure 3-1 : Diagram of laboratory set up

Interference from light of a different excitation wavelength must be avoided. Since it is necessary to be sure that when exciting with 1064 nm light, for example, that all of the signal is due solely to that excitation wavelength in order that the emitted signal is due only to incandescence. This would not be the case if there was any other light in the measurement volume. Therefore the fundamental and frequency doubled Nd:YAG light was separated using dichroic mirrors, Figure 3-1, which transmit at 1064 nm and reflect 532 nm. Two Pellin Broca prisms within the dye laser were used to separate the frequency doubled light from the fundamental dye laser wavelength.

When the beam exits the Nd:YAG laser it is collimated and has a Gaussian spatial profile. If a beam with a Gaussian spatial profile was used to heat or excite the particles in the flame the particles at the centre of the beam would receive much higher energy than those at the fringes of the beam. The fluence (the laser power per unit area) measured by averaging the power of the beam over the area of the beam would therefore be an underestimate for the centre of the beam and an overestimate for the outside of the beam. It is important that all the particles in the measurement volume are heated to the same temperature and as such a beam with a uniform spatial profile (a tophat profile) should be used. The importance of the choice of the fluence its influence on peak particle temperature is outlined in section 1.6.

In order to obtain a top hat profile the central 1 mm of the 7 mm Gaussian beam is selected using a 1 mm diameter pin-hole. This is a small enough portion of the beam at its peak that it can be considered to be uniform as illustrated in Figure 3-2. The pin-hole was located 70 mm from the centre of the flame. The positioning close to the flame is important in order that the change in spatial profile due to diffraction is minimal.

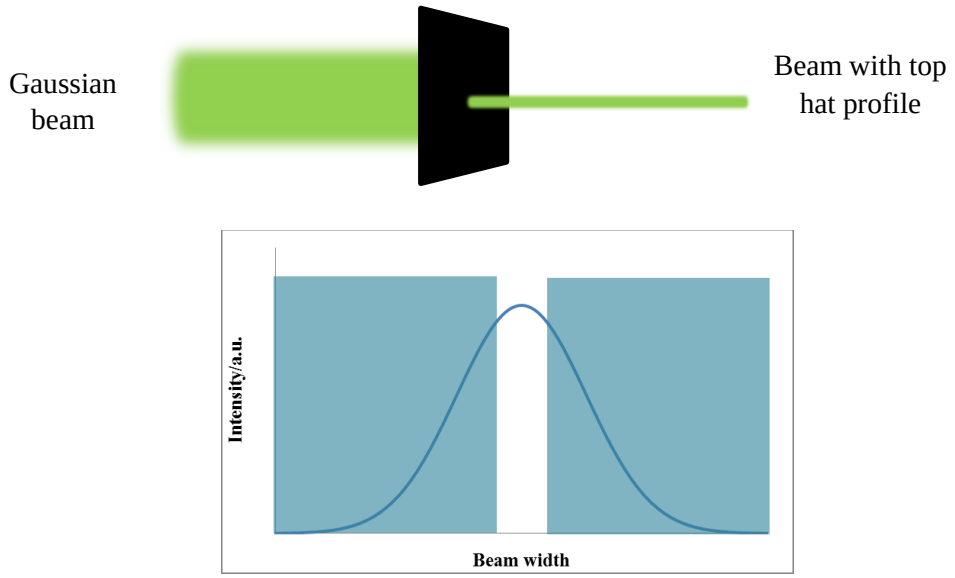

Figure 3-2 : Selection of middle section of Gaussian beam to give a top hat profile

In order to ensure that the beam was not divergent after the pinhole the beam diameter was measured using burn paper immediately after the pinhole, at the centre of the burner and immediately after the burner. As the beam diameter was identical at all three measurement points there could be confidence that the beam was collimated through the measurement volume.

In order that measurements could be made as a function of height above burner without adjusting the sensitive optical set-up the burner was mounted on an adjustable platform. The height "zero" was set by measuring the power after the burner, using a power meter, and adjusting the burner height until the beam intensity was attenuated by half.

3.2 DETECTION SETUP

During this work two different detection schemes were employed, one for making measurements at a single detection wavelength over a range of heights above burner and one for making spectrally resolved measurement at two heights above the burner surface. The main equipment is outlined below and an outline is given of the two detection setups and what they are used for.

3.2.1 Detection set up I

The incandescence and fluorescence signals are emitted over a range of wavelengths. When making measurements at a fixed detection wavelength a bandpass filter was used in front of the photomultiplier tube. It is known that fluorescence is predominantly emitted at longer wavelengths than that of excitation. However, in PAHs due to the high levels of conjugation the electronic energy levels are closely spaced. As a result of this the thermal population will be in a state higher than the ground state. This makes it

possible that excited electrons falling to the ground state are losing higher amounts of energy than they gained through excitation and thus fluorescence being emitted at wavelengths shorter than the excitation wavelength would be expected.

It is important when selecting a detection wavelength for LII measurements to avoid the region where laser induced breakdown of hydrocarbons may lead to Swan (radical C2) or Swing (radical C3) bands[1]. This is especially important if 532 nm excitation will be used at a fluence of greater than 0.2 J cm^{-2} [1] – which will be the case in this work. Thus for this work is was decided that a bandpass filter of 450 ± 10 nm FWHM would be placed directly in front of the PMT as recording over this small range of wavelengths will avoid Swan bands[1].

In order to achieve greater spatial resolution a pinhole of diameter 650 µm was placed directly in front of the PMT. This resulted in the signal being collected from 1 mm in diameter 650 µm in the z-plane. This gives a total measurement volume of 0.332 mm^3. A focal lens is used between the burner and the photomultiplier with a 150 mm focal length used in a 2f-2f set up; that is with 2 x focal length both before and after the lens, giving a total distance of 60 cm between the centre of the flame and the detector.

The signal registered by the PMT was digitised by an oscilloscope (Tektronix DPO 2024) which was triggered upon the Q-switch trigger. The Q-switch trigger, photodiode signal and signal emitted from the flame were all recorded simultaneously on a different channel. The emitted signal displayed was an average of 64 shots with only the average being recorded.

3.2.2 Detection set up II

In order to spectrally resolve the incandescence and fluorescence signals a grating monochromator was used. This allowed for a wide range of detection wavelengths to be employed with the signal being recorded over a range of either 400 – 800 nm or 300 – 700 nm.

In order to eliminate any interference due to scattered 532 nm excitation light getting through the monochromator and onto the detector a 533 nm notch filter (FWHM = 20 nm) was placed in front of the PMT. The transmission band filter that was being used ended at 400 nm and the spectrally resolved measurements were therefore made between 400 nm and 800 nm for excitation with 1064 nm and 532 nm. There was no need for the notch filter when exciting with 283 nm light and so measurements could be taken as low as 300 nm. Since much of the fluorescence emitted upon 283 nm excitation is at wavelengths below 400 nm this was seen as advantageous even although there could be no direct comparison below 400 nm of the signal obtained with 283 nm light and that obtained with 532 nm and 1064 nm.

A LabView programme was written to coordinate the monochromator movement and signal recording. Through this is was possible to select the wavelength interval and the wavelength spacing between data points and averaging of the data to be gathered. The programme worked by moving the monochromator grating to give the required detection wavelength and records and recording an average of 64 signals. This is automatically repeated until the signal is collected over the desired range of detection wavelengths.

There had to be a compromise between the length of time for which the flame is stable, as shown in section 3.3 to be 20 minutes and the time taken to record the signal over a given range of detection wavelengths – which is affected by the number of scans, the averages, the range and the time the monochromator grating takes to move between detection wavelengths. With these factors in mind it was decided that a resolution of 2 nm would be used with 64 scans at each wavelength.

3.3 BURNER CONFIGURATION

3.3.1 Choice of Burner

As a topic at the LII meeting of 2005[2] there was discussion around the benefit of identifying and working with standard burners and conditions. This facilitates not only the comparison of work between groups but also generation of large datasets under identical conditions as reference data for modelling.

As a result three sets of conditions each for a different burner, the Gülder, McKenna and Santoro, were identified as so called "target flames". The recommended settings to obtain the target flame in a McKenna burner are outlined in Table 1 as this shares many similarities with the burner employed in this work

Table 1 : Target flame conditions for McKenna burner as decided at LII workshop 2005[2]

	MCKENNA (premixed)
Fuel	Ethylene/air, equivalence ratio 2.1
Flow	Total flow 10 slm
Coflow	n/a
Materials	Porous plug of brass/stainless steel
Measurement position	12 mm above burner surface at centreline (15 minutes after ignition)
Stabilisation	Plate (60 mm in diameter and 20 mm thick) 21 mm above the burner surface Shroud gas of N2/air/ethylene air lean mix with flow rate of 15 slm

In this work a McKenna type burner was used to stabilise flat premixed flames of ethylene and air. This makes the results very amenable to modelling because the flame can be considered to be one dimensional in the region where measurements were made, and also makes the flame conditions very reproducible (as the flame is easily stabilised).

3.3.2 Burner configuration

Unlike the burner outlined in Table 2 as the standard, the burner employed in this work had a smaller plug diameter, of 35 mm, and as such the flow had to be scaled to reproduce the mass flux accordingly meaning a total flow of 3.200 sL min^{-1} was used. By using Equation 3-1 and keeping the flow rate constant the conditions for five different stoichiometries, Table 2, were chosen.

$$\Phi = \frac{x_{air,stoich} / x_{fuel,stoich}}{x_{air} / x_{fuel}}$$

Equation 3-1

Where: x = mole fraction

Φ = equivalence ratio

Table 2 : Flow rates for range of stoichimetries to be employed

Φ	$x_{C_2H_4}$	x_{air}	Flow rate C_2H_4 (sL min^{-1})	Flow rate air (sL min^{-1})
1.7	10.61	89.39	0.38	3.22
1.8	11.17	88.83	0.40	3.20
1.9	11.71	88.29	0.42	3.18
2.0	12.26	87.75	0.44	3.16
2.1	12.79	87.21	0.46	3.14

These stoichiometries were selected because they gave sooting flames ranging from near the threshold of soot formation to highly sooting conditions, Figure 3-3 and Figure 3-4.

Figure 3-3: Ethylene:air premixed flame Φ= 1.7

Figure 3-4: Ethylene:air premixed flame Φ= 2.1

It can be seen even visually, due to the orange glow, that there is a great deal more particulate material in the flame where Φ = 1.7 compared to that of Φ = 2.1. The zone prior to large PAH or soot formation is also visible, due to the lack of any orange colouring below around 5 mm in the flame.

3.3.3 Burner Stability

A further difference with the burner used was that there was no capability for co-annular flow of shroud gas. This could, in principle, influence the stability of the flame by making it susceptible to currents of ambient air in the laboratory. Therefore it was

important to carefully examine the stability of the flame and ensure that the flame was stable by thoroughly repeating experiments at all flame conditions studied this resulted in highly reproducible results as shown in chapter 4.

As is outlined in Table 1, a cylindrical plate (of the same diameter as the burner plate and 20 mm thick) was placed at a height of 21 mm above the burner surface [3-6] as shown in Figure 3-5

This helps to stabilise the flame by acting as a heat sink. A well-defined procedure must be carefully followed to ensure that reproducible flame conditions are obtained. Initially the stabilisation plate must reach thermal equilibrium; instabilities can arise later due to the build-up of soot on the plate surface. The accumulation of soot on the plate leads to a risk of the laser beam clipping the soot or the soot building to such a level that it breaks off and falls into the flame, which could damage the burner. Furthermore if the soot build up is uneven, that is not parallel with the stabilisation plate surface this will serve to destabilise the flame.

To this end it was decided that measurements would be made to a maximum height of 15 mm above the burner surface allowing for several height above burner measurements to be made yet still ensuring a little soot build up will not clipping the wing of the laser beam.

An appropriate time had to be selected to allow for the plate temperature to stabilise before measurements were begun the signal emitted from the flame upon laser excitation was recorded every 30 seconds over a period of 30 minutes at 15 mm above the burner surface in a flame where $\Phi = 2.1$. The results are shown in Figure 3-6. These conditions were chosen as this was the highest fuel to air ratio used in this study. Furthermore 15 mm corresponds to the highest position at which measurements were to be made at so if the measurement was unaffected here the soot build up is unlikely to affect measurements at points lower than this in the burner.

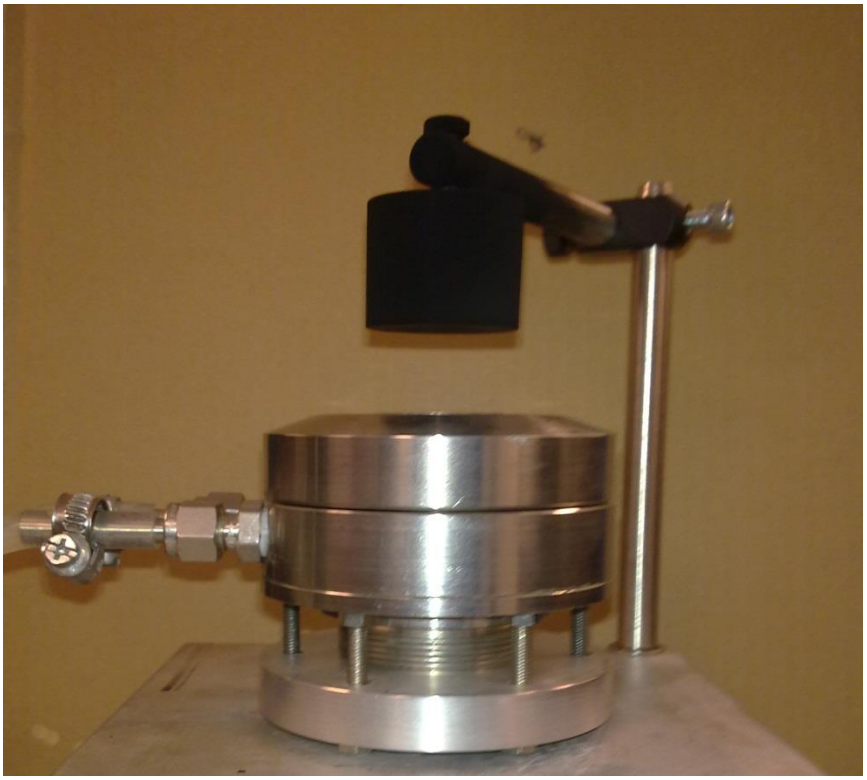

Figure 3-5 : Burner with stabilisation plate 21 mm above burner surface

As can be seen there is an initial period of few minutes where the emitted signal increases in intensity. This suggests that during this period the plate and burner are equilibrating and that this is not an ideal time for measurements to be made in the flame. After this the flame remains stable for a further 20 minutes, and it is during this period that it is optimum for measurements to be made. Beyond a total time of 25 minutes there begins to be a large soot build up on the plate, so it is no longer advisable to make measurements when there is a risk of the soot breaking off and falling into the flame. The effect of this can be seen in the above plot when, after around 20 minutes the signal starts to decrease.

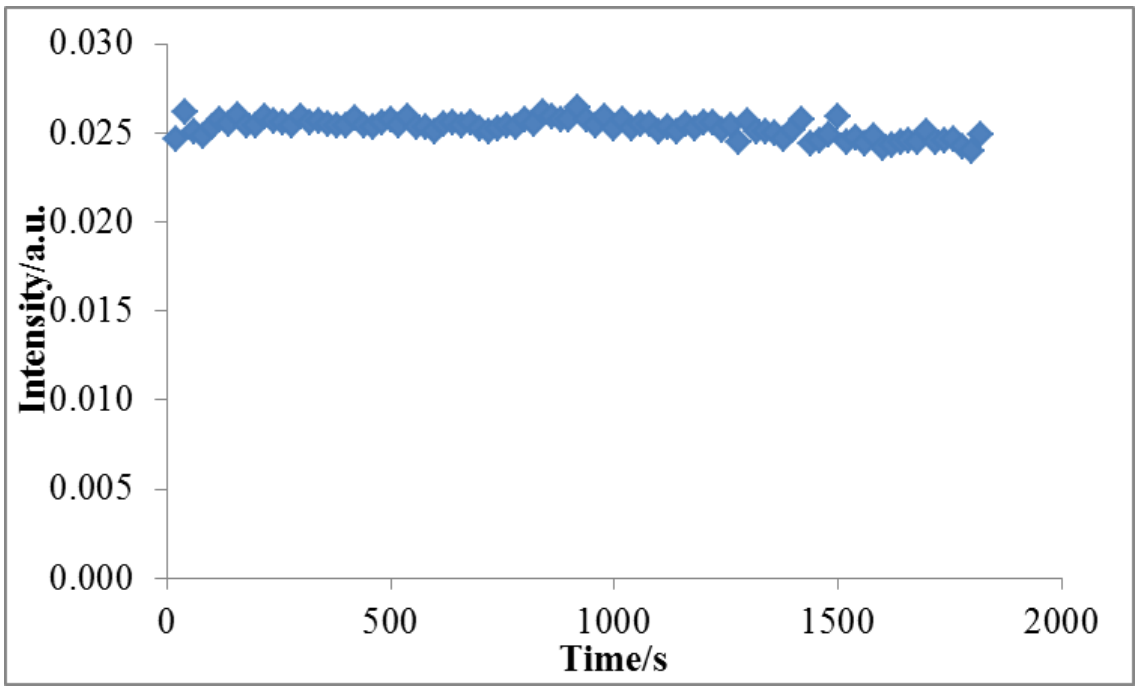

Figure 3-6 : change in signal intensity over time, Φ = 2.1, HAB = 15 mm, λ_{ex} = 532 nm

Once the stability of the burner with respect to time has been checked and maximum height above burner had been selected it was necessary to investigate the horizontal profile to ensure that the flame was one dimensional despite the burner surface being slightly narrower than the standard one. This was achieved by moving the burner horizontally in 1 mm increments and recording the emitted signal from the flame at each point. The results are shown in Figure 3-7.

As can be seen from the figure there is very little variation in the emitted signal in the central 15 mm of the flame, which shows that in this region the flame can be considered to be flat. Beyond this central 15 mm the signal decreases towards the edge of the flame. This is due to the effect of the surrounding atmosphere interfering directly with the flame and is what would be expected in the absence of an inert shielding gas. Since the centre of the flame is the region of interest these edge effects seem to be of little

consequence. This demonstration of the stability and the one-dimensional nature of the flame demonstrate that the measurements obtained here can meaningfully be compared to those obtained in the standard McKenna burner described above and to the results of one dimensional laminar flame models.

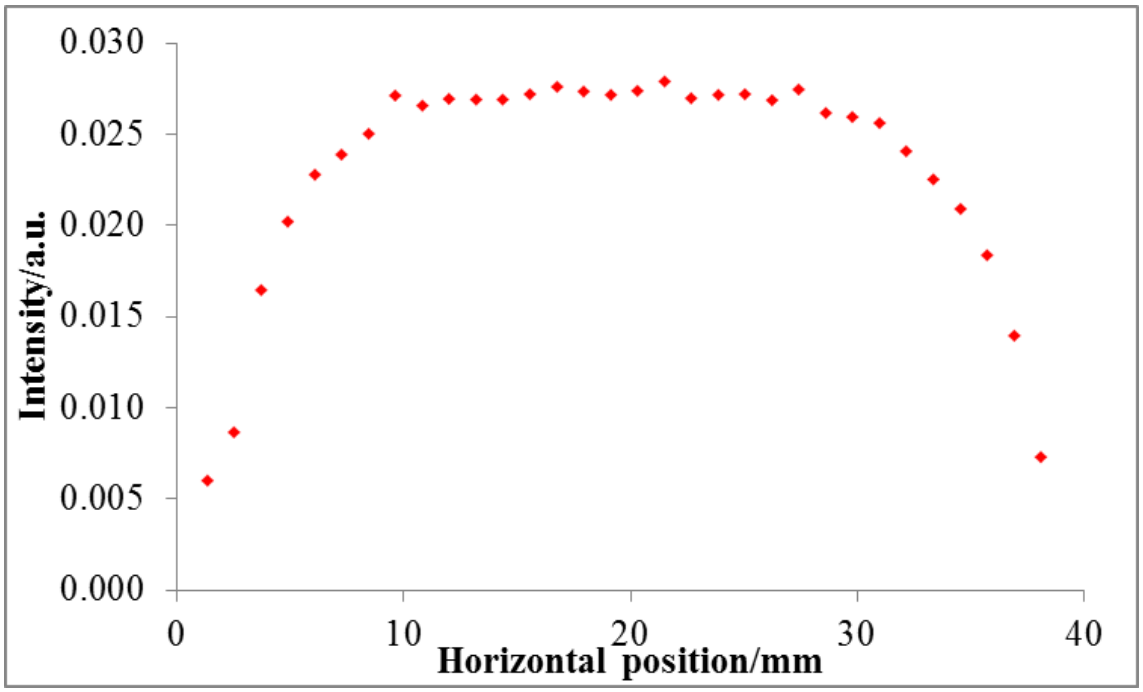

Figure 3-7 : Peak intensity across width of burner Φ = 2.1, HAB = 15 mm, λ_{ex} = 532 nm

3.4 AVOIDANCE OF INTERFERENCE

One of the major issues when making measurements of this type is the background interference which can occur. This can be due to stray light from the laser being

reflected around the room. This can have a large impact on the signal and can even mask the signal, especially the fluorescence, due to the short timescales for which fluorescence exists. The short duration of the laser pulse eliminates other sources of interference, such as flame luminosity or ambient light.

When initial measurements were made over the range of heights above burner it can be seen from the results that there was a large problem with scattered laser light, Figure 3-8

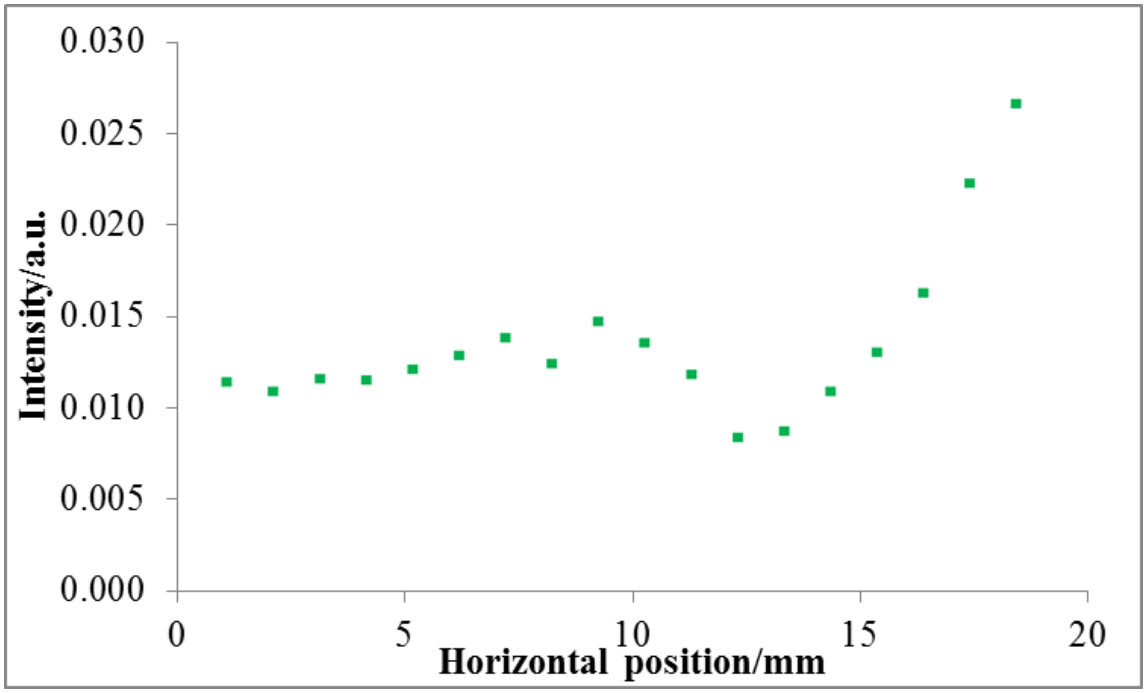

Figure 3-8 : Intensity at peak Φ = 1.9, HAB = 15 mm, λ_{ex} = 532 nm with no shielding

As can be seen there appears to be a signal present at all heights above the burner, which is not what would be expected. Additional shielding was added around the laser beam and pinhole, to minimise scattered light, and there was additional shielding placed between the flame and the detector to eliminate any remaining stray light.

Initially the shielding which had been designed was put in place from a safety. An enclosure was constructed around the Nd:YAG laser and along the laser pathway

between the Nd:YAG laser and the dye laser, Figure 3-9

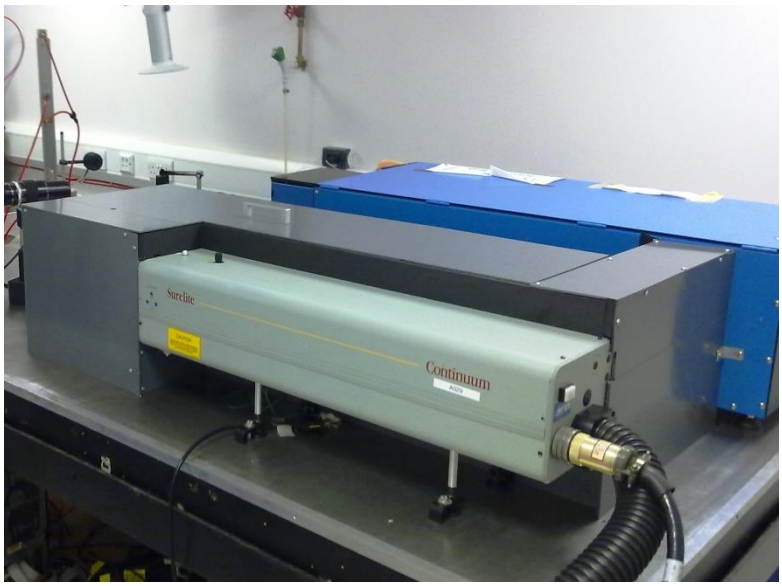

Figure 3-9 : laser shielding

However in order to allow the 1064 nm and 532 nm light to exit the enclosure there was a circular opening cut in the shielding. Unfortunately though, this resulted in scattered 532 nm light also escaping, irrespective if 532 nm light or 1064 nm light was being used. This caused the effect which was highlighted in Figure 3-8 where there is a constant offset of the signal due to the scattered light reaching the detector. In order to combat this further shielding was added between the burner and the detector in the form of plastic tubing. This ensured that the signal emitted from the flame could carry on its path to the detector unperturbed but any stray light will be stopped from reaching the detector, unless it is coming from the measurement volume.

The measurement was subsequently repeated and the data shown in Figure 3-10 was obtained.

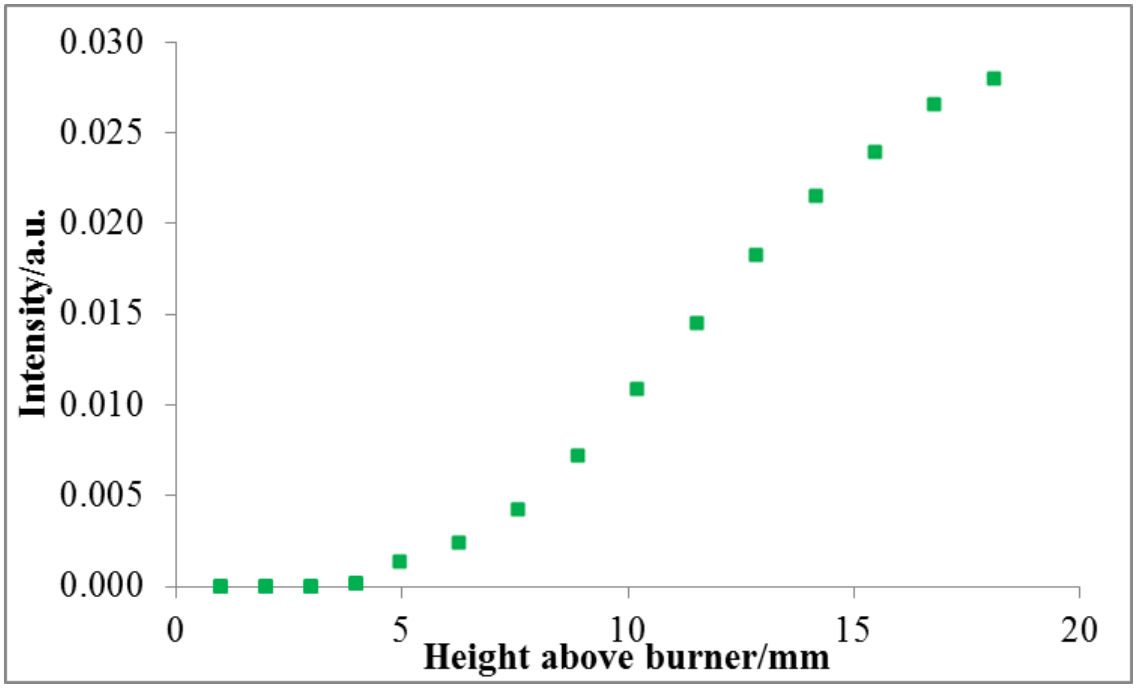

Figure 3-10 : Intensity at peak Φ = 1.9, HAB = 15 mm, λ_{ex} = 532 nm with shielding

Here it can be seen that there is no signal below 4 mm with increasing signal intensity over the rest of the range. This is what would be expected and it can be accepted that there is sufficient shielding for the measurements to continue.

3.5 CORRECT IDENTIFICATION OF INCANDESCENCE SIGNAL

It was first important to ensure that the signal being recorded was attributable to incandescence and not due to scattered laser light. On directing laser light through a flame there will be light emitted both due to fluorescence of molecules and incandescence of particulate material. There may also be light that gets onto the detector as a consequence of scattered excitation light, and while this can be minimised through

the experimental set up one must not become complacent that it will be entirely absent in the signal.

The key attribute which differentiated incandescence from either scattered light or fluorescence is the decay time. While incandescence will have a lifetime of hundreds of nanoseconds, scattered light and fluorescence are on the scale of tens of nanoseconds. Therefore even by visually examining the time decay it is possible to differentiate between incandescence and fluorescence or scattered light. It is also known that both the decay time and intensity of the incandescence signal change upon altering the fluence, that is the power per unit area of the laser.

Therefore the signal which was emitted from the flame was recorded upon passing a laser through a flame where $\Phi = 2.1$ at 15 mm and altering the fluence, by changing the Q-switch delay) as can be seen in Figure 3-11.

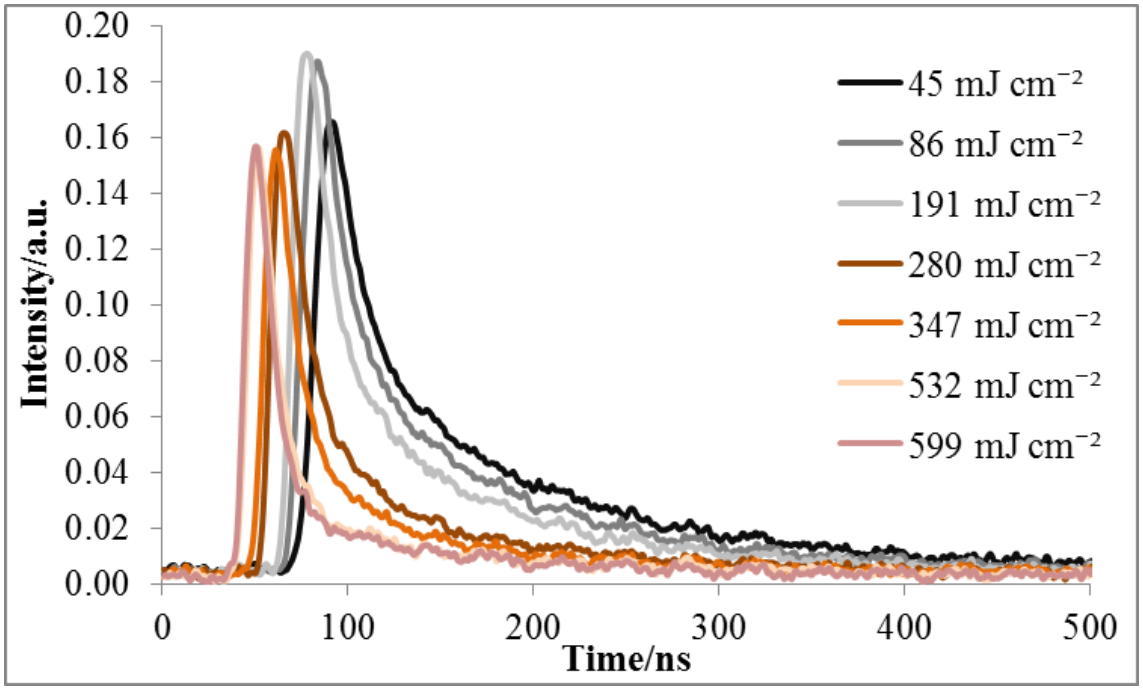

Figure 3-11 : Emitted signal resulting from λ_{ex} = 532 nm over range of fluences

As can be seen the decay time is of a significantly long time that the signal could not be due to either scattered light or fluorescence. Also it can be seen that the peak height of the signal and the decay time changes when altering the fluence. It can also be seen that the signals obtained appears to fall into two groups. These groups split between fluences of 198 mJ cm^{-2} and 280 mJ cm^{-2} which is as would be expected as it is around a fluence of 220 mJ cm^{-2} that the particles begin to sublime. Therefore, there could be confidence that the signals which were being obtained were primarily due to incandescence.

3.6 CHOICE OF FLUENCE

When making laser measurements within a flame one of the first considerations is which fluence should be used. There is no general agreement in the literature about what the optimum fluence should be, and indeed higher or lower fluences have various advantages and disadvantages. Use of lower fluences is often favoured when wanting to obtain information on particle size through fitting the decay of the LII signal. This is because at fluences below sublimation none of the energy should be lost to sublimation. However, there are difficulties when working at a low fluence regime with making robust measurements as any small fluctuations in the laser power will have a great impact on the peak incandescence, unlike at higher fluences where there is a plateau region. Thus for measurements involving obtaining the soot volume fraction, which is calculated from the peak incandescence, it is advantageous to use a fluence which falls in the plateau region. Furthermore as highlighted by Zerbs *et al.* in 2009[6] there will be small changes as to what the optimum choice of fluence will be depending on what set up is being employed as a result of the optical set up and gate width being used in the LII collection.

It is therefore important before making any measurements to investigate what fluence is best to use. This is especially important in the work where multiple excitation wavelengths will be used. In order for the subtraction of the signal from 1064 nm from

the signal obtained for other excitation wavelengths to be valid it is important that the particles are being heated to the same temperature by each of the excitation wavelengths[7].

It has been shown in numerous papers that as the fluence increases the LII signal also increases, that is until around the point where sublimation of the particles begins to occur[2, 3, 7-15]. After this point there is a plateau region or a region of slow decrease. This is the optimal place to make LII measurements as small fluctuations in the laser power, or any attenuation of the beam, will not greatly impact the signal[16], however it is important to choose a fluence as close to the beginning of the plateau as possible in order to minimise the effect of mass loss to sublimation.

In order to identify an optimal fluence, a "fluence curve" was created by plotting the LII intensity 200 ns after the Q-switch trigger, corresponding to around 100 ns after the peak LII signal, against the fluence being used. By using the signal after a delay, rather than at the peak, ensures there is no interference in the signal from short lived fluorescence. However, in doing so the peak LII signal shifts from a higher to lower fluence, meaning that in order to ensure the LII signals were correct, and that sublimation was occurring at the fluence expected, the fluence obtained at the peak had to first be examined as shown in Figure 3-12. The fluence was changed by altering the Q-switch delay, allowing for a steady increase in fluence used. This was carried out for all excitation wavelengths in order that the same point on the fluence curves could be used for each measurement ensuring particle heating was consistent for the different excitation wavelengths.

This showed that the signal reached a maximum at around 430 mJ cm^{-2} which corresponds to what has been seen in the literature. This confirms that sublimation is occurring at after this point and as such a fluence greater than this must be used for incandescence measurements.

Figure 3-12 also shows the fluence for 1064 nm excitation in a flame with a stoichiometry of 2.1 at a height of 15 mm observed 200 ns after the Q-switch trigger.

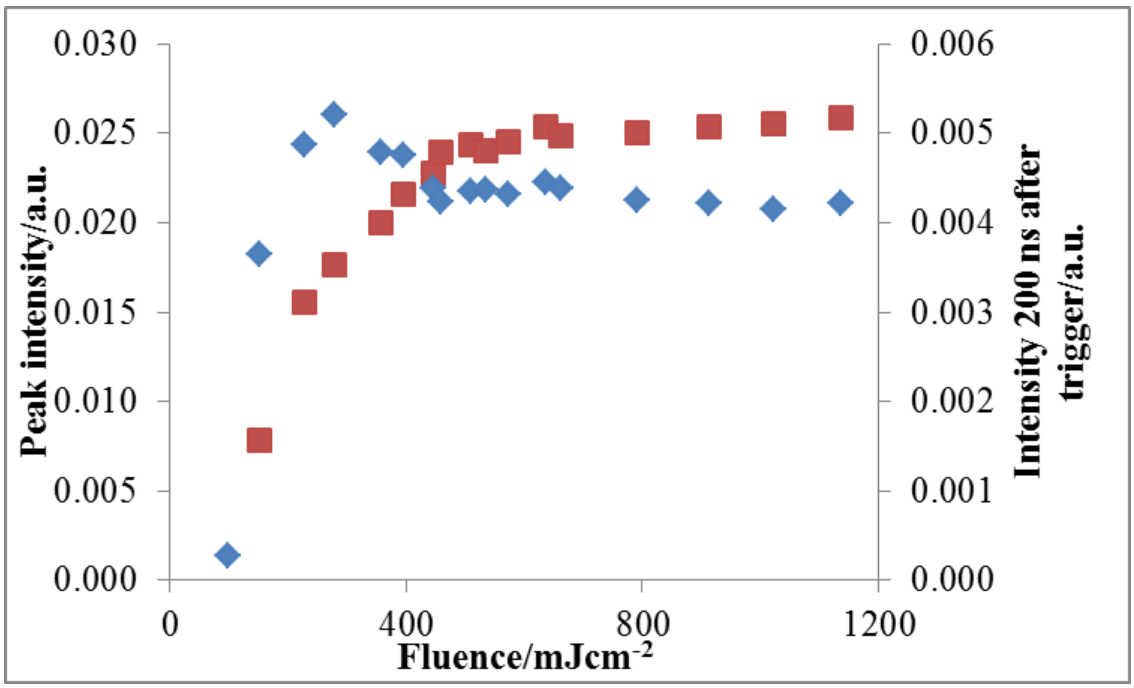

Figure 3-12 : Intensity at peak (■) and 200 ns after the laser trigger (♦) Φ = 2.1, HAB = 15 mm, λ_{ex} = 1064 nm

As can be seen there is a shift in the maximum value to just over 200 mJ cm^{-2}. The plateau region is clearly seen and this is matched to the plateau region seen for 532 nm excitation. This process was repeated with 532 nm and 283 nm excitation wavelengths, which are shown below in Figure 3-13 and Figure 3-15 plotted alongside the 1064 nm data. For ease of comparison and to eliminate the effect of any small changes to the detection setup between these measurements the signals have been normalised so that the peak signals are equal.

From this it can be seen that the plateau region of the LII signal when exciting with 532 nm is at around 220 mJ cm^{-1}, which is as would be expected[10] as at fluences greater than this the particle will undergo sublimation[1]. Hence in order to heat the particles to the same temperature fluence of 480 and 280 mJ cm^{-1} were used with 1064 nm and 532 nm respectively.

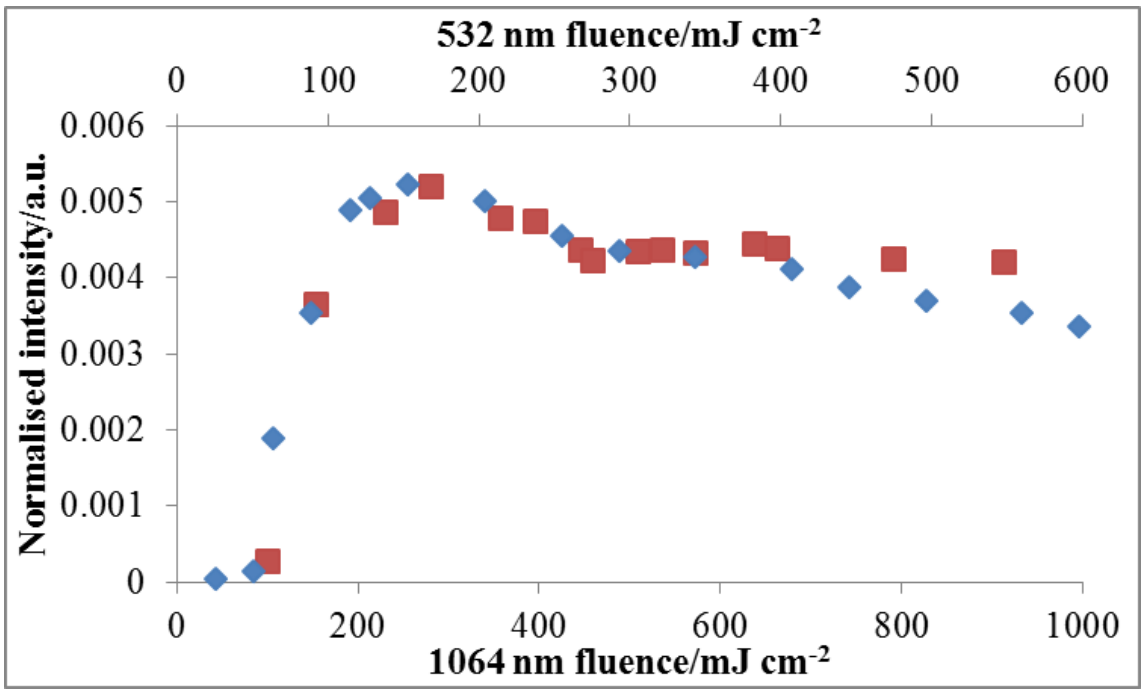

Figure 3-13 : Intensity after 100 ns Φ = 2.1, HAB = 15 mm, λ_{ex} = 1064 nm (■) and λ_{ex} = 532 nm (♦)

Due to constraints with the equipment it was not possible to increase the power and obtain a full fluence curve for the 283 nm excitation, with a maximum obtainable fluence of 127 mJ cm^{-2}. A telescope could have been used to reduce the beam diameter before passing through the pin-hole to increase the fluence but this would have led to a poorer top-hat spatial profile. However, the difference between the 283 nm curve obtained and the 532 nm and 1064 nm curves are consistent with what would be expected with the fluence required to reach sublimation with 283 nm lower than the fluence required for 532 nm[7, 17]. In order to show the fluence on the same axis the 532 nm and 283 nm fluences were multiplied by 1.84 and 2.00 respectively.

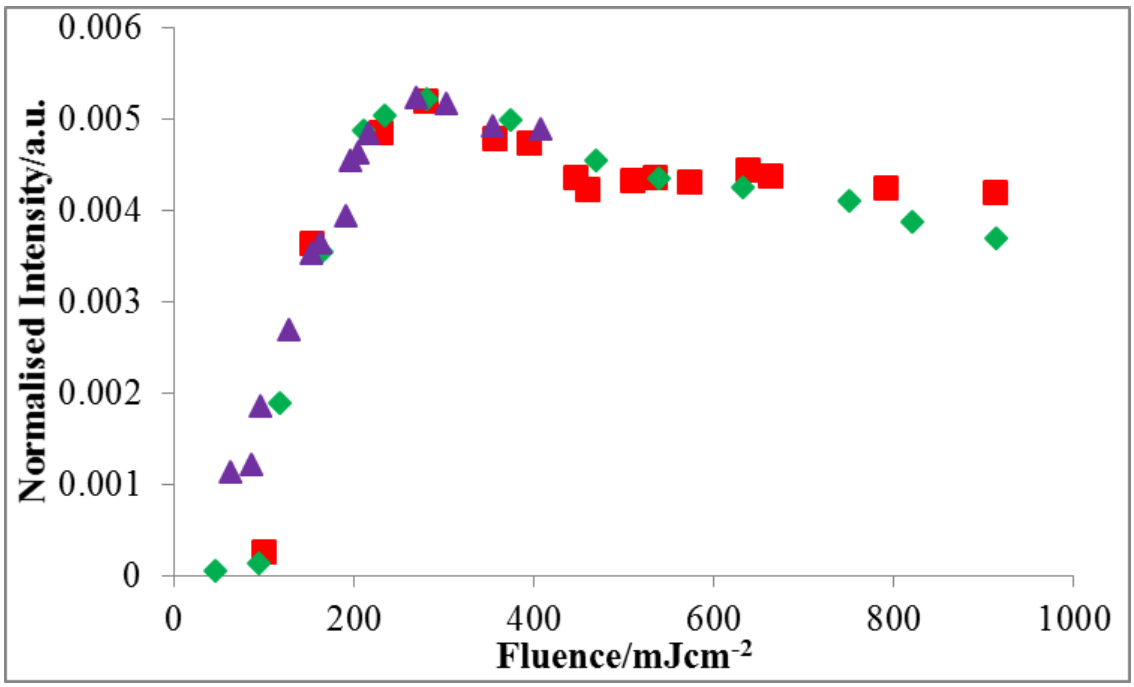

Figure 3-14 : Intensity after 200 ns Φ = 2.1, HAB = 15 mm, λ_{ex} = 1064 nm (■), 532 nm (♦) and 283 nm (▲)

Therefore a fluence of 127 mJ cm^{-1} was chosen for use. This ensured that the particles were being heated in the same way as the particles being heated with 532 nm or 1064 nm light. In this way the incandescence decay for each should be equal, allowing for the subtraction of the 1064 nm signal from that of the 532 nm and 283 nm.

By normalising fluence curves to the highest fluence which are taken for a range of heights above burner there is no clear evidence of a variation in shape, Figure 3-15

These curves were taken over a smaller range of fluences than those shown in previous figures, and therefore it appears the peak signal is at an earlier fluence. This would not be the case, as would be seen if smaller fluence incrementaitons had been used. As can be seen the shape appears to be the same over a range of heights above the burner. This suggests that the particles are being heated in the same way and therefore that the physical properties of the soot appear no to be changing substantially over this range of heights above burner. It has been highlighted in the literature that this may not be the

case for fluences over the range of heights above burner but this is clearly shown not to be the case in this work.

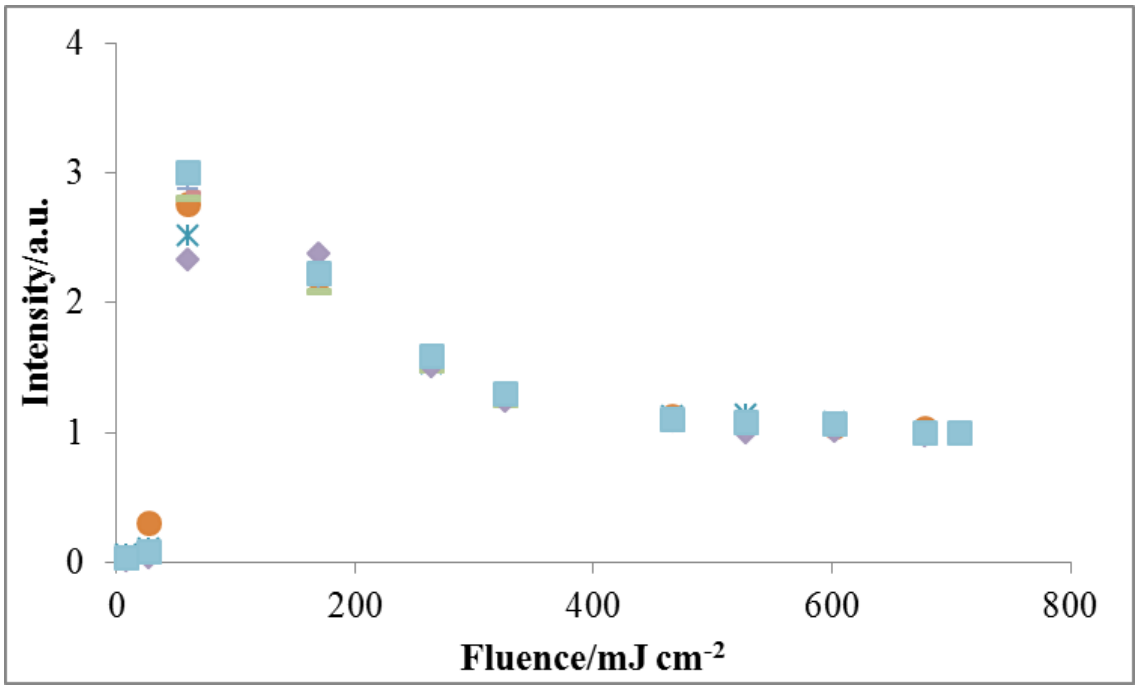

Figure 3-15 : Intensity 200 ns after the Q-switch trigger normalised to maximum fluence where Φ = 2.1, HAB = 9 – 15 mm, λ_{ex} = 532 nm

3.7 DATA OBTAINED

Throughout this work care was taken to be both methodical and thorough in order to obtain a robust measurement set. The following table outlines the measurements that were taken along with the number of repeat measurements

Table 3 : Signals recorded using detection set-up I

Flame condition (Φ)	Wavelength of excitation	Heights above burner	Repeats
2.1	1064 nm	0 mm – 15 mm	4
	532 nm	0 mm – 15 mm	8
	283 nm	0 mm – 15 mm	4
2.0	1064 nm	0 mm – 15 mm	4
	532 nm	0 mm – 15 mm	8
	283 nm	0 mm – 15 mm	4
1.9	1064 nm	0 mm – 15 mm	4
	532 nm	0 mm – 15 mm	8
	283 nm	0 mm – 15 mm	4
1.8	1064 nm	0 mm – 15 mm	4
	532 nm	0 mm – 15 mm	8
	283 nm	0 mm – 15 mm	4
1.7	1064 nm	0 mm – 15 mm	4
	532 nm	0 mm – 15 mm	8
	283 nm	0 mm – 15 mm	4

Table 4 : Signals recorded using detection set-up II

Flame condition (Φ)	Wavelength of excitation	Heights above burner	Repeats
2.1	1064 nm	10 mm and 15 mm	2
	532 nm	10 mm and 15 mm	2
	283 nm	10 mm and 15 mm	2

2.0	1064 nm	10 mm and 15 mm	2
	532 nm	10 mm and 15 mm	2
	283 nm	10 mm and 15 mm	2
1.9	1064 nm	10 mm and 15 mm	2
	532 nm	10 mm and 15 mm	2
	283 nm	10 mm and 15 mm	2
1.8	1064 nm	10 mm and 15 mm	2
	532 nm	10 mm and 15 mm	2
	283 nm	10 mm and 15 mm	2
1.7	1064 nm	10 mm and 15 mm	2
	532 nm	10 mm and 15 mm	2
	283 nm	10 mm and 15 mm	2

3.8 DATA PROCESSING

The data which was obtained throughout the work shown here was recorded in one of two ways. When single measurements were made using set up 1 the light which passed through the filter and was incident on the detector was digitised by an oscilloscope. The data was saved on the oscilloscope. This worked by recording an average of 64 signals, triggered from the laser Q-switch, and saving them as a text file. The time window to save over was selected manually and restricted to around 2000 ns from the trigger. When saved in this way each new signal was saved as the filename_x, with x increasing with the signal number. This allowed a script to be written in order that the available files could be imported to Matlab and saved in one file, making the data easier to manipulate.

In order to record the signals which were obtained while employing set up 2 a method had to be developed to coordinate moving the grating in the monochromator (*i.e.*

changing to another detection wavelength) and acquiring the signal. This was achieved through use of a LabView programme which was custom written for this work. This worked by initially moving the grating to the desired detection wavelength before waiting for the trigger. In this case the trigger used was a photodiode which was placed near the exit slit in the laser shielding. The average of 64 signals obtained was recorded. This resulted in huge amount of data and therefore, in order to make the data more manageable, the data was cropped (to 2000 ns after the trigger) prior to being saved as a data file. Since it was known from previous work that the signal would be expected to decay within a few hundred nanoseconds this was considered a more than ample signal length to record.

3.9 REFERENCES

1. F. Goulay, P. E. Schrader, L. Nemes, M. A. Dansson and H. A. Michelsen, *Proceedings of the Combustion Institute*, 2009, **32**, 963-970.
2. C. Schulz, B. F. Kock, M. Hofmann, H. Michelsen, S. Will, B. Bougie, R. Suntz and G. Smallwood, *Applied Physics B-Lasers and Optics*, 2006, **83**, 333-354.
3. B. Axelsson, R. Collin and P. E. Bengtsson, *Applied Optics*, 2000, **39**, 3683-3690.
4. H. Bladh, J. Johnsson and P. E. Bengtsson, *Applied Physics B-Lasers and Optics*, 2009, **96**, 645-656.
5. S. A. Lawton, *Combustion Science and Technology*, 1988, **57**, 163-169.
6. J. Zerbs, K. P. Geigle, O. Lammel, J. Hader, R. Stirn, R. Hadef and W. Meier, *Applied Physics B-Lasers and Optics*, 2009, **96**, 683-694.
7. C. S. Moreau, E. Therssen, X. Mercier, J. F. Pauwels and P. Desgroux, *Applied Physics B-Lasers and Optics*, 2004, **78**, 485-492.

8. J. Delhay, Y. Bouvier, E. Therssen, J. D. Black and P. Desgroux, *Applied Physics B-Lasers and Optics*, 2005, **81**, 181-186.
9. H. Bladh and P. E. Bengtsson, *Applied Physics B-Lasers and Optics*, 2004, **78**, 241-248.
10. H. Bladh, P. E. Bengtsson, J. Delhay, Y. Bouvier, E. Therssen and P. Desgroux, *Applied Physics B-Lasers and Optics*, 2006, **83**, 423-433.
11. G. Cleon, T. Amodeo, A. Faccinetto and P. Desgroux, *Applied Physics B-Lasers and Optics*, 2011, **104**, 297-305.
12. C. R. Shaddix and K. C. Smyth, *Combustion and Flame*, 1996, **107**, 418-452.
13. S. De Iuliis, F. Migliorini, F. Cignoli and G. Zizak, *Applied Physics B-Lasers and Optics*, 2006, **83**, 397-402.
14. P. E. Bengtsson and M. Alden, *Applied Physics B-Lasers and Optics*, 1995, **60**, 51-59.
15. P. Desgroux, X. Mercier, B. Lefort, R. Lemaire, E. Therssen and J. F. Pauwels, *Combustion and Flame*, 2008, **155**, 289-301.
16. R. L. Vander Wal and K. A. Jensen, *Appl. Opt.*, 1998, **37**, 1607-1616.
17. E. Therssen, Y. Bouvier, C. Schoemaecker-Moreau, X. Mercier, P. Desgroux, M. Ziskind and C. Focsa, *Applied Physics B-Lasers and Optics*, 2007, **89**, 417-427.

4 IMPACT OF EXCITATION WAVELENGTH ON THE ACCURACY OF LASER INDUCED INCANDESCENCE MEASUREMENTS OF SOOT VOLUME FRACTION

In order that LII measurements are effective and reliable it is important to minimise any interferences which may occur during the measurement. A significant source of interference is the result of laser induced fluorescence of PAHs in the measurement volume.

There are two approaches which are commonly taken to eliminate fluorescence in LII measurements: either use of an excitation wavelength which will not induce fluorescence at the detection wavelength; or the measurement is taken at a suitable time after the signal onset in order that the fluorescence (which has a shorter lifetime than incandescence) will have completely decayed. It is shown in this chapter that fluorescence contributes significantly to the recorded signals if the excitation wavelength is not considerably longer than the detection wavelength.

Ideally, the first method will be employed and an excitation wavelength such as 1064 nm is employed together with a detection wavelength in the visible spectral region. However, it is often advantageous to maximise the information which can be obtained from one measurement by carrying out simultaneous light scattering measurements, for which a visible wavelength of light, such as 532 nm, must be used. There is also the added benefit of ease alignment when using visible wavelengths, which can make them a favourable choice in complex set-ups. Although it is known that there can be interference from fluorescence at the peak of the LII signal there are still measurements seen in the literature where the peak signal obtained with 532 nm excitation is used. The early part of this chapter shows the impact of using the peak signal, even if the detection wavelength is below the excitation wavelength where it would not be expected that large amounts of fluorescence would occur. This is achieved through comparison of the peak

signal obtained over a range of conditions with 1064 nm excitation being compared to the peak signal obtained over the same range of conditions with 532 nm excitation.

Due the possibility of fluorescence impacting the signal the second approach to minimise this, by recording the signal at a time after the trigger where fluorescence should have decayed, is often employed. When using the delayed signal approach care must be taken that information is not lost as a result of the delay time being too long, and equally a time where all of the fluorescence has decayed must be carefully selected. Either of these considerations being neglected could lead to degradation in the quality of data which is obtained. However, even with this in mind, there is little consistency shown within the literature of what is the ideal delay time and, if gated detection is being used, what the window should be.

Given the numerous examples in the literature of delayed detection it is perhaps surprising that this is the case and that little explanation beyond the delay time being after the fluorescence has decayed is given. The initial part of this chapter aims to begin to address this by looking carefully at the signal which is given for each of the approaches which have been outlined.

By examining the signal recorded at the peak with 1064 nm excitation and comparing with the signals recorded 200 ns after the Q-switch trigger with 532 nm excitation. In both cases the signal will be attributable only to incandescence but a difference can be seen in the signal which is obtained after a delay due to the effects which particle size will have on the measurement, as larger particles will cool more slowly than smaller particles.

The impact of using an excitation wavelength shorter than the detection wavelength was then investigated. This was carried out with the hope that if successful it would demonstrate the ability highlight considerations which would need to be made in order to observe LII using a wavelength with could also be used for OH LIF. This was achieved by employing an excitation wavelength of 283 nm, well below the detection wavelength of 450 nm.

4.1 MEASUREMENT CONDITIONS AND CORRECT IDENTIFICATION OF LII SIGNAL

As discussed extensively in chapter 3 it is of the utmost importance to ensure that the measurements are being carried out under the optimal conditions. For successful measurements it is important to select a stable sooting flame which is reproducible and a fluence which is suitable for obtaining LII[1]. For this section of the work it was decided that the light which was being emitted from the flame, as a result of excitation, would be recorded at one wavelength, using set up I (as fully described in chapter 3). Due to the spectral bandpass of the filter, rather than the emitted light being detected at one distinct wavelength it was recorded over a small range of wavelengths according to the bandwidth of the filter, which was 450 ± 10 nm FWHM. The other conditions which were chosen are fully described in chapter 3 and are summarised in Table 4-1.

Table 4-1 : Experimental conditions

Stoichiometry	1.7, 1.8, 1.9, 2.0, 2.1
Excitation wavelength/fluence	283 nm 127 mJ cm^{-2}
	532 nm 280 mJ cm^{-2}
	1064 nm 480 mJ cm^{-2}
Fuel	Ethylene
HAB range	"0" mm (burner surface) to 15 mm
Detection wavelength	450 ± 10 nm

These conditions allowed for the maximum amount of information to be obtained for a sooting flame in the burner which was available in the laboratory. The maximum height was chosen in order that the signal could be obtained in a consistent way without the build-up of soot on the stabilisation plate interfering with the measurement. The stoichiometries chosen were over a range where the flame was sooting and could be stabilised when the total flow rate was kept constant. These conditions were used for all of the work which is presented in this chapter.

4.1.1 Normalisation of signal

As the results which are presented in this chapter were gathered over a period of months small changes arose due to minor differences in the set-up. In order to account for this all of the measurements which are taken are normalised so that the signal for $\Phi = 2.1$ at 15 mm above the burner surface for any given excitation wavelength is equal to one 200 ns after the Q-switch trigger. The signals for the other stoichiometries are corrected by the factor which is used for the $\Phi = 2.1$ signal for each excitation wavelength.

This was considered acceptable as in later measurements, which will be shown in chapter 6, the signals were recorded over a much shorter timeframe without having to move the set-up and there was quantitative agreement between the signals recorded for all three wavelengths. This was as would be expected as the fluence was carefully chosen in order that the particles would be heated to the same temperature at any given point in the flame irrespective of the excitation wavelength. As such with the normalisation being carried out at 200 ns after the Q-switch trigger it is in a region where there should be no fluorescence and as such the signals should be equal.

4.2 HEIGHT ABOVE BURNER MEASUREMENTS

The temporal decay of emitted incandescence is dependent upon the size of the particle since smaller particles cool more rapidly than larger ones[2, 3]. The peak signal level is often considered to be linearly proportional to soot volume fraction[4]. Therefore, when taking measurements over a range of heights above the burner surface it would be expected that the signal would not only be more intense as the height of measurement is increased but that the signal would also have a longer decay time.

As has been discussed, 1064 nm is a favourable excitation wavelength since fluorescence at the detection wavelength is avoided and as such will be used as the reference case in the first part of the work described in this chapter. The signals which are obtained from 1064 nm excitation are compared to those obtained with 532 nm and 283 nm. The signals obtained upon excitation with 532 nm and 283 nm have a higher signal initially, under the same flame conditions, due to fluorescence.

4.2.1 Calibration of results

Without suitable calibration LII is only useful as a qualitative technique. While useful information can still be obtained without calibration the information which is gathered can only be considered on a relative basis. For example if the intensity increases there are more of the particles or larger particles present. This though is only relative to an arbitrary point where the first measurement is made and the change cannot be quantified.

However, by calibration the information which is obtained can become much more useful. If the soot volume fraction is identified then it can be seen in which regions of the flame there is a higher soot concentration, either due to there being more soot particles or due to there being larger soot particles. Since the particle size can be calculated there can be the development of a more complete picture of what is happening in the flame.

In order to calibrate the LII measurements which have been made in this work the classic technique of light extinction was used[13, 15-17]. In order to carry this out the power from the laser was measured before and after the flame at each height in the flame where $\Phi = 2.1$.

In order to obtain the calibration for the soot volume fraction the intensity of the excitation laser light was measured before and after the flame using a power meter, Figure 4-4.

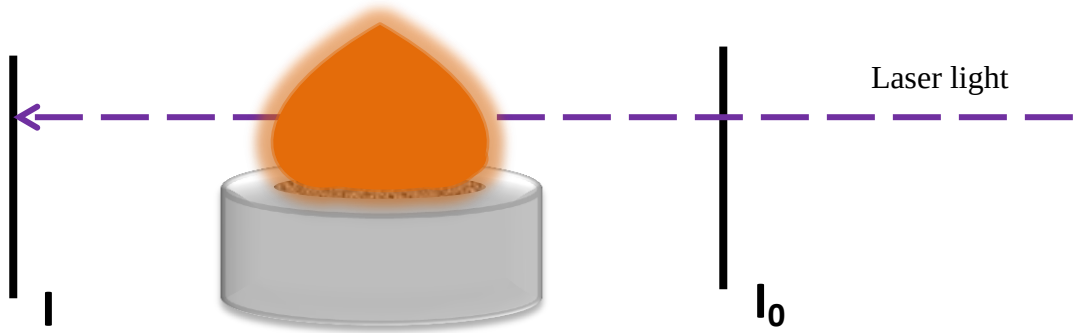

Figure 4-1 : set up for light extinction measurement

By making measurements in this way it is possible to calculate the light extinction which occurs as the light passes through the flame according to Figure 4-1.

$$ln\frac{I_T}{I_0} = -k_{ext}d$$

Equation 4-1

Where I = transmitted (therefore attenuated) light intensity

I_0 = incident light intensity

d = optical path length

k_{ext} = extinction coefficient

By employing the extinction coefficient, and assuming that the soot particles have a radius which is less that the wavelength of light being employed, the soot volume fraction, f*v*, can be calculated, Figure 4-2. This theory relies upon the assumption that the extinction coefficient is largely equivalent to the absorption coefficient.

$$k_{ext} \approx k_{abs} = f_v \frac{6\pi E(m)}{\lambda}$$

Equation 4-2

Where k_{abs} = absorption coefficient

fv = soot volume fraction

$E(m)$ = soot absorption function

λ = laser wavelength

As highlighted by Smyth and Shaddix in 1996 there has historically been an issue with the soot absorption function which is being used[18]. This arose from the misapplication of the soot refractive index value which was obtained by Dalzell and Sarofim in 1969[19]. This lead to the majority of papers working in the visible wavelength to quote soot refractive index as being $\bar{m}$ = 1.57 – 0.56i. To further complicate matters even although this has been brought to the attention of the community this value is still used as it makes it possible to compare new measurements to those which have been previously made. For this study the value used by Axelsson *et al.*[6, 20] of m = 1.56 – 0.46i which was used to calculate the soot volume fraction under similar flame conditions was chosen for use.

The calculated absorbance values which were obtained through this method with 1064 nm excitation where Φ = 2.1 are shown in Figure 4-2.

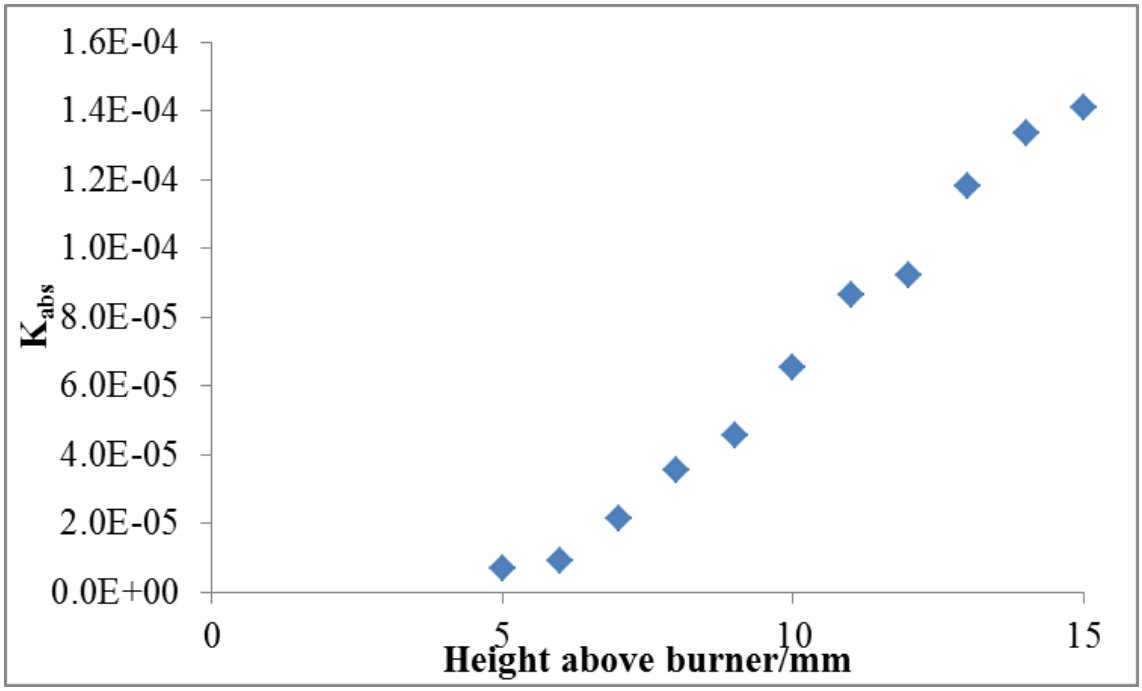

Figure 4-2 : Light extinction measured for 1064 nm excitation 5 – 15 mm above the burner surface in a flame where Φ = 2.1

As can be seen there are no values below 5 mm in the flame, this is due to there being no change between the power measured before and after the flame. This could be due to the power meter not being sensitive enough to measure the small change. This agrees with what has been shown above - that there is extremely little, if any incandescence below this point – suggesting no soot being present, which would mean absorbance of the laser light would be very low.

This could be compared to the incandescence signal which was obtained in the same flame with 1064 nm excitation (as shown in section 4.2.2), Figure 4-3.

It can be seen that the calculated soot volume fractions largely agree, within error, with the incandescence signal which was obtained. This means that all of the incandescence signals which have been obtained can be related to the soot volume fraction by using the

scale presented above. This is useful for illustrating by how much the soot has grown between two heights in the flame.

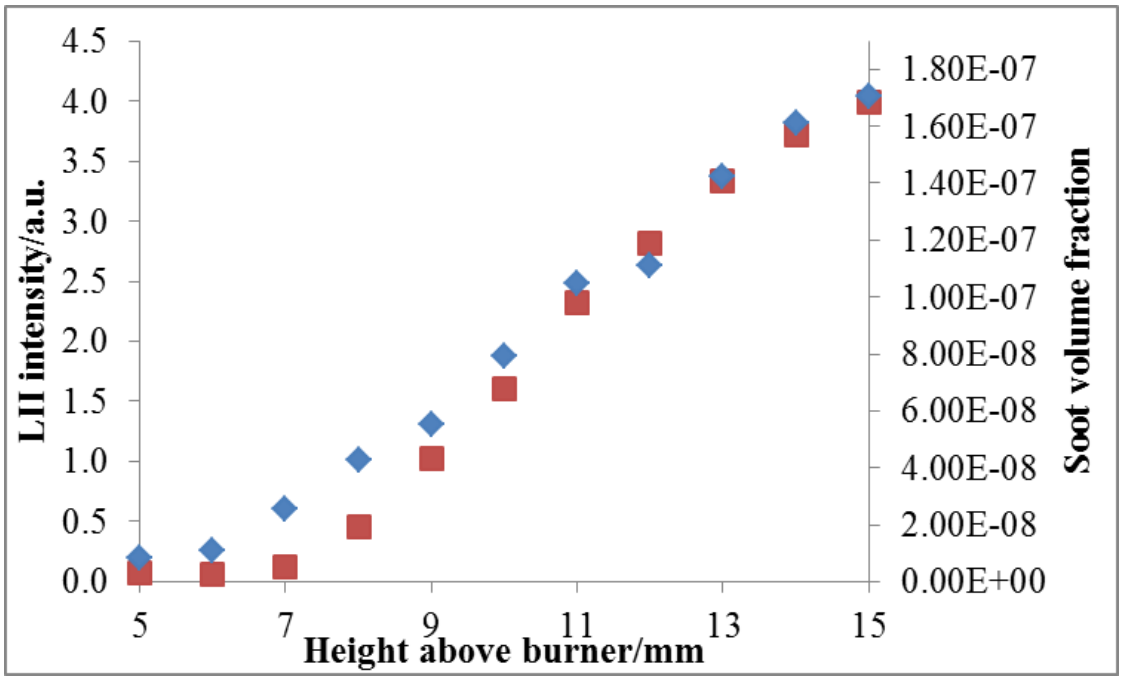

Figure 4-3 : Light extinction measured for 1064 nm excitation 5 – 10 mm above the buner surface in a flame where Φ = 2.1 (♦) and peak LII signal recorded for excitation with 1064 nm (■) in the same flame

4.2.2 Excitation with 1064 nm light

Since the burner which is employed for this work is a flat flame burner then the particles would grow as they proceed downstream and no incandescence signal is therefore expected at lower heights. The incandescent signal will increase, both in intensity and decay time, as the measurement height increases. This increase will slow and may, if the measurement height is high enough, begin to decrease if oxidation becomes a competing process[5].

Therefore to illustrate this and to investigate the flame which would be used in this work the emitted signal upon excitation with 1064 nm of light was recorded at 1 mm intervals over a range of 0 – 15 mm above the burner surface. Initially the stoichiometry used was 2.1 because as the highest sooting flame this would give the highest incandescence signal. Each signal was averaged 64 times before recording and each signal was recorded 8 times, before the average was taken. The peak signal was then plotted as a function of height above burner, Figure 4-4, with the error bars showing the standard deviation of the 8 signals recorded. In order that any fluctuations in the baseline did not effect the measured intensities the baseline before the peak was averaged and subtracted from the signal.

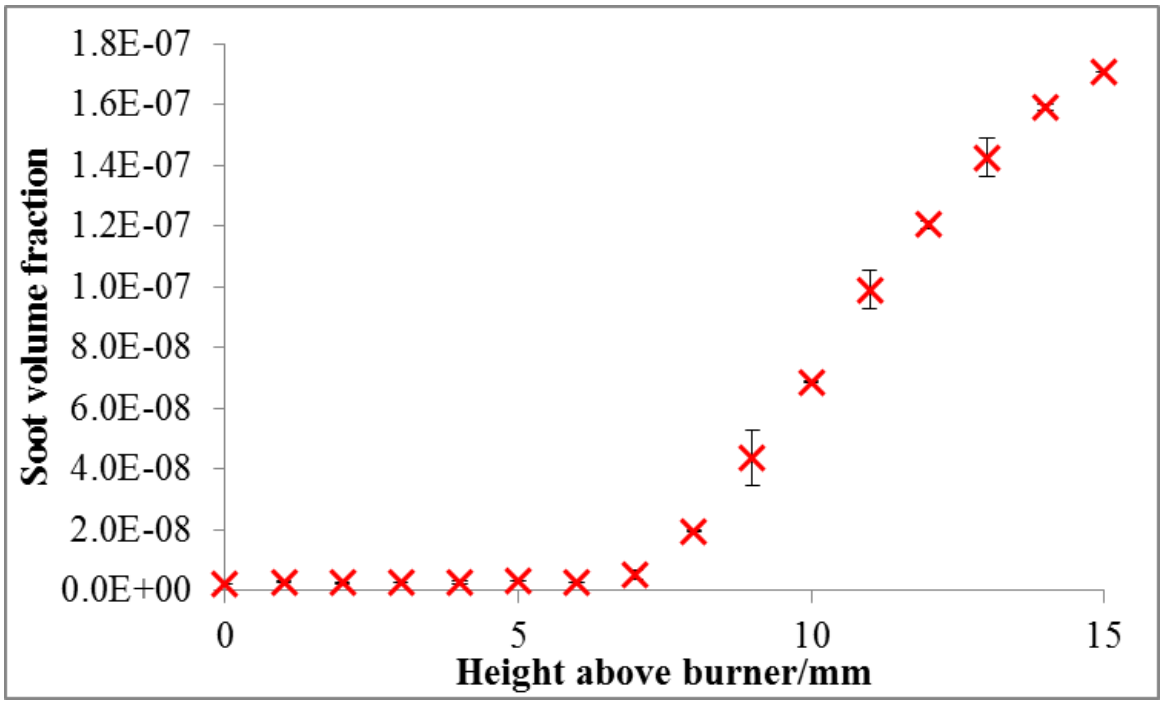

Figure 4-4 : Peak emitted intensity recorded over range of heights above burner from 0 to 15 mm for 1064 nm excitation in flame with stoichiometry Φ = 2.1. The error bars shown correspond to the standard deviation obtained from the four signals averaged to obtain each point shown

Initially it is seen that the standard deviation at each height above burner is small. As a percentage it is always less than 6 % of the sample. This confirms that the flame is stable and that the measurement is both repeatable and reliable.

It can be seen that, as would be expected, the incandescence signal increases as the measurement height is increased. Below a height of 6 mm there is no signal detected under these conditions. This suggests that there is no particulate material present at this height in the flame which is large enough to incandesce and the 1064 nm light not inducing any fluorescence in any PAHs which are present. By visually examining the flame this corresponds with what would be expected as it can be seen that there is no orange colour lower in the flame, Figure 4-5. This orange glow is characteristic of there being particulate material in the flame which is large enough to incandesce.

Figure 4-5 : Flame where Φ = 2.1. In orange region soot is present

As the signals obtained for Φ = 2.1 were successful and were as would be expected the study was expanded to include the range of target flames which had been identified – Φ = 1.7, 1.8, 1.9 and 2.0. Therefore, the above measurement was repeated with these flame conditions and again the peak signal intensity for each condition over the range of heights above burner plotted, Figure 4-6

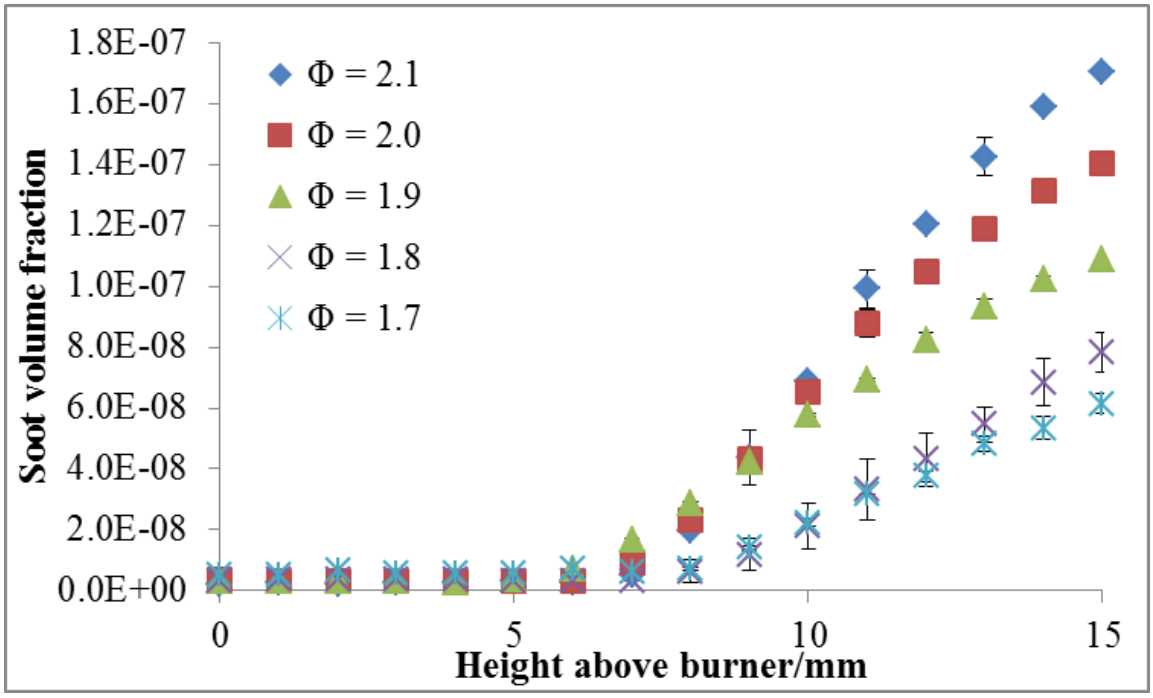

Figure 4-6 : Peak emitted intensity recorded over range of heights above burner from 0 to 15 mm for 1064 nm excitation in flame where Φ = 1.7, 1.8, 1.9, 2.0 and 2.1

As can be seen upon decreasing the stoichiometry the absolute intensity at a given height above burner also decreases. This is as would be expected as there is less fuel in the flame and there will either be larger particles or more particles as the stoichiometry increases. This can be further investigated by comparing the decay times of the signals, as if the decay times are equivalent there are simply more particles but if there is an

increase in decay times the particles are also larger in size[6]. This will be further discussed in chapter 5.

For all flame conditions there is no signal below 5 mm suggesting that in none of the flame conditions outlined is there any particulate material large enough to incandesce in this region. This is as we would expect as after the initial breakdown of soot there will be a region of gaseous PAHs (which will not incandesce) and it will not be until these particles reach a larger size of a few hundred amu that there will be any potential for them to incandesce. It can be hypothesised that if this is indeed the case within the flame, and that if the soot growth is sequential, that upon exciting the particles with a shorter excitation wavelength there should be signal in the region prior to incandescence which is attributable only to fluorescence. In order to further investigate the above was repeated using 532 nm excitation.

It can also be seen that the signal for Φ = 1.7 and 1.8 the signal is much lower after 7 mm than the signals obtained for Φ = 1.9, 2.0 and 2.1. This suggests that there is either more soot or soot of a larger size forming at 7 mm for Φ = 1.9, 2.0 and 2.1 than Φ = 1.7 and 1.8. The signal for Φ = 1.9, 2.0 and 2.1 the signals are similar until 10 mm, suggesting in the early stages of soot formation there is much the same growth for these flames.

4.2.3 Excitation with 532 nm light

It is known that upon excitation with 532 nm part of the signal is attributable to fluorescence. Although this is well known it is still common for 532 nm to be used for incandescence measurements due to the ability to make simultaneous light scattering measurements, the ease of access to this wavelength of light in many laboratories[7] and the ease of alignment it gives. As a result of this fluorescence contribution, if 532 nm is being used as the excitation wavelength a more careful approach must be taken to the evaluation of soot volume fraction based on recorded signals. Two possible approaches are available and the signal either gathered at a time after the laser pulse where it is

assumed the fluorescence will have decayed or the signal should be recorded in a region where the signal should not have a fluorescence contribution. The latter is an unreliable method this is shown to be the case with measurements recorded using a bandpass filter.

In order to illustrate the large effect which the fluorescence contribution can have the measurements which were made with 1064 nm excitation wavelength were repeated using 532 nm of light, Figure 4-7

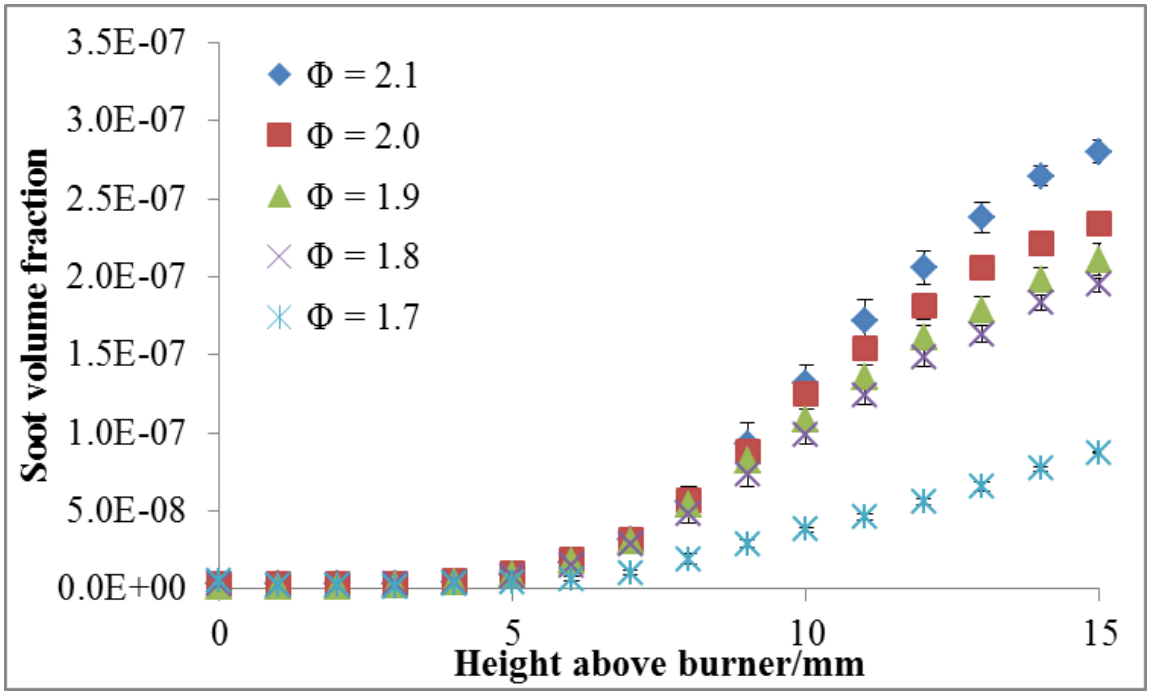

Figure 4-7 : Peak emitted intensity recorded over range of heights above burner from 0 to 15 mm for 532 nm excitation in flame over range of stoichiometries Φ = 1.7, 1.8, 1.9, 2.0 and 2.1

Here it can be seen that the increase in peak signal is not constant. This can only be attributed to the inclusion of LIF in the signal. This shows that although the detection wavelength being employed is shorter than that of the wavelength of excitation, and hence it may be expected that there will be no fluorescence contribution to the signal,

this is not the case. As has been previously stated in PAHs due to the high levels of conjugation the electronic energy levels are closely spaced. This results in thermal population will being in a state higher than the ground state. This makes it possible that excited electrons falling to the ground state are losing higher amounts of energy than they gained through excitation. As a consequence of this it is possible for the fluorescence to occur at a wavelength which is shorter than the wavelength of excitation.

This displays why, when exciting with shorter wavelengths of light, the peak signal is not suitable for use as a representation of the amount of incandescence being emitted. Therefore for the calculation of soot volume fraction, where it is usual for the peak signal to be used, it is advisable to use a long wavelength of excitation light.

It can also be seen that there is a signal, albeit small, from 5 mm. This can be attributed to small molecules fluorescing, as although the same flame conditions are used no signal is recorded in this region upon excitation with 1064 nm light.

This can be further seen in Figure 4-8 where the signal with 1064 nm and 532 nm of light are compared to each other with the differences between the signals being great in some cases.

The difference between the 1064 nm excitation and 532 nm excitation is clearly seen, with the greatest difference seen at higher stoichiometries. As has been discussed this difference will be attributable to the fluorescence in the signal. It can also be seen that there is a signal for 532 nm excitation at a lower height in the flame than is seen with 1064 nm excitation. This would be as expected since as the particles grow from gaseous to solid soot particles they will fluoresce before they are of sufficient mass to incandesce.

By looking at the peak of the LII signal it can be seen that even though the detection wavelength is less than 532 nm there is a contribution to the signal which is due to fluorescence. Since fluorescence is a short lived process it would be expected that this will have decayed after tens of nanoseconds, i.e. in a much shorter time than incandescence.

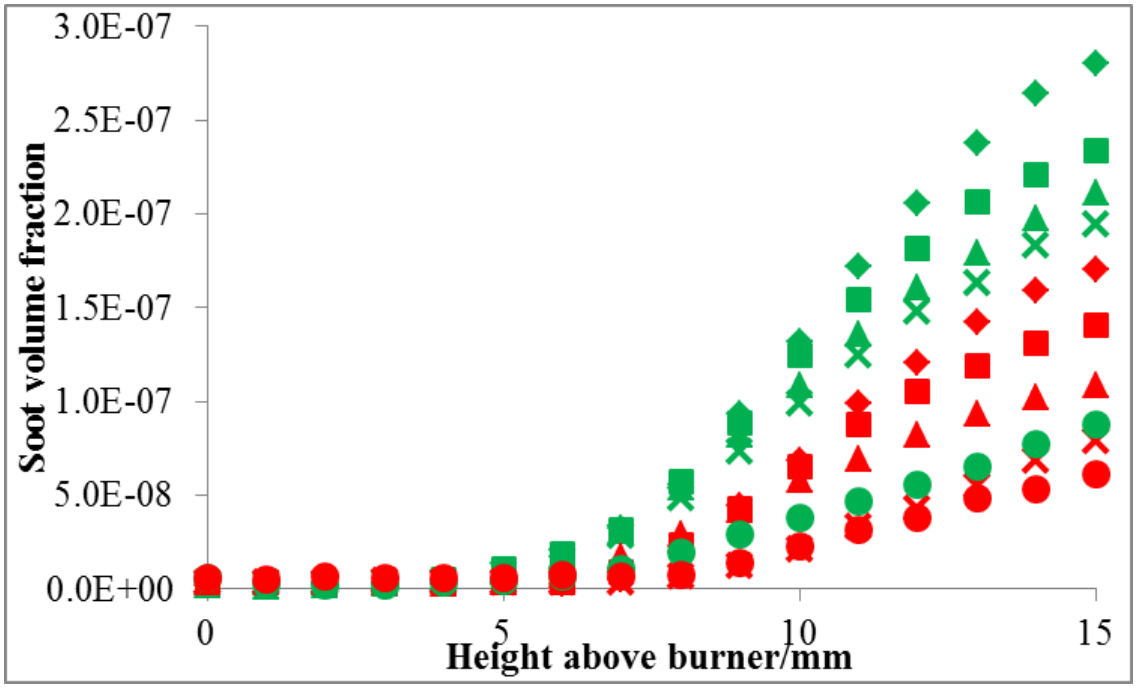

Figure 4-8 : Comparison of peak emitted intensity recorded over range of heights above burner from 0 to 15 mm for 1064 nm (red) and 532 nm (green) excitation in flame over range of stoichiometries Φ = 1.7 (●), 1.8 (x), 1.9 (▲), 2.0 (■) and 2.1(♦)

By examining the decay of the signal obtained in a flame with a stoichiometry of 2.0 with each of the excitation wavelengths it can be clearly seen that any difference which occurs in the signal does so in the first 50 ns, Figure 4-9. The ripples which are seen on the signal are as a result of an electrical pick up and can therefore be ignored.

It can be seen that by 200 ns after the Q-switch trigger the signals are equal, and therefore attributable only to incandescence.

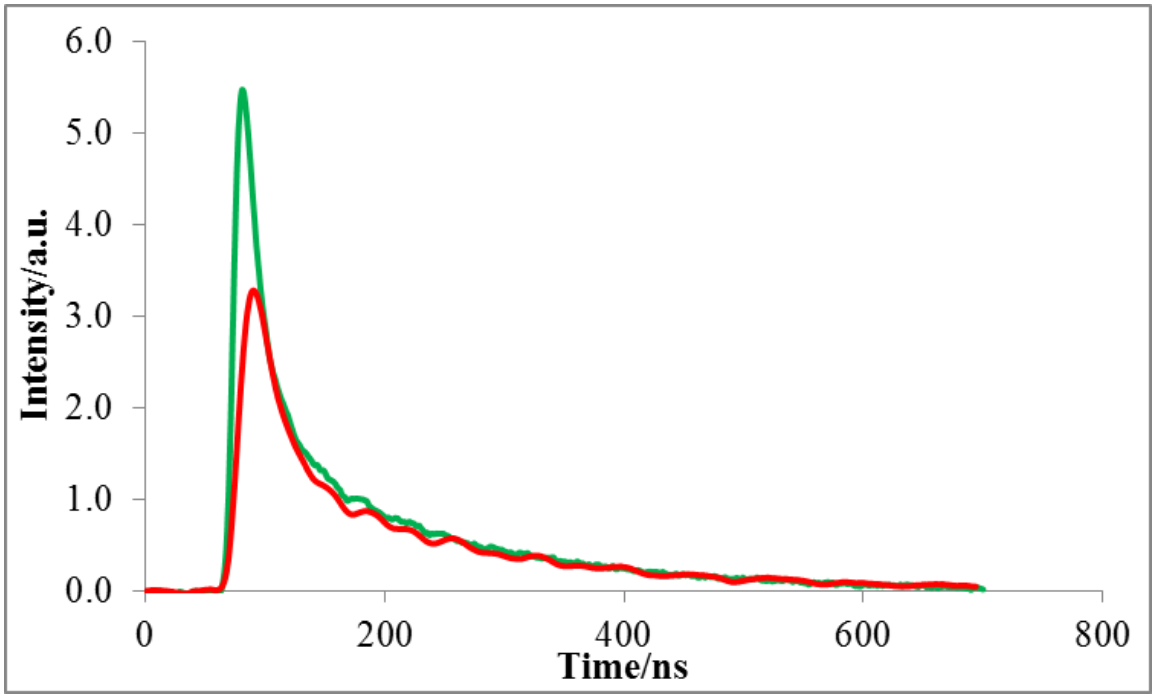

Figure 4-9 : Comparison of decay profile obtained with 532 nm and 1064 nm excitation 15 mm above the burner surface where Φ = 2.0

In order to determine whether this was consistently the case the signal was potted at all heights above the burner, both at the peak and 200 ns after the Q-switch trigger, Figure 4-10

As can be seen at all heights in the flame there is a clear separation between the peak signals where for all heights the signal after 200 ns is equal. The difference between these signals can therefore be attributed to fluorescence. It can be seen that if the 532 nm signal at the peak was used to evaluate the soot volume fraction very different results would be obtained. It is for this reason that delayed detection is often employed when exciting with 532 nm of light.

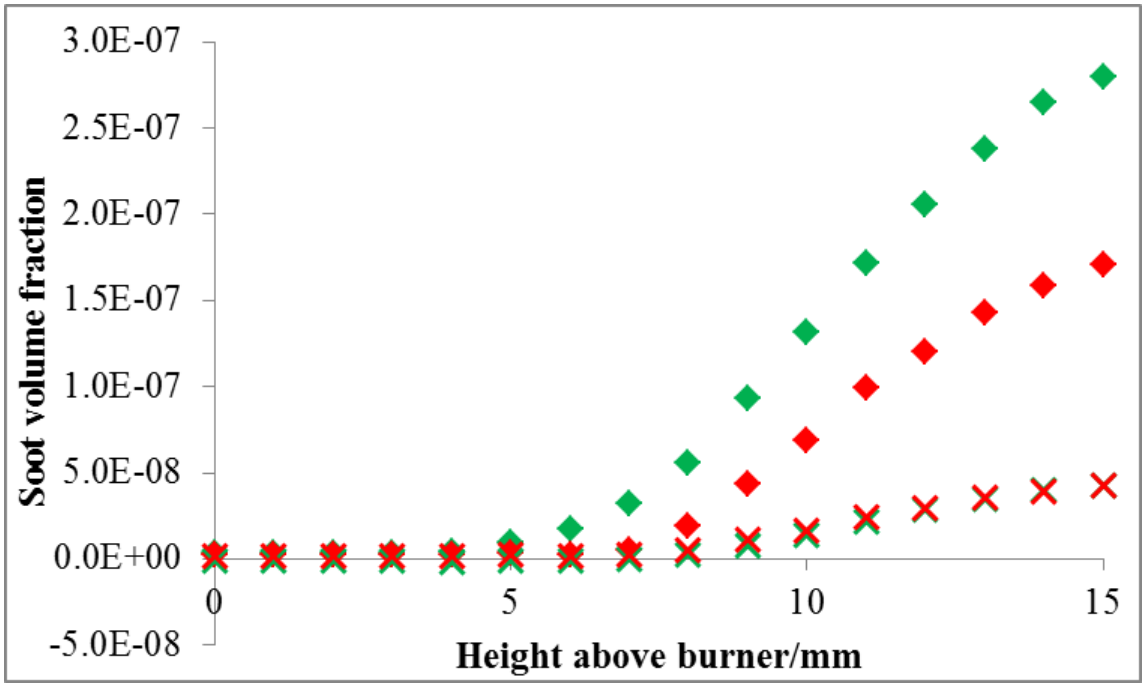

Figure 4-10 : Peak signal (♦) and signal 200 ns after the Q-switch trigger (x) where Φ = 2.1 with 532 nm (green) and 1064 nm (red) excitation over height above burner 0 – 15 mm

Similarly this can be plotted for all of the stoichiometries which were employed, Figure 4-11 - Figure 4-14

It can be seen here that a difference is seen in the fluorescence contribution between the different stoichiometries. It can also be seen that there is little incandescence until around 9 mm above the burner surface in the cases for Φ = 1.8 and 1.7. This highlights that in these cases there is no soot or PAHs which are large enough to fluoresce at these heights between 6 mm and 9 mm. This again highlights a difference in the soot volume fraction between the different stoichiometries.

Since a clear difference can be seen between the peak signal obtained for 1064 nm excitation and 532 nm excitation this offers the possibility to comment on the fluorescence which is present in the signal. This will be expanded upon and discussed fully in chapter 5.

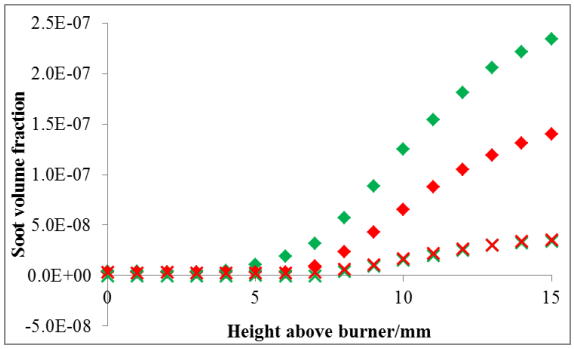

Figure 4-11

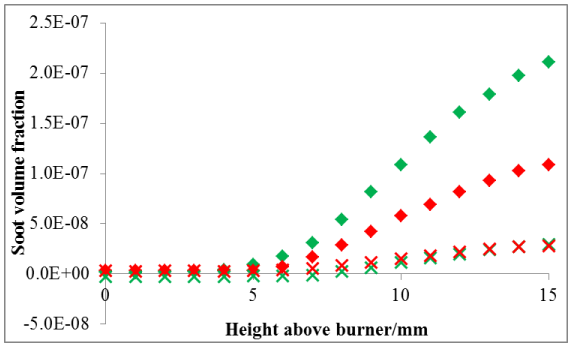

Figure 4-12

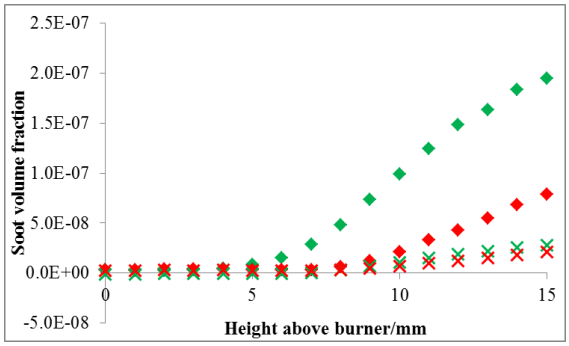

Figure 4-13

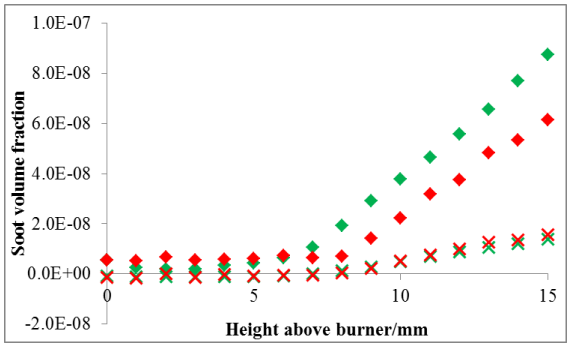

Figure 4-14

Figure 4-11 - Figure 4-14: Peak signal (♦) and signal 200 ns after the Q-switch trigger (x) where Φ = 2.0 – 1.7 with 532 nm (green) and 1064 nm (red) excitation over height above burner 0 – 15 mm

4.3 IMPACT OF SHORT WAVELENGTH USE FOR CALCULATING SOOT VOLUME FRACTION

As has been discussed previously there are two approaches to making LII measurements – prompt and delayed.

- PROMPT LII: The peak of LII signal or the value coinciding with the peak of the laser pulse is taken as representative of the LII signal. This method is used when it is unlikely that there will be interference from fluorescence and is generally employed with longer wavelengths of excitation light, e.g. 1064 nm. Prompt LII is used in order to obtain the soot which is present in a given measurement volume in the flame, that is the soot volume fraction[2, 9, 10].

- DELAYED LII: The signal is obtained over a small time range at a time, usually around 100 ns, after the laser pulse[8, 11, 12]. This method is used to eliminate any short lived interference which may occur at earlier times (i.e. as a result of fluorescence or stray light) and is generally used when short wavelengths of excitation are used, e.g. 532 nm. Delayed LII is used to obtain information about soot particle size.

Although it is well known that there is a fluorescence portion to any signal which results from the excitation of PAHs, and other small molecules, when short wavelengths of excitation are used, there are still many examples in the literature where signals resulting from short wavelengths of excitation light are used for calculating soot volume fraction[8]. This is often considered acceptable if the emitted light is recorded at a wavelength below that of excitation. However, as has been shown above there can be a significant fluorescence contribution to the LII signal even when the detection wavelength is lower than the excitation wavelength. Furthermore, the increase in fluorescence is not constant with the increase in incandescence, and therefore cannot be corrected for by a linear relationship and is not thus not insignificant.

By forcing the maximum signal, that is the signal obtained at 15 mm in the flame, to be equal for both excitation with 532 nm and 1064 nm, the issues surrounding the interference of fluorescence can clearly be seen, Figure 4.12 – Figure 4.16.

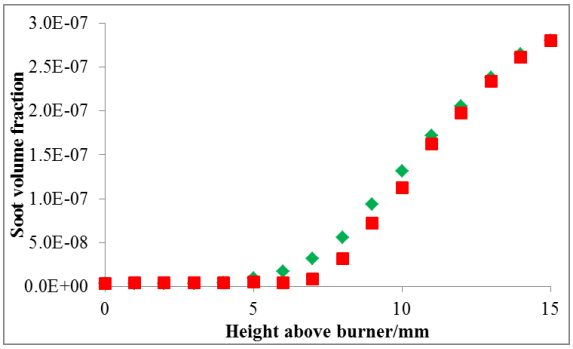

Figure 4-15

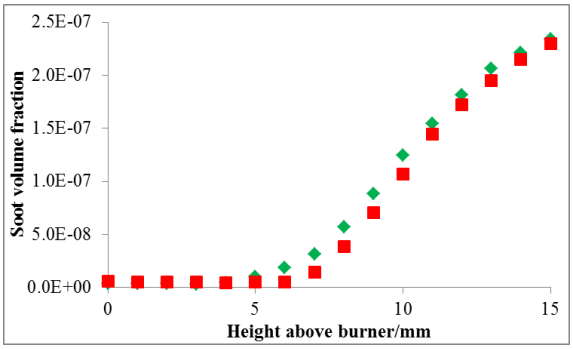

Figure 4-16

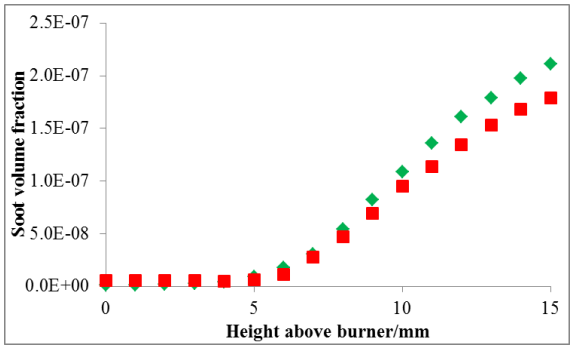

Figure 4-17

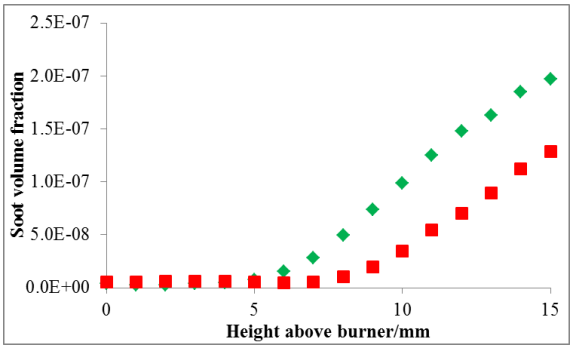

Figure 4-18

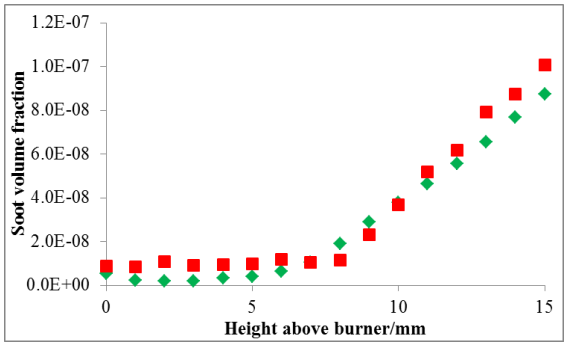

Figure 4-19

Figure 4-15 - Figure 4-19: Peak signal obtained for 1064 nm excitation (■) and the peak signal obtained for 532 nm excitation (♦) in a flames where Φ = 2.1 – 1.7, each normalised so the signal at 15 mm is equal to the peak signal for 1064 nm at 15 nm in a flame where Φ = 2.1

As can be seen at the majority of stoichiometries a separation, especially at lower heights above burner, can be seen. This is as a result of the fluorescence intensity not being related in any single way to the incandescence. The resulting errors are therefore impossible to compensate for without prior information about the quantities which are being measured. For all conditions except $\Phi = 1.7$ the signal which is obtained for 532 nm excitation is higher than would be expected. In the case of $\Phi = 2.1$ and 2.0 the greatest difference in the signal is at lower heights in the burner, for $\Phi = 1.9$ and 1.8 the greatest difference is seen at higher heights in the burner. This highlights that in the two more sooting flames there are less PAHs higher in the burner, which could be expected, and that in lower sooting flames there are proportionally more PAHs at higher heights in the flame. This shows that if the signal is recorded over a range of heights above burner and a range of stoichiometries the difference in the signal due to the inclusion of PAHs in the signal cannot be accounted for. This makes it difficult to extract information on the soot volume fraction accurately with overestimation being an issue throughout.

Due to the low signal levels observed with measurements where the stoichiometry is 1.7 it is difficult to infer information, however, it again appears that there is a constant increase of the fluorescence signal.

Through observing the signals obtained in this way it is reinforced that regardless of if the signal is recorded at a lower wavelength than that of excitation or not the fluorescence contribution will impact any attempt to calculate the soot volume fraction. This is an issue which must be taken into consideration and from the results shown above it would be recommended that this method should never be used to calculate soot volume fraction from shorter wavelength excitation.

4.4 IMPACT OF DETECTION WITH 532 NM EXCITATION ON THE ACCURACY OF LII MEASUREMENTS OF SOOT VOLUME FRACTION

Irrespective of which wavelength of light is employed it is usual to record the signal (if not employing a range of detection wavelengths) at a wavelength shorter than that of the excitation to further avoid fluorescence. However, as has been shown above if a short wavelength of light is employed there can still be fluorescent interference if prompt LII is used, and as such it is usual to always use delayed detection with shorter excitation wavelengths.

Although disadvantageous due to the possibility of interference from fluorescence 532 nm light is often used for carrying out LII measurements[7]. As discussed this is because in many laboratories 532 nm light is readily available, or because it offers the ability of performing simultaneous light scattering measurements as the lights is in the visible region. It is widely accepted that the use of this light does not pose a problem so long as delayed detection is employed, however, there is a lack of understanding around whether this has an impact on the relative signal obtained when compared to prompt LII. There are examples in the literature where 532 nm is used to obtain information on the soot volume fraction[13], where there is the argument that if a detection wavelength between 400 and 450 nm detection is used, and the regions where Swan bands occur avoided, that 532 nm is suitable for these kind of measurements[14]. However as has been shown above there is still the potential to obtain a significant amount of fluorescence in the signal in the flame conditions presented here, which therefore should be further investigated.

For this reason an investigation was undertaken in order to assess any small differences which may exist, and if these may impact the information which can be extracted from the signal. This was achieved by using the results which were shown previously and comparing the signal which was obtained using prompt LII with 1064 nm excitation with that obtained when using delayed LII with 532 nm excitation. The signal for 532

nm was taken 200 ns after the Q-switch trigger. This is in the order of the time delay used when making most delayed measurements, that is around 100 ns after the peak signal.

Through forcing the signal obtained for Φ = 2.1 to be equal and applying this normalisation to all subsequent stoichiometries, Figure 4-20, any differences which are seen in the signals are highlighted.

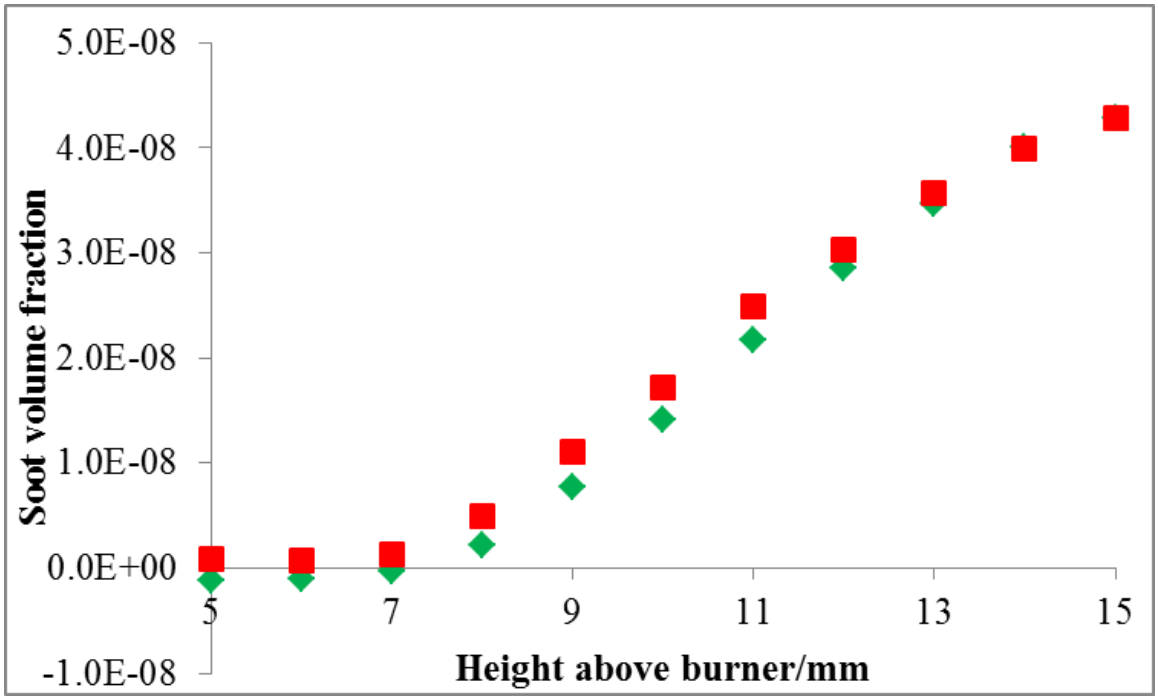

Figure 4-20 : Peak signal obtained for 1064 nm excitation (■) and signal 200 ns after Q-switch trigger for 532 nm excitation (♦) normalised so the signal at 15 mm is equal to the peak signal for 1064 nm at 15 mm in a flame where Φ = 2.1

As can be seen when correcting to the highest measurement the signal for progressively lower heights above the burner surface are progressively lower than they would be expected to be. This is because at lower heights above the burner surface the particles are smaller and therefore cool at a quicker rate than those higher in the flame. This

underestimation may lead to an incorrect assessment of the relative values within the flame and an inherent bias towards larger particles in the flame.

This was expanded to assess the impact of this at different heights above the burner surface if the normalisation was kept constant, Figure 4-21 - Figure 4-24.

Figure 4-21 shows much the same as had been seen in the $\Phi = 2.1$ flame. As was seen under the previous conditions this will lead to a bias towards larger particles within the flame.

Figure 4-22 shows an even greater under estimation of the soot volume fraction which would be obtained if the signal after 200 ns with 532 nm excitation was used. Furthermore, if the signals are normalised such that the signals obtained with 532 nm and 1064 nm excitation at 15 mm in a $\Phi = 2.1$ flame there is an over estimation of the soot volume fraction at 14 mm and 15 mm above the burner surface, before an increasing under-estimation from 12 mm to 7 mm above the burner surface. This shows that not only are measurements which are made in this way unreliable when comparing different heights above burner but there is no sensible way of comparing the results obtained at different stoichiometries. The seemingly negative signals are due to there being no strong incandescence signal below 7 mm in this flame, therefore the averaged signal used takes into account negative noise, which when normalised it appears that there has been a significant negative signal.

When normalising the signal obtained for $\Phi = 1.8$, Figure 4-23, the over exaggeration due to the normalisation is even more pronounced with there being no signal at any height in the burner which shows an underestimation. There is sequentially less of an over-estimation, however, on going to lower heights above the burner surface.

The signals obtained for $\Phi = 1.7$, Figure 4-24, go against this trend of increasing overestimation with decreasing stoichiometry. This is most likely due to the very low signals which are obtained for excitation at this stoichiometry and the proportionally larger noise levels seen. Furthermore in figure 4-8 it can be seen that the peak signal for $\Phi = 1.7$ for 532 nm and 1064 nm excitation is very similar – suggesting only low levels

of fluorescent interference in the flame. As a result of this it would be expected that the normalised signals will be more similar, as is shown

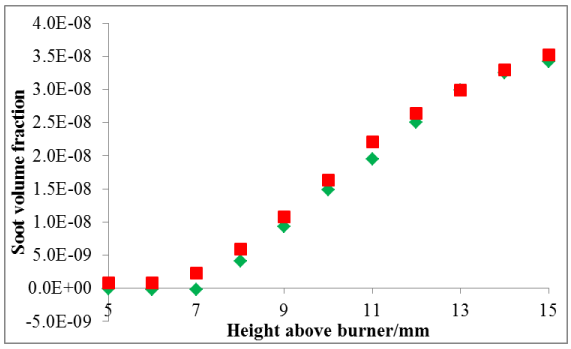

Figure 4-21

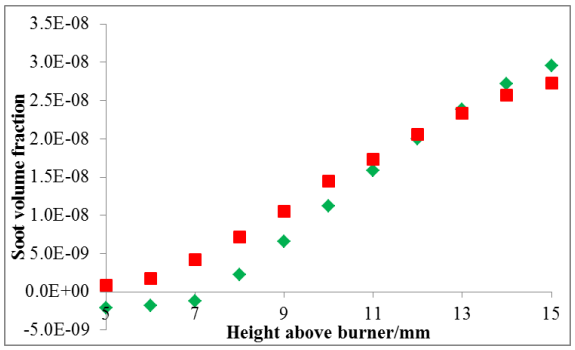

Figure 4-22

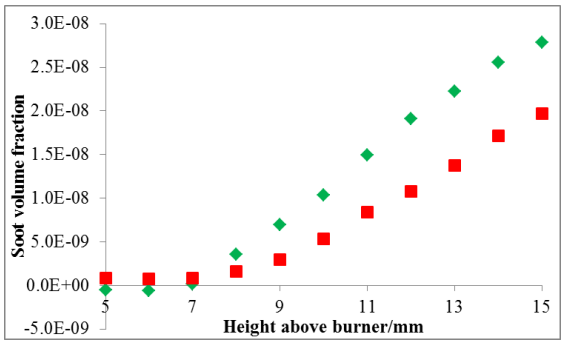

Figure 4-23

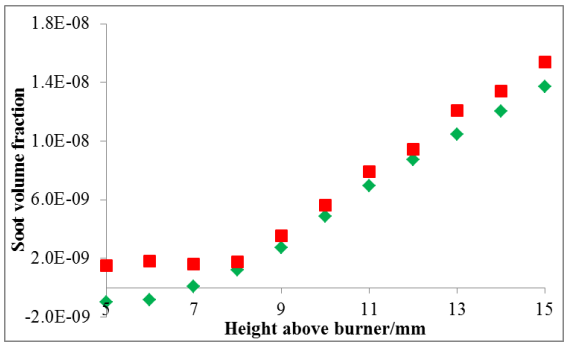

Figure 4-24

Figure 4-21 - Figure 4-24: Peak signal obtained for 1064 nm excitation (■) and the peak signal obtained for 532 nm excitation (♦) in a flames where Φ = 2.1 – 1.7, each normalised so the signal at 15 mm is equal to the peak signal for 1064 nm at 15 nm in a flame where Φ = 2.1

These figures clearly highlight the issues associated with using the signal after a delay compared to using the peak signal. This suggests that although the use of 532 nm has obvious advantages with respect to simultaneous light scattering measurements care must be taken if the delayed signal is used to infer anything about soot volume fraction.

It is important, therefore, to at least have an appreciation of the impact of making measurements using shorter wavelengths. It has also been highlighted that there are cases where there is not the difference which would be expected.

Since these measurements were recorded in such a way that it would be expected that sufficient steps have been taken in order to minimise any opportunity of fluorescence such great impact from fluorescence interference may not have been expected. However, this has been shown not to be the case, giving a clear indication that the extent to which fluorescence can impact the measurement is specific to the measurement set up. This should, therefore, be considered if a visible wavelength of light is going to be used and an investigation undertaken as to the effect that could be had upon the signal obtained.

4.5 EXCITATION WITH 283 NM LIGHT

A common wavelength of light which is used to obtain OH LIF is 283 nm. It was considered that it may be interesting if it were possible, by tuning this wavelength so it is off resonance, to obtain information about the soot volume fraction present without having to employ a longer wavelength of light. This would open the possibility for labs equipped with UV wavelengths of light to make LII measurements at wavelengths where it would be possible to obtain fluorescence information, eliminating the need for more than one laser source.

This wavelength of light was selected due to its commonality in fluorescence measurements and the ease of access to it if a dye laser is available. As has been described 283 nm light is obtained from 532 nm light via excitation of a dye in the dye laser. However, through this process there is a significant power drop, as can be seen when selecting the fluence in chapter 3. This meant that the fluence being used was at the threshold of its maximum, which could have led to issues with laser power

fluctuation, however from the results which follow this can be seen to have been an unfounded concern.

It was expected that by the inclusion of a third wavelength which is shorter the fluorescence signal which is observed should differ to that obtained with 532 nm excitation. In general smaller PAHs should be excited by shorter wavelengths than larger PAHs. Therefore it would be expected that there would be more fluorescence in lower regions of the flame with excitation of 283 nm than with 532 nm.

If the decay of the 283 nm signal is plotted along with the decay signals for 532 nm and 1064 nm it can be seen that the decay times are, as seen when comparing 1064 nm and 532 nm decays, in good agreement as displayed in Figure 4-25.

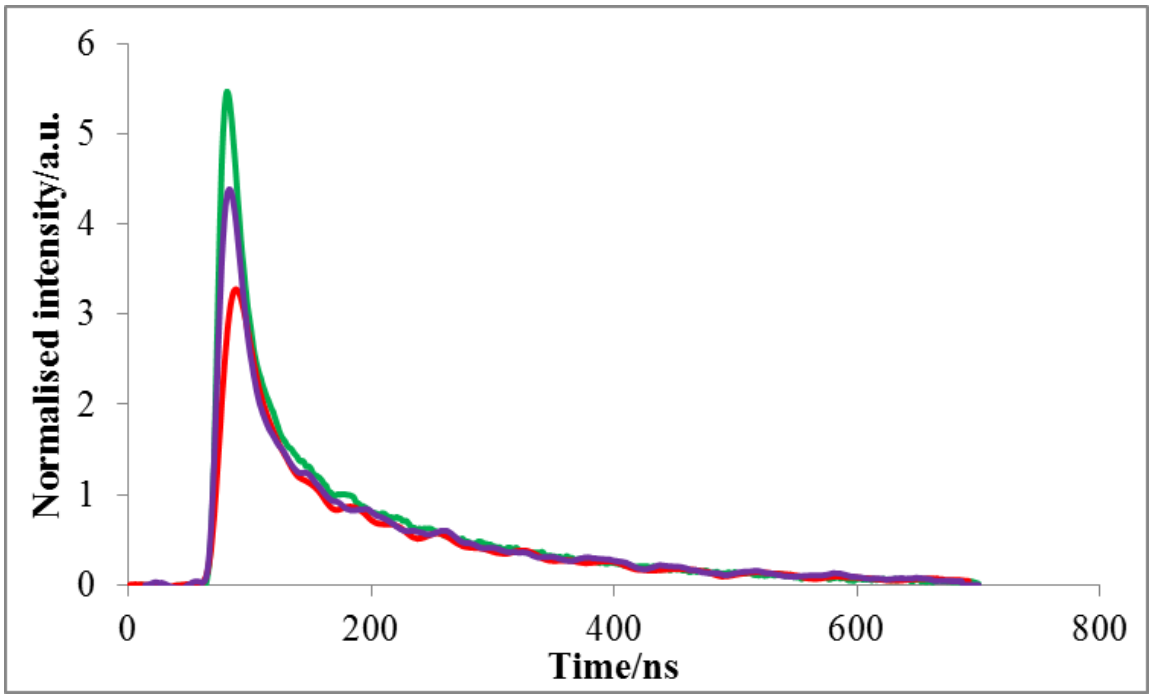

Figure 4-25 : Comparison of decay profile obtained with 283 nm (—), 532 nm (—) and 1064 nm (—) excitation 15 mm above the burner surface where Φ = 2.0

As before this illustrates that the particles are being heated to the same temperature as the incandescence decay is equivalent in all there cases. Again, this illustrates that any difference which is seem between the signals observed with different wavelengths of excitation is attributable to a contribution from fluorescence.

Initially in order to ascertain that the signal is what would be expected from a signal attributable to incandescence and a small amount of fluorescence the peak signal obtained in a flame where $\Phi = 2.1$ over the range of heights above burner, Figure 4-26.

This shows the characteristic increase in peak signal as the height above burner is increased. It can be seen that there is a measurable signal after 3 mm, which is a lower height than that where a signal is first seen upon excitation with 532 nm or 1064 nm. This is as would be expected as smaller PAHs should be excited with 283 nm than with 532 nm.

As previously the measurements were repeated for a range of flame conditions, Figure 4-26. It is expected that as well as seeing a difference, attributable to fluorescence, between the 283 nm and 1064 nm measurement there will also be a difference seen between the 283 nm and 532 nm signal which can be attributed to differences in the fluorescence signal.

Again there is the overwhelming increase in the signal upon increasing the height above burner, though in this case the shape is different than that which is seen with 532 nm and 1064 nm excitation with the increase being much more linear. This suggests that the fluorescence contribution is altering in a different way than the fluorescence contribution which is seen with 532 nm excitation.

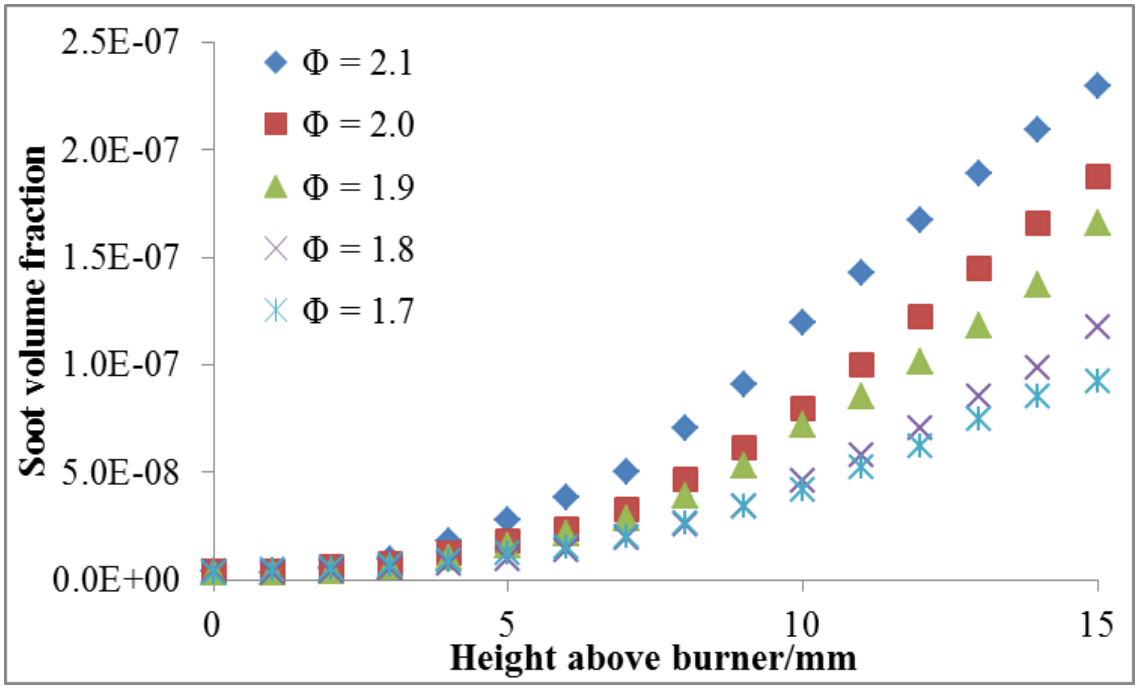

Figure 4-26 : Peak emitted intensity recorded over range of heights above burner from 0 to 15 mm for 283 nm excitation in flame over range of stoichiometries Φ = 1.7, 1.8, 1.9, 2.0 and 2.1

In order to see how the peak signal intensities compare the 1064 nm peak signals at each stoichiometry were plotted against those obtained with 283 nm excitation, Figure 4-27. Here it can clearly be seen that there is a higher signal level with the signal obtained with 283 nm excitation compared to the 1064 nm excitation. However, this is not seen to the same extent as when there is excitation with 532 nm. This is expected as fluorescence is most likely to occur at wavelengths close to that of the excitation wavelength and 450 nm is considerably longer than 283 nm. Examining the signal it can be seen that there is a measurable signal with 283 nm of light from 4 mm. This is lower than with either of the other wavelengths of light, which would be expected due to the 283 nm light causing smaller molecules to fluoresce than 532 nm light. If the PAHs and subsequent soot molecules are growing stepwise, as would be expected, there would be smaller PAHs in the flame prior to there being larger PAHs (which would be excited by

532 nm of light). Being able to detect this is of some interest and requires further investigation.

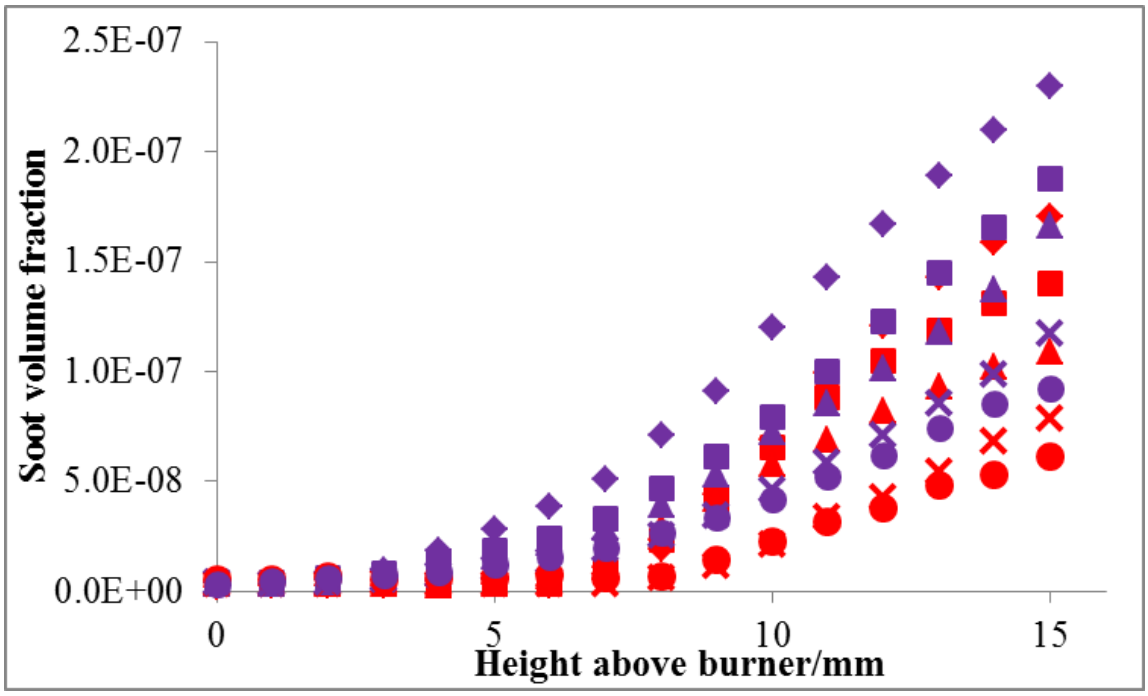

Figure 4-27 : Comparison of peak emitted intensity recorded over range of heights above burner from 0 to 15 mm for 1064 nm (red) and 283 nm (purple) excitation in flame over range of stoichiometries Φ = 1.7 (●), 1.8 (x), 1.9 (▲), 2.0 (■) and 2.1(♦)

In order to assess that the decay, as with 532 nm excitation and ensure it will converge with the 1064 nm excitation signal at a time where the fluorescence has ceased the signal both at the peak and 200 ns after the trigger were plotted, Figure 4-28 - Figure 4-32

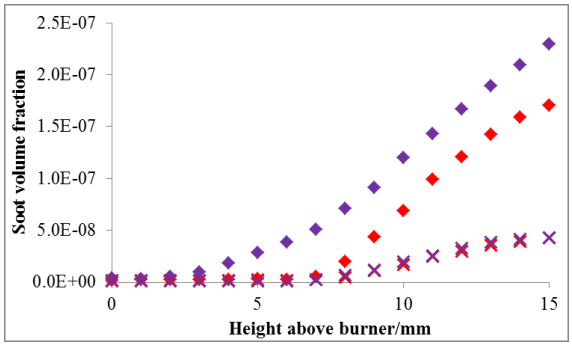

Figure 4-28

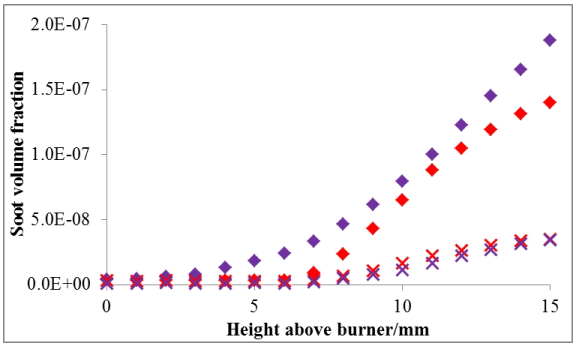

Figure 4-29

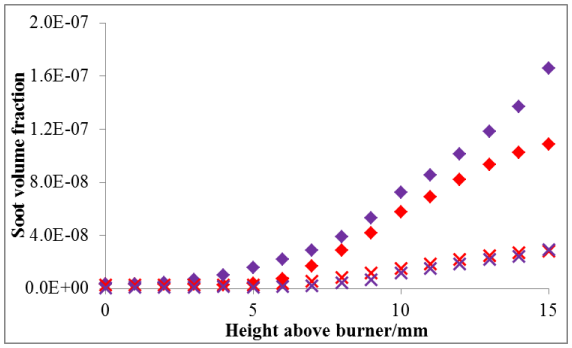

Figure 4-30

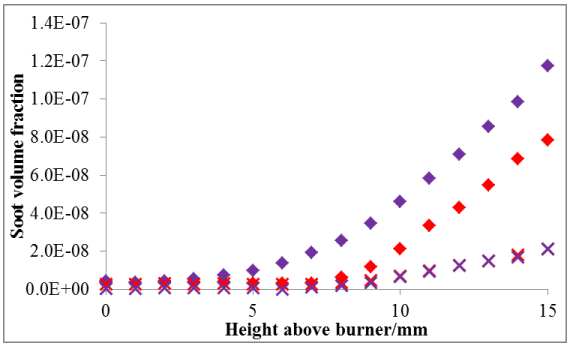

Figure 4-31

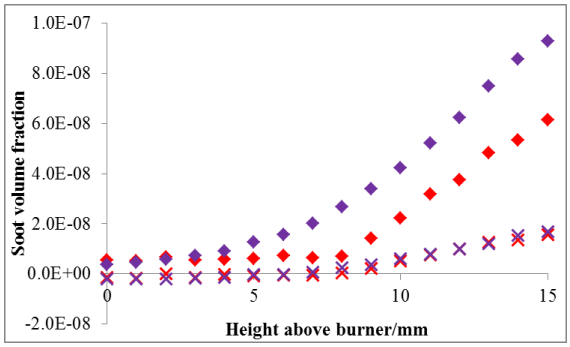

Figure 4-32

Figure 4-28 - Figure 4-32: Peak signal (♦) and signal 200 ns after the Q-switch trigger (x) where Φ = 2.1 – 1.7 flame with 283 nm (purple) and 1064 nm (red) excitation over height abover burner 0 – 15 mm

From this data it can be seen that the signal after 200 ns after the Q-switch trigger the signal for both 1064 nm and 283 nm are equivalent. This shows that, like with 532 nm, the difference in the early part of the signal is due to fluorescence before only the incandescence signal remains. The fluorescent contribution to the signal, as well as how it compares to the fluorescent signal obtained with 532 nm excitation. This will be further discussed in chapter 5

The signal can be compared to that obtained with the 532 nm excitation in order to assess the difference between the signals, Figure 4-33

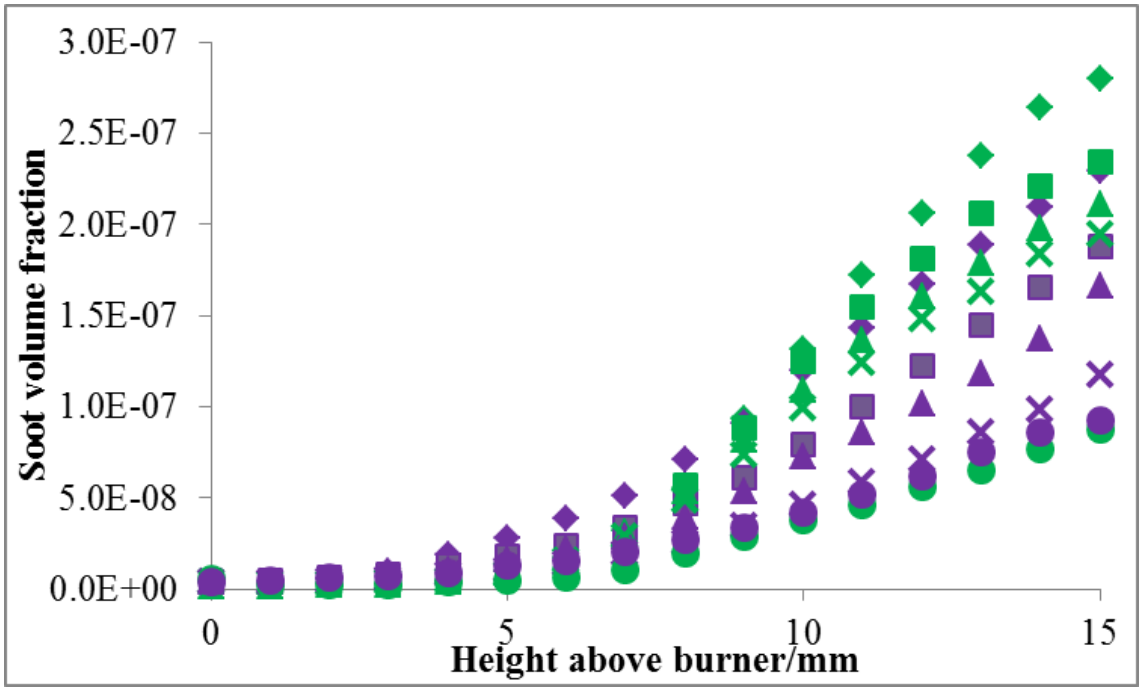

Figure 4-33 : Comparison of peak emitted intensity recorded over range of heights above burner from 0 to 15 mm for 532 nm (green) and 283 nm (purple) excitation in flame over range of stoichiometries Φ = 1.7 (●), 1.8 (x), 1.9 (▲), 2.0 (■) and 2.1(♦)

This suggests that there is, as would be expected a difference in the fluorescence contribution to the signal. It can be seen that the fluorescence contribution to the signal is greater for 532 nm excitation than 283 nm excitation.

This can be further investigated through plotting the peak signal against the signal obtained 200 ns after the Q-switch trigger, Figure 4-34 to Figure 4-38

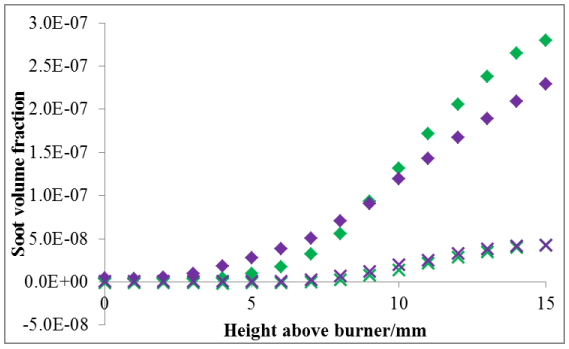

Figure 4-34

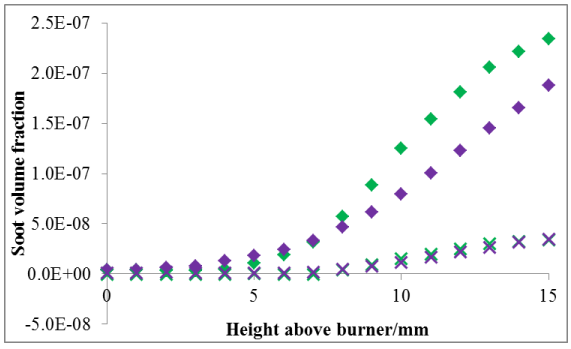

Figure 4-35

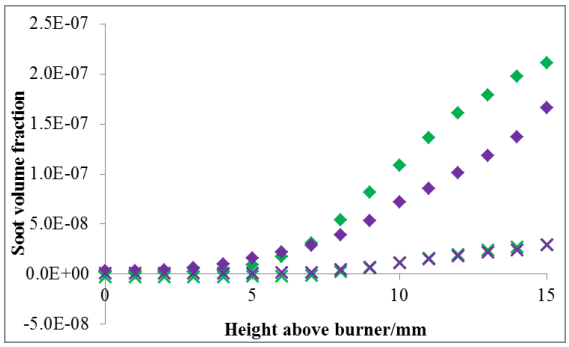

Figure 4-36

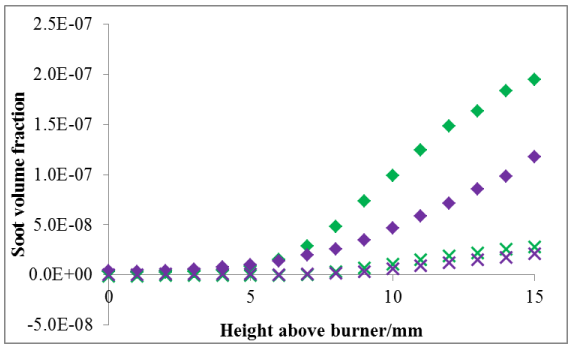

Figure 4-37

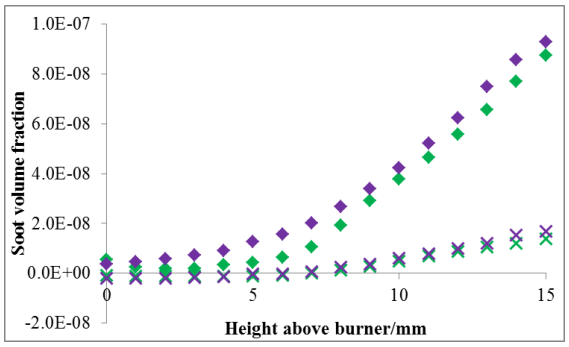

Figure 4-38

Figure 4-34 : Figure 4-38: Peak signal (♦) and signal 200 ns after the Q-switch trigger (x) where Φ = 2.1 flame with 283 nm (purple) and 532 nm (green) excitation over height abover burner 0 – 15 mm

As can be seen there is a difference not only in the peak signal intensity but in the shape of the height above burner profile. Although this was expected examining the signal in this way suggests that if the fluorescence could be studied, without the incandescence contribution, that valuable information could be yielded. This idea will be examined further in chapter 5.

4.6 CONCLUSIONS

It has been shown that using the set up as described that it is possible to obtain highly reproducible LII signals in the flames which were selected for this study. Through examination of the peak signal which was obtained upon excitation with 532 nm and 1064 nm excitation it could clearly be seen that there is a significant difference. This is attributable to the LIF contribution to the signal obtained with 532 nm excitation. Upon normalisation of the equivalent signals so the signal at 15 mm in $\Phi = 2.1$ are equal for each excitation wavelength leads to an over-estimation of the LII signal upon 532 nm excitation at lower heights in the flame. This shows that it is not appropriate to make measurements at the peak with 532 nm of light and expect that the signal would be equivalent to that obtained with 1064 nm excitation, even if the detection wavelength is shorter than that of the excitation wavelength.

It is shown that through using delayed LII with 532 nm excitation light that there is again disagreement between what would be obtained with this compared to what would be obtained with the peak signal obtained upon 1064 nm excitation. Again there is an underestimation of the signal which is obtained at lower heights in the burner. This is due to smaller particles, that is those lower in the flame, cooling at a faster rate than particles which are larger, that is those higher in the flame. This highlights that although there is the benefit of the signal not being effected by LIF if a range of particle sizes are being examined there will be a discrepancy in the signal. This highlights issues

encountered when attempting to infer information about soot volume fraction when using 532 nm. Although not routinely used for soot volume calculations it is useful to highlight what impact this can have.

Comparing the signals obtained with 532 nm at the peak and after a delay there are errors with each method. On obtaining the signal at the peak the errors are due to LIF and after a delay due to particle size differences. Therefore care should be taken when deciding which method to use. If measuring soot volume fraction it may be advisable to use the peak, even with the LIF contributions.

4.7 REFERENCES

1. S. De Iuliis, F. Migliorini, F. Cignoli and G. Zizak, *Applied Physics B-Lasers and Optics*, 2006, **83**, 397-402.
2. B. Mewes and J. M. Seitzman, *Applied Optics*, 1997, **36**, 709-717.
3. H. Bladh, J. Johnsson and P. E. Bengtsson, *Applied Physics B-Lasers and Optics*, 2008, **90**, 109-125.
4. R. L. Vanderwal and K. J. Weiland, *Applied Physics B-Lasers and Optics*, 1994, **59**, 445-452.
5. H. Richter and J. B. Howard, *Progress in Energy and Combustion Science*, 2000, **26**, 565-608.
6. B. Axelsson, R. Collin and P. E. Bengtsson, *Applied Optics*, 2000, **39**, 3683-3690.
7. R. L. Vander Wal, *Applied Physics B-Lasers and Optics*, 2009, **96**, 601-611.
8. T. Ni, J. A. Pinson, S. Gupta and R. J. Santoro, *Applied Optics*, 1995, **34**, 7083-7091.

9. S. Will, S. Schraml and A. Leipertz, *Twenty-Sixth Symposium (International) on Combustion,* 1996, 2277-2284.
10. S. De Iuliis, F. Cignoli and G. Zizak, *Appl. Opt.*, 2005, **44**, 7414-7423.
11. P. O. Witze, S. Hochgreb, D. Kayes, H. A. Michelsen and C. R. Shaddix, *Applied Optics*, 2001, **40**, 2443-2452.
12. R. L. VanderWal, *Applied Optics*, 1996, **35**, 6548-6559.
13. J. Appel, B. Jungfleisch, M. Marquardt, R. Suntz and H. Bockhorn, *Twenty-Sixth Symposium (International) on Combustion*, 1996, 2387-2395.
14. P. Desgroux, X. Mercier and K. A. Thomson, *Proceedings of the Combustion Institute*, 2013, **34**, 1713-1738.
15. K. A. Thomson, K. P. Geigle, M. Kohler, G. J. Smallwood and D. R. Snelling, *Applied Physics B-Lasers and Optics*, 2011, **104**, 307-319.
16. R. J. Santoro, H. G. Semerjian and R. A. Dobbins, *Combustion and Flame*, 1983, **51**, 203-218.
17. J. Zerbs, K. P. Geigle, O. Lammel, J. Hader, R. Stirn, R. Hadef and W. Meier, *Applied Physics B-Lasers and Optics*, 2009, **96**, 683-694.
18. K. C. Smyth and C. R. Shaddix, *Combustion and Flame*, 1996, **107**, 314-320.
19. W. H. Dalzell, G. C. Williams and H. C. Hottel, *Combustion and Flame*, 1970, **14**, 161-169.
20. B. Axelsson, R. Collin and P. E. Bengtsson, *Applied Physics B-Lasers and Optics*, 2001, **72**, 367-372.

5 LASER INDUCED FLUORESCENCE OF POLYCYCLIC AROMATIC HYDROCARBONS WITH EXCITATION WAVELENGTHS OF 283 NM AND 532 NM

As has been demonstrated in chapter 4 the signal obtained upon excitation with 532 or 283 nm light will be a combination incandescence and fluorescence. This was shown to be the case for signals recorded below that of the excitation wavelength, suggesting that although it would be expected that fluorescence will predominantly occur at wavelengths greater than the excitation wavelength, there is a significant fluorescence contribution at 450 nm.

As has been shown, through careful selection of the fluences, the particles can be heated to the same temperature with each excitation wavelength. The temporal decay of the incandescence signal will therefore be the same, irrespective of the excitation wavelength[1]. The decay time of each signal was calculated in order to demonstrate this consistency between the excitation wavelengths. The decay times also serve to show the changing particle size in the flames. It is expected that upon increasing the measurement height the particle size will increase and that this will result in a longer incandescence decay time[2, 3].

Any differences which are see in the recorded signal resulting from 1064 nm excitation and that of 532 nm or 283 nm excitation can therefore be attributed to fluorescence[4]. This allows the opportunity to obtain useful information from the fluorescence contribution rather than eliminating any fluorescence contribution as an interference useful information can be obtained from it. This has been carried our previously in the literature but never before recorded in the way shown here or over such a range of flame conditions and heights above burner.

The results shown in chapter 4 are used here to show how the measured fluorescence signal changes over the range of stoichiometries and heights above burner which have

been employed. The results obtained via this method are comparable with what is seen in the literature when samples are removed from the flame for PAH identification[5, 6]. While further work is still needed to develop this method so classes of PAH can be identified this is encouraging, especially as these results are obtained in-situ. This is especially true as one of the main issues in making measurements in sooting flames is that it is difficult to obtain accurate PAH data through extractive sampling[7].

5.1 DECAY TIMES

As has been discussed when larger particulate material in the flame absorbs laser light passing through the flame it will gain energy causing heating of the particle. Any of this particulate material, if of significant mass, will act as a near black body and will lose energy through the emission of light. This will be accompanied by both conductive cooling and, if the laser energy is high enough, sublimation[8].

In the case of the work presented here the fluences which were employed for each excitation wavelength were carefully chosen. This was to ensure that the particles are being heated to the same temperature with each excitation wavelength, so that the prompt signal is proportional to the soot volume fraction[1]. By employing a flat flame burner we can therefore assume that, although the measurements with each excitation wavelength are not being made simultaneously, the flame conditions are reproducible so the results can meaningfully be captured[9]. This flame stability is confirmed by the reproducibility of the results in chapter 4 – as highlighted in figure 4-4.

Following from this it can therefore be expected that the decay of the signal for each wavelength of light will be equivalent after a time where any fluorescence has fully decayed. Therefore any difference seen between the signals cannot be due to incandescence and can be identified as being fluorescence.

In order to assess this, the decays of the signals recorded were examined. To eliminate the period where fluorescence is present the decay was fitted from a time of 200 ns after the laser trigger, which represents a time of around 100 ns after the peak of the LII signal. For each of the flame conditions the repeat signals which were obtained were averaged prior to the fit. Figure 5-1 shows the signal obtained upon 1064 nm excitation at 15 mm above the burner surface along with the fitted decay curve, shown on a log scale.

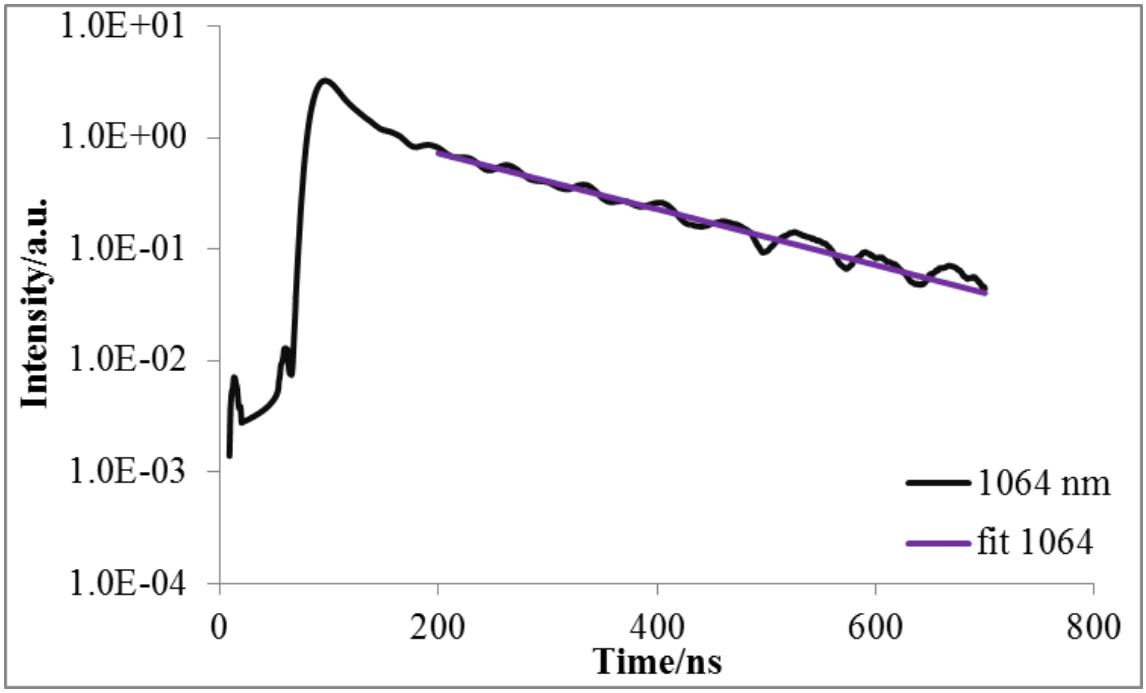

Figure 5-1 : Decay signal recorded at for λ_{ex} = 1064 nm 15 mm in Φ = 2.1 flame and fitted exponential curve (fit from 200 ns after laser trigger)

As can be seen the fit of an exponential decay to the signal, is in good agreement with the signal. The exponential decay fitted follows Equation 5-1, where A and φ are specific to the exponential fitted, and as such are constant throughout the decay, and t is the time at any given point in the signal.

$$Decay = Aexp(-\varphi t)$$

Equation 5-1

The decay time is related to the decay rate (φ) by the relationship φ = 1/decay time and can thus be calculated. Through obtaining the decay it is possible to infer information about the particle size[10]. Larger particles will have longer decay times than smaller particles and therefore the relative particle sizes can be obtained. Since it has been shown that there is a higher incandescence signal going up the flame, and that the particles grow in a stepwise fashion, then upon going from lower to higher heights in the flame the decay time, and therefore the particles size, will increase[10].

It can clearly be seen that the signal decays more rapidly the lower in the burner the measurement is made. This shows that the smaller particles are cooling at a slower rate than the larger particles. This is in good agreement with and shows little variation from the decay times presented by Axelsson *et al*.[2] which were obtained in a similar flame.

As such the decay time was obtained for each of the heights above burner at which the measurements were made for 1064 nm excitation. Due to the weakened signal at lower heights above burner it was not possible to obtain reliable exponential fits lower than 9 mm in the burner. This was to be expected from earlier work which showed the maximum intensity below 9 mm as being very low. The decay times at each height above burner were plotted against the height above burner surface as shown in Figure 5-2.

As can be seen there is a steady increase in the decay time moving to higher measurement heights in the flame. This is as would be expected as due to the laminar and steady nature of the flame the soot particles will grow in a linear fashion with the particles at each subsequent height having larger soot particles[11]. This also agrees with what was seen when the peak intensity over the range of heights above burner were plotted.

As has been discussed due to the fluences which have been chosen were selected in order that the particles are being heated to the same temperature with each excitation wavelength the incandescence decay should be the same in each case. This should be seen at any given height above burner where particles of the same size are being excited by any given wavelength. If this holds true it would be expected that any differences which are seen between the equivalent decay profiles are due to short lived fluorescence and therefore will not be a feature in the region where the exponential decay is being fitted. Therefore comparing the decay times for each of the three excitation wavelengths at a given condition the decay times should be equivalent for each of the wavelengths.

It can be seen from Figure 5-2 there is a good correlation between the decay time obtained with the signal resulting from 283 nm, 532 nm and 1064 nm excitation. It was expected that there may be a slight deviation from the decay times seen for 1064 and 532 nm due to the fluence being used for the 283 nm excitation being at the threshold of where it would ideally be. This was due to the lower intensity which is obtained from the dye laser and the inability to increase this. However, this was proven to be unfounded with the decay time being similar to that obtained with 1064 nm and 532 nm.

The similarity of the decay time suggests that for all employed excitation wavelengths at a given height the particles are cooling in the same way. From this level of similarity we can assume, since incandescence decay is a single exponential, that for the duration of the decay the incandescence signal is equivalent for all three.

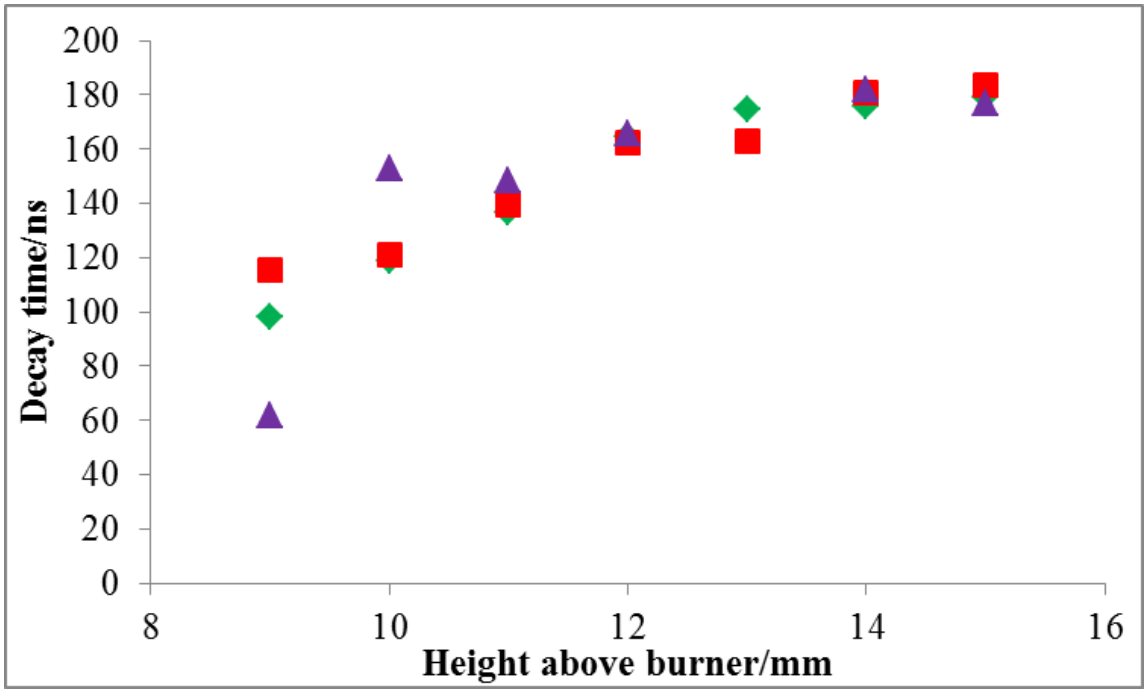

Figure 5-2 : Decay times for heights 9 – 15 mm in Φ = 2.1 flame with λ_{ex} = 1064 nm (■), 532 nm (♦) and 283 nm (▲)

From the figure shown it can also be seen that the particles have a decay time of around 100 ns at 9 mm above the burner surface, growing to around 180 ns at 15 mm above the burner. The growth looks to be stable, with most growth occurring below 12 mm.

In order to assess this over the range of stoichiometries which have been employed the above process was repeated for all of the stoichiometries over the range of heights above burner shown in Figure 5-3 to Figure 5-6.

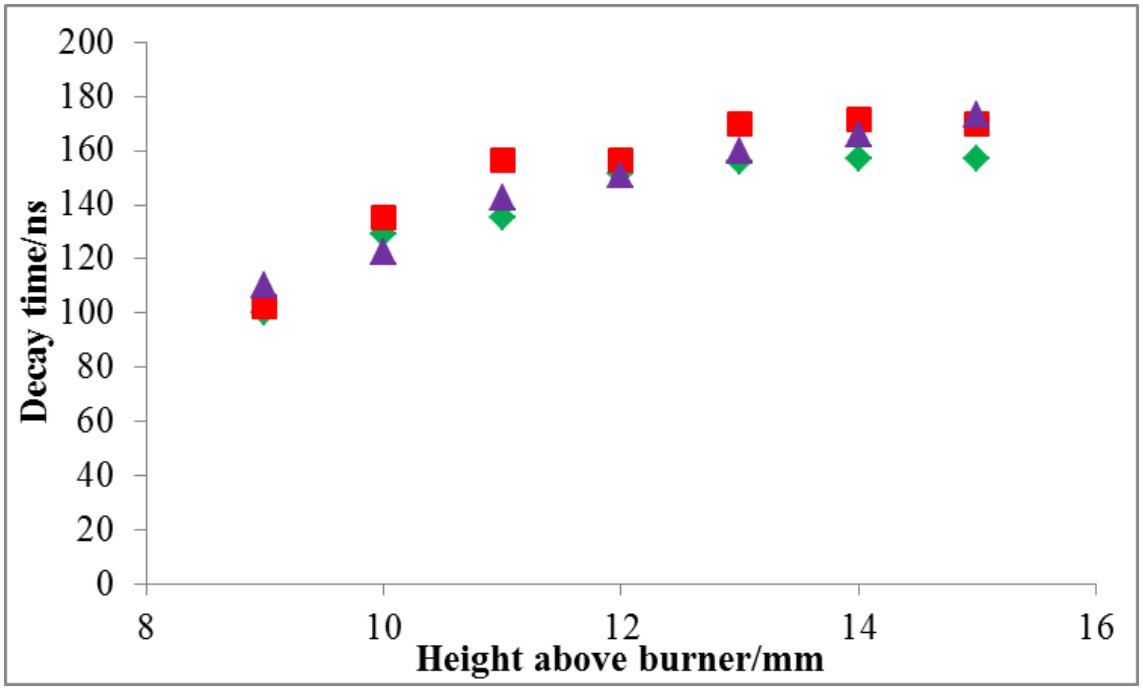

Figure 5-3 : Decay times for heights 9 – 15 mm in Φ = 2.0 flame with λ_{ex} = 1064 nm (■), 532 nm (♦) and 283 nm (▲)

Again it is shown that the decay times which are obtained for each of the three excitation wavelengths at a given height in the flame are comparable. Here the signal has a decay time of around 100 ns, reaching around 160 – 170 ns for the particles at 15 mm above the burner surface. This is slightly lower than was seen in the case where Φ = 2.1. This may be expected as there may be more particles which grow larger at a faster rate in a flame with a higher stoichiometry. It is seen the main period of growth appears to occur before 12 mm in the flame, which was also the case in the flame where Φ = 2.1.

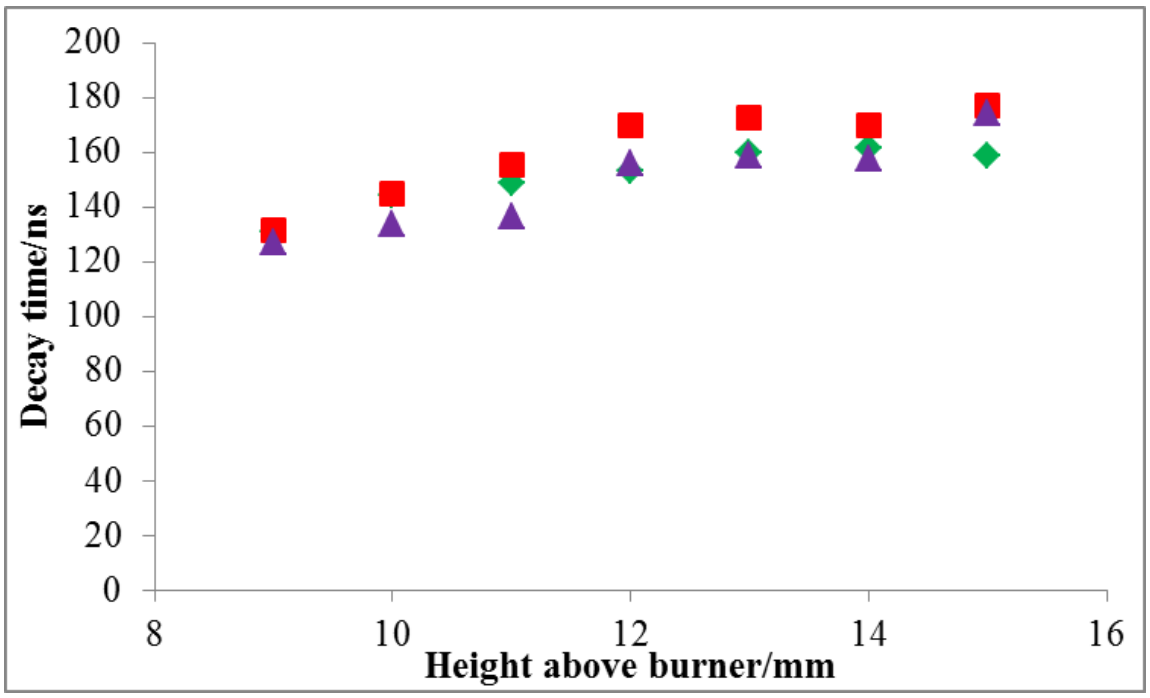

Figure 5-4 : Decay times for heights 9 – 15 mm in Φ = 1.9 flame with λ_{ex} = 1064 nm (■), 532 nm (♦) and 283 nm (▲)

In this case there is less of a change seen in the decay times between 9 mm and 15 mm above the burner surface. Here at 9 mm the decay time is around 130 ns with a maximum decay time in the region of 170 ns. This may suggest that the initial growth rate of particles in this flame is quicker, therefore the particles reach a larger size quicker, the growth from this point then slows so there is not the same degree of change seen as with the previous cases.

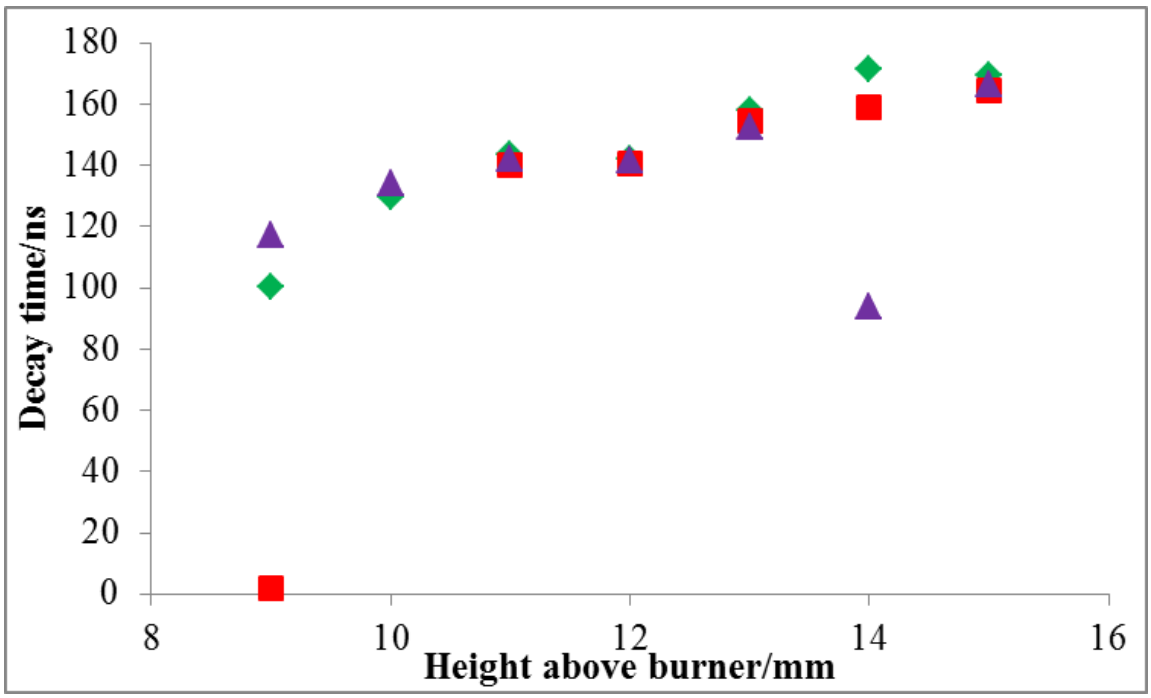

Figure 5-5 : Decay times for heights 9 – 15 mm in Φ = 1.8 flame with λ_{ex} = 1064 nm (■), 532 nm (♦) and 283 nm (▲)

Again it can be seen that there is good correlation between the decay time of recorded signals for the three excitation wavelengths. It is interesting to note here that the decay time increases from 9 – 11 mm in each case, before plateauing at 12 mm, and then increasing for the last 3 mm.

There is one extreme outlier seen at 14 mm with 283 nm excitation. When the signal which is being fitted is examined it can be seen that the fit is poor due to a great deal of noise in the signal, which is not seen to such a degree with the other data recorded. The reasons for this would require further investigation.

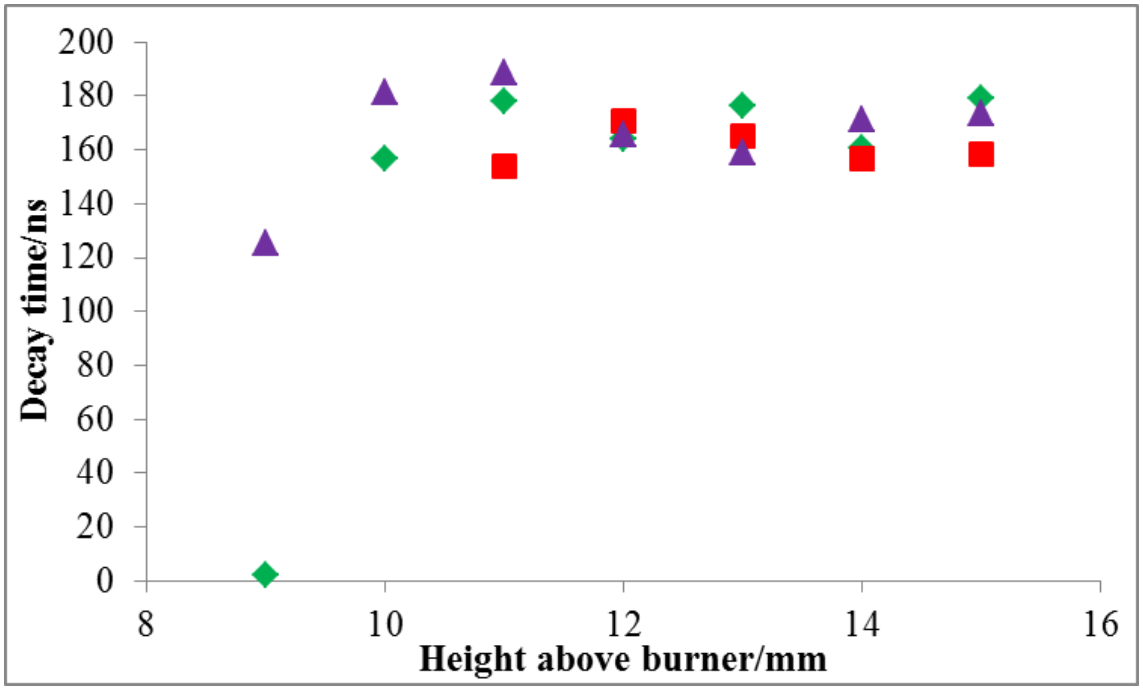

Figure 5-6 : Decay times for heights 9 – 15 mm in Φ = 1.7 flame with λ_{ex} = 1064 nm (■), 532 nm (♦) and 283 nm (▲)

The signals obtained for Φ = 1.7 were very low in comparison to the other samples obtained and therefore it was difficult to obtain a good fit for them. This can be seen in the measurements at 9 mm in the flame where the signal for both 532 nm and 1064 nm gives a time of 0 ns. However, the decay times for higher in the flame were more akin to what would be expected, though slightly higher than may have been supposed, with a maximum decay time of 180 ns. This would suggest that the particles which are being formed in this flame are larger even than those being formed in the flames of higher stoichiometries, with Φ = 2.1.

Through examination of these decay times it can be ascertained that there is generally good agreement between the signals which were obtained under specific conditions for the three excitation wavelengths. Therefore we can say with some confidence that the particles which are present in a given measurement zone are being heated to the same temperature by each of the three excitation wavelengths, and hence have the same

incandescence profile. It can be assumed, due to incandescence being an exponential decay that if the decay time fitted above is in good agreement that the incandescence signal prior to this point will also be the equivalent.

It is then possible to compare the decay times for the signals which are obtained over the range of stoichiometries as shown in Figure 5-7

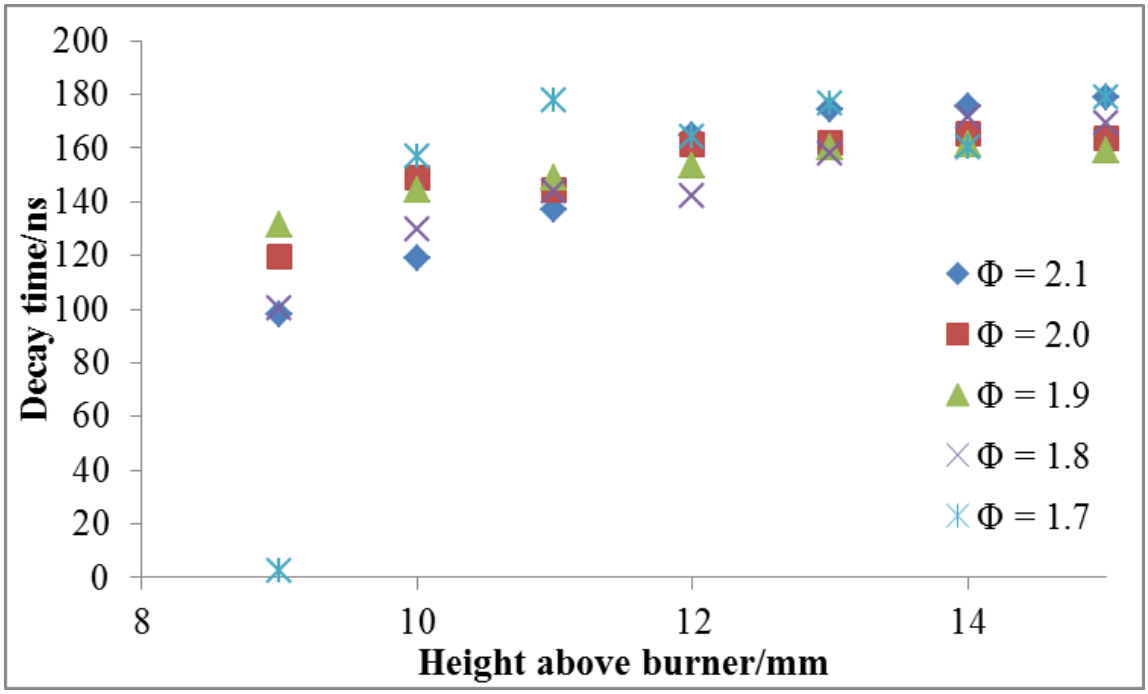

Figure 5-7 : Decay times for heights 9 – 15 mm where Φ = 1.7, 1.8, 1.9, 2.0 and 2.1 with λ_{ex} = 1064 nm

It can be seen that the decay rates for each of the signals obtained over the range of heights above burner for each stoichiometry are very similar. This suggests that the particles in each flame may be of a similar size. However, it appears that the signals obtained for 1.7, 1.8 and 1.9 show more of a gradual increase in the decay time than the signals obtained for 2.0 and 1.9 which are more constant. This suggests in flames for stoichiometries 2.0 and 1.9 that the maximum soot size seen here is reached earlier in the

flame. When comparing with the peak signal of LII there is still an increase in signal during this period, but it is possible that this is due to more particles of this size forming, rather than the existing particles undergoing further growth.

Furthermore, it has previously been seen that there is a large difference in absolute intensity of the signals. Therefore it can be inferred that in the flames which have been used in this study the growth of soot largely follows the same pathway, with the soot particles growing at the same rate in each case. Thus the difference in absolute intensity is predominantly due to more of the same particles being present in sequentially more sooting flames rather than different sized particles existing. It can be surmised, therefore, that the growth rate of individual particles is the same in all flames which were used in this study.

5.2 VALIDITY OF SUBTRACTION OF LASER INDUCED INCANDESCENCE FROM EMITTED SIGNAL

It has been discussed that in most of the examples in the literature where LII signals are obtained any fluorescence which is present in the obtained signal is considered as an interference and steps are taken to either to eliminate or minimise the fluorescence. However, there have been examples from Schoemaeker Moreau *et al.*[12] and Lemaire *et al.*[1] where the fluorescence which is present in the signal is examined for the additional information it can yield.

This is possible if 1064 nm is used as the excitation wavelength because a signal attributable solely to incandescence will be obtained. Thus if the emitted signal is then recorded in the same conditions but using an excitation wavelength which leads to a combination of incandescence and fluorescence, the incandescence signal will be

equivalent to that obtained with 1064 nm excitation. This allows the incandescence signal to be subtracted from the signal which is a combination of incandescence and fluorescence, resulting in the fluorescence signal being obtained.

This only holds true if it can be ensured that the particles in the measurement volume are being heated to the same temperature[1] (and hence will result in the same incandescence signal) with both wavelengths of excitation light. This is achieved through using an equivalent fluence for both lasers, and this is discussed in detail in chapter 3. It can be confirmed that this is the case when the decay times of the signals resulting from the different wavelengths of light are considered. It has been described that the decay times at each height above burner are equivalent with the three different wavelengths of light which were employed. Since it was shown in chapter 4 that at each of the heights above burner there is a difference in the signal, which we could be confident was attributable to fluorescence. This allows for the subtraction of the incandescence contribution from the signal obtained with 532 nm and 283 nm of light to obtain the fluorescence at each height above burner for all conditions.

By looking at the decay of the signal which is obtained for 1064 nm excitation at 15 mm above the burner surface in a flame where $\Phi = 2.1$ compared to the signal obtained under the same conditions for an excitation of 532 nm the difference in the early part of the signal is evident to see as shown in Figure 5-8

This agrees with what has been highlighted above with the large difference in the signals occurring within the first 50 ns after the laser pulse. This is attributable to the fluorescence contribution which arises from the 532 nm excitation light exciting large PAHs within the measurement volume.

Therefore by subtracting the signal which is obtained with 1064 nm excitation from the signal obtained with 532 nm the resultant signal, which is attributed to fluorescence, can be obtained as shown in Figure 5-9.

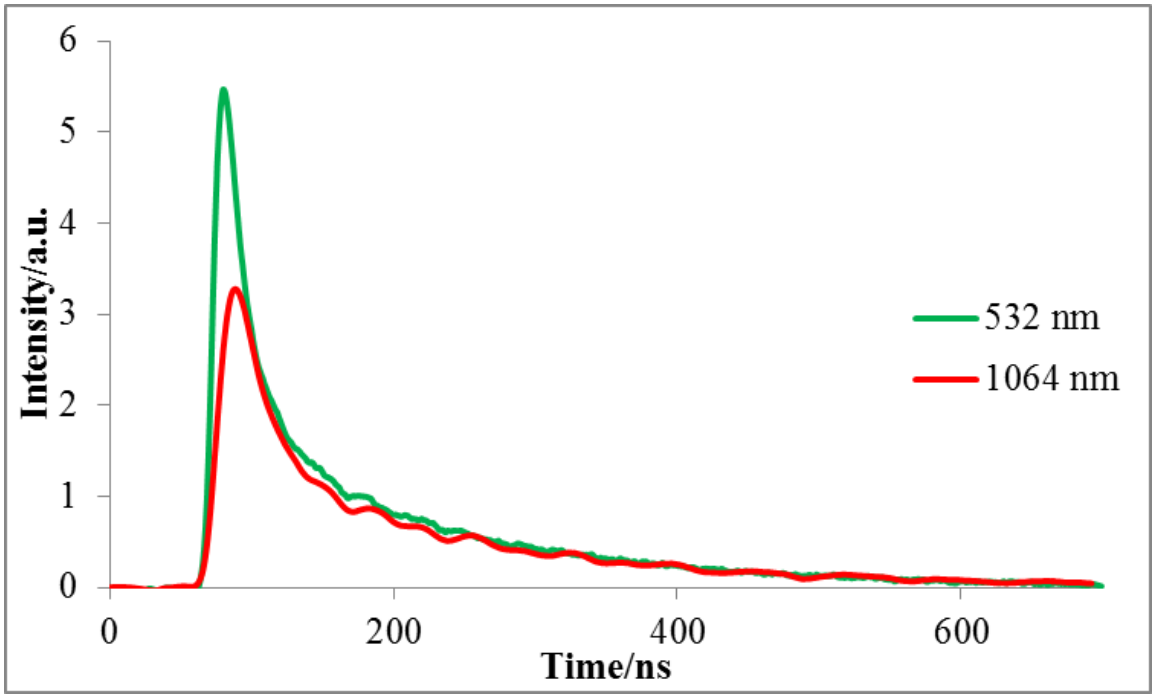

Figure 5-8 : Decay time at 15 mm above the burner surface where Φ = 2.1 and λ_{ex} = 1064 nm and 532 nm

The signal which is shown here has a FWHM of 16 ns, which is significantly longer than the FWHM of the laser pulse, which is a maximum of 8 ns. This indicates that the signal is attributable to fluorescence and not as a result of the laser pulse. This shows that by recording using more than one excitation wavelength there is the benefit that simultaneous information can be obtained about a particular flame. This is advantageous as it allows fluorescence signals to be obtained in regions where otherwise it would be very difficult due to the larger soot particles in the measurement volume.

It is known that the fluorescence signal is dependent on the wavelength of excitation which is used. This is as longer wavelengths of excitation light will tend to excite larger molecules compared to shorter wavelengths of light which will excite smaller molecules. Therefore looking at the signal obtained with 283 nm excitation light the procedure followed above can be shown to hold true and give a fluorescence signal, Figure 5-10 and Figure 5-11

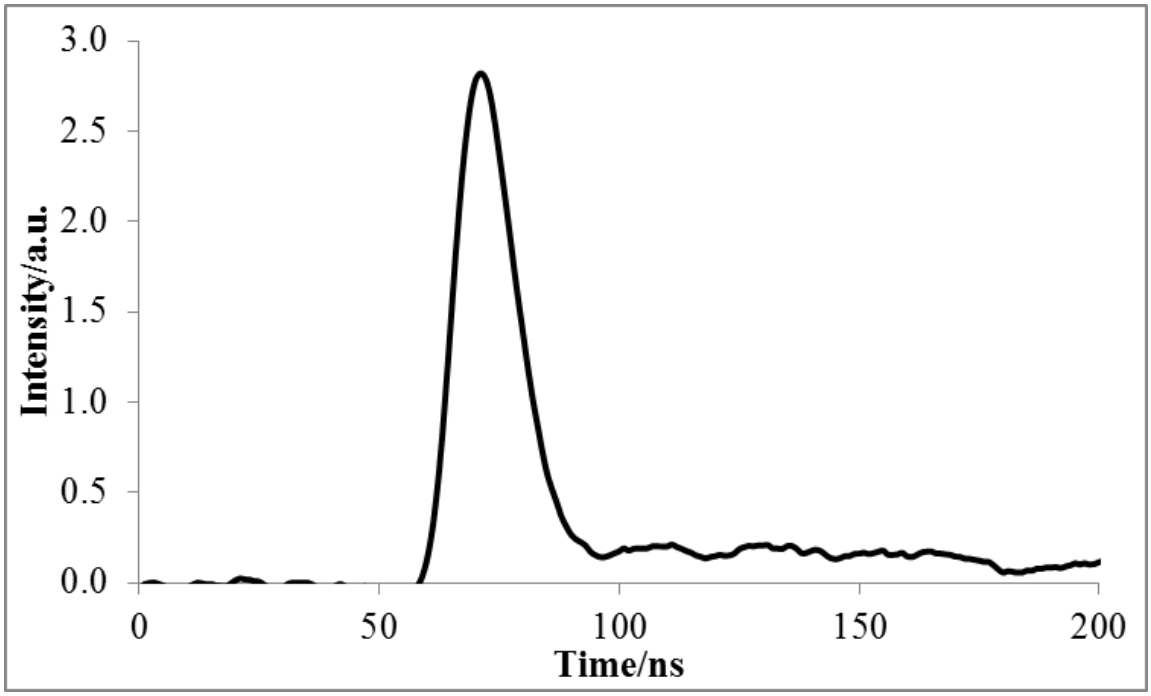

Figure 5-9 – Decay signal resulting from subtraction of signal obtained for λ_{ex} = 1064 nm from that of λ_{ex} = 532 nm in a flame where Φ = 2.1 at 15 mm above the burner surface

As can be seen the signal obtained for 532 nm differs in the magnitude of the difference between it and the signal obtained for 283 nm excitation. This is as a result of each of the excitation wavelengths exciting different classes of PAH. It may be hypothesised that lower in the flame there will be a signal obtained for 283 nm excitation where there is none for 532 nm excitation. This can be explained by the soot growth being a linear reaction where smaller PAHs, which will be excited by 283 nm, being formed before larger PAHs, which will be excited by 532 nm.

There is however an important aspect which must be kept in mind when inferring information from studies such as these – that is that the intensity of fluorescence emitted with different excitation wavelengths is not comparable. That is that if the LIF intensity is higher with 283 nm excitation this does not mean that there are less molecules being excited by 532 nm. In order to draw such information from fluorescence measurements

there must be an appreciation of what molecules are being excited by each wavelength. This cannot be achieved through looking at measurements such as above, and further work outwith the scope of this work would have to be undertaken.

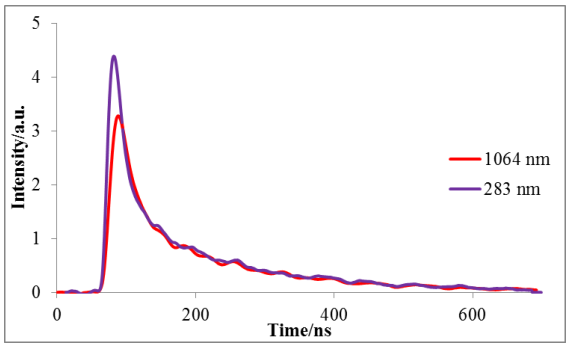

Figure 5-10 : Decay time at 15 mm above the burner surface where Φ = 2.1 and λ_{ex} = 1064 nm and 532 nm at 15 mm above the burner surface

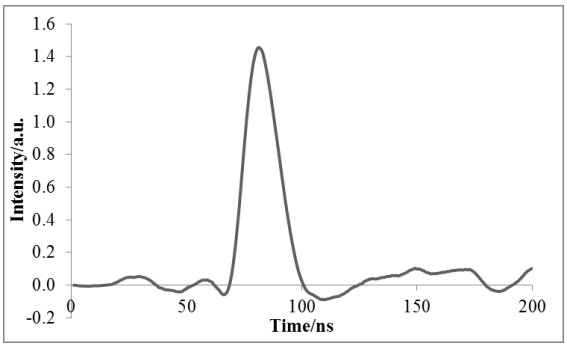

Figure 5-11 : Decay signal resulting from subtraction of signal obtained for λ_{ex} = 1064 nm from that of λ_{ex} = 283 nm in a flame where Φ = 2.1 at 15 mm above the burner surface

5.3 LASER INDUCED FLUORESCENCE OVER RANGE OF HEIGHTS ABOVE BURNER

Since it has been shown that it is possible to obtain fluorescence in this way it can be shown that there is an advantage to using two excitation wavelengths as pseudo-simultaneous information can be obtained on both PAHs and soot which is present within the measurement volume. However, by looking at the signal as described above it is difficult to obtain qualitative information of how the fluorescence changes with the

height above burner for each of the excitation wavelengths. Therefore, for each of the measurements which were shown in chapter one the signal which was emitted for 1064 nm excitation was subtracted from the signal which was obtained with both 532 nm and 283 nm. This gave a fluorescence signal for each of the measurements. This was then plotted as prompt LII would be, that is by taking the maximum of the LIF signal and plotting it against the height above burner where the measurement is carried out for the range of stoichiometries.

Although fluorescence is not as straightforward as for the maximum signal to be used quantitatively, and much more information would be needed for this to be the case, it is assumed that each wavelength of excitation light is only exciting a small range of PAHs and as such for the purposes of comparing the signal obtained for "smaller" PAHs and "larger" PAHs this holds. The relative amounts can also be compared when the same excitation wavelength is used so long as it is recognised that a range of PAHs are being excited, rather than a single PAH, and that this may mean that there is a potential the signal is weighted to a specific class within this grouping.

Since the incandescence increases as the height of the measurement increases, and similarly the decay time increases, it can be concluded that the soot is growing in a largely linear way from the base to the top of the measurement range. It is known that the fluorescence signal is due to the PAHs which join together to form the soot and as such it is expected that the signal will fall upon increasing the height where the measurement is made. However, the PAHs which will be excited depends on the excitation wavelength which will be employed, with longer wavelengths exciting larger PAHs. Since PAHs also grow in a linear fashion it will be expected that lower down in the flame there will be no fluorescence signal, with the signal increasing as larger PAHs are formed. Thus it is expected that the fluorescence signal will initially increase as the measurement height is increased before reaching a maximum and then decreasing.

Following this however, there may be a period where oxidation becomes a key mechanism. This will cause a breakdown of some of the soot molecules, leading to a re-increase of PAHs within the flame. This re-increase will be seen depending on the size

of the PAHs which form during this phase and if they are appropriate for the excitation wavelengths of light to excite. This would correspond to work which has been carried out in Lille using a jet cooled LIF technique[5].

As has been shown above by subtracting the signal which was obtained for 1064 nm from that with 532 nm or 283 nm there will be a resultant signal due to the fluorescence present. By subtracting the 1064 nm signal from the 532 nm and 283 nm signal over the range of heights above burner for each of the signals which were previously obtained it will be possible to see how the fluorescence signal changes over the range of heights above burner and conditions which were employed.

Initially the peak signal for 1064 nm was subtracted from the peak signal which was obtained when 532 nm excitation both for the flame conditions for $\Phi = 2.1$. This was compared with the signal which was obtained when the peak 1064 nm was subtracted from the peak signal obtained with 283 nm excitation. For this section of the work the subtraction is at the peak of the signal in order to attempt to alleviate any small inconsistences, which would be seen in the signal if taken at x ns after the laser trigger resulting from a jitter. This was not a great issue when monitoring the LII signal as it has a longer decay time so mis-positioning by 6 ns will not have an overall effect on the value reported. However, as a result of fast decay times associated with fluorescence moving the measurement point by 6 ns would have a large effect on the value being reported. The values obtained were then plotted against the height above burner where the signal had been obtained, Figure 5-12

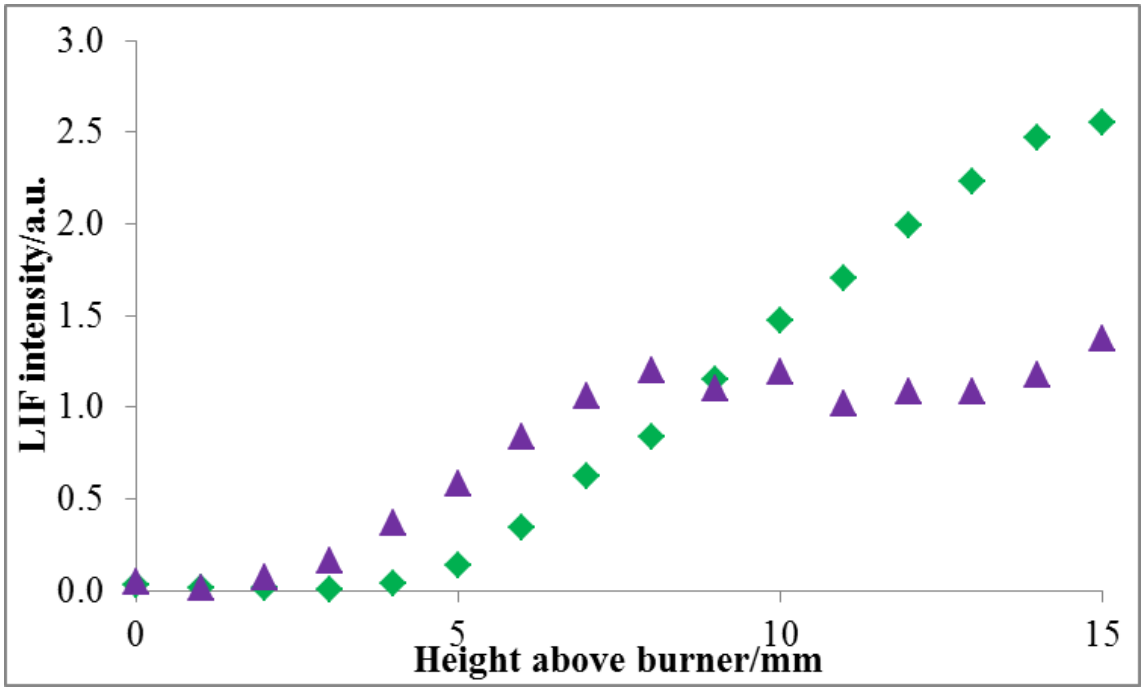

Figure 5-12 : Fluorescence contribution at peak over range of heights above burner where Φ = 2.1 where λ_{ex} = 532 nm (♦) and 283 nm (■)

Here it can be seen that there is a clear fluorescence signal at 3 and 4 mm above the burner surface when 283 nm excitation is used, while there is no signal observed for 532 nm excitation. This suggests that at this height in the burner although there are PAHs present, causing the fluorescence seen with 283 nm excitation, there are no PAHs which are large enough to be excited with 532 nm light. This is as would be expected as the PAHs grow in a stepwise fashion and therefore there should be a smaller PAHs and therefore they would be expected to fluoresce upon excitation with the shorter 283 nm excitation wavelength. It must be remembered that the excitation wavelength will not excite one specific PAH but rather a small range of PAHs, so looking at the plot above there may not be an increase in one specific PAH but rather larger numbers of PAHs of that class being formed. As the signal cannot be quantified this could mean that the increase is indicating growth as well as increase in particle number.

It can then be seen that from 5 to 8 mm in addition to the fluorescence signal resulting from 283 nm there is also a signal from 532 nm excitation. This suggests that in this region there begins to be larger PAHs than those which are excited with 283 nm excitation light. This is as would be expected as it has been described that due to the stepwise growth of soot within the flame there will first be small PAHs, which will then grow to become larger PAHs.

The decrease of the signal which is obtained with 283 nma fter 8 mm is a result of the PAHs growing into larger PAHs and soot particles, resulting in a concentration drop and hence a drop in the fluorescence signal. The signal then remains at a constant level before again rising. This rise can be said to coincide with the phase where oxidation becomes a competing process and the breakdown of large PAHs and soot particles leads to the re-emergence of smaller PAHs. This decrease and increase agrees with the studies of Mercier and co-workers[5, 6] in the jet cooled experiments discussed previously.

Looking at how the fluorescence signal changes over the range of height above burner upon excitation with 532 nm the same increase-decrease-increase is not seen. This can be explained by the PAHs which are excited being of a significant size that by the end of the measurement volume the PAHs have not been utilised in the soot formation. Without knowing which class of PAHs this signal is attributable to it is impossible to give an accurate answer as to why this is the case.

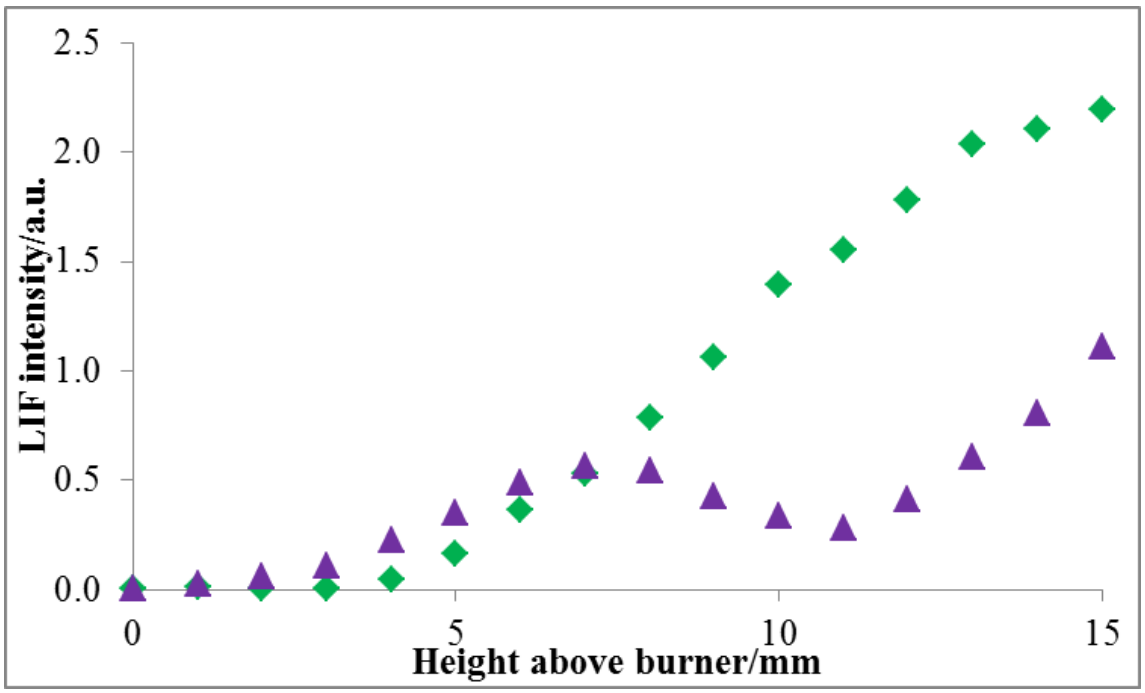

Figure 5-13: Fluorescence contribution at peak over range of heights above burner where Φ = 2.0 where λ_{ex} = 532 nm (♦) and 283 nm (■)

It can be seen, Figure 5-13, that the signals which are obtained in a flame with a stoichiometry of 2.0 follow much the same trend as the fluorescence signals which are obtained in the flame with a stoichiometry of 2.1. However, the drop in intensity of the signals obtained with 283 nm excitation is much more pronounced than in the previous case. This means that the PAHs which are being excited in this flame are being consumed in the region of the flame from 7 to 10 mm before PAHs which are excited by 283 nm begin to reform. Due to it being impossible using this technique to identify individual PAHs it cannot be said with any certainty that the PAHs which are being consumed and those which lead to the increase in the signal are equivalent. It can clearly be seen though that there is a consumption of smaller PAHs at a region in the flame where there is rapid soot growth.

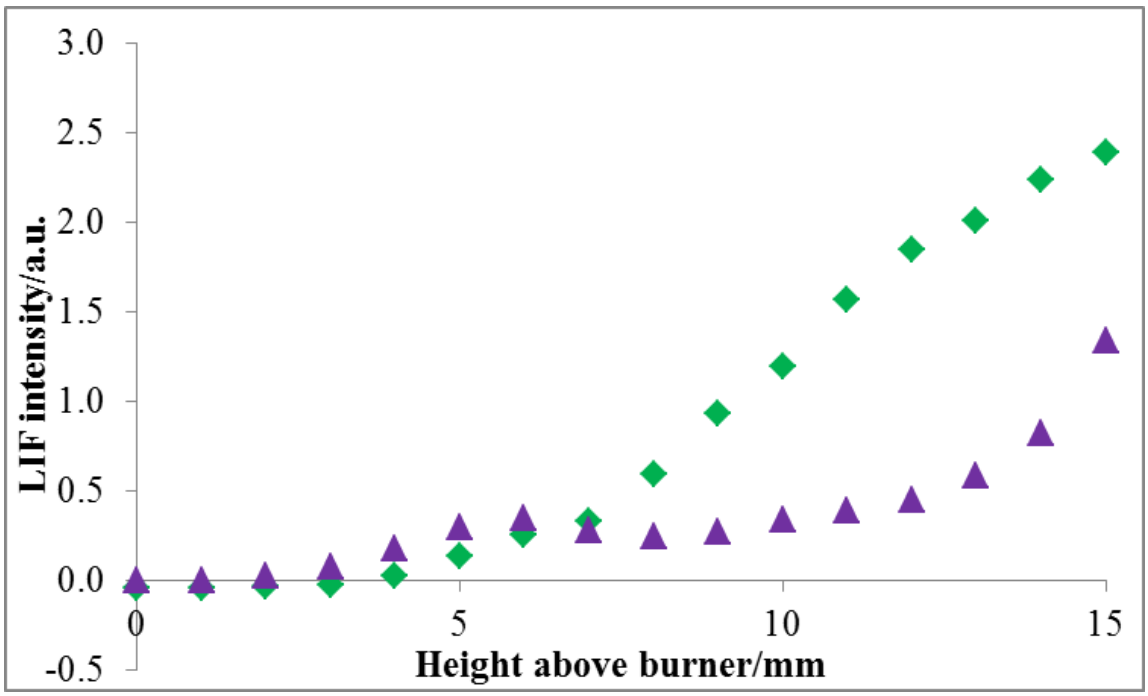

Figure 5-14 : Fluorescence contribution at peak over range of heights above burner where Φ = 1.9 where λ_{ex} = 532 nm (♦) and 283 nm (■)

Here, Figure 5-14, the drop in signal which is seen with 283 nm excitation occurs at a lower height in the burner than the previous cases and the re-increase is qualitatively much greater. This shows that although the PAHs are initially in small quantities this increases rapidly in the last few millimetres of the measurement zone. This suggests that although it has been shown previously from the decay time data that the flames, although different stoichoimetries, have soot of almost equivalent size at any given height in the flame the mechanism of the growth is not the same, or the ratio of soot produced to the PAHs formed is not equivalent in all flames.

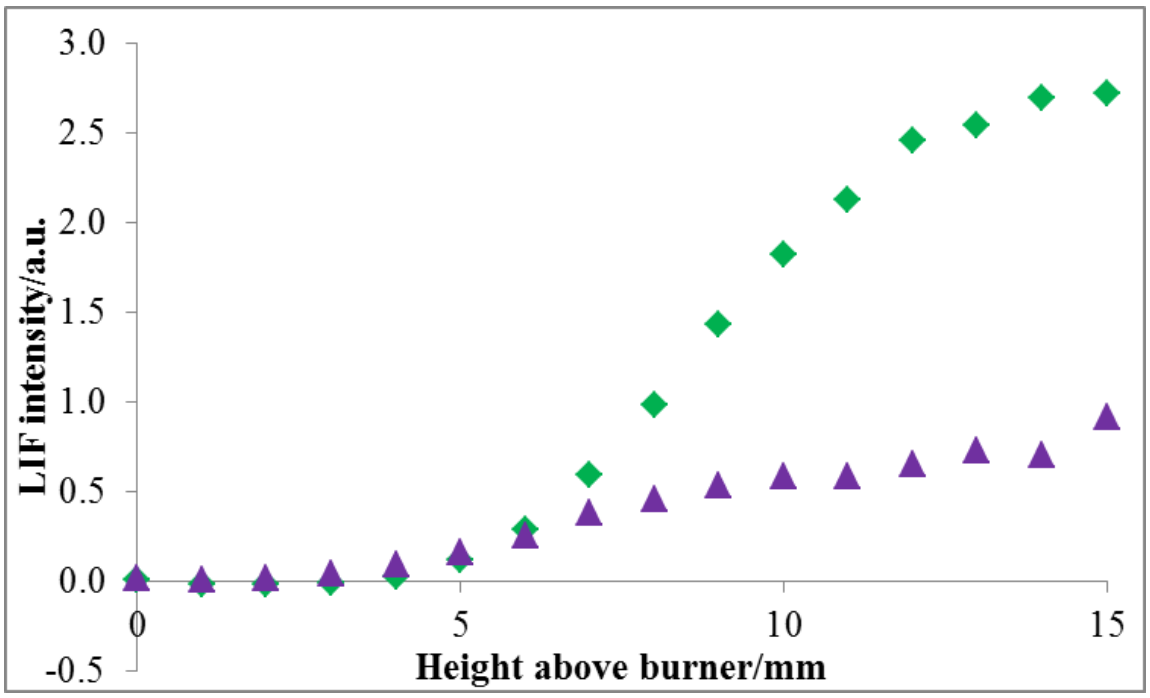

Figure 5-15 : Fluorescence contribution at peak over range of heights above burner where Φ = 1.8 where λ_{ex} = 532 nm (♦) and 283 nm (■)

The case here for a stoichiometry of 1.8, Figure 5-15, is markedly different from the previous conditions with no decrease and increase seen in the signal for 283 nm excitation. This suggests that the PAHs being excited by the 283 nm light are not being consumed during the reaction, or that if they are this is being masked by the formation of other PAHs of the same class. The slight increase in the signal obtained with 283 nm occurs after a brief plateau at 10 and 11 mm. This coincides with where the slight dip in decay time is seen in with all three of the excitation wavelengths. This could suggest that equilibrium is never reached in this flame, though this would require further investigation.

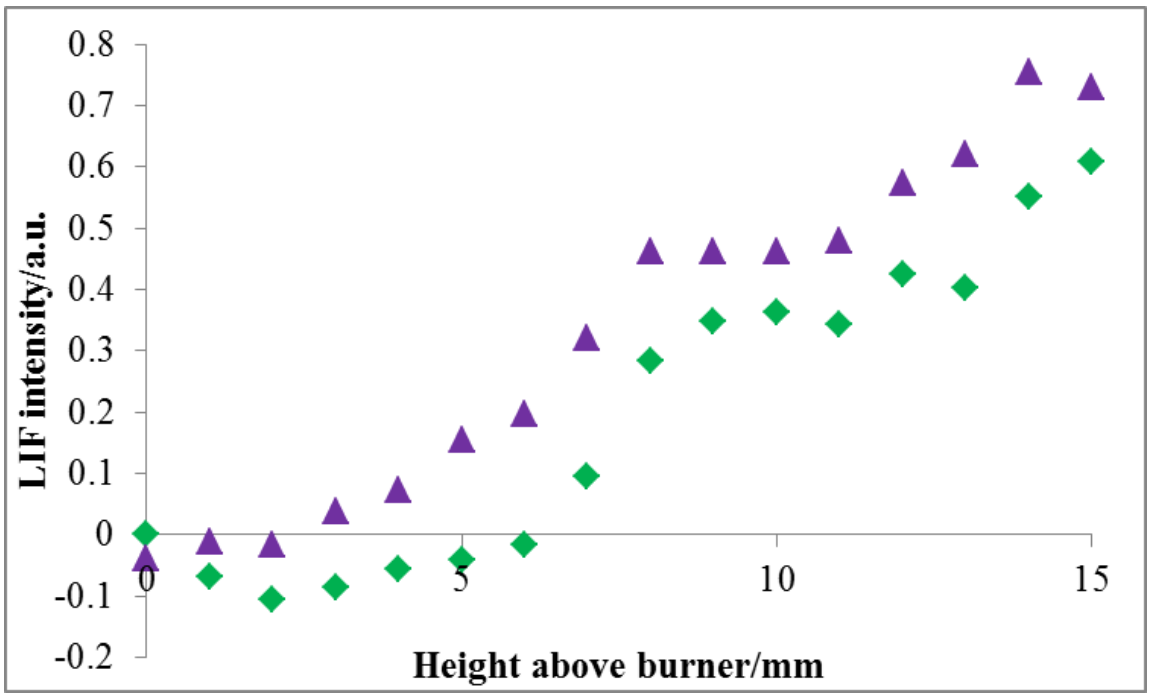

Figure 5-16 : Fluorescence contribution at peak over range of heights above burner where Φ = 1.7 where λ_{ex} = 532 nm (♦) and 283 nm (■)

Finally in the case for stoichiometry equal to 1.7, Figure 5-16, the signal is very weak, and hence it is difficult to extract any real information in the current set-up. However, it can be seen that the signals largely follow the same path as height above burner is increased. This correlates with what was seen initially when comparing the absolute signal obtained for 532 nm with that for 1064 nm (Figure 4-8) excitation as compared to the difference which is seen for the other stoichiometries where a large difference due to the fluorescence contribution is seen.

Therefore, it is not surprising with such little soot being formed, little LIF signal suggesting low formation of PAH, and the signal being similar for 1064 nm and 532 nm, that any PAHs which are present are in low concentrations as there is by far relatively less soot being formed under this flame condition.

5.4 EFFECT OF CHANGING STOICHIOMETRY ON LASER INDUCED FLUORESCENCE

In order to assess how the fluorescence is being impacted by the change in stoichiometry, the fluorescence contribution for 532 nm excitation was plotted as a function of height above burner, Figure 5-17

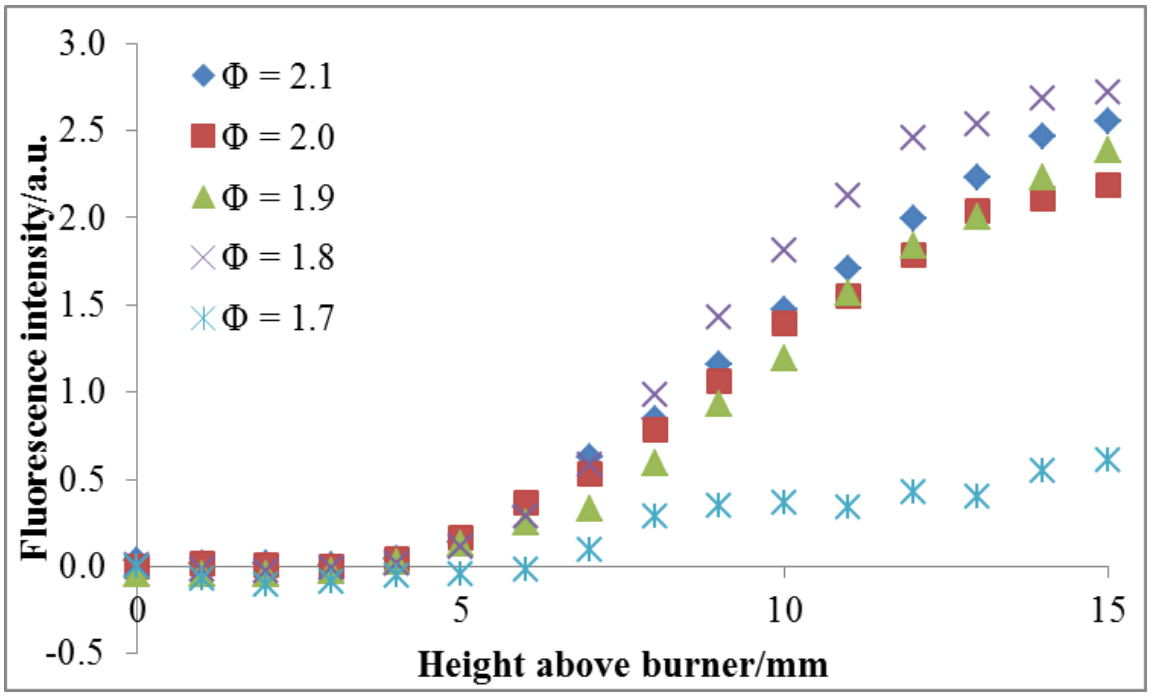

Figure 5-17 : Fluorescence contribution at peak over range of heights above burner where Φ = 1.7, 1.8, 1.9, 2.0 and 2.1 where λ_{ex} = 532 nm

When comparing signals obtained at one wavelength it is possible to infer something about the relative amounts of PAHs which are present in the flame. This is not absolute as the excitation wavelength will excite a range of PAHs but if they are present in similar relative quantities at each stoichiometry comparison can be made.

It can be seen that for stoichiometries 1.8 to 2.1 the signals obtained for 532 nm excitation are very similar. This is perhaps surprising as it may be expected that the PAHs which are present in the flame would show more difference between the stoichiometries.

Furthermore there appears to be no order to the data with $\Phi = 1.8$ giving the highest fluorescence contribution and $\Phi = 2.0$ giving the lowest, although these differences may be within the region of error. This may, in principle, be due to differences in the relative amounts of different PAHs are being excited in each of the flame conditions as well as the total PAH concentration. In order that this can be investigated there would need to be further studies into the specific PAHs which are present under a given set of flame conditions.

The same can be plotted for the fluorescence signal obtained with 283 nm excitation light at each stoichiometry, Figure 5-18

The relatively high signal for $\Phi = 2.1$ suggests that there are more free PAHs in this flame than the other conditions.

As can be seen the signal for $\Phi = 1.7$ which is obtained with 283 nm excitation is much more comparable with the signals obtained with $\Phi = 1.8$, 1.9 and 2.0. This suggests that there are smaller PAHs in this flame in similar quantities in each flame but a lower concentration of larger PAHs, as seen in the signal obtained with 532 nm. This could be explained by all the PAHs which are formed quickly progressing to form soot, without there being the same level of free PAHs which are seen in the other flame conditions.

All of the results outlined here are interesting, and encouraging with respect to the development of the technique. However, by only recording at one detection wavelength valuable information could be being eliminated. This will be further explored in the following chapter.

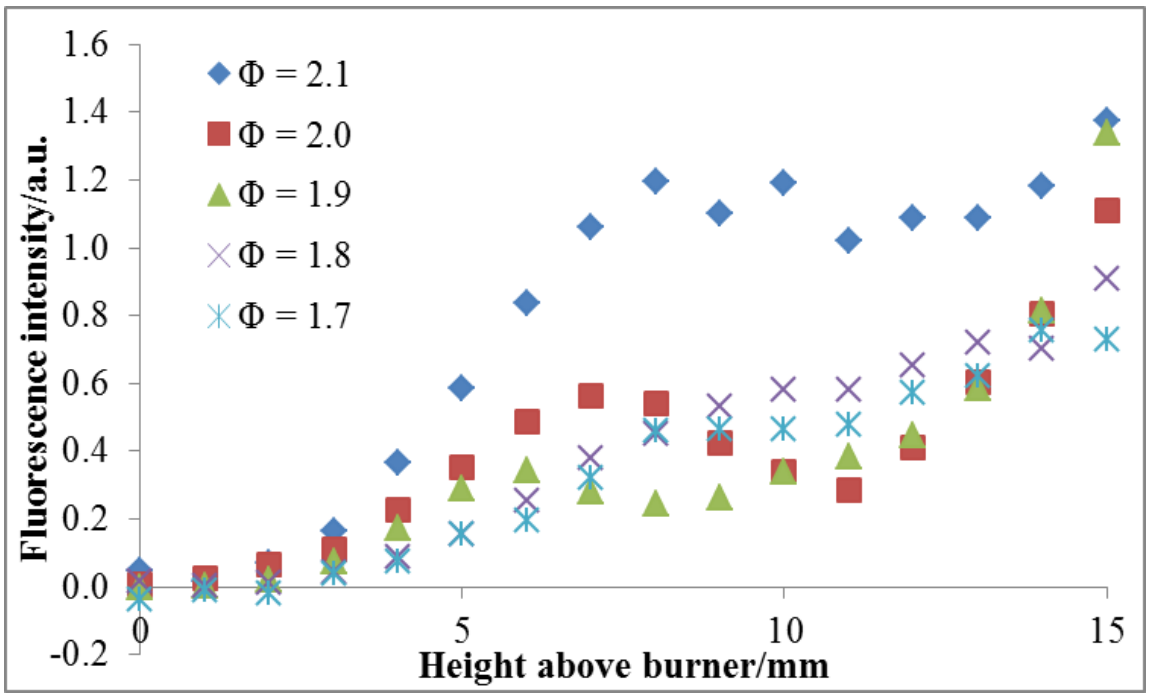

Figure 5-18 : Fluorescence contribution at peak over range of heights above burner where Φ = 1.7, 1.8, 1.9, 2.0 and 2.1 where λ_{ex} = 283 nm

5.5 LIF DECAY TIME

Further information can be obtained on the LIF lifetime in the same way at the decay time for the incandescence is obtained. This is achieved by taking the subtracted signal and fitting the decay time from the peak of the signal. This gives the times which are reported in Figure 5-19

It can be seen that for 532 nm excitation the decay time is fairly constant at all heights above the burner. The decay times do though correlate with what would be expected form fluorescence decays and are in the order of nanoseconds, unlike the incandescence signals which are in the order of hundreds of nanoseconds.

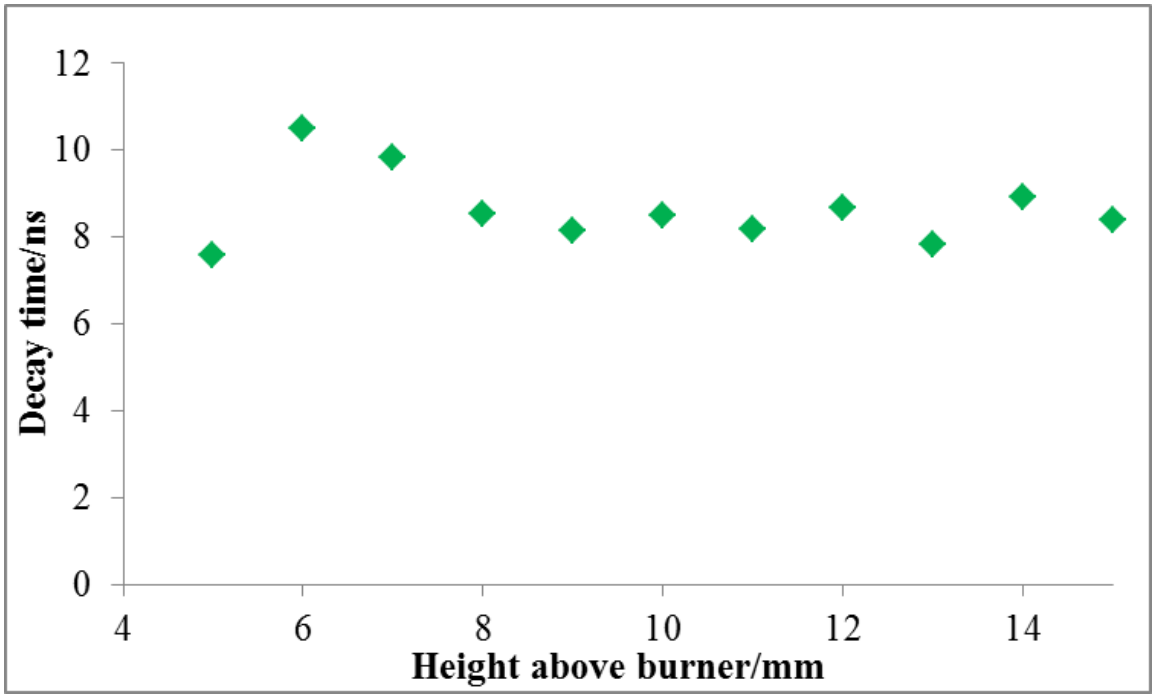

Figure 5-19 : Decay times for fluorescence signal obtained with λ_{ex} = 532 nm in flame where Φ = 2.1 from 5 – 15 mm above the burner surface

Care, however, must be taken when interpreting this as the rise time of the detector and pulse duration of the laser must be taken into consideration. The fluorescence lifetime seems to be too short to be measured with the equipment used during the present work. Additionally, the temporal profiles of the 1064 nm and 532 nm trigger may not be identical due to jittering, and as such slight offset in the timing of the pulses would significantly influence the LIF signals shown in Figure 5-9 and Figure 5-11.

In reality due to the different PAHs being excited the fluorescence signal will be a combination of different decays and hence the decay seen here may not be a true single exponential. As such in order to infer any real information from the fitted decay times an investigation must be undertaken in order to better understand what PAHs are present. For example if it were possible to deconvolute the decay times which were characteristic of specific PAHs much more valuable information could be gained. This may never,

though, be achievable, due to the short lifetime of fluorescence and the vast number of potential PAHs which it could be possible to obtain.

5.6 CONCLUSIONS

It has been shown that through use of this method it is possible to obtain signals with three different wavelengths of excitation light which have an equivalent incandescence signal. This has been shown to be the case through calculation of the decay time for each signal, after a time where any fluorescence and scattered light will have fully decayed, the decay times are largely equal for each wavelength. This is as had been hypothesised through careful choice of fluence. These results also show that although the optimum fluence was chosen from measurements which were made at a height of 15 mm in the flame, it is equally applicable in all sooting regions of the chosen flames. This was expected from the height above burner fluence curves seen in chapter 3.

It was then illustrated that as a result of the signal for 532 and 283 nm being as a result of a combination of fluorescence and incandescence it is possible to subtract the incandescence signal (as the 1064 nm signal will be due only to this) and obtain the fluorescence contribution. This means that it is possible, rather than treating the fluorescence contribution as an interference, to obtain information on the fluorescence. This is highly encouraging due to the difficulties associated with obtaining fluorescence information from sooting flames. Through use of this technique over the range of flame conditions which have been used in this work and it has been possible, by examining the height above burner measurements, to see the formation, consumption and reformation of PAHs within a given flame. This is especially encouraging as it shows agreement with what has been seen by the combustion group in Lille in samples which have been

extracted from the flame. The ability to obtain information which is comparable with extractive measurements without perturbing the flame is an exciting development.

However, due to the fluorescence signal not being directly related to a concentration in order for further information to be obtained via this method more understanding of the PAHs which are being formed would be required. The next chapter aims to begin to develop a method for this, whereby through recording the emitted signal over a range of wavelengths, rather than at one wavelength, could be used to obtain information on which PAHs are present.

5.7 REFERENCES

1. R. Lemaire, A. Faccinetto, E. Therssen, M. Ziskind, C. Focsa and P. Desgroux, *Proceedings of the Combustion Institute*, 2009, **32**, 737-744.
2. B. Axelsson, R. Collin and P. E. Bengtsson, *Applied Optics*, 2000, **39**, 3683-3690.
3. R. L. Vander Wal, T. M. Ticich and A. B. Stephens, *Combustion and Flame*, 1999, **116**, 291-296.
4. R. L. Vander Wal, K. A. Jensen and M. Y. Choi, *Combustion and Flame*, 1997, **109**, 399-414.
5. M. Wartel, J. F. Pauwels, P. Desgroux and X. Mercier, *Applied Physics B*, 2010, **100**, 933-943.
6. X. Mercier, M. Wartel, J. F. Pauwels and P. Desgroux, *Applied Physics B-Lasers and Optics*, 2008, **91**, 387-395.
7. P. Desgroux, X. Mercier and K. A. Thomson, *Proceedings of the Combustion Institute*, 2013, **34**, 1713-1738.

8. H. Bladh, J. Johnsson and P. E. Bengtsson, *Applied Physics B-Lasers and Optics*, 2008, **90**, 109-125.
9. G. Sutton, A. Levick, G. Edwards and D. Greenhalgh, *Combustion and Flame*, 2006, **147**, 39-48.
10. S. Will, S. Schraml and A. Leipertz, *Optics Letters*, 1995, **20**, 2342-2344.
11. R. J. Santoro, H. G. Semerjian and R. A. Dobbins, *Combustion and Flame*, 1983, **51**, 203-218.
12. C. S. Moreau, E. Therssen, X. Mercier, J. F. Pauwels and P. Desgroux, *Applied Physics B-Lasers and Optics*, 2004, **78**, 485-492.

6 SPECTRALLY RESOLVED LASER INDUCED FLUORESCENCE OF POLYCYCLIC AROMATIC HYDROCARBONS

It has already been highlighted that it is possible to separate the contribution of signals emitted from the flame which are attributable the fluorescence of small molecules and PAHs and the incandescence of soot. It was shown in chapter 5 that it is possible to isolate information from fluorescence through the subtraction of the incandescence signal from the total signal. However, the limitations of studying fluorescence in this way were highlighted – with one of the major issues being around the inability to identify the PAHs which are present or be able to quantify them. This issue echoes what is seen in ICCD images of flames which are presented in the work of Vander Wal[1], Schoemaeker Moreau[2] and Lemaire[3]. While this yields valuable information about the regions in the flame where PAHs are present and where soot is present in two dimensions in the flame it also cannot either quantify or identify PAHs which are present.

The work presented in this chapter aims to address this by presenting a new method of handling the emission of light from a flame which has been excited from laser light. This is achieved by recording the emitted light, not at one wavelength, but over a range of wavelengths from 400 – 700 nm for 532 and 1064 nm excitation light and 300 – 700 nm for 283 nm excitation light. The same process of subtraction as before was then used in order to obtain spectral data attributable to fluorescence. Through the success of this it would be possible if the spectra of known PAHs were obtained that it would be possible to identify the PAHs which are present from the fluorescence spectra.

It is of importance to be able to identify PAHs in flames which are sooting[4]. Through use of the technique outlined here it is possible to obtain information on both the soot

particles and the fluorescing molecules simultaneously. While this has been shown with imaging techniques this method obtains enough information that it would be possible through two sets of measurements (that is one with 1064 nm excitation and one with a shorter excitation wavelength) to obtain information on the regions in the flame where there is soot and the regions of fluorescence, the soot volume fraction, the soot particle size and information on the relative amounts of PAH present. This is a comprehensive set of information and can yield a great deal of information about a flame without having to extractively sample[5-8].

6.1 MEASUREMENT CONDITIONS AND COLLECTION OF SIGNAL

In the results shown in the previous two chapters five different stoichiometries were used and measurements were made at sixteen locations in each flame. These were repeated several times in each case so that reliable results could be obtained. Since the measurements in each of these flame conditions were only recorded at one wavelength the measurements were relatively quick to obtain. However, measurements that are both temporally and spatially resolved take much longer as the signal must be sequentially gathered at each wavelength. Therefore instead of using all of the flame conditions, 6 measurement points were chosen, covering a broad range of conditions. Additionally only three stoichiometries were selected for use – Φ = 2.1, 1.9 and 1.7, with the signal recorded at two measurement heights in each flame – 10 mm and 15 mm. These heights were selected as from work shown in chapters 4 and 5 it could be seen that for each excitation wavelength there is an incandescence signal at this height and for 532 nm and 283 nm excitation a fluorescence signal was also obtained here.

The set up employed for this section is fully outlined in chapter 3 as set up II. It involves the use of a monochromator in order to obtain the signal over a range of wavelengths.

However, through early preliminary measurements it was found that when either 532 nm or 1064 nm light were being used for excitation there was an interference in the measured signal as a results of small amounts of scattered green light getting onto the PMT. Therefore in order to eliminate this a notch filter was employed at 533 ± 17 nm FWHM, (OD = >6.0 at 533 nm) and positioned immediately prior to the PMT to block the majority of any green light which was making it through the monochromator to the detector. However, this notch filter also blocks wavelengths shorter than 400 nm. In equivalent preliminary measurements using 283 nm light it was found that there was little interference from green stray light, even without the use of the notch filter. This was expected as the 283 nm light is being emitted from the dye laser, allowing the whole of the light which is being emitted from the Nd:YAG to be enclosed, whereas even when making 1064 nm measurements there needs to be a gap in the shielding, through which small amounts of scattered 532 nm light can escape. Therefore, for 283 nm measurements it was possible to extend LIF spectra down to 300 nm. Athough there could be no direct subtraction of 1064 nm in the range 300 – 400 nm this was still recorded, and will still be shown as it is interesting to see how the signal at such wavelengths varies when a short wavelength of excitation is used. There are limited examples using short wavelengths of light seen in the literature, however D'Anna[9] has shown that using 366 nm similar work can be carried out. However, in her work the incandescence signal does not come from experimental measurements but is a fitted curve.

The upper wavelength was chosen to be 800 nm for 1064 nm and 532 nm excitation and 700 nm for 283 nm excitation. At wavelengths which are longer than this due to the efficiency of the PMT employed the signals begin to get low. This means that attributing the signal to either LII or LIF and not noise becomes increasingly difficult. This left a wavelength range of 300 nm for use which was considered ample for the work which is to be presented here. Due to the time taken to obtain measurements, and the resolution of the monochromator, it was decided that recording the signal every 2 nm would be a sufficient resolution to use.

For this section of work due to the collection of measurements being taken over a shorter period of time than the first section of work, with no changes to the set-up during this time, there was absolute quantitative agreement seen between the LII signals which were obtained, as shown in Figure 6-1

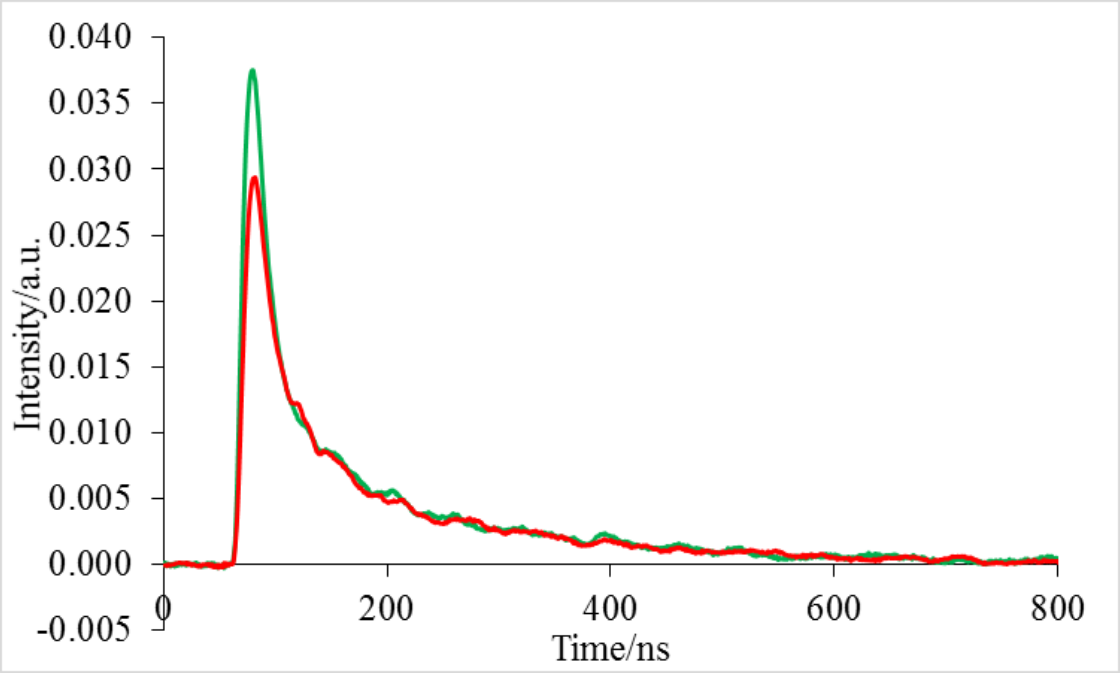

Figure 6-1 : Comparison of decay profile obtained with 532 nm and 1064 nm excitation 15 mm above the burner surface where Φ = 2.1

As can be seen with no normalisation the signals are equivalent by 100 ns after the trigger at this wavelength, showing that there is quantitative agreement in the LII signal allowing for subtraction of the signals obtained with 283 nm and 532 nm excitation from that obtained with 1064 nm excitation. The fact that there is such good quantitative agreement confirms the validity of normalising the signals obtained in chapters 4 and 5 at 200 ns after the Q-switch trigger.

It should be noted that unlike in previous chapters where the Q-switch trigger was used in order to begin the signal recording, in this chapter a photodiode was used as the

trigger. This means if comparing the signal to one obtained in chapters 4 or 5 the signals occur 20 ns earlier in this chapter (as the PD triggers 20 ns after the Q-switch trigger).

6.2 INITIAL MEASUREMENT

As with the measurements in chapter 4 it is methodical to begin such measurements in the flame which will give the highest signal. This initially allowed for an optimisation of the process and also the settings can be adjusted in order that the maximum values are just below the threshold, allowing the best possible conditions for the lower stoichiometries.

Therefore, initially the signal obtained for $\Phi = 2.1$ at 15 mm above the burner surface using 532 nm excitation was recorded. By plotting the signal obtained at the peak compared to the signal obtained 180 ns after the trigger the change in the shape of the signal can be seen as shown in Figure 6-2.

As can be seen, and as would be expected there is a difference in the spectral shape obtained for the peak signal and the signal 180 ns after the trigger. This is because, as has been highlighted, the peak signal is a combination of both LII and LIF, where the signal obtained 180 ns after the trigger will only be due to incandescence. It is evident that the difference in shape is considerable, especially in the region around the excitation wavelength. This is as would be expected due to the majority of fluorescence occuring close to this excitation wavelength[1, 10].

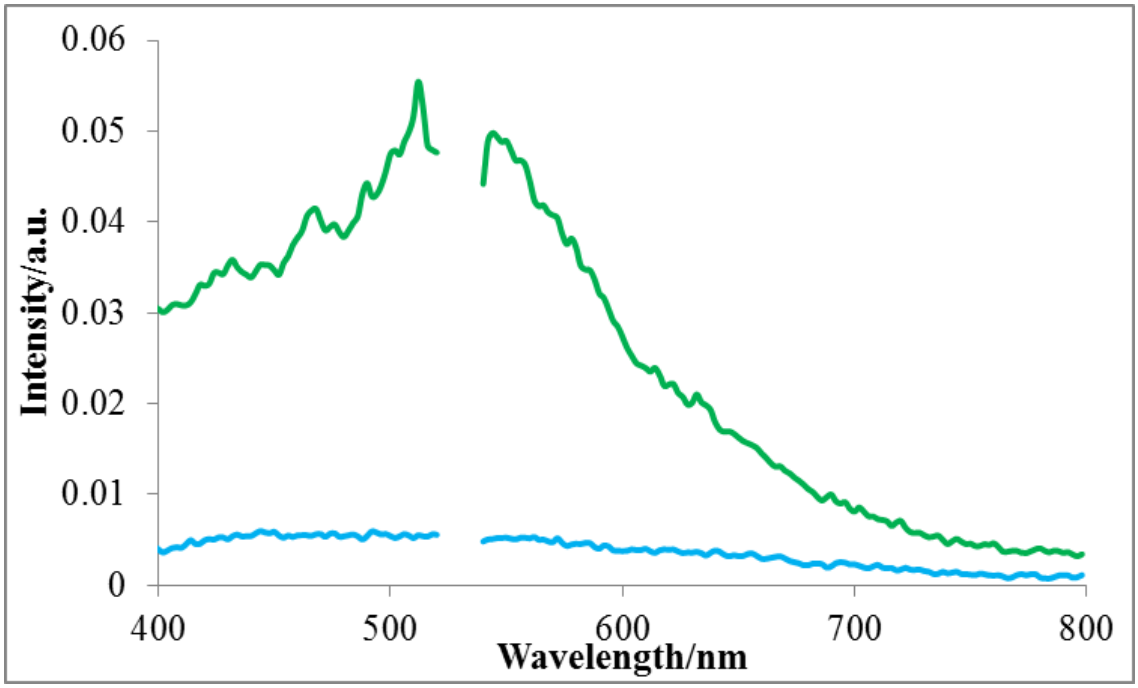

Figure 6-2 : Peak signal (—) and signal after 180 ns after the photodiode trigger (—) obtained in a flame with a stoichiometry where Φ = 2.1 with λ_{ex} = 532 nm excitation at 15 mm above the burner surface

6.2.1 Correction of the signal

Initially the first observation which comes to mind when looking at the signal after 180 ns which is obtained is that it does not look like one would expect an incandescence signal to over the wavelength range shown for particles of a temperature such as those found in the flame, circa 2400 K[11]. However, it must be remembered that some corrections which must be applied. Firstly there must be a correction for the soot emissivity over the wavelength range. Then there must be a correction for the PMT (Hamamatsu R636-10) response[12], which dictates that above 600 nm the efficiency drops steeply, giving progressively lower signals on increasing the wavelength of collection. Finally there is an error associated with the monochromator as a result of the grating efficiency. If these are corrected for the signal will look more akin to what would be expected from such measurements as shown in Figure 6-3.

It can be seen that when compared to a perfect blackbody curve little difference is seen between the incandescence and the blackbody curve. It is expected that there would be some differences as a laser heated particle within the flame will not cool only via incandescence and there will be losses via sublimation and conduction. The greatest degree of variation is seen at the highest wavelengths. This is due to the efficiency of detector decreasing upon increasing wavelength. In order to better investigate the correlation between the incandescence signal and blackbody radiation it would be advantageous to use a PMT which has greater efficiency at longer wavelengths.

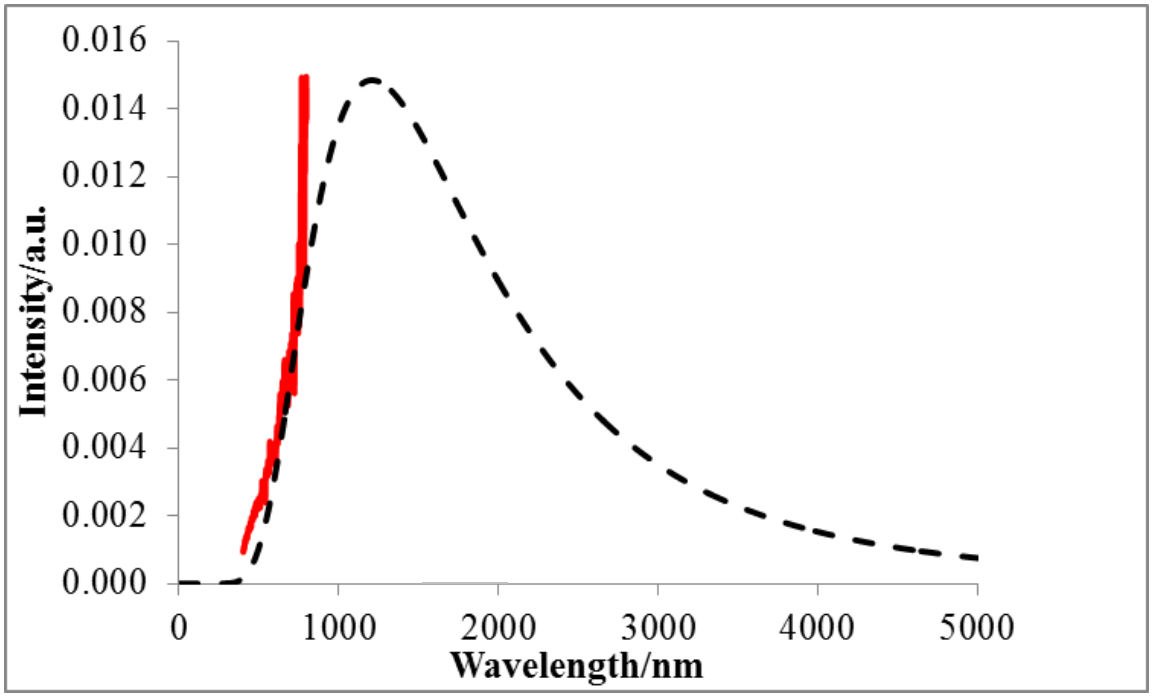

Figure 6-3 : Corrected spectrum for the peak signal obtained with λ_{ex} = 1064 in a flame where Φ = 2.1 at 15 mm above the burner surface with blackbody curve (--) for a body emitting light at 2000 K

For the remainder of the work presented here there will be no such corrections carried out. This is because upon correcting the signals at longer collection wavelengths for

weaker signals there is more noise present, which is emphasised by the correction, especially after longer detection times. This makes it more complicated to compare the results and as such the raw signal will be shown.

6.2.2 Comparison of signal obtained with 532 nm excitation with that obtained with 1064 nm excitation

Conversely to the signal obtained with 532 nm excitation, the signal obtained when exciting with 1064 nm will be attributable only to incandescence and as such while it would be expected that the peak signal and the signal 180 ns after the trigger would differ in intensity they would differ less substantially in shape, as shown in Figure 6-4.

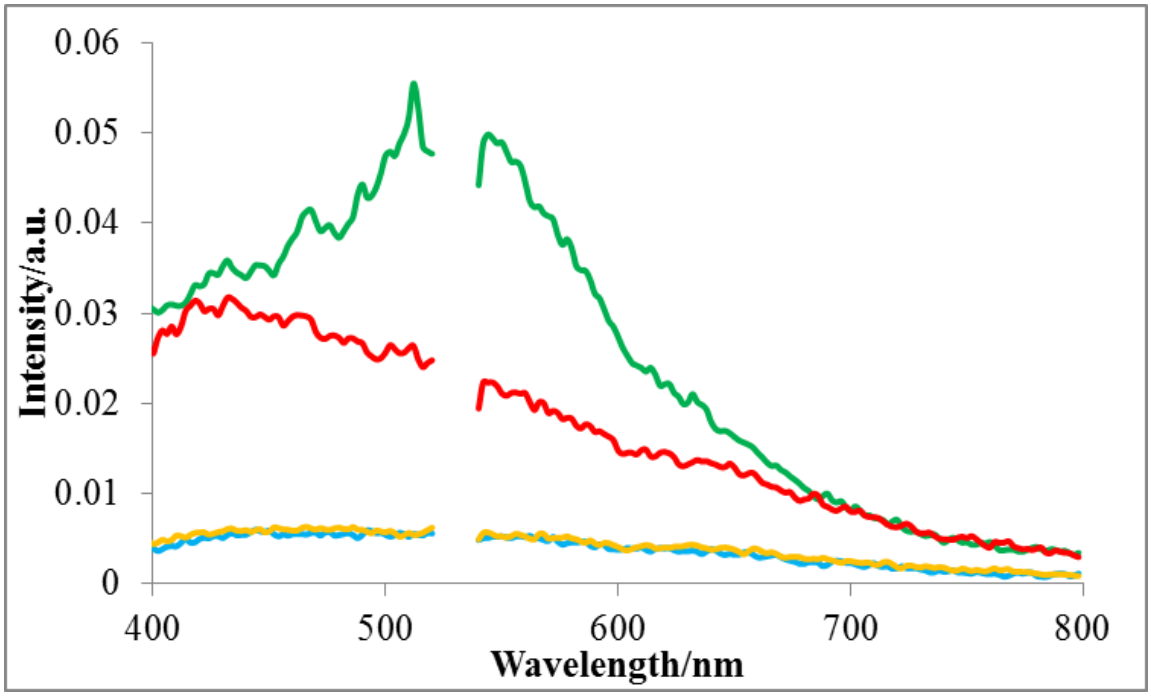

Figure 6-4 : Peak signal and signal after 180 ns obtained in a flame where Φ = 2.1 with λ_{ex} = 532 nm (— and — respectively) and λ_{ex} = 1064 nm (— and — respectively) at 15 mm above the burner surface

Any changes in the incandescence spectral shape as a function of time is seen to be more prevalent at shorter wavelengths. This is because the incandescence signal decays faster at shorter wavelengths causing the black-body spectrum to shift towards longer wavelengths as the particle cools.

As has been shown in previous chapters any difference between the signal resulting from 1064 nm excitation and that of 532 nm excitation can be attributed to fluorescence. By plotting the signal obtained over the wavelength range as a function of time this is clearly shown to be the case.

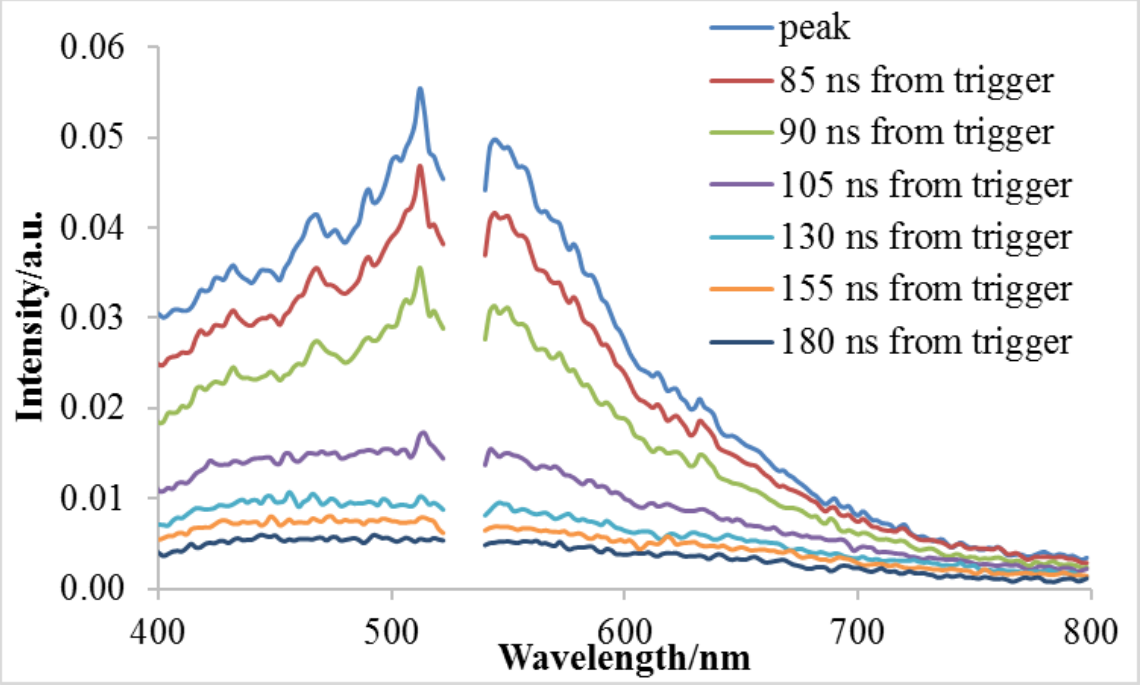

Figure 6-5 : Peak signal and signal at range of times after trigger obtained at 15 mm above the burner surface in a flame where Φ = 2.1 with λex = 1064 nm excitation

Thus it can be seen that the peak signals for 1064 nm and 532 nm excitation are very different, especially in the range 450 – 700 nm, with the signal with 532 nm excitation

being much higher at the peak than the equivalent signal obtained with 1064 nm excitation. This is not the case after 180 ns where the signals are equivalent, which is as would be expected when there is no remaining fluorescence contribution.

Since the decay of the fluorescence occurs gradually the change in the shape of the 532 nm spectra can be seen over time. This can be seen in the signal obtained with 532 nm excitation at 15 mm above the burner if plotted at a range of times after the peak signal shown Figure 6-5

The contribution of LIF to the signal can clearly be seen in the region between the peak and 180 ns after the signal. After 50 ns the decay has been such that the shape of the decay is like that which is seen with the incandescence only signal recorded with 1064 nm excitation.

To illustrate this the above was plotted again but with the signal obtained for 1064 nm excitation 130 ns, 155 nm and 180 ns after the trigger included and is shown in Figure 6-6

This shows that the 532 nm signal decays to converge with the 1064 nm signal, and therefore attributable only to incandescence by 130 ns after the trigger, which relates to around 50 ns after the peak LII signal. This is as would be expected as, as has been discussed, the particles are being heated to the same temperature and therefore, as with the measurements in the previous chapter, the incandescence signal should be equivalent at all detection wavelengths for both excitation wavelengths. However, it can be seen that the fluorescence differs across the detection wavelengths, which again is as could be expected as the wavelength where the fluorescence will be emitted is dependent on the structure of the molecule which has been excited. It is also known that fluorescence will predominantly occur around the excitation wavelength and as such it would be expected that the largest proportion of fluorescence will surround 532 nm.

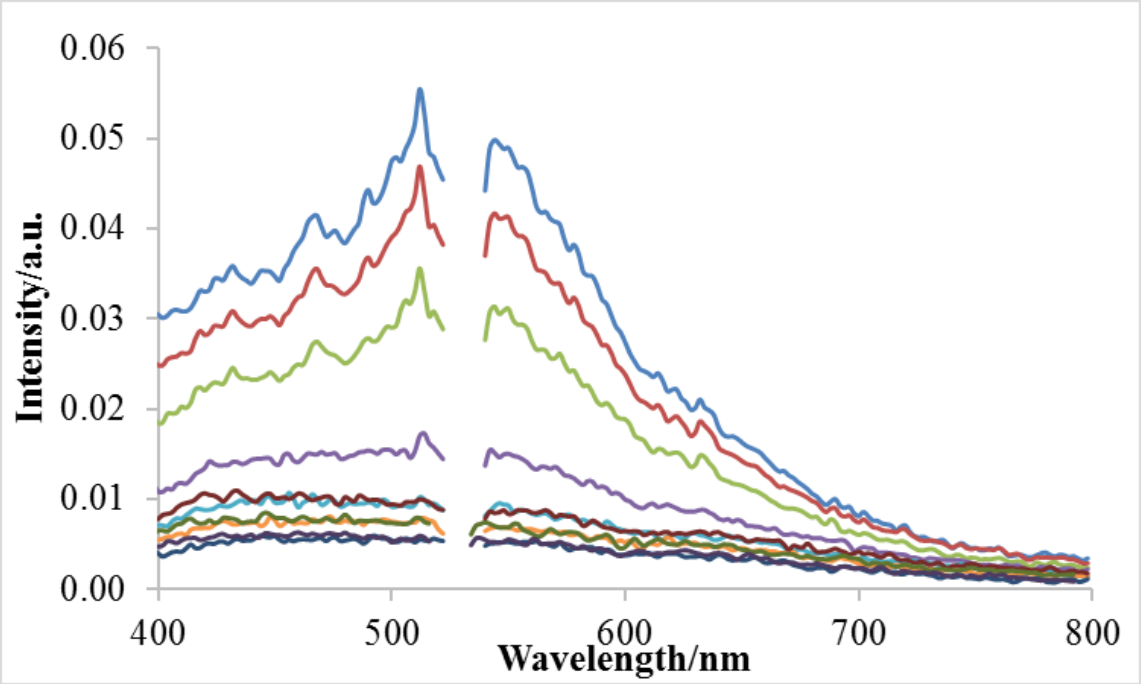

Figure 6-6 : Peak signal and signal at range of times after trigger obtained at 15 mm above the burner surface in a flame where Φ = 2.1 with λ_{ex} = 532 nm excitation and at time 130 ns, 155 ns and 180 ns after the trigger with λ_{ex} = 1064 nm (—)

This being the case by the subtraction of the signal obtained with 1064 nm excitation from the signal obtained with 532 nm excitation the resultant signal will be, as with the point measurements, attributable only to the fluorescence signal. As the signal has been recorded at a range of detection wavelengths this will result in a fluorescent spectra. As has been discussed this will be characteristic of the PAHs which are present in the flame.

In order to illustrate this the signal obtained for 1064 nm in a flame of Φ = 2.1 at 15 mm was subtracted from the signal obtained in the same flame conditions with 532 nm excitation. This was plotted at both the peak and a range of times after the trigger in order to observe the fluorescence decay, Figure 6-7

This shows that the fluorescence is decreasing rapidly over time. There is no signal above 700 nm, which is as would be expected due to a combination of it being expected

that fluorescence will occur closer to the excitation wavelength and the increasing inefficiency of the detector above this wavelength. As can be seen by 130 ns after the trigger, corresponding to around 50 ns after the peak, all of the signal has decayed completely and there is no signal observed.

It appears that there are some features which it could be possible to identify, namely those occurring at 446 nm, 480 nm, 492 nm, 550 nm, 570 and 576 nm, and there is definitely a characteristic shape present. Some peaks decay quicker than others and this could be attributable to specific features of the PAHs. However, the peaks which occur around 468 nm and 516 nm are potentially as a result of laser induced C_2 and termed Swan bands[13]. This is one of the main interferences which can occur when employing laser diagnostics in the study of flames. This is an especially large problem in Raman studies[14, 15] and becomes more prevalent as the fluence used is increased. This is due to C_2 radicals being a product of the laser induced breakdown of molecules upon excitation with 532 nm light. It would be possible, by increasing the laser fluence to a sufficiently high level as to deliberately induce Swan bands to identify if what is shown in the above figure is definitely attributable to C_2 radicals.

There appears, from looking at Figure 6-7 to be anomaly in the data from 400 – 450 nm where the signal is negative. This is due to the 532 nm signal being slightly lower than that obtained with the 1064 nm data. However, this is within the normal variation of the data and is only accentuated here due to the relatively low fluorescence signal level. Also the random noise in the spectrum is exaggerated when taking the difference between two similar values.

As has been discussed above the fluorescence signal appears to be centred around the excitation wavelength, but this appears to be a consequence of the detectors efficiency.

It would be possible, through use of known fluorescence spectrum of PAHs, to fit these to spectra which have been obtained in the way outlined above. This would open the possibility to use this method to identify classes of PAH which are present at a given point in the flame. This would open the door identification of PAHs in a way that is only

possible through intrusive methods presently. Although this method would not give great enough resolution to identify specific PAHs any possibility to identify PAHs in the sooting region would be welcomed[4].

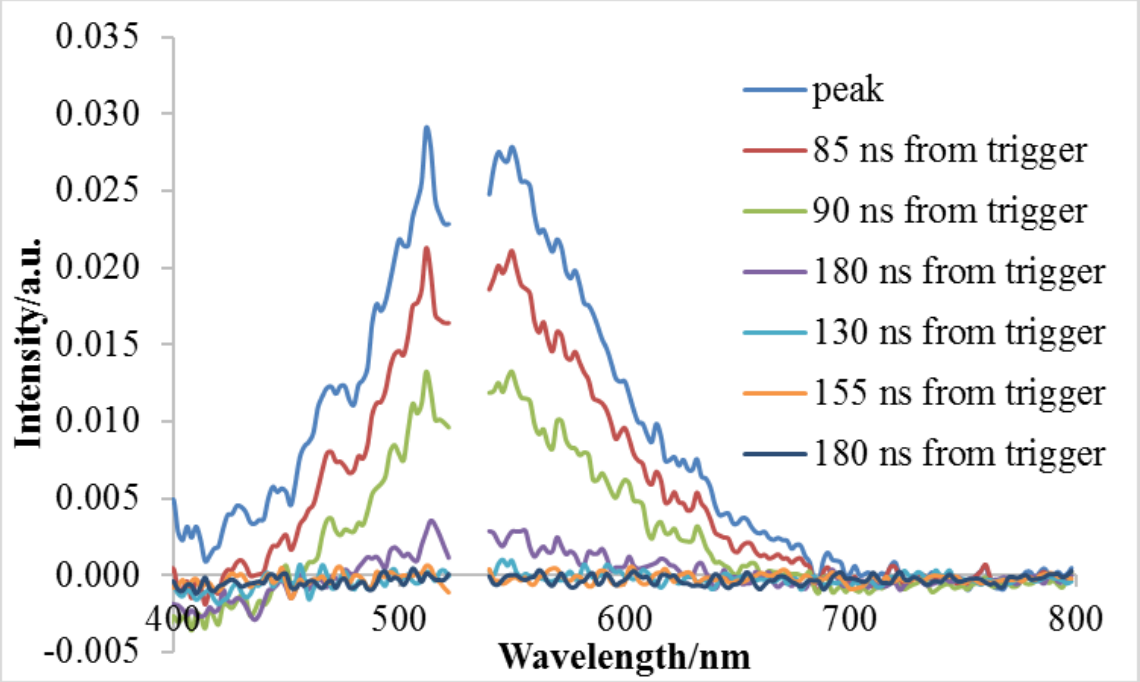

Figure 6-7 : signal obtained over wavelength range 400 – 700 nm at variety of time delays after the trigger where λex = 1064 nm signal is subtracted from the signal obtained for λex = 532 nm at 15 mm in a flame where Φ = 2.1

6.3 IMPACT OF CHANGING STOICHIOMETRY

By changing the stoichiometry it is possible to ascertain how the incandescence signal and fluorescence signal change over the range. Initially this was carried out using 532

nm and 1064 nm excitation at the three different stoichiometries, Figure 6-8 and Figure 6-9.

As can be seen the signals resulting from 532 nm excitation show the same features at 436 nm and 494 nm for each stoichiometry. This is as would be expected as in chapter 5 with the point measurements it seems that upon changing the stoichiometry there is only very little change in the soot particle properties at a given height above burner, but rather the change comes in the soot volume fraction. As such it may not be expected that there would be a different class of PAHs present at 15 mm in the different flames. If there was a large change in the PAH structure at each stoichiometry it may be expected that there would be difference features seen in the spectra. This will be further confirmed by looking at the subtraction of the 1064 nm spectra in order to see the signal attributable only to PAHs, and thus any differences in the spectra would be highlighted. It also must be remembered that any given excitation wavelength will only excite a small range of PAHs and as such there may be differences in other classes of PAHs which are being formed.

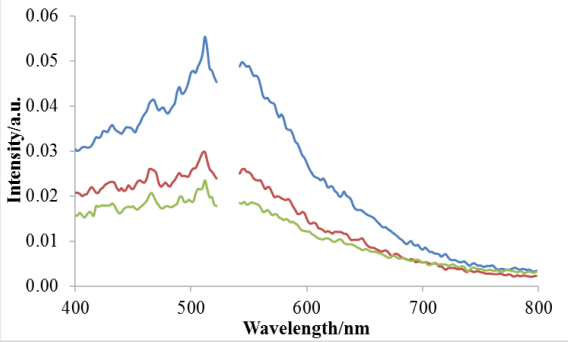

Figure 6-8 : signal obtained at peak over wavelength range 400 – 800 nm in a flame where Φ = 2.1 (—), 1.9 (—) and 1.7 (—) and λ_{ex} = 532 nm at 15 mm above the burner surface

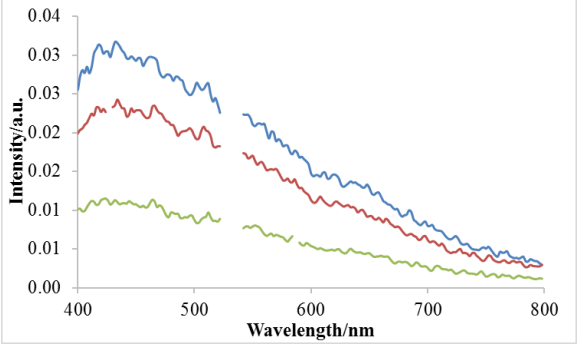

Figure 6-9 : signal obtained at peak over wavelength range 400 – 800 nm in a flame where Φ = 2.1 (—), 1.9 (—) and 1.7 (—) and λ_{ex} = 1064 nm at 15 mm above the burner surface

As would be expected there is no change in the shape of the signal obtained when exciting with 1064 nm excitation. This is because the incandescence signal, no matter the concentration or size of the soot particles, will always have the same spectral shape if the particles are heated to the same temperature. The increase in intensity which is seen between the signals of different stoichiometry is due to the increased soot volume fraction ensuring that there are a larger number of particles incandescing in the measurement volume.

As in chapter 5, it is possible to subtract the signal which is obtained from 1064 nm excitation from that which is obtained for 532 nm excitation. In this case we are left with a spectrally resolved signal which is solely attributable to fluorescence, Figure 6-10.

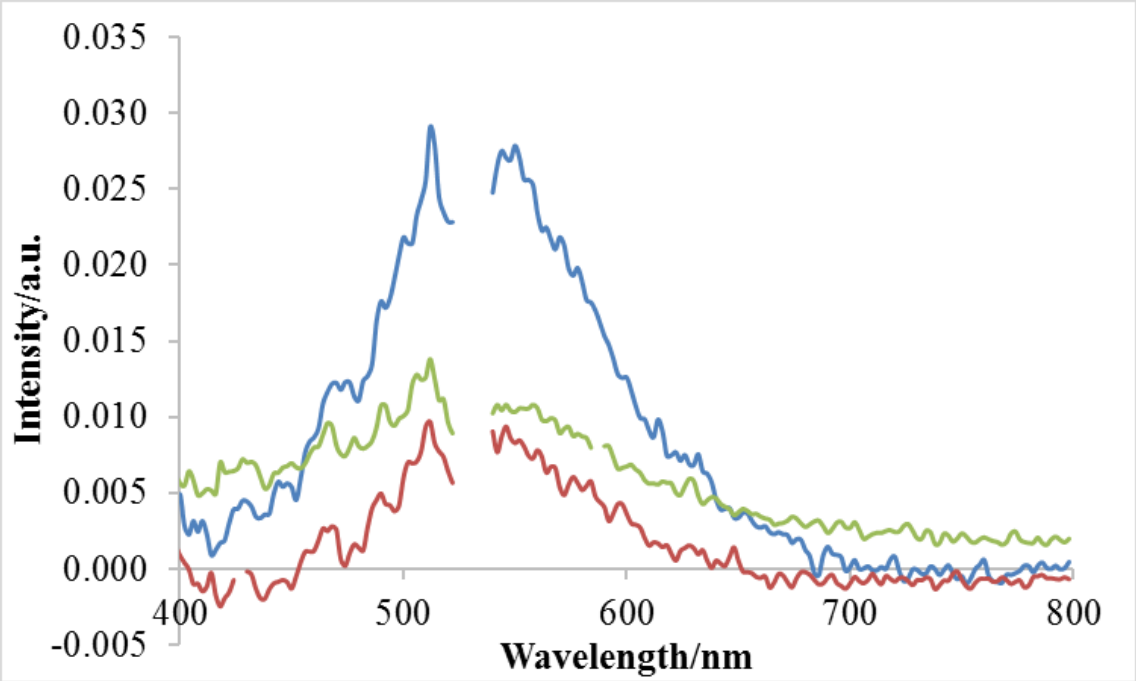

Figure 6-10 : signal obtained at peak over wavelength range 400 – 800 nm for λ_{ex} = 1064 nm subtracted from signal obtained for λ_{ex} = 532 nm in a flame where Φ = 2.1 (—), 1.9 (—) and 1.7 (—) at 15 mm above the burner surface

As can be seen there is a higher intensity of the fluorescence which is found in the flame where Φ = 2.1. However, the signals which were obtained for Φ = 1.9 and 1.7 are largely similar in magnitude. This suggests that there are very similar quantities of PAH present in the Φ = 1.9 and 1.7 flames. At both shorter and longer wavelengths, however, the signal in the Φ = 1.7 flame are higher than those observed in the Φ = 1.9 flame but this may well be due to experimental errors since no LIF signal is expected at 800 nm. This could have been due to measurement issues and if the spectrum was shifted so that it had a baseline value of zero at 800 nm the Φ = 1.7 data would fall below the Φ = 1.9 data at almost all wavelengths. It can be seen that the signal obtained for Φ = 2.1 shows a high degree of fluorescence over the region 450 – 650 nm. This region differs in shape from what is seen for the other stoichiometries and could indicate the presence of different classes of PAHs. This would have to be further investigated in order to draw firm conclusions.

6.4 IMPACT OF CHANGING HEIGHT ABOVE BURNER

It has been discussed how the signal changes on increasing the height above the burner surface where the measurement is being made. In order to investigate this the measurements described above were recorded at 10 mm above the burner surface. It was hypothesised that there would be a difference in the signal which is obtained when compared to the signals obtained at 15 mm, Figure 6-11and Figure 6-12.

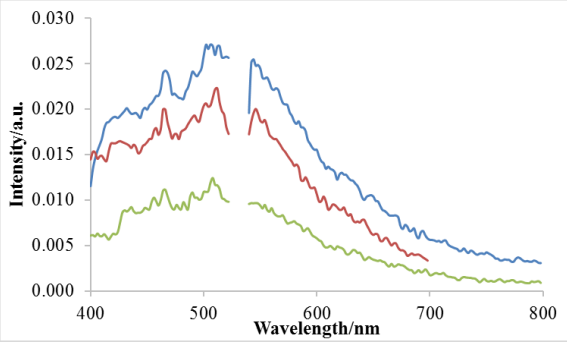

Figure 6-11 : signal obtained at peak over wavelength range 400 – 800 nm in a flame where Φ = 2.1 (—), 1.9 (—) and 1.7 (—) and λ_{ex} = 532 nm at 10 mm above the burner surface

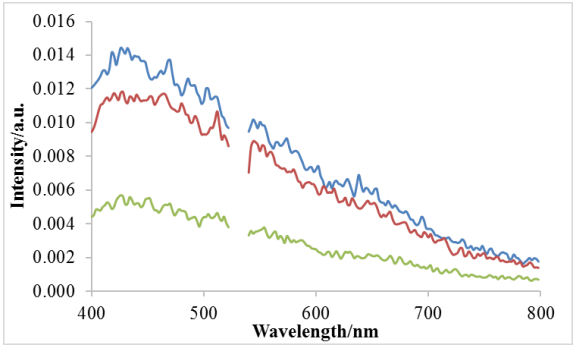

Figure 6-12 : signal obtained at peak over wavelength range 400 – 800 nm in a flame where Φ = 2.1 (—), 1.9 (—) and 1.7 (—) and λ_{ex} = 532 nm at 10 mm above the burner surface

As with the measurements recorded at 10 mm as a result of 532 nm excitation there are features which are seen between 400 nm and 550 nm which are common to the signal obtained for each stoichiometry. Again this suggests that there are similar PAHs present in each flame. Largely these occur around the same regions as that observed at 15 mm, however they are stronger at 10 mm. This agrees with what has been seen in chapter 5, where the LIF signal resulting from 532 nm excitation increases in an almost linear way between 10 mm and 15 mm.

As expected the signal obtained form 1064 nm excitation is the same shape for each of the stoichiometries, because the signal is attributable only to incandescence. However, in this case, and unlike what is observed at 15 mm in the flame, the signal is much more similar for Φ = 1.9 and 2.1. This suggests there are far fewer particles in the flame where Φ = 1.7.

This allowed for the subtraction of the signal obtained with 1064 nm excitation from that obtained with 532 nm excitation, Figure 6-13.

The signal for Φ = 2.1 is greater than the signal for Φ = 1.7 and 1.9, however, greater of understanding of the PAHs which are present in this region of the flame would be required to infer information about the relative concentrations present. There is less of a difference, however, than is observed at 15 mm in the flame. This suggests that there are relatively more PAHs by 15 mm compared to 10 mm.

Although the signals which are shown here may at first appear incomparable to those shown in previous chapters, with a seemingly high Φ = 1.7 signal, this is not entirely the case. When comparing with figures 4.6 and 4.7 it can be seen that relatively there is not a great deal of difference in the relative intensities at 450 nm. Also through comparing the signal seen at 450 nm in figure 6.13 with figure 5.17 the signal for Φ = 1.7 is not significantly greater than what would be expected. This suggests that any small discrepancy seen in the intensity of the LIF signal shown above could be due to experimental variation. There is no evidence that if the signal had been measured at a slightly different wavelength in previous chapters that the signal would be as low as seen at 450 nm.

We can then compare the fluorescence which is seen for each stoichiometry at the two different selected heights. Figure 6-14 shows the comparison of the signal obtained at 15 mm and 10 mm where Φ = 2.1 It can be seen from this comparison that there is a lower signal obtained at 10 mm in the flame compared to that obtained at 15 mm. From the results shown in chapter 4 this is what would be expected. The highest degree of separation between the signals occurs between 475 and 650 nm, which is as would be expected when 532 nm excitation is used – with the majority of the fluorescence to occur beyond this wavelength.

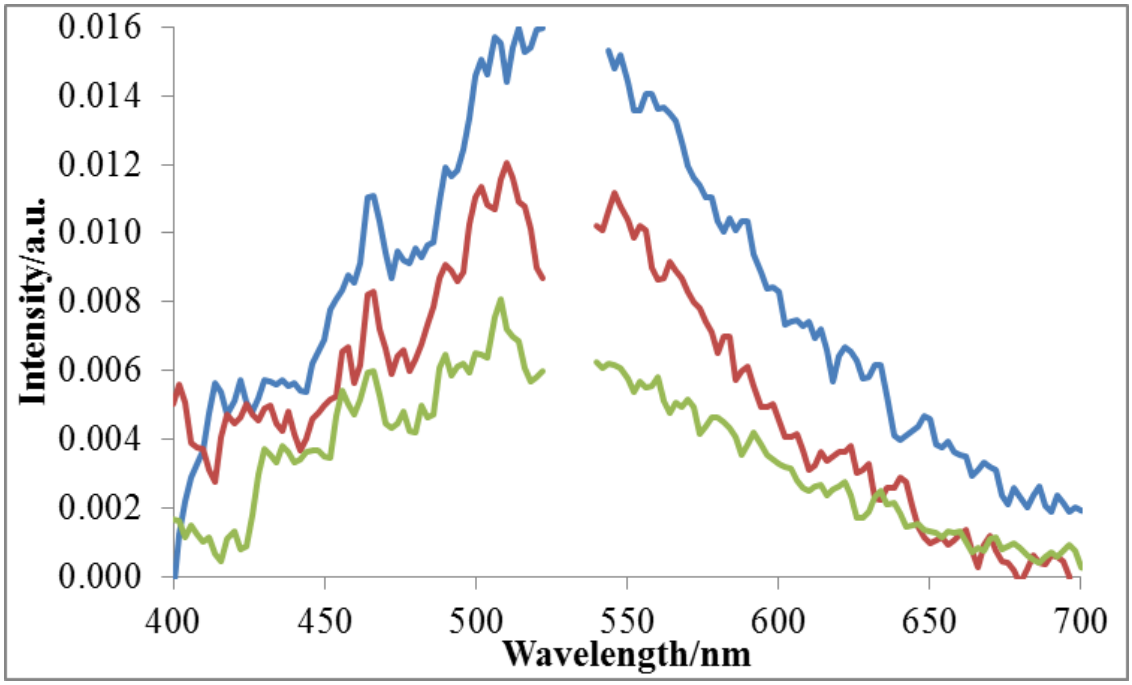

Figure 6-13 : signal obtained at peak over wavelength range 400 – 700 nm for λ_{ex} = 1064 nm subtracted from signal obtained for λ_{ex} = 532 nm in a flame where Φ = 2.1 (—), 1.9 (—) and 1.7 (—) at 10 mm above the burner surface

Although many of the spectral features between the two signals are similar there are regions where a difference in signal can be seen. At 450 nm there is what appears to be a peak at the higher height, though not at the lower, and again in the region around 475 nm. Similarly, in the region from 550 nm – 575 nm there are peaks seen in the 15 mm spectrum but not in the 10 mm. Equally, there are peaks occurring in the 10 mm spectra which are not present in the 15 mm, notably from 575 nm – 600 nm. This suggests that while the spectra are similar there are different PAH classes at each of the heights recorded. This presents the possibility, if there were spectra readily available to known spectra, to identify the PAHs which are present in each case and see the evolution of the PAHs with increasing measurement height.

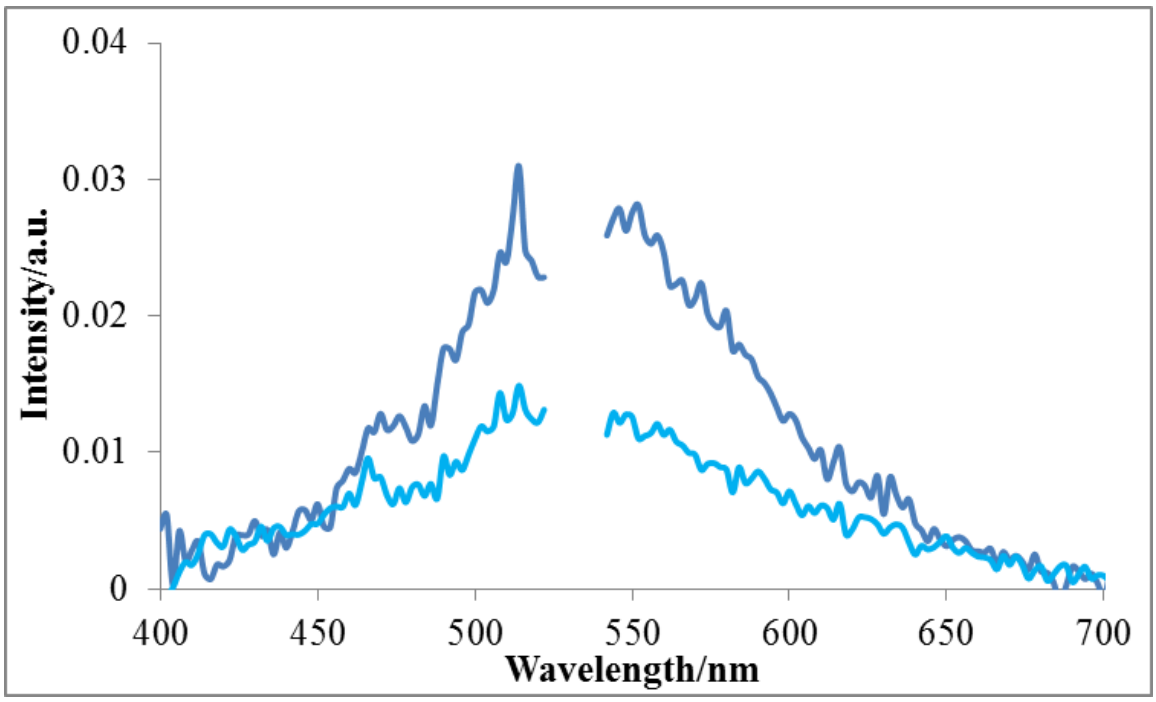

Figure 6-14 : signal obtained at peak over wavelength range 400 – 700 nm for λ_{ex} = 1064 nm subtracted from signal obtained for λ_{ex} = 532 nm in a flame where Φ = 2.1 15 mm (—) and 10 mm (—) above the burner surface

This was similarly plotted for Φ = 1.9 spectra as shown in Figure 6-15. Here there is not a great deal of difference observed between the signals recorded at the two heights in the flame, with the signal recorded at 15 mm seemingly lower than that recorded at 10 mm. However, it can be seen that the signal recorded at 15 mm falls below the zero line, suggesting there may have been an error with the measurement. If the spectra is corrected so that this is equal to zero the result is more as would be expected with the 15 mm signal higher over all wavelengths than the signal recorded at 10 mm.

As with the spectra obtained in the flame where Φ = 2.1 there are some spectral features which are similar and some which are different between the signals. This suggests that although the same classes of PAHs are present at each height there are, as would be expected, differences in the PAHs giving rise to the signal.

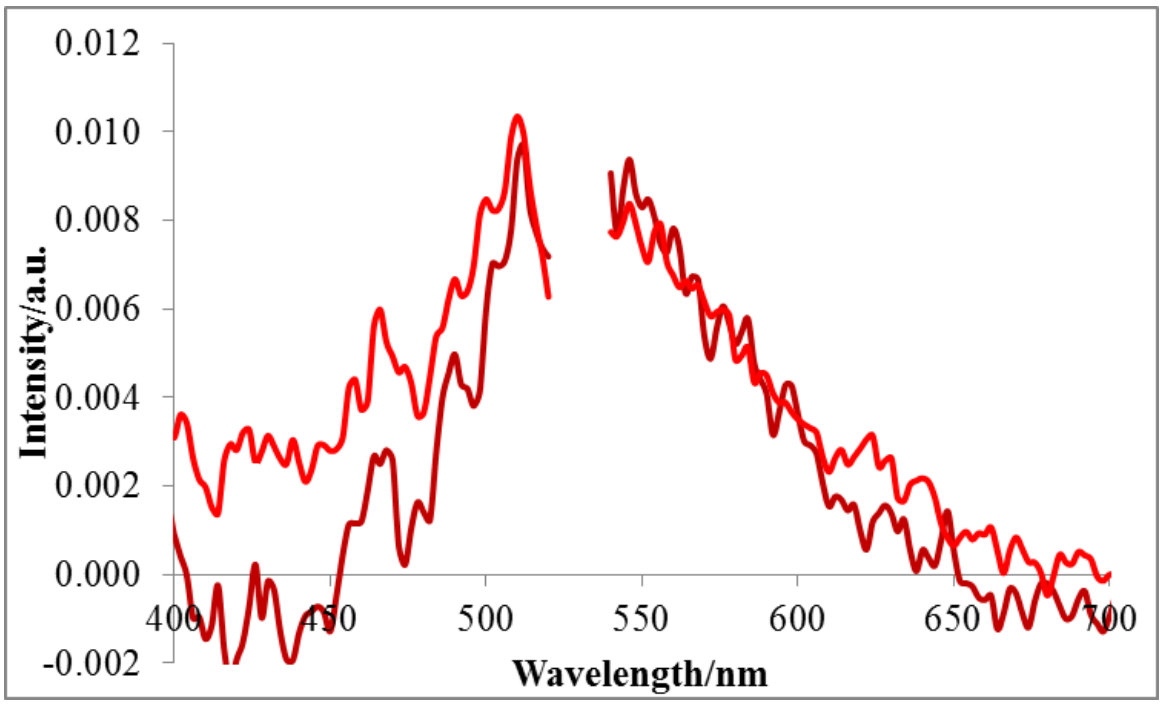

Figure 6-15 : signal obtained at peak over wavelength range 400 – 700 nm for λ_{ex} = 1064 nm subtracted from signal obtained for λ_{ex} = 532 nm in a flame where Φ = 1.9 15 mm (—) and 10 mm (—) above the burner surface

Finally, this was repeated for Φ = 1.7, Figure 6-16 Here there is a separation in the fluorescence seen for the entire wavelength range, though still with the greatest difference seen in the range 475 – 640 nm. As has been discussed there is a possibility that the measurement at 15 mm has suffered an offset. Should this have been corrected for it would suggest that the signals are as those outlined for the other stoichiometries with there being little difference below 450 nm or above 650 nm.

Again there are differences noted between the two spectra and this could be attributable to differences in the PAHs present. However with signals at low levels, such as those obtained for Φ = 1.7, caution will have to be applied so as not to confuse "real" peaks in the data, attributable to a particular spectral feature, with peaks which are as a result of noise being present in the data.

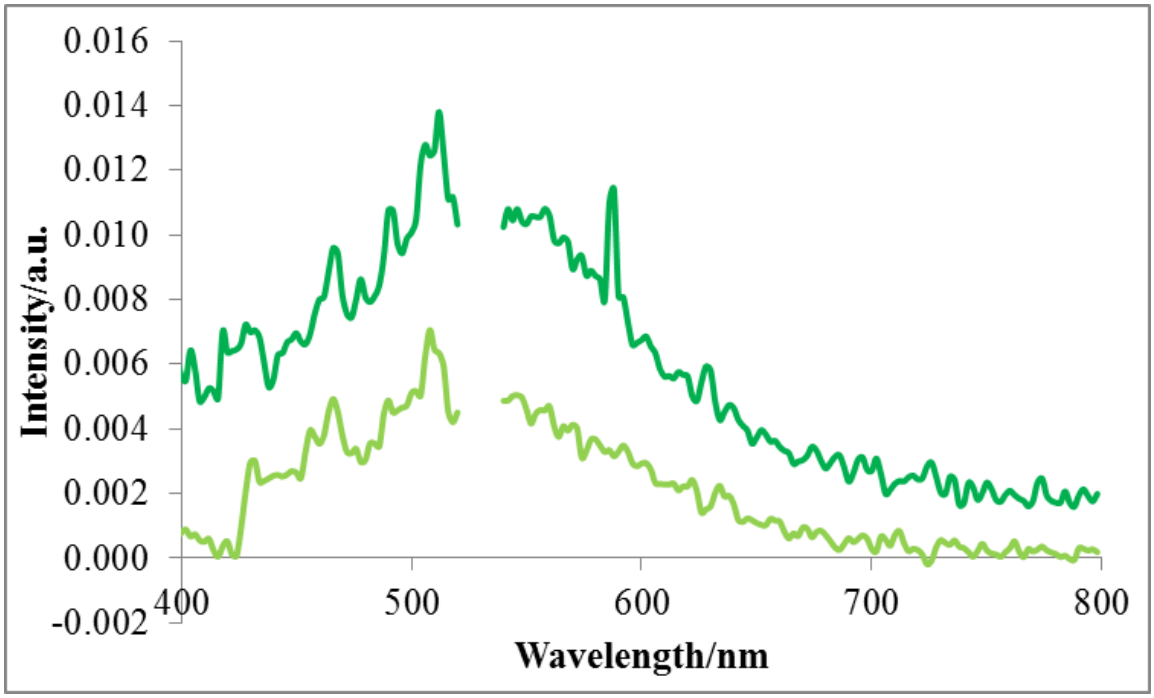

Figure 6-16 : signal obtained at peak over wavelength range 400 – 700 nm for λ_{ex} = 1064 nm subtracted from signal obtained for λ_{ex} = 532 nm in a flame where Φ = 1.7 15 mm (—) and 10 mm (—) above the burner surface

6.5 EXCITATION WITH 283 NM

It has been demonstrated that by observing the signal over a range of wavelengths a great deal of information can be obtained. In chapter 5 it was shown that there is a difference in the fluorescence information obtained when exciting with 532 nm and 283 nm and this was attributed to the size of the PAHs being excited. It was thus decided to build on this by using 283 nm for the excitation of the flames selected above and recording the emitted signal over the range of wavelengths.

As it would be expected that the fluorescence would be strongest at wavelengths which are closest to the excitation wavelength it was decided that it would be advantageous to measure to a shorter wavelength when using 283 nm excitation. This would not have been possible when exciting with 1064 or 532 nm as it was necessary to use a notch filter immediately before the detector in order to eliminate stray 532 nm light. This was, however, unnecessary when exciting with 283 nm as it is possible to block all light surrounding the Nd:YAG laser, and no green light makes it through the dye laser. This is not the case when exciting with 1064 or 532 nm as there has to be a hole in the shielding to allow the light to pass out the enclosure. Due to there being scattered light within the enclosure even when exciting with 1064 nm some green light will escape.

6.5.1 Measurements with 283 nm excitation at 15 mm above the burner surface

Initially as with the measurement with the measurement above the signal was recorded at the peak and 180 ns after the trigger in a flame where $\Phi = 2.1$ at 15 mm above the burner surface, Figure 6-17. This was to ensure that using 283 nm for the experiment yielded the results which would be expected, with the signal decaying to give the characteristic incandescent shape.

As can be seen as with the 532 nm signal there is a high degree of difference in the shape between the signal at the peak and the signal 180 ns after the trigger. The difference in signal shape is attributable to the fluorescence contribution to the total signal. It can also be observed that the biggest difference in the signal occurs a lower wavelength than when 532 nm excitation is used, which is as would be expected.

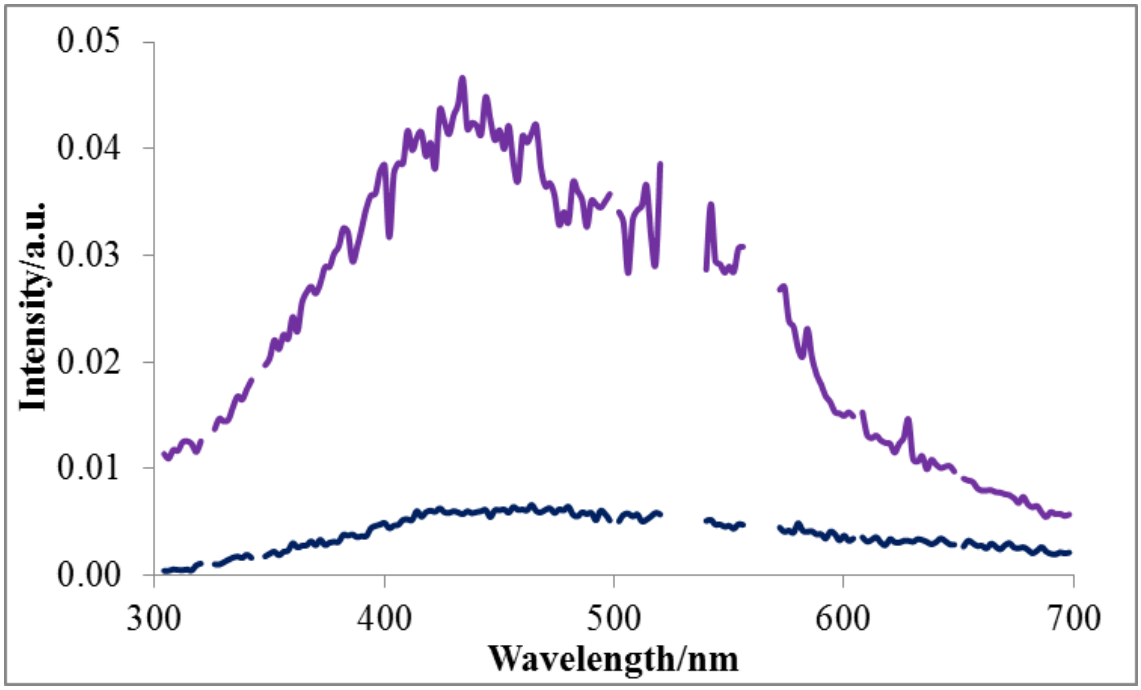

Figure 6-17 : Peak signal (—) and signal 180 ns after the trigger (—) obtained at 15 mm above the burner surface in a flame with a stoichiometry where Φ = 2.1 with λ_{ex} = 283 nm excitation

The fluorescent contribution can be better seen through the comparison of the signal obtained with 1064 nm excitation, Figure 6-18 Unfortunately, as was discussed, due to the necessity of employing a notch filter to remove interfering green light from the signal it was not possible to measure the 1064 nm signal below 400 nm. However, by comparing the signals it can clearly be seen that by 180 ns after the trigger the signals are almost equal. Conversely there is a large difference seen in the peak signal. This highlights the presence of PAHs which are being excited by 283 nm causing a fluorescent contribution in the signal.

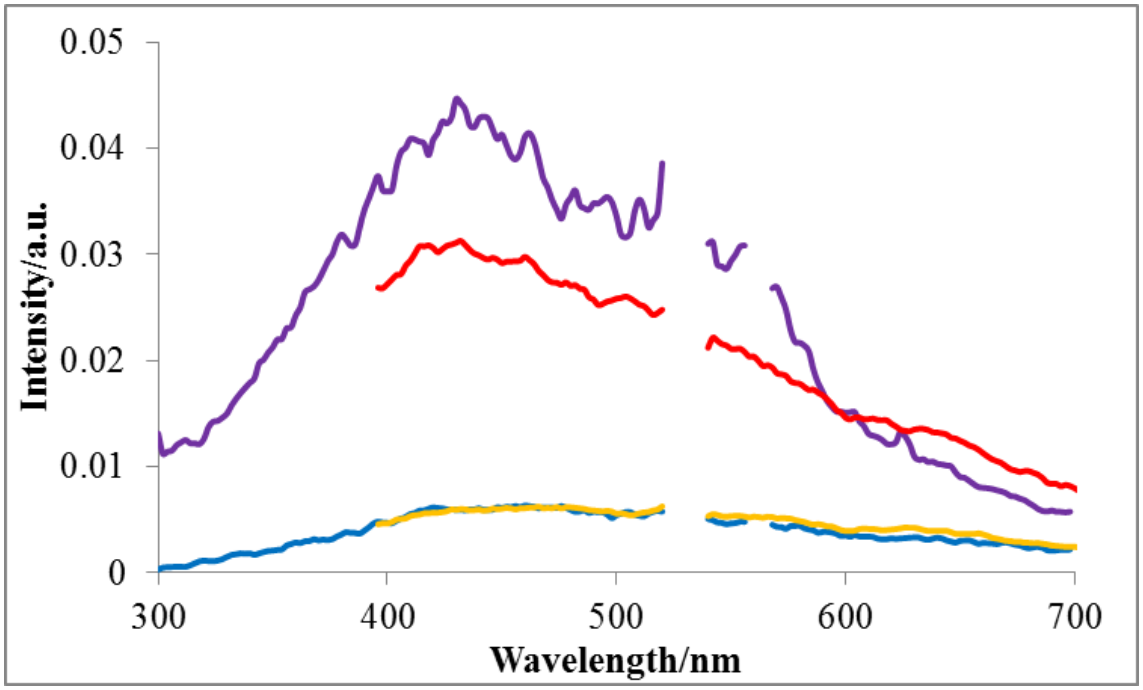

Figure 6-18 : Peak signal and signal 180 ns after the trigger obtained at 15 mm above the burner surface where Φ = 2.1 with λ_{ex} = 283 nm (— and — respectively) and λ_{ex} = 1064 nm (— and — respectively)

Similarly the signals can be compared to those obtained with 532 nm excitation, Figure 6-19. This yields some very interesting results from which it is possible to begin to obtain information about the small particulate material in the flame. It can be seen that in both cases there is definite contribution to the signal as a result of fluorescence in the signal. However, with 283 nm excitation there is a peak in the signal around 440 nm, whereas with 532 nm the signal peaks around 540 nm. This is as would be expected as the 283 nm excitation light will reflect smaller PAH molecules, which will fluoresce at shorter wavelengths than those recorded with 532 nm excitation light. This shows that as well as there being large PAHs present there are also smaller PAHs at 15 mm in the flame.

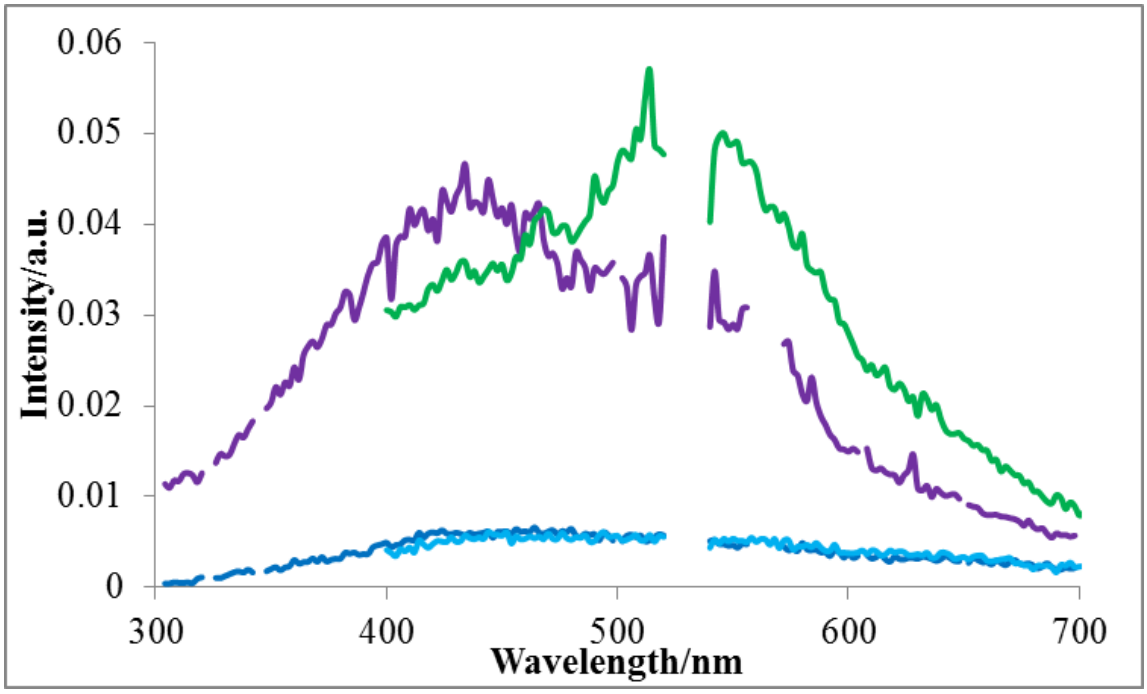

Figure 6-19 : Peak signal and signal 180 ns after the trigger obtained at 15 mm above the burner surface in a flame where Φ = 2.1 with λ_{ex} = 283 nm (— and — respectively) and λ_{ex} = 532 nm (— and — respectively)

This is highlighted upon subtracting the 1064 nm signal from that obtained with 283 nm excitation, Figure 6-20. There is a slight discrepancy in the signal recorded with 283 nm above 600 nm where the signal falls below zero when the 1064 nm signal is subtracted. This is primarily due to variation in the low signal levels present.

This clearly shows though that there are small particles which are causing fluorescence at shorter wavelengths, which are excited by the 283 nm light. When exiting with 532 nm light there is more fluorescence at higher wavelengths suggesting larger PAH molecules. This can be inferred purely from the general shape of the fluorescence signal because larger PAHs are not only excited by longer wavelengths but subsequently fluoresce at longer wavelengths.

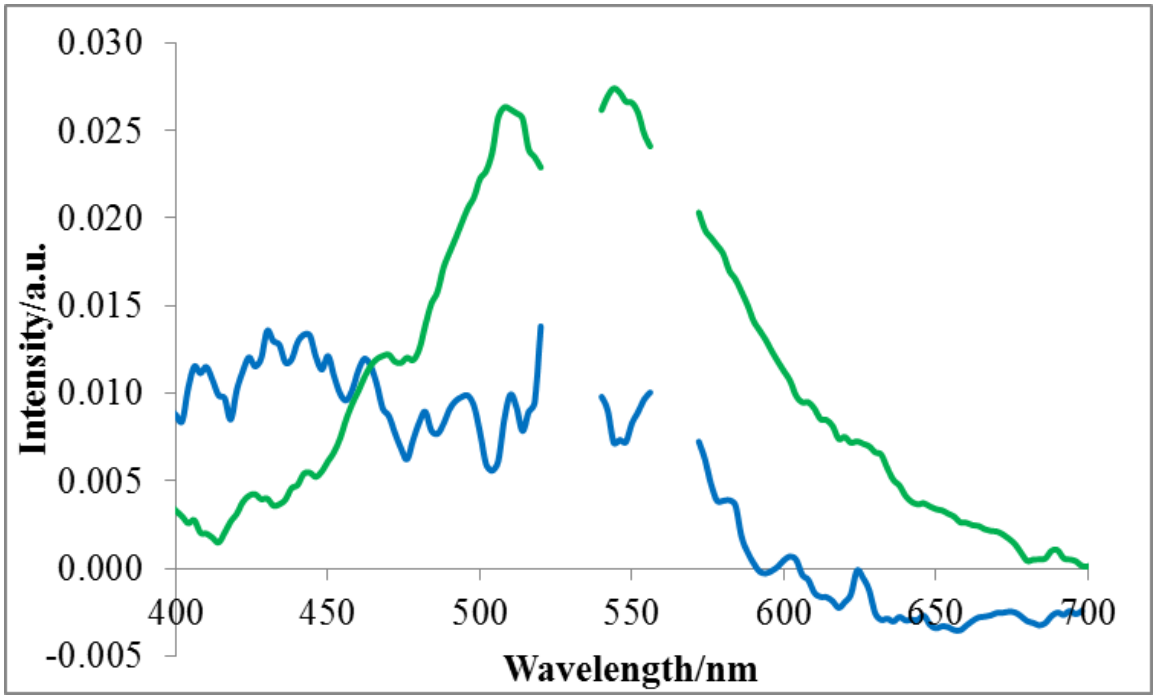

Figure 6-20 : signal obtained at peak over wavelength range 400 – 700 nm for λ_{ex} = 1064 nm subtracted from signal obtained for both λ_{ex} = 532 nm (—) and λ_{ex} = 283 nm (—) in a flame where Φ = 2.1 at 15 mm above the burner surface

This is the foundation for a potential to identify the classes of PAHs which are present within the flames. Since each PAH will have a characteristic fluorescence spectra then it should be possible to fit known spectra to the spectra obtained through subtraction measurements as above. It can clearly be seen that it is possible to observe and differentiate between relatively smaller and larger PAHs within the flame. Were it possible to attribute these to classes of PAH the method shown here would offer an in-situ method for the examination of PAHs. This is something which until now has been difficult to achieve – especially in sooting flames, such as those which are used here.

As with the previous measurements this study was extended to include measurements at different stoichiometries – Φ = 1.7 and 1.9, Figure 6-21 and Figure 6-22.

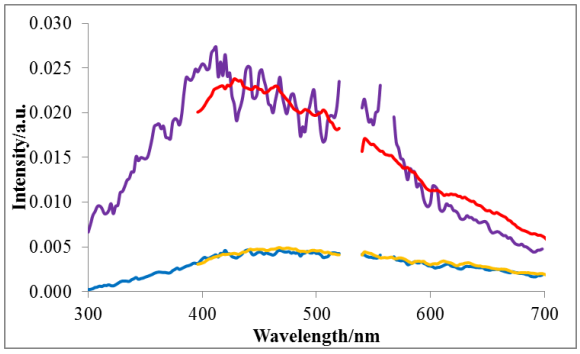

Figure 6-21 : Peak signal and signal 180 ns after the trigger obtained at 15 mm above the burner surface where Φ = 1.8 with λ_{ex} = 283 nm (— and — respectively) and λ_{ex} = 1064 nm (— and — respectively)

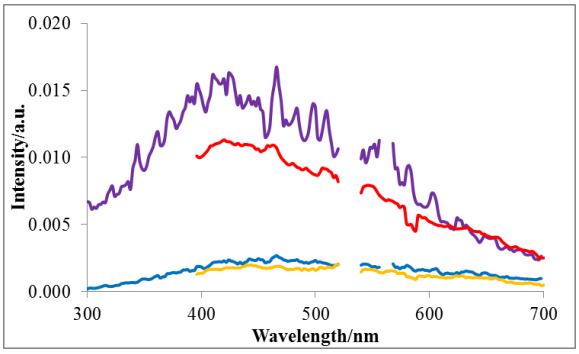

Figure 6-22 : Peak signal and signal 180 ns after the trigger obtained at 15 mm above the burner surface where Φ = 1.7 with λ_{ex} = 283 nm (— and — respectively) and λ_{ex} = 1064 nm (— and — respectively)

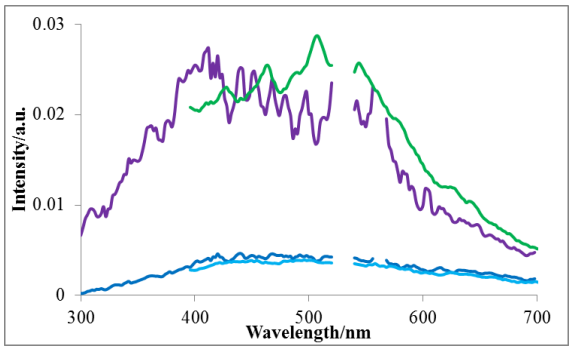

Figure 6-23 : Peak signal and signal 180 ns after the trigger obtained at 15 mm above the burner surface in a flame where Φ = 1.7 with λ_{ex} = 283 nm (— and — respectively) and λ_{ex} = 532 nm (— and — respectively)

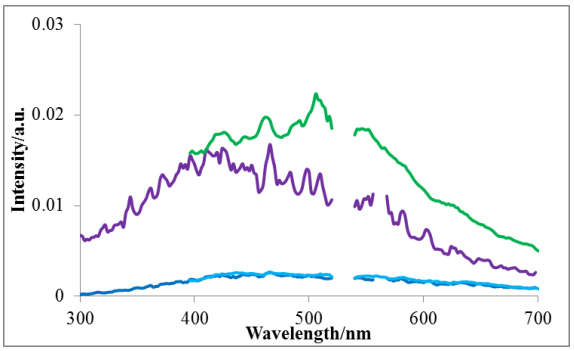

Figure 6-24 : Peak signal and signal 180 ns after the trigger obtained at 15 mm above the burner surface in a flame where Φ = 1.7 with λ_{ex} = 283 nm (— and — respectively) and λ_{ex} = 532 nm (— and — respectively)

Here it can be seen that there is less difference in the signal obtained with 283 nm than with 1064 nm than has been seen in the case where Φ = 2.1. This suggests that there are

fewer small PAHs in this flame than have been seen in the previous flame. This is not the case where Φ = 1.7 where there is again a greater difference in the peak signal between that obtained with 283 nm and 1064 nm excitation.

Again a comparison to the signal obtained with 532 nm can be made, Figure 6-23 and Figure 6-24.

As with the Φ = 2.1 conditions with Φ = 1.7 there is a much higher signal with 532 nm excitation compared to 283 nm excitation. This occurs to a much lesser extent with Φ = 1.9.

Due to the low intensities of the signals involved and the noise which is present in the signal it is almost impossible to obtain usable information from the signals obtained for Φ = 1.9 and 1.7 when the fluorescence is obtained through subtraction of the 1064 nm signal from the 283 nm.

6.5.2 Measurements with 283 nm excitation at 10 mm above the burner surface

As before this was repeated at 10 mm above the burner surface, Figure 6-25 - Figure 6-27. As above due to the low signal levels there is difficulty with subtracting the signal obtained at 1064 nm excitation from that obtained with the shorter wavelengths. However, it is possible to compare the signals without subtraction in a relative way.

As can be seen in the flame where Φ = 2.1 there is a significant difference between where the signal obtained for 283 nm excitation compared to that obtained for 1064 nm excitation. This difference shows high amounts of fluorescence are present under these conditions.

For the case where Φ = 1.9 the signals are much more similar than for the previous case, suggesting that there is not a great deal of fluorescence found here. This is unexpected, when compared to other results obtained, but it is not inconceivable that under these

conditions all of the PAHs which would be excited by 283 nm will have been consumed by the reaction.

When a stoichiometry of Φ = 1.7 is used the signal obtained for 283 nm excitation is very low. A possible explanation for this behaviour lies in the type of PAHs which may be present at this height in the flame. As has been extensively discussed the formation of spot is a stepwise process, with first gaseous PAHs forming, which will grow to larger solid PAHs which will eventually form soot. It has been hypothesised that between these gaseous and solid species there is a brief zone where the PAHs are liquid like structures[1, 18-20]. This leads to a so called dark zone where the particles cannot incandesce but show weak fluorescence.

Comparing the signals to those observed with 532 nm is easier achieved by comparing without the subtraction of the signal obtained with 1064 nm. Since the signal which would be subtracted in each case is identical this is a valid way of comparing the signals without having to worry about the high levels of noise which prevent the spectra from giving meaningful information. This is shown in Figure 6-28 to Figure 6-30It must be remembered throughout this comparison that no information can be inferred from the intensity of the signal. The difference in the shape of the spectra under each condition is clear to see however. This highlights that if spectra of known PAHs were obtained then the valuable information which it would be possible to obtain from data such as this.

It can be seen that in flames Φ = 2.1 and 1.9 the signals which are seen are relatively similar. There is a difference in the intensity of the signal but the general shape are very alike. This is comparable to what has been seen earlier where it is suggested that the growth mechanisms for the different flames are almost the same but with different concentrations present.

The comparison between 532 nm and 283 nm excitation is difficult due to the low level of the signal attributable to 283 nm excitation. This would require further investigation in order to properly understand what is taking place in the flame at this point. As

previously hypothesised this could be due to the particles present in the flame being due to liquid like particles. This would be an interesting area for further study.

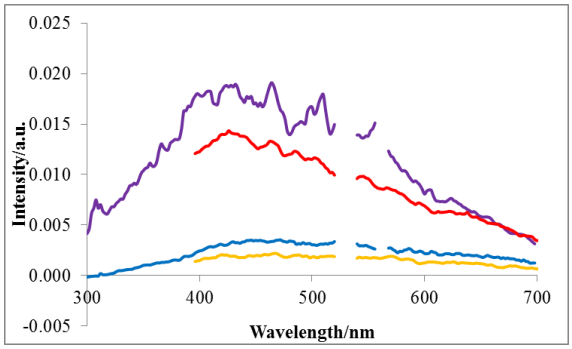

Figure 6-25 : Peak signal and signal 180 ns after the trigger obtained at 10 mm above the burner surface where Φ = 2.1 with λ_{ex} = 283 nm (— and — respectively) and λ_{ex} = 1064 nm (— and — respectively)

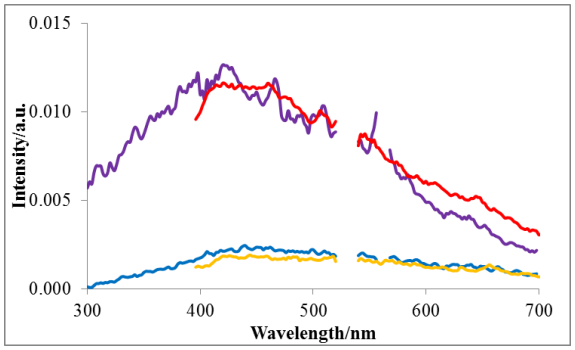

Figure 6-26 : Peak signal and signal 180 ns after the trigger obtained at 10 mm above the burner surface where Φ = 1.9 with λ_{ex} = 283 nm (— and — respectively) and λ_{ex} = 1064 nm (— and — respectively)

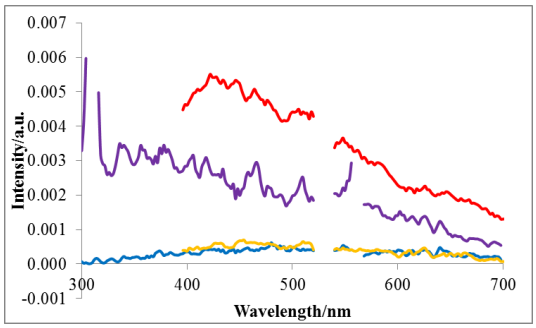

Figure 6-27 : Peak signal and signal 180 ns after the trigger obtained at 10 mm above the burner surface where Φ = 1.7 with λ_{ex} = 283 nm (— and — respectively) and λ_{ex} = 1064 nm (— and — respectively)

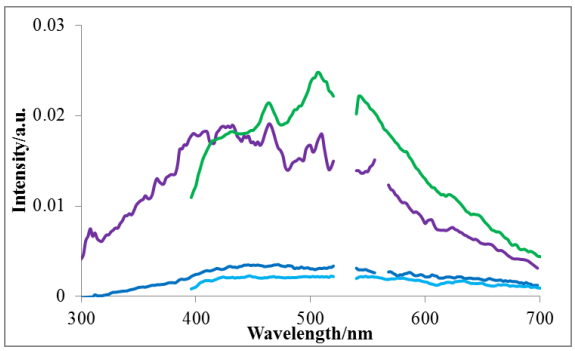

Figure 6-28 : Peak signal and signal 180 ns after the trigger obtained at 10 mm above the burner surface in a flame where Φ = 2.1 with λ_{ex} = 283 nm (— and — respectively) and λ_{ex} = 532 nm (— and — respectively)

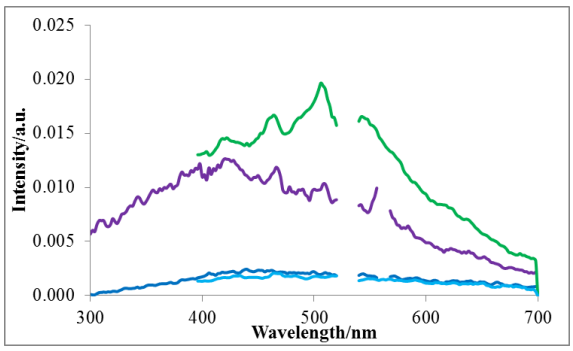

Figure 6-29 : Peak signal and signal 180 ns after the trigger obtained at 10 mm above the burner surface in a flame where Φ = 1.9 with λ_{ex} = 283 nm (— and — respectively) and λ_{ex} = 532 nm (— and — respectively)

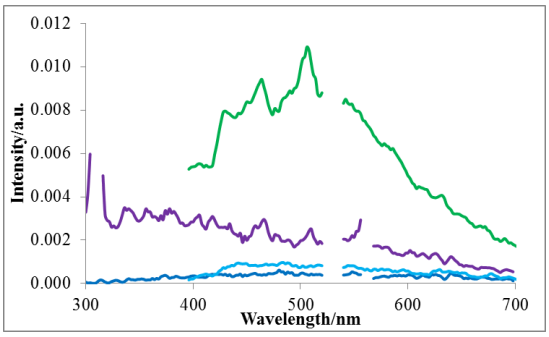

Figure 6-30 : Peak signal and signal 180 ns after the trigger obtained at 10 mm above the burner surface in a flame where Φ = 1.7 with λ_{ex} = 283 nm (— and — respectively) and λ_{ex} = 532 nm (— and — respectively)

6.6 DECAY TIMES

As has been discussed signals which are detected at higher wavelengths will have a lower decay rate than those which are recorded at shorter wavelengths[16, 17]. This is due to the blackbody spectrum shifting to increasing wavelength as the temperature falls. Thus by plotting the decay time of the incandescence signals which are obtained at each of the detection wavelengths there should be an increase in the decay time from 400 to 800 nm detection wavelength[12].

The decay at each wavelength for each flame condition was fitted as per the method outlined in chapter 5. Here the decay is fitted from a time after the photodiode trigger where the LIF will have decayed and the signal will only be due to incandescence.

6.6.1 15 mm height above burner surface

Initially the decay was fitted for $\Phi = 2.1$ at 15 mm above the burner surface. By plotting the decay time for each detection wavelength it can be seen that there is an increase in decay time, therefore a decrease in decay rate upon increasing the detection wavelength as shown in Figure 6-31.

The decay has been fitted between 150 ns (as it has been demonstrated that any fluorescence in the signal has decayed by this point) and 1000 ns (which is significantly after the signal has decayed to zero).

The fitted decay has a higher degree of scatter at longer wavelengths because the PMT rapidly loses its efficiency in this region, especially above 600 nm. Due to this the signal levels are lower and the signal to noise ratio decreases, making it more difficult to obtain a good fit. However, the general increase in the decay time can be seen and the agreement between the two excitation wavelengths is apparent. In order to assess the impact of changing the stoichiometry the above process was repeated with the signals which were obtained at 15 mm for both $\Phi = 1.9$ and 1.7, Figure 6-31 to Figure 6-33

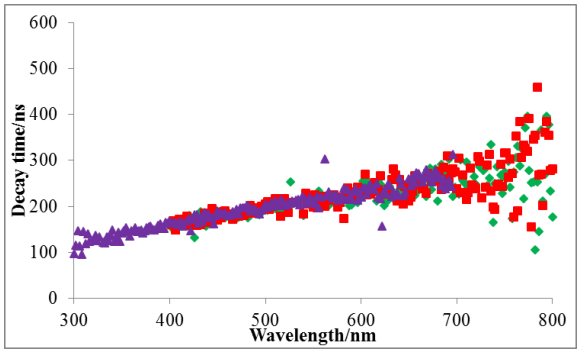

Figure 6-31 : fitted decay for signals obtained over wavelength range 400 – 800 nm where Φ = 2.1 with λ_{ex} = 1064 nm (■), λ_{ex} = 532 nm (♦) and λ_{ex} = 283 nm (▲) at 15 mm above the burner surface

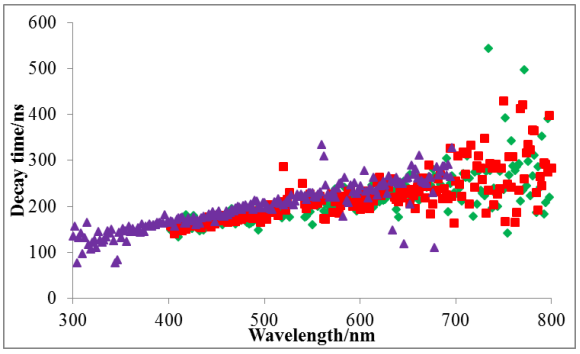

Figure 6-32 : fitted decay for signals obtained over wavelength range 400 – 800 nm where Φ = 1.9 with λ_{ex} = 1064 nm (■), λ_{ex} = 532 nm (♦) and λ_{ex} = 283 nm (▲) at 15 mm above the burner surface

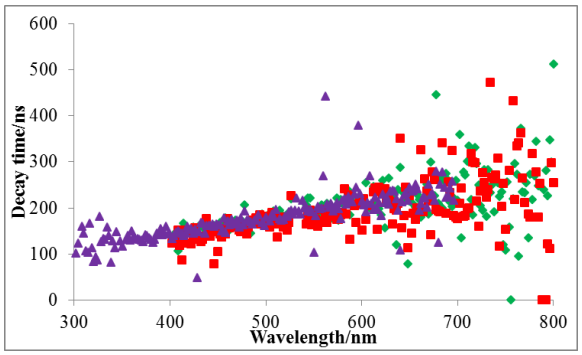

Figure 6-33 : fitted decay for signals obtained over wavelength range 400 – 800 nm where Φ = 1.7 with λ_{ex} = 1064 nm (■), λ_{ex} = 532 nm (♦) and λ_{ex} = 283 nm (▲) at 15 mm above the burner surface

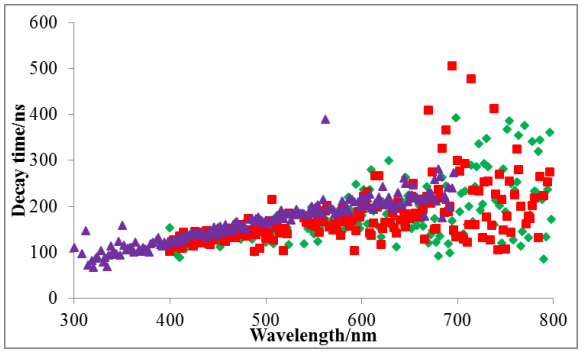

Figure 6-34 : fitted decay for signals obtained over wavelength range 400 – 800 nm where Φ = 2.1 with λ_{ex} = 1064 nm (■), λ_{ex} = 532 nm (♦) and λ_{ex} = 283 nm (▲) at 10 mm above the burner surface

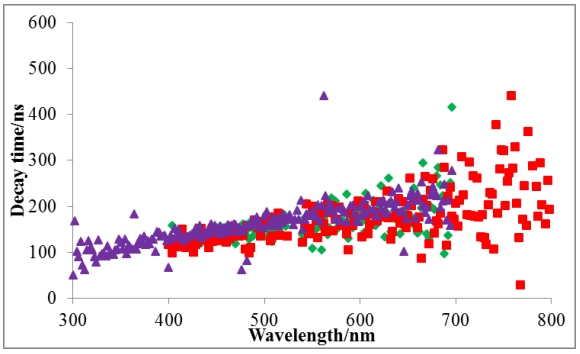

Figure 6-35 : fitted decay for signals obtained over wavelength range 400 – 800 nm where Φ = 1.9 with λ_{ex} = 1064 nm (■), λ_{ex} = 532 nm (♦) and λ_{ex} = 283 nm (▲) at 10 mm above the burner surface

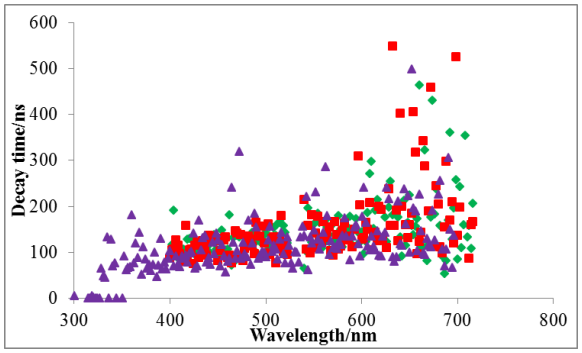

Figure 6-36 : fitted decay for signals obtained over wavelength range 400 – 800 nm where Φ = 1.7 with λ_{ex} = 1064 nm (■), λ_{ex} = 532 nm (♦) and λ_{ex} = 283 nm (▲) at 10 mm above the burner surface

Again, for both cases, the increase in decay rate on increasing the wavelength can be seen. The decrease in the signal which has been recorded can be seen with the fitted

signals becoming more variable upon increasing the wavelength. This is, as has been said above, due to low signal levels and poor signal to noise ratio, and is thus seen to a greater extent at lower stoichiometries where the recorded signal is weaker.

6.6.2 10 mm height above burner surface

This was then repeated at 10 mm above the burner surface. The fit for the incandescent decay at these heights, especially at longer detection wavelengths, the signal will be low and have a poor signal to noise ratio, meaning that it is difficult to obtain a good fit as shown in Figure 6-34 - Figure 6-36.

As can be seen in each of the cases at 10 mm above the burner surface there is the, once again, good agreements between the signal which is obtained for each of the excitation

wavelengths. This tends to confirm the conclusion that across the range of conditions it is possible to subtract the signal attributable to incandescence from that attributable to a combination fluorescence and incandescence.

The ability to accurately fit the decay time to data which is obtained in this way shows the possibility of being able to calculate the particle size in such measurements. This means from one data set collected in this way there can be information obtained on the soot volume fraction, particle size as well as the fluorescence spectra which are obtained.

6.7 POTENTIAL TO FIT BLACKBODY RADIATION TO INCANDESCENCE SPECTRA

It has been shown through the method described above that it is possible to obtain

incandescence, when exciting with 1064 nm, over a range of wavelengths. It has also been discussed that this incandescence is akin to that which would be emitted by blackbodies when heated to such a temperature as they glow. Thus the peak signal over the range of wavelengths is able to be likened to a blackbody curve.

With blackbody radiation the light emitted is relative only to the temperature to which it is heated, irrespective of the chemical properties. As such if we assume that the incandescence in this case is behaving in the same way and fit a blackbody curve to it we can derive the temperature of the particles. This would allow for the temperature of the soot particles to be non-invasively obtained, offering many advantages over inserting a thermocouple in the flame. There are other non-invasive methods of obtaining the temperature of soot particles, however this method can be coupled with the other information which can be obtained from the afore mentioned data.

6.8 CONCLUSIONS

In previous chapters the potential for separating the light emitted from the flame as a result of incandescence and fluorescence have been proven. However, there was limited information which could be obtained from measurements which were obtained at one wavelength. Therefore, a method was developed in order to record the emitted light over a range of wavelengths, in order that fluorescence spectra could be obtained which would pave the way for the possibility of being able to compare the obtained fluorescence signal to fluorescence spectra of known PAHs in order that it be possible to identify classes of PAH which are present at a given position in the flame for given flame conditions. This would require a significant amount of further work but the potential has been highlighted and an effective method proposed. This has great advantages over methods which require the withdrawl of samples from the flame in

order to be able to analyse them. This causes problems not only with obtaining a sample but surrounding whether the sample is representative of the other species present in that region, or if due to the sample transportation or perturbation of the region of the flame by a probe, that the sample analysed is significantly different from what it should be. The method presented eliminates any need for assumptions to be made on this.

The potential for obtaining the temperature of the flame through fitting of a blackbody curve to the emitted incandescence signal is also highlighted, however, this would require use of a set up which had greater sensitivity in long wavelength ranges than that which was employed here. It has also been shown that information on the decay time can be accurately gathered, which will allow for particle size information to be obtained, and in the same way as shown in previous chapters it will also be possible to obtain soot volume fraction. This paves the way for a great deal of information to be obtained from data which is gathered in the way shown in this chapter, which is greatly advantageous.

6.9 REFERENCES

1. R. L. Vander Wal, K. A. Jensen and M. Y. Choi, *Combustion and Flame*, 1997, **109**, 399-414.
2. C. S. Moreau, E. Therssen, X. Mercier, J. F. Pauwels and P. Desgroux, *Applied Physics B-Lasers and Optics*, 2004, **78**, 485-492.
3. R. Lemaire, A. Faccinetto, E. Therssen, M. Ziskind, C. Focsa and P. Desgroux, *Proceedings of the Combustion Institute*, 2009, **32**, 737-744.
4. P. Desgroux, X. Mercier and K. A. Thomson, *Proceedings of the Combustion Institute*, 2013, **34**, 1713-1738.
5. C. S. McEnally, L. D. Pfefferle, B. Atakan and K. Kohse-Hoinghaus, *Progress in Energy and Combustion Science*, 2006, **32**, 247-294.

6. K. Siegmann, K. Sattler and H. C. Siegmann, *Journal of Electron Spectroscopy and Related Phenomena*, 2002, **126**, 191-202.
7. C. Lou, C. Chen, Y. P. Sun and H. C. Zhou, *Science China-Technological Sciences*, 2010, **53**, 2129-2141.
8. X. Mercier, M. Wartel, J. F. Pauwels and P. Desgroux, *Applied Physics B-Lasers and Optics*, 2008, **91**, 387-395.
9. A. D'Anna, *Proceedings of the Combustion Institute*, 2009, **32**, 593-613.
10. R. L. Vander Wal and K. J. Weiland, *Applied Physics B*, 1994, **59**, 445-452.
11. K. N. Palmer, *Fire research notes*, 1958, **356**.
12. https://www.hamamatsu.com/jp/en/R636-10.html, accessed August 2013.
13. P.-E. Bengtsson and M. Aldén, *Combustion and Flame*, 1990, **80**, 322-328.
14. A. R. Masri, R. W. Bilger and R. W. Dibble, *Combustion and Flame*, 1987, **68**, 109-119.
15. J. M. Seitzman, J. Haumann and R. K. Hanson, *Applied Optics*, 1987, **26**, 2892-2899.
16. B. Axelsson, R. Collin and P. E. Bengtsson, *Applied Optics*, 2000, **39**, 3683-3690.
17. R. J. Santoro, H. G. Semerjian and R. A. Dobbins, *Combustion and Flame*, 1983, **51**, 203-218.
18. R. A. Dobbins, R. A. Fletcher and H. C. Chang, *Combustion and Flame*, 1998, **115**, 285-298.
19. A. D'Alessio, A. D'Anna, A. D'Orsi, P. Minutolo, R. Barbella and A. Ciajolo, *Symposium (International) on Combustion*, 1992, **24**, 973-980.
20. Ü. Ö. Köylü, C. S. McEnally, D. E. Rosner and L. D. Pfefferle, *Combustion and Flame*, 1997, **110**, 494-507.

7 CONCLUSIONS AND FUTURE WORK

7.1 CONCLUSIONS

The work which is shown here aimed firstly to assess the different methods (namely prompt and delayed detection) of LII. This was achieved and it was shown that there are significant errors which are obtained if 532 nm is used for excitation, regardless of whether prompt or delayed detection is employed. It has been shown that due to PAHs present in the measurement volume there will be an over estimation of the soot volume fraction present at a given point in the flame as a result of fluorescence. Conversely, it is shown that if delayed detection is employed there will be an underestimation of the soot volume fraction at low heights in the burner, resulting from the effects of soot particle size. These findings highlight that if either of these methods are to be used to obtain soot volume fraction significant care must be taken. It is seen that it is more accurate to use delayed detection as the errors are seen as being lower than the error associated with prompt detection.

The implication, bearing in mind the findings of the first section, of using a UV excitation wavelength to calculate soot volume fraction was also considered. This was shown to be effective and it was highlighted that, as would be expected, a significant difference in the intensity of the fluorescence contribution was seen.

It has also been demonstrated that it is possible to isolate fluorescence signals from the measurements over a range of flame conditions and heights above burner. This relied upon the heating of the particles to the same temperature with the three excitation wavelengths in order that the incandescence decay is equivalent. The LII signal can then be subtracted to leave only the fluorescence contribution. The fluorescence profiles obtained show similar features to those seen in the literature for invasive measurements, including a reduction in the fluorescence signal generated by 283 nm excitation at

intermediate heights above the burner surface followed by a re-increase, which is of great interest as the measurements shown here were performed entirely *in-situ.* These measurements allowed for the inference of changing concentration of the classes of PAHs within the flame.

Through use of a monochromator it was possible to spectrally resolve the fluorescence signal obtained. This highlighted the possibility of the use of this method to obtain *in-situ* information about PAHs which cannot otherwise be obtained. Collectively through use of this method there is the possibility to obtain soot volume fraction, soot particle size and information of the PAHs near simultaneously. This shows a large advantage over the methods which are shown in the literature.

7.2 FUTURE WORK

As was stated by the American economist and sociologist Thorstein Veblen in 1908 *"the outcome of any serious research can only be to make two questions grow where only one grew before"*. As such there are many things which are within the scope of the research discussed here that it would be interesting to study given the opportunity.

While this work has shown the power of using different excitation wavelengths in order to obtain spectral information pertaining to fluorescing PAHs. It has been discussed that it may be possible to identify classes of PAH from these spectra and that this could, unlike anything published thus far, be carried out *in-situ*. This would progress the work to begin to develop a better picture of which PAHs are present in the different flame positions. This could be achieved by comparing the spectra which are obtained in the flame with the fluorescence spectra of known PAHs which have been obtained elsewhere.

In order for this to be successful care will have to be taken when assigning particular PAHs to the spectra obtained. It must be remembered that each of the spectra which are obtained *in-situ* will be as a result of a combination of more than one PAH – that is pure spectra will not be obtained. However, if the fluorescence spectra of several potential PAHs can be identified then the standard spectra could be combined in order to obtain the spectrum which would result from a mixture of these PAHs. Obviously this would be dependent on the relative combinations of PAHs and it could be possible to write a programme which combines different ratios of suspected PAHs and identifies the best fit for the spectra obtained within the flame.

Another way of obtaining spectra of known PAHs for comparison, and to influence the PAH pathway taken within the flame, would be to seed the flame with a known PAH. This could either be achieved by mixing known PAHs with the premix of fuel and air or injecting directly into the flame. It must be noted however that the PAHs added to the flame will remain as when added, they can undergo either breakdown or growth, just as other PAHs in the flame are. However, by injecting a relatively large volume of the known PAH there is a greater chance that a proportion of it will not react and hence be able to be identified in the flame in greater quantities.

It can already be seen through comparison of the 283 nm and 532 nm excitation obtained fluorescence spectra that there are different sizes of PAH at different heights in the flame (as would be expected). This can be seen as the 283 nm excitation will cause fluorescence of smaller molecules than the excitation with 532 nm. This could be further resolved through use of a wider range of excitation wavelengths. This could be achieved in the UV range relatively easily by changing the dye which is used in the dye laser.

It has also been shown that for certain flame conditions the signal drops to such an extent that it is proposed that this is the so called “dark zone” which occurs during the formation of nascent soot[1-3]. As has been highlighted this is a region of great interest in the study of soot formation and as such this should be investigated further.

Initially it could be suggested that under the same conditions for excitation with 283 nm in a flame where $\Phi = 1.7$ the study should be extended to cover a wider range of heights above burner around 10 mm. This would show at what height in the flame the dark zone is occurring and where it can be inferred that the nascent soot is forming. This, however, is a time consuming process and care would have to be taken that value was being obtained through making these measurements.

With larger changes to the set up this could be further studied through using the same type of burner in a low pressure chamber. This would have the effect of expanding the flame front so that it could be possible to better resolve this region. This would give the opportunity to examine how small a region it is possible to identify PAHs in. In other flame conditions where the fluorescence signal is stronger having better resolution would also offer the possibility to determine how finely divided the different classes of PAHs identified can be.

Further work beyond this would include extending the study to involve a wider range of burners, perhaps the other two identified as standard, a wider range of stoichiometries and a wider range of detection wavelengths. For example, through employing a notch filter which extends below 400 nm, this would have led to better subtractions for the 283 nm LIF spectra.

It would also be interesting to apply the developed method to other combustion studies, through monitoring of exhaust emissions. There is already an extensive body of work in this area showing the benefit of LII and LIF and as such it can be hypothesised that this would be successful in obtaining similar information to that which is obtained in flames.

Although outwith the scope of the study of combustion it would be interesting to transfer the method which has been developed here to different disciplines. For example there is the potential to monitor the growth of other nanoparticulate material which can be equally difficult to investigate through other techniques[4, 5]. Since the study of nanoparticulate material is currently growing this could be a good area in which to progress the method in potentially more stable environments.

7.3 REFERENCES

1. R. L. Vander Wal, K. A. Jensen and M. Y. Choi, *Combustion and Flame*, 1997, **109**, 399-414.
2. A. D'Alessio, A. D'Anna, A. D'Orsi, P. Minutolo, R. Barbella and A. Ciajolo, *Symposium (International) on Combustion*, 1992, **24**, 973-980.
3. Ü. Ö. Köylü, C. S. McEnally, D. E. Rosner and L. D. Pfefferle, *Combustion and Flame*, 1997, **110**, 494-507.
4. F. Cignoli, C. Bellomunno, S. Maffi and G. Zizak, *Applied Physics B-Lasers and Optics*, 2009, **96**, 593-599.
5. K. J. Daun, J. T. Titantah and M. Karttunen, *Applied Physics B-Lasers and Optics*, 2012, **107**, 221-228.